UNIVERSIDADE D
COIMBRA

Marta Cristina Filipe Simões

Tailoring Challenging Drug Properties through Solid Dispersions

Tese no âmbito do Doutoramento em Ciências Farmacêuticas, ramo de Tecnologia Farmacêutica, orientada pelo Professor Doutor Sérgio Paulo de Magalhães Simões e pelo Doutor Rui Miguel de Aguiar Pinto, e apresentada à Faculdade de Farmácia da Universidade de Coimbra.

Dezembro de 2020

Faculdade de Farmácia
da Universidade de Coimbra

TAILORING CHALLENGING DRUG PROPERTIES THROUGH SOLID DISPERSIONS

Marta Cristina Filipe Simões

Dissertação de Doutoramento na área científica de Ciências Farmacêuticas, ramo de Tecnologia Farmacêutica, orientada pelo Professor Doutor Sérgio Paulo de Magalhães Simões e pelo Doutor Rui Miguel de Aguiar Pinto, apresentada à Faculdade de Farmácia da Universidade de Coimbra.

Dezembro de 2020

UNIVERSIDADE D
COIMBRA

The work presented in this thesis has been carried out under the supervision of Professor Sérgio Paulo de Magalhães Simões (PharmD, PhD, Associate Professor with habilitation in the Faculty of Pharmacy of the University of Coimbra), and Rui Miguel de Aguiar Pinto (PharmD, PhD, Head of Project Management of Bluepharma – Indústria Farmacêutica, SA).

Agradecimentos

Muitos foram aqueles que dedicaram um pouco do seu tempo e conhecimento a este projeto. Seja de forma direta ou indireta, a verdade é que este trabalho não teria sido possível sem vocês.

Em primeiro lugar, devo o meu reconhecimento às pessoas que me supervisionaram, mas mais que isso, ensinaram e desafiaram diariamente. O meu agradecimento profundo ao Professor Sérgio Simões, pelo seu guia constante, pela sua disponibilidade, pelo incentivo, pela exigência, pelos desafios (muitas vezes "maiores do que eu"), pelo exemplo e, sobretudo, pela confiança. E ao Rui Pinto, por me ensinar a pensar de forma diferente, pelo guia científico, pela partilha de conhecimento, pelas discussões, por me ensinar a crescer no mundo da ciência e, não menos importante, pela amizade. Sem dúvida, sem vocês não estaria aqui hoje.

Da equipa Bluepharma, muitos são aqueles a quem devo o meu agradecimento. Aos meus colegas do Desenvolvimento Galénico, pela ajuda no trabalho experimental e pelos momentos de partilha e bom-humor! Ao pé de vocês tudo se torna mais fácil. À Drª Sonia e ao Gabriel, pelos constantes desafios e oportunidades. Ao Desenvolvimento Analítico, pelo apoio analítico no projeto, e em especial à Alexandra Gonçalves, Marcos Monteiro, Alexandra Roxo, Alexandra Pereira, e Rute Ambrósio, pela disponibilidade e por alinharem nas minhas aventuras. Aos restantes colegas da Formulação e "vizinhos", em especial a Branca, a Patrícia Freitas, a Rita, a Matilde e a Amélia, obrigada pelos desafios, pelo companheirismo, pelas gargalhadas, pelos bons conselhos, por me fazerem acreditar. À Administração da Bluepharma, por me receberem e incentivarem e por nunca deixarem de apostar na ciência e na inovação. É uma honra poder fazer parte desta família.

O meu profundo agradecimento também ao Professor Rui Fausto e equipa do departamento de Química da Universidade de Coimbra, nomeadamente ao Bernardo e à Andreia, que hoje pertence à Bluepharma, pelo apoio inestimável com a espectroscopia Raman.

Agradeço também o apoio financeiro (PD/BDE/135149/2017) à Fundação para a Ciência e Tecnologia, que permitiu completar o trabalho descrito nesta tese.

A todos os meus amigos, alguns já mencionados, que me acompanharam ao longo deste capítulo, o meu muito obrigada. Não posso mencionar todos, porque felizmente são muitos. Obrigada pela vossa paciência, por me ajudarem a ver o lado bom da vida, e por me fazerem rir. Um especial

obrigada à Ana, minha amiga de sempre, por estar sempre do meu lado e pelos incentivos certos nos momentos certos.

Acima de tudo, devo o meu profundo agradecimento à minha família. Aos meus pais, Carlos e Conceição, pelo seu amor e suporte incondicional, pelo exemplo de luta, determinação, altruísmo e sacrifício. Vocês fizeram de mim o que sou hoje. À minha irmã Teresa, pela ajuda em algumas das figuras desta tese, mas principalmente por estares sempre por perto. Obrigada pelo teu pensamento positivo e alegria de viver, por me obrigares a desligar o computador, a relaxar, e a dar atenção às coisas importantes. Ao João, pelo incentivo, por me deixares voar, por não me deixares desistir, pela compreensão pelas compridas horas de trabalho, por leres os meus trabalhos, por não estar ao teu lado quando devia. Às minhas avós Amélia e Alice, obrigada pelo vosso amor e por me ensinarem que não há limites para a bondade. Em especial à avó Amélia, que naqueles olhos doces nos ensinou que devemos sempre ver o mundo com a curiosidade de uma criança. Olha por nós.

A todos vós, muito obrigada.

The work presented in this thesis was performed at Bluepharma - Indústria Farmacêutica, S.A. (Portugal) in collaboration with the Faculty of Pharmacy of the University of Coimbra (Portugal). The work was funded by Bluepharma - Indústria Farmacêutica, S.A. (Portugal) and by the fellowship PD/BDE/135149/2017 from the Fundação para a Ciência e a Tecnologia (Portugal).

Table of Contents

Abstract

Solid dispersions are systems where one component is dispersed in a carrier, and the whole system is solid. The solubility, drug release, chemical and physical stability, and *in vivo* performance of these compositions vary depending on the chemical characteristics of the main components and the physical structure of the composition. Solid dispersions are considered one of the most complex pharmaceutical systems, and an in-depth understanding of their properties is essential to control and modulate product performance. The use of Hot-melt extrusion (HME) to prepare solid dispersions has made it a technology that changed the entire paradigm of the pharmaceutical industry research and manufacturing. It is recognizably able to overcome formulation barriers and tailor drug performance and has been used successfully for already marketed products and many others under development. The enhancement of solubility is the primary use of HME, but others include taste-masking, stabilization of amorphous drugs, and controlled drug delivery.

In this work, HME technology was applied in three different scopes, particularly in the solubility enhancement of a poorly soluble compound, in the physical stabilization of an unstable amorphous drug, and in the controlled release of a highly soluble drug in low drug load. A combination of chromatographic (high and ultra performance liquid chromatography (HPLC and UPLC)), microscopic (optical microscopy, polarized light microscopy (PLM), scanning electron microscopy (SEM)), thermal (standard differential scanning calorimetry (DSC), modulated temperature DSC (mDSC), thermogravimetric analysis (TGA), and polarized light thermal microscopy (PLTM)), diffraction (X-ray powder diffraction (XRPD)), and spectroscopic techniques (Raman spectroscopy coupled to confocal microscopy, or in some cases to variable temperature) were used. Dissolution testing and stability studies were as well crucial for the in-depth characterization of the prepared systems. High-throughput screening methods, thermodynamic predictions, and statistical analysis were also of great importance.

In this work, a systematic step-by-step methodology for the development of solid dispersions was presented, where thermodynamics, screening approaches, multivariate statistics, and process optimization were combined (Chapter I). It was focused on pharmaceutical development under the Quality by Design principles and practical methods from early development to regulatory approval. The technical and scientific specificities of HME-based formulations were discussed in line with the state of the art of product development and current regulatory guidance.

Then, an amorphous solid dispersion (ASD) of Etravirine was prepared to enhance the solubility of this poorly soluble drug (Chapter II). An extensive investigation of the solubilization capacity and physical stability of different compositions was performed, where theoretical predictions, high-throughput screening, and Principal Components Analysis were combined. The dissolution rate was improved more than two times, and the ASD demonstrated to be physically and chemically stable for at least three months, even when stored at accelerated conditions. Although not expected, it was later explained by Raman spectroscopy, where molecular interactions affecting the CN groups of Etravirine were observed. Moreover, Raman's high potential to distinguish solid-state forms was demonstrated, including differentiating amorphous and crystalline states.

A different aim of the investigation was described in the Ibrutinib research (Chapter III), where HME was applied to improve the physical stability of the amorphous drug. Although with a high tendency to convert into the most stable crystalline form, stability until at least six months at accelerated conditions was achieved through HME in a very high drug load of 50%. Intermolecular interactions characterized by thermal analysis and Raman spectroscopy involving the α, β unsaturated ketone of ibrutinib supported the physical strength of the prepared systems. This application of HME technology is not common but demonstrated a remarkable interplay between HME, drug loading, polymeric carriers, solid state, and intermolecular interactions that can also be applied to other drugs.

Lastly, the well-known technological challenge of controlling the release of a highly soluble drug was overcome through an innovative platform involving HME (Chapter IV). The selected prototype is not standard in the field and consists of microtablets tableted into tablets, where HME is coupled with double compression as downstream processing. Its performance was exhaustively characterized, and near zero-order kinetics for 6 to 8 hours observed on dissolution. The mechanistic drug release was explored through the Weibull function and SEM, and revealed a combination of swelling, diffusion, and erosion.

The research performed had several goals, but it is possible to stand out the overcome of formulation barriers, tailoring challenging drug properties through the use of the potentialities of HME. Also important is the contribution to an improved understanding of the complex solid-state characterization of solid dispersions, including physicochemical properties of drugs and formulated systems. However, further efforts and expertise are still required to achieve the purpose of this work. The research identified gaps, challenges, and future areas of study to, finally, take these products - better products - to market.

Keywords

Hot-melt extrusion, Solid Dispersions, Solubility enhancement, Bioavailability enhancement, Etravirine, Ibrutinib, Multivariate Statistics, Principal Components Analysis, Polymers, Extruder, Amorphous materials, Pharmaceutical Development, Quality by Design, Design Space, Critical Quality Attributes, Regulatory Evaluation.

Resumo

As dispersões sólidas são sistemas em que um determinado componente está disperso num veículo, e o sistema existe no estado sólido. A solubilidade, dissolução do fármaco, estabilidade física e química, e comportamento *in vivo* destas formulações varia consoante as características químicas dos componentes principais e a estrutura física da composição. As dispersões sólidas são consideradas um dos tipos de sistemas farmacêuticos mais complexo, e a caracterização profunda das suas propriedades é essencial para controlar e modular o comportamento do produto. O uso da extrusão a quente fez com que o paradigma da investigação e fabrico na indústria farmacêutica fosse completamente alterado no que concerne à preparação de dispersões sólidas. Esta tecnologia é reconhecidamente capaz de ultrapassar barreiras de formulação e modular a performance de fármacos, e tem sido utilizada com sucesso em produtos já comercializados e muitos outros em desenvolvimento. A utilização principal da extrusão a quente é a melhoria da solubilidade, mas pode ser também aplicada para mascarar o sabor, estabilizar fármacos amorfos ou para a libertação controlada de substâncias ativas.

Neste trabalho, a tecnologia de extrusão a quente foi aplicada em três contextos diferentes, nomeadamente, na melhoria de solubilidade de um fármaco pouco solúvel, na estabilização do estado físico de uma substância amorfa reconhecidamente instável, e na libertação controlada de um composto altamente solúvel e de baixa dosagem. Para isso, foi utilizada uma combinação de técnicas cromatográficas (cromatografia líquida de alta e ultra eficiência (HPLC e UPLC)), microscópicas (microscopia ótica, microscopia de luz polarizada (PLM), microscopia eletrónica de varrimento (SEM)), térmicas (calorimetria diferencial de varrimento convencional (DSC) e com modulação de temperatura (mDSC), análise termogravimétrica (TGA), e microscopia térmica com luz polarizada (PLTM)), difração (difração de raios X de pó (XRPD)), e espectroscópicas (espectroscopia Raman acoplada a microscopia confocal e combinada, em alguns casos, com variação de temperatura). Os ensaios de dissolução e estudos de estabilidade foram também críticos para a caracterização detalhada dos sistemas preparados. Os métodos de rastreio de alto rendimento, os cálculos termodinâmicos e a análise estatística foram também importantes para o sucesso da investigação.

Neste trabalho, foi apresentada uma metodologia sistemática passo-a-passo para o desenvolvimento de dispersões sólidas, onde se combinou a termodinâmica, as estratégias de

rastreio, a estatística multivariada e a otimização de processos (Capítulo I). O foco foi o desenvolvimento farmacêutico segundo os princípios de *Quality by Design* e abordagens práticas, desde os primeiros estudos de desenvolvimento até à aprovação regulamentar. As especificidades técnica e científica das formulações baseadas em extrusão a quente foram discutidas, em linha com o estado da arte do desenvolvimento de produtos farmacêuticos e atuais diretrizes regulamentares.

Posteriormente, foi preparada uma dispersão sólida amorfa (ASD) de Etravirina, para melhorar a solubilidade deste fármaco considerado pouco solúvel (Capítulo II). Foi feita uma investigação extensiva da capacidade de solubilização e estabilidade física de composições diferentes, onde se combinaram cálculos termodinâmicos, com o rastreio de alto rendimento e a análise de componentes principais. A taxa de dissolução foi melhorada mais de duas vezes, e a dispersão amorfa demonstrou ser física e quimicamente estável por, pelo menos, três meses, mesmo quando armazenada em condições aceleradas de envelhecimento. Este resultado foi explicado posteriormente através da espectroscopia Raman, onde foram observados sinais de interações intermoleculares nos grupos CN da Etravirina. Foi ainda demonstrado o alto potencial da espectroscopia Raman para distinguir diferentes estados sólidos, nomeadamente para diferenciar o estado amorfo do cristalino.

Na investigação aplicada ao Ibrutinib (Capítulo III), o alvo da análise foi distinto e a extrusão foi aplicada para melhorar a estabilidade física de um fármaco no estado amorfo. Apesar de apresentar uma tendência elevada para conversão para o estado cristalino mais estável, foi possível atingir seis meses de estabilidade em condições aceleradas através do uso da extrusão a quente, mesmo utilizando uma elevada quantidade de fármaco na formulação, 50%. A análise térmica e espectroscópica permitiu detetar interações intermoleculares na cetona α, β-insaturada do Ibrutinib, que justificam a resiliência física dos sistemas preparados. Esta aplicação da extrusão não é comum, mas permitiu estabelecer uma relação notável entre extrusão a quente, quantidade de fármaco, excipientes, estado físico e interações intermoleculares, que poderão ser aplicadas a outros compostos.

Por último, um conhecido desafio da tecnologia farmacêutica - a libertação de um fármaco muito solúvel em baixa dosagem - foi também ultrapassado, através da criação de uma plataforma tecnológica inovadora baseada na extrusão a quente (Capítulo IV). O protótipo selecionado não é considerado padrão na área, e consiste em microcomprimidos num comprimido, onde a extrusão é acoplada a jusante a uma dupla compressão. O comportamento deste sistema foi exaustivamente caracterizado, tendo-se observado, em dissolução, uma cinética próxima de ordem-zero durante 6

a 8 horas. O mecanismo de libertação foi também explorado através da função de Weibull e SEM, revelando a combinação de intumescimento, difusão e erosão.

A investigação realizada teve vários objetivos, destacando-se a transposição de barreiras de formulação, através da modulação de fármacos difíceis recorrendo às potencialidades da extrusão a quente. Não menos importante, contribuiu para uma melhor compreensão da caracterização complexa do estado sólido de dispersões sólidas, incluindo propriedades físico-químicas de fármacos e seus sistemas formulados. No entanto, ainda se verifica a necessidade de esforço e especialização adicionais, de modo que seja atingido o desígnio deste trabalho. Foi possível identificar lacunas, desafios e eventuais áreas de investigação futura para, finalmente, levar os produtos - melhores produtos - até ao mercado.

Palavras-chave

Extrusão a quente, Dispersões sólidas, Melhoria de solubilidade, Melhoria de biodisponibilidade, Etravirina, Ibrutinib, Estatística multivariada, Análise de componentes principais, Polímeros, Extrusora, Materiais amorfos, Desenvolvimento farmacêutico, *Quality by Design*, Espaço de desenvolvimento, Atributos de qualidade críticos, Avaliação regulamentar.

EXECUTIVE SUMMARY

The emerging trends in the high-throughput screening for drug discovery have led to new and very challenging new drugs, most of them with high molecular weight and low bioavailability. Pharmaceutical scientists and pharmaceutical industries, along with process, physical, mechanical, and chemical engineers, have worked in the last years in solutions, and novel drug delivery technologies emerged to allow the formulation and oral administration of these high potency compounds.

In this context, Hot-melt extrusion (HME) emerged as a novelty for product development and represents a promising technology to prepare solid dispersions. The enhancement of solubility and bioavailability through the manufacturing of amorphous solid dispersions (ASDs) is the primary use of HME, but it has also been applied for taste masking, preparation of shaped-systems, controlled drug delivery, and nanoparticles. Other applications not so common include, for instance, the stabilization of amorphous drugs.

Solid dispersions are complex solid systems where the drug is dispersed in a carrier. The drug may be molecularly dispersed or exist in crystalline or amorphous clusters distributed over the carrier. A comprehensive understanding of their properties is essential to control drug solubility, bioavailability, and even stability of the formulation. A full toolbox of characterization methods is currently available, where microscopic, thermal, spectroscopic, diffraction and computational methods may be applied to support the pharmaceutical development of this type of system.

HME has several benefits for implementation in the pharmaceutical industry, and its interest has been rising exponentially. It is a solvent-free, cost-effective, and continuous process, able to manufacture a variety of pharmaceutical forms in a consistent and reproducible manner. Therefore, the research work described in this thesis took place in a pharmaceutical industry context, where HME is currently regarded as a technology able to solve complex formulation issues, to optimize drug delivery, and tailor product performance.

HME was proposed as an answer in three different technical challenging issues, fully described and explored throughout this thesis. Due to the high technical skills and scientific specificities of solid dispersions, including regulatory, HME was applied to solve real formulation issues and complex drug delivery problems that required an advanced solution. The aims of this work, the structure of the thesis, and scientific publications are described in the following sections. The results clearly

demonstrate the potential of HME to solve solubility and physical stability issues, and to modulate the drug delivery.

This thesis was performed in a pharmaceutical company, Bluepharma. Most of the work was executed at the Product Development department, in the sub-group of the oral solid formulations. Our goals include pre-formulation studies, formulation and process development, optimization, scale-up, product manufacturing following the current Good Manufacturing Practices, and process validation. The work described in this thesis is populated with teamwork, where formulation and analytical scientists cooperate with medical and technical specialists, project and team managers, the board, and third-party organizations as clients or partners. Science and advanced technical skills are important for any effective product development, but people and cooperation are, in fact, the base of a successful project.

Aims

The main goal of this work was to overcome formulation barriers in the pharmaceutical development path, tailoring the behavior of the formulation through Hot-melt extrusion. Therefore, HME was applied in three different scopes, with three compounds with very different physicochemical properties. Detailing, HME was used to enhance the solubility of a poorly soluble compound (Etravirine), in the physical stabilization of an unstable amorphous drug (Ibrutinib), and in the controlled release of a highly soluble drug[1]. Specific aims of this work were:

1. To predict, understand and explore the possible carriers for HME application concerning different drugs;
2. To fully characterize different extrudates, through comparison of stability, thermal behavior, drug-polymer interaction, biopharmaceutical properties, and physical state;
3. To understand the relationship between the physical structure and stability, as well as understand the stabilization factors of an HME solid dispersion and determine the critical storage conditions that lead to a longer shelf-life;
4. To gain insights into the relationship between the physical structure and dissolution behavior (linking amorphicity to enhanced dissolution profile);
5. To understand and explore possible carriers for extended-release through HME technology and to explore alternative technological platforms to modify the drug release rate;
6. To correlate the drug release kinetics with the molecular mechanisms for the controlled release;
7. To assure consistency and robustness of the manufacturing process and analytical methods following Quality by Design guidelines, identifying Critical Process Parameters and characterizing formulation and manufacturing variables.

Overall, this project also aims to contribute to in-depth the knowledge on the complex solid-state of amorphous drugs and their systems prepared by HME, taking into account the assurance of quality, safety, and efficacy of the novel dosage forms.

[1] Compound not disclosed for confidentiality reasons.

Outline of the Thesis

This thesis is organized into five parts, as described below.

Chapter I – *Solid Dispersions and Hot-Melt Extrusion in the Pharmaceutical Industry: from bench to market* provides an overview of the issues investigated in the succeeding chapters. It aims to contextualize the reader with the theme, describes major aspects of HME technology and its application in pharmaceutical development. It discusses the concept of Quality by Design applied to HME, as well as regulatory specificities, challenges, and development strategies. Moreover, a systematic step-by-step approach for a fast and effective screening of promising formulations is presented, established to increase the success of HME-based drug product developments.

In Chapter II – *Five-Stage Approach for a Systematic Screening and Development of Etravirine Amorphous Solid Dispersions by Hot-melt Extrusion,* HME is applied in the solubility enhancement of a poorly-soluble drug, Etravirine. Moreover, it describes the successful application of the step-by-step approach presented in Chapter I in the systematic screening of promising systems for Etravirine. The drug release rate was improved more than two times, and the manufactured systems demonstrated to be physically and chemically stable.

In Chapter III – *Enhanced Solid-state Stability of Amorphous Ibrutinib Formulations Prepared by Hot-melt Extrusion*, HME was used as a technique able to improve the physical stability of a drug, stabilizing the amorphous form and avoiding the conversion into the most thermodynamically stable form. It described a systematic screening approach to identify polymeric compositions targeting high physical stability, and the physical strength of the prepared systems corroborated by stability studies until six months.

Chapter IV - *Novel technological platform for extended-release tablets by combining hot-melt extrusion and MUPS* describes the application of HME in the development of a drug delivery platform for the controlled-release of a highly soluble drug in a low drug load. The study was initiated by the systematic screening of release controlling polymers coupled with different downstream processing technologies. An uncommon technological platform was selected, based on Multi-Unit Particulate Systems. It demonstrated to have the intended release kinetics, which release mechanism was experimentally studied and characterized.

Chapter V – *Conclusion* presents the main conclusions and discusses future perspectives and ongoing work.

The results and achievements presented in this thesis led to the scientific publications described in the following section.

Scientific Publications and Conferences

International Peer-Reviewed Publications

1. Simões MF, Nogueira BA, Tabanez AM, Fausto R, Pinto RMA, Simões S. Enhanced solid-state stability of amorphous ibrutinib formulations prepared by hot-melt extrusion. Int J Pharm. 2020 Apr 15;579:119156. doi: 10.1016/j.ijpharm.2020.119156.

2. Simões MF, Pereira A, Cardoso S, Cadonau S, Werner K, Pinto RMA, Simões S. Five-Stage Approach for a Systematic Screening and Development of Etravirine Amorphous Solid Dispersions by Hot-Melt Extrusion. Mol Pharm. 2020 Feb 3;17(2):554-568. doi: 10.1021/acs.molpharmaceut.9b00996.

3. Simões MF, Pinto RMA, Simões S. Hot-melt extrusion in the pharmaceutical industry: toward filing a new drug application. Drug Discov Today. 2019 Sep;24(9):1749-1768. doi: 10.1016/j.drudis.2019.05.013.

4. Simões MF, Rocha-Gonçalves A, Pinto RMA, Simões S. Novel technological platform for extended-release tablets by combining hot-melt extrusion and MUPS. Submitted for publication.

5. Simões MF, Pinto RMA, Simões S. Hot-melt extrusion: a Roadmap for Product Development. Submitted for publication (under review).

Other Publications from the collaboration in other projects

1. Simões MF, Silva G, Pinto AC, Fonseca M, Silva NE, Pinto RMA, Simões S. Artificial Neural Networks applied to Quality-by-Design: from Formulation Development to Clinical Outcome. Eur J Pharm Biopharm. 2020 July; 152: 282 - 295. doi: 10.1016/j.ejpb.2020.05.012

Poster Communications

1. Simões MF, Silva G, Pinto RMA, Simões S. An innovative combination of technological platforms for a zero-order drug release kinetics: Hot-Melt Extrusion and Multi-Units Particulate systems for the oral delivery of a BCS class III drug. Poster *to be* presented at[2]: 12th World Meeting on Pharmaceutics, Biopharmaceutics and Pharmaceutical Technology; 2021; Vienna, Austria.

2. Simões MF, Pinto RMA, Simões S. HME-based amorphous solid dispersions to enhance the physical stability of an amorphous BCS class II drug. Poster presented at: Controlled Release Society Annual Meeting & Exposition; 2019 Jul 21-24; Valencia, Spain.

3. Simões MF, Silva G, Pinto RMA, Simões S. Combined approach for a Fast Forward Screening of Amorphous Solid Dispersions prepared by Hot-Melt Extrusion using a BCS class IV drug. Poster presented at: Controlled Release Society Annual Meeting & Exposition; 2018 Jul 22-24; New York, U.S.A.

4. Simões MF, Silva G, Pinto RMA, Simões S. Fast Forward Screening for Hot-Melt Extrusion: an effective tool for formulation development of poorly soluble drugs. Poster presented at: XII Spanish-Portuguese Conference on Controlled Drug Delivery; 2018 Jan 14-16; Coimbra, Portugal.

Other Poster Communications from the collaboration in other projects

1. Simões MF, Silva G, Pinto AC, Pinto RMA, Simões S. Application of Artificial Intelligence to Generic Drug Product Development: a Quality-by-Design case study. Poster *to be* presented at[3]: 12th World Meeting on Pharmaceutics, Biopharmaceutics and Pharmaceutical Technology; 2021; Vienna, Austria.

2. Simões MF, Silva G, Simões S. Multivariate Statistical Comparison of *In Vitro* Dissolution Profiles: getting away from f_2 statistics and Mahalanobis Distance. Poster presented at: Controlled Release Society Annual Meeting & Exposition; 2019 Jul 21-24; Valencia, Spain.

[2] The short paper was accepted for presentation in March 2020, but the conference was postponed to 2021.

[3] The short paper was accepted for presentation in March 2020, but the conference was postponed to 2021.

3. Simões MF, Monteiro M, Mota C, Silva G, Simões S. A Quality-by-Design study for an immediate-release tablet formulation of a BCS class IV drug: the critical impact of drug particle size on product quality attributes. Poster presented at: Controlled Release Society Annual Meeting & Exposition; 2018 Jul 22-24; New York, U.S.A.

Oral Communications

1. Simões MF. *Desenvolvimento Farmacêutico e escolha de formulações*. Lecture in the Investigational Medicinal Products and the Pharmacy of Clinical Studies module of the Training Programme in Pharmaceutical Medicine and Clinical Investigation, promoted by the Pharmaceutical Medicine Academy; 2020 Oct 2; online session, Portugal.
2. Simões MF. *Desenvolvimento Farmacêutico e escolha de formulações*. Lecture in the Investigational Medicinal Products and the Pharmacy of Clinical Studies module of the Training Programme in Pharmaceutical Medicine and Clinical Investigation, promoted by the Pharmaceutical Medicine Academy; 2018 Oct 19; Porto, Portugal.
3. Simões MF. Hot-Melt Extrusion through the Eye of the Pharmaceutical Industry. Presented at: Merck Seminar: Technology and Regulatory Trends in the Pharma Market; 2018 Sept 26; Lisbon, Portugal.

List of Figures

Chapter I

Chapter II

Chapter III

List of Tables

Chapter I

Chapter II

Chapter III

Chapter IV

List of Abbreviations and Symbols

AG	Adam-Gibbs
ANDA	Abbreviated New Drug Approval
ANN	Artificial Neural Network
ASD	Amorphous solid dispersions
BA	Bioavailability
BCS	Biopharmaceutical Classification System
BiTABS	Bilayer tablets
cGMP	current Good Manufacturing Practices
CMA	Critical Material Attribute
CPP	Critical Process Parameter
CQA	Critical Quality Attribute
CTD	Common Technical Document
DC	Direct Compression
DDS	Drug Delivery Systems
DMF	N,N-dimethylformamide
DoE	Design of Experiments
DS	Drug substance
DSC	Differential Scanning Calorimetry
EC	Ethylcellulose
EMA	European Medicines Agency
ETR	Etravirine
EU	Europe
FDA	Food and Drug Administration US
FMEA	Failure Mode and Effects Analysis
HDPE	High-density polyethylene
HME	Hot-Melt Extrusion
HPC	Hydroxypropyl cellulose
HPLC	High Performance Liquid Chromatography

HPMC	Hydroxypropyl Methylcellulose (hypromellose)
HPMCAS	Hypromellose Acetate Succinate
HSM	Hot Stage Microscopy
HTS	High-throughput screening
IBR	Ibrutinib
ICH	International Council for Harmonisation
IPC	In-process control
IVIVC	*In vitro - in vivo* correlation
KWW	Kohlrausch-Williams-Watts
MAD	Mean absolute difference
MCC	Microcrystalline cellulose
mDSC	Modulated Temperature Differential Scanning Calorimetry
MLP	Multi-layer perceptron
MLR	Multiple linear regression
MPD	Melting point depression
MUPS	Multi-unit particulate system
MW	Molecular weight
NMR	Nuclear Magnetic Resonance
NNRTI	Nonnucleoside reverse transcriptase inhibitor
P407	Poloxamer grade 407 micro
PAR	Proven Acceptable Ranges
PATs	Process Analytical Technologies
PBPK	Physiologically Based Pharmacokinetic
PCA	Principal Components Analysis
PEG	Polyethylene glycol
PK	Pharmacokinetic
PLM	Polarized Light Microscopy
PLTM	Polarized Light Thermal Microscopy
PVAc	Polyvinyl acetate
PVOH	Polyvinyl alcohol
PVP	Poly(vinylpyrrolidone) (povidone)
PVPVA	Poly(vinyl pyrrolidone-vinyl acetate) copolymer (copovidone)
QbD	Quality by Design
QTPP	Quality Target Product Profile

REM	Risk Estimation Matrix
RH	Relative Humidity
RMSE	Root mean squared error
SDS	Sodium dodecyl sulfate
SEM	Scanning Electron Microscopy
SLP	Soluplus
SSE	Sum of squared errors
T_g	Glass transition temperature
TGA	Thermogravimetric analysis
THF	Tetrahydrofuran
T_m	Melting temperature
UPLC	Ultra Performance Liquid Chromatography
US	United States of America
USP	United States Pharmacopeia
XR	Extended-release
XRPD	X-Ray Powder Diffraction
Δ	Difference between two variables, or one variable in two different states
δ	Hansen solubility parameters
ρ	Density
χ	Flory-Huggins interaction parameter

CHAPTER I. SOLID DISPERSIONS AND HOT-MELT EXTRUSION IN THE PHARMACEUTICAL INDUSTRY: FROM BENCH TO MARKET

Abstract

Hot-Melt Extrusion has found widespread application as a viable pharmaceutical technological option over recent years. HME applications include solubility enhancement, taste masking, and sustained drug release. As bioavailability enhancement is a hot topic of today's science, one of the most important applications of HME is centered on solid dispersions. This review describes major aspects of HME technology and its application on the preparation of solid dispersions. It also addresses critical molecular and thermodynamic aspects governing the physicochemical properties of these systems, mainly in what concerns miscibility and physical stability. A systematic step-by-step approach is presented, where thermodynamics, polymers screening, multivariate statistics, and process optimization are combined, to increase the success of HME-based drug product development. The Quality by Design concept is introduced and applied to HME, and steps and tools for its effective implementation provided, including a risk assessment highlighting critical points. The technical and scientific specificity of HME-based solid dispersions are discussed in light of the current paradigm of drug development, and in line with regulatory guidelines from the ICH regions.

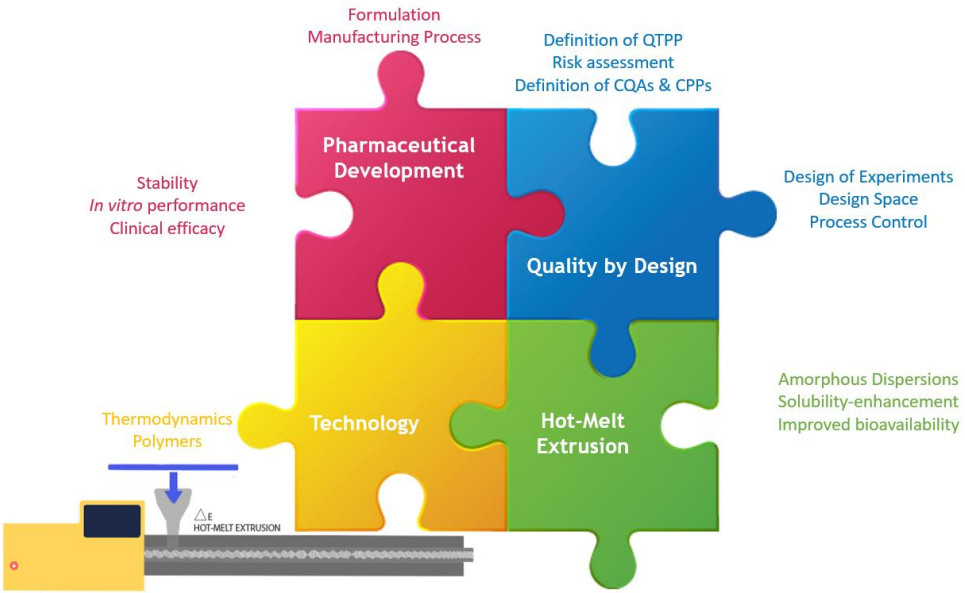

Figure 1.1. Graphical abstract of chapter I. Correlation between pharmaceutical development under Quality by Design principles and the HME technology.

The literature review presented in this chapter was published in Simões MF, Pinto RMA, Simões S. Hot-melt extrusion in the pharmaceutical industry: toward filing a new drug application. Drug Discov Today. 2019 Sep;24(9):1749-1768. doi: 10.1016/j.drudis.2019.05.013; and Simões MF, Pinto RMA, Simões S. Hot-Melt Extrusion: A Roadmap for Product Development. Submited for publication (under review).

This chapter is not an integral copy of the published work.

1. Introduction

Hot-melt extrusion (HME) has been revealed as a successful technology for a large spectrum of applications in the pharmaceutical industry, with proven robustness for numerous drug delivery systems (DDS) [1, 2]. Some of the most well-known applications are for taste masking of drugs [3-5], solubility enhancement of poorly water-soluble compounds [6-10], controlled [11-13], extended [14], sustained [15, 16], and targeted drug delivery [17-21], and also preparation of nanoparticles [22-24].

The versatility of HME for the development and manufacturing of very different DDS (Figure 1.2) has made it a technology that shifted the entire paradigm of pharmaceutical industry research and manufacturing. The enhancement of solubility and bioavailability (BA) through the manufacturing of amorphous solid dispersions (ASDs) is the primary use of HME [25, 26], as indicated by the multiple papers and patents. Indeed, ASDs have been proven effective in optimizing the solubility of poorly soluble materials [25, 26]. Therefore, significant effort has been devoted to understanding solid dispersions lately, in various aspects, such as manufacturing processes, polymeric carriers' applications, and the physical properties of prepared systems. Considered complex formulations, a complete understanding of the physical structure and chemical properties is essential to predict solubility, BA, and even stability of the solid dispersion.

This is more and more important as in the last three decades, the high-throughput screening (HTS) methodology created many new drug candidates with low aqueous solubility, classified as II or IV by the Biopharmaceutical Classification Systems (BCS) [27]. The low aqueous solubility of these molecules is typically the bottleneck for absorption, which leads to the low BA and justifying their failure as therapeutic agents. Diverse approaches have been employed to overcome solubility barriers, such as reducing particle size, ASDs, lipid-based strategies, surfactants, and cyclodextrins, among others [25, 26].

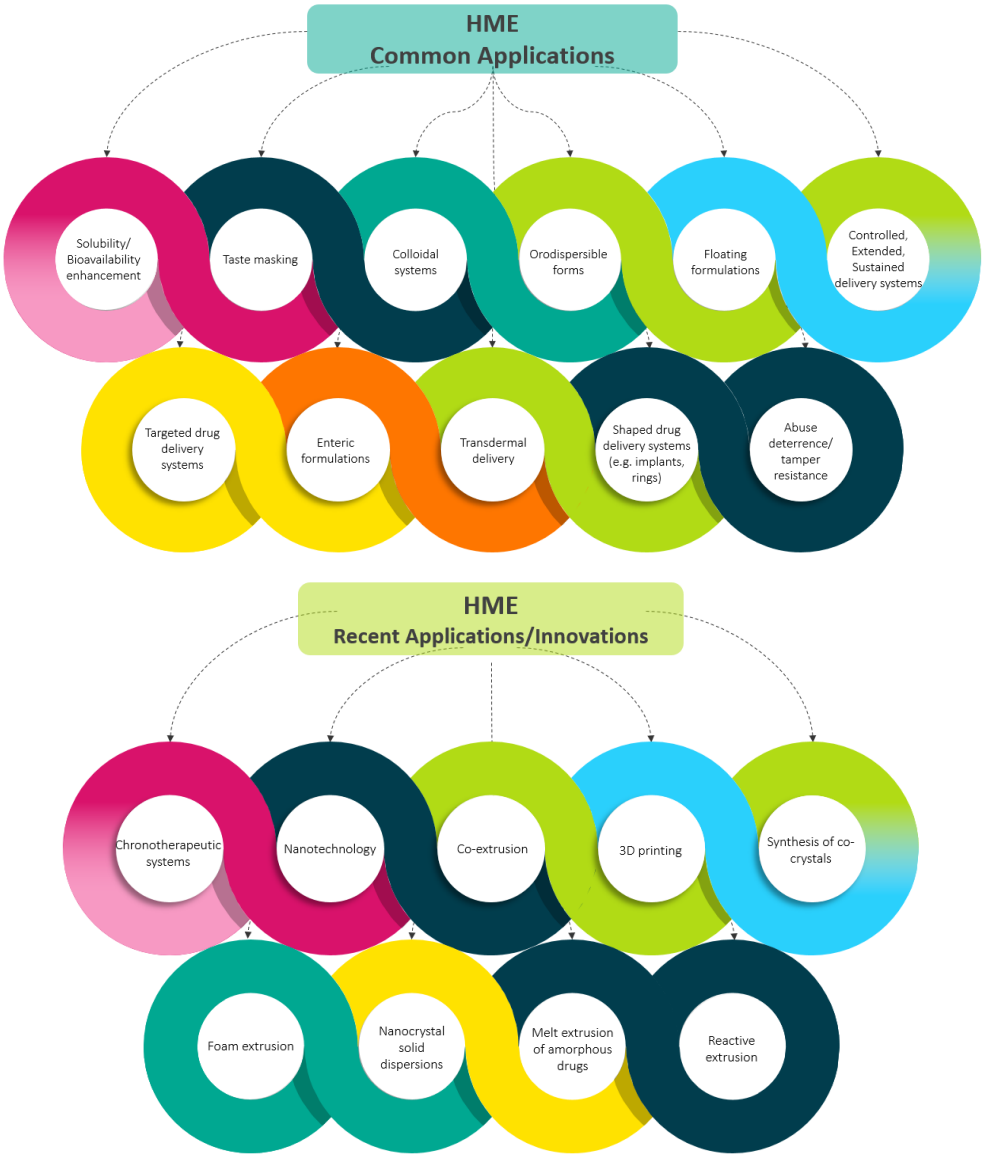

Figure 1.2. Common and recent applications of HME technology [28-31].

Solid dispersions are systems where one component is dispersed in a carrier, and where the whole system appears to be solid [32-37]. A drug can remain molecularly dispersed within the polymer or exists in a crystalline or amorphous phase, and the solubility characteristics of these types of solid dispersions differ [38, 39]. Therefore, ASDs are the outcome of the kinetic entrapment of the amorphous active compound, where it is molecularly solubilized in the carrier. These systems have an improved dissolution rate, but they also tend to revert to the more stable thermodynamic form, the crystalline [39]. Indeed, this is the primary concern of ASD, which leads to phase separation and recrystallization and can eventually affect product performance on dissolution [32-37]. This phenomenon leads to the failure of the entire formulation strategy of using ASDs to improve BA

and justify, at least partially, why there are only a few ASD-based formulations in the market [36, 40].

Besides HME, preparation techniques of ASDs include spray drying, freeze-drying, and supercritical fluid drying (Table 1.1). HME found its place in the pharmaceutical area, and many researchers embraced this technique due to its promising performances [1, 29]. The extruder applies energy through shear and temperature to the drug and the thermoplastic excipients. The energy produced by the combination of temperature and friction can overpass the crystal lattice energy and turn the polymer molten. During extrusion, the material is simultaneously mixed and dispersed.

Table 1.1. Comparison of HME to other technologies for the manufacture of ASD. Adapted from [39].

Manufacturing process	Advantages	Disadvantages
Hot-melt extrusion	Strict control of temperature; Continuous process and solvent-free; Customizable and modular; Easy scale-up even for large scale.	Use of high temperatures; Blend requires thermoplastic behavior; Physical instability over time; High energy consumption.
Spray drying	Applies mild temperatures; Robust and scalable preparation process; Possible to manufacture on a large scale.	Use of organic solvents, with concerns on toxicology, safety during processing, and residual solvent content; Costly manufacturing process.
Freeze drying	Low temperatures adequate for thermolabile products; Robust process; Large-scale production is standardized.	Costly, slow, and high-energy process; Stability concerns highly dependent on the moisture content.
Supercritical fluid processing	Rapid process with high yield; Uses carbon dioxide, which is safe and not expensive; Application in highly susceptible drugs to hydrolysis.	Technical hurdles for practical implementation due to clogged nozzles and congealing; Application depends on formulation solubility in supercritical carbon dioxide; Not widespread.

Comparing to other manufacturing processes for ASD, HME presents unique characteristics that justify the high interest of formulation scientists and pharmaceutical companies over the world. It allows continuous manufacturing, it is solvent-free, relatively fast, and requires a narrow footprint. Nonetheless, the high process temperatures, the requirement for downstream processing, and the large energy consumption are significant drawbacks. Besides, there are not many excipients with thermoplastic properties approved for pharmaceutical applications, and the metastable nature of the final drug product is always challenging. In the daily routine of laboratories and factories, some

technical difficulties still exist, and the full potential of HME is yet to be met, like any breakthrough innovation [2].

This work intends to drive the formulation scientist into the HME technology with a focus on the pharmaceutical industry, in order to develop and submit new products to regulatory authorities. A systematic step-by-step approach for the development of HME products is presented. As a core in product development, the Quality by Design (QbD) paradigm applied to HME is discussed, including steps and tools for its implementation and a risk assessment that can be followed to support dossier filing. The focus is primarily on frequently ignored topics, as useful and practical approaches, rather than heavy and unfeasible ones in the routine of product development, from early development to regulatory approval. Moreover, possible questions from dossier reviewers are listed and reflect technical and scientific specificities of this type of formulations. Finally, the latest approvals are analyzed as case studies within the QbD paradigm.

2. Overview of HME-based marketed drug products

At the end of the eighteenth century, HME was invented and applied in the manufacturing of lead pipes. It has been used in other industries since then, like plastic, rubber, and food. The technology was also found useful in the pharmaceutical industry [1, 2, 29], and the interest is rising exponentially with over 500 papers published during the last 10 years. HME is now employed to produce different DDS, such as for oral administration (granules [41-43], pellets [44, 45], films [46, 47] and tablets [48, 49]), but also transdermal [50, 51], transmucosal [52, 53] and subcutaneous (implants [54-57]). Although there is a huge potential for formulating poorly soluble drugs into ASDs, few have been commercialized so far (Table 1.2). Nonetheless, this trend is clearly changing as more and more HME-based drug products appear in the pipeline of many pharmaceutical companies.

Companies are now specialized in HME, including SOLIQS (Germany) and PharmaForm (USA). SOLIQS has developed Meltrex® formulation and redeveloped Kaletra® from Abbot. Kaletra® (lopinavir/ritonavir) is a well-known example of a formulation that represents the impact of HME in product performance. In addition to the BA enhancement, the redeveloped HME product brought significant benefits for patients with a reduced dosage, frequency of administrations, and improved stability at room temperature [39]) and this was recognized by the Food and Drug Administration US (FDA) through a fast-track approval [2]. Similarly, PharmaForm, a service provider for HME R&D, has published more than 40 peer-reviewed publications on the topic and has developed a significant intellectual property. One of the technologies, known as PharmaForm Abuse-Deterrent Technology (PADT), has been specially designed to prevent drug abuse focusing on opioids. HME is generally a sought solution for abuse-deterrence as the solid forms are not crushable or chewable [2].

Table 1.2. Currently marketed HME products [27, 30, 39, 40, 58-64].

Pharmaceutical form	Commercial name	Owner	Drug(s)	Therapeutic Indication	Polymer	HME purpose
Ophthalmic insert	Lacrisert®	Merck	-	Dry eye syndrome	HPC	Shaped (rod) system
	Ozurdex®	Allergan	Dexamethasone implantable device	Macular edema	PLGA	Shaped System
Implants	Zoladex®	AstraZeneca	Goserelin	LHRH agonist	PLGA	Shaped (rod) system
	Depot-Profact®	Sanofi Aventis	Buserelin	Carcinoma of the prostate gland	PLGA	Shaped (rod) system
	Probuphine® *(2016, US)*	Titan [a]	Buprenorphine	Opioid dependence	EVA	Shaped (rod) system
Devices	Implanon®	Schering-Plough	Etonogestrel	Contraceptive	EVA	Shaped (rod) system
	NuvaRing®	NV Organon	Etonogestrel /ethinylestradiol	Contraceptive	EVA	Shaped (ring) system
	Annovera® *(2018, US)*	Therapeutics MD	Ethinylestradiol/ segesterone acetate	Contraceptive	Silicone	Shaped (ring) and multilayer system
Oral	Kaletra®	Abbott	Lopinavir/Ritonavir	HIV	PVPVA	Amorphous dispersion
	Isoptin® SRE	Abbott	Verapamil	Hypertension	HPC/HPMC	Shaped system (oval)
	Covera-HS®	Pfizer	Verapamil HCl	Hypertension and angina pectoris	HPC	Melt granulation
	Nurofen Meltlets lemon®	Reckitt Benckiser Healthcare	Ibuprofen	Analgesic	HPMC	Melt granulation
	Norvir®	Abbott	Ritonavir	HIV	PEG-glyceride	Amorphous dispersion
	Gris-PEG®	Penidol Ph.	Griseofulvin	Onychomycosis	PEG	Crystalline dispersion

Pharmaceutical form	Commercial name	Owner	Drug(s)	Therapeutic Indication	Polymer	HME purpose
	Rezulin®	Parke-Davis	Troglitazone	Diabetes	PVP	Amorphous dispersion
	Cesamet®	Meda Pharmaceuticals	Nabilone	Antiemetic drug	PVP	Solid dispersion
	Adalat SL®	Bayer	Nifedipine	Antianginal agent	HPMC/PEO	Controlled release
	Eucreas®	Novartis	Vildagliptin/Metformin HCl	Diabetes type 2	HPC	Melt granulation
	Zythromax®	Pfizer	Azithromycin enteric-coated multiparticulates	Antibiotic	Pregelatinized starch	Melt granulation
	Fenoglide®	Life cycle Pharma	Fenofibrate	Dyslipidaemia	PEG 6000	Solid dispersion
	Noxafil®	Merck	Posaconazole	Antifungal	HPMCAS	Amorphous dispersion
	Onmel®	Merz	Itraconazole	Onychomycosis	HPMC	Amorphous dispersion
	Palladone®	Purdue Pharma	Hydromorphone HCl	Pain relief	HPMC/Ethylcellulose[b]	Controlled release
	Nucynta®	Janssen	Tapentadol	Pain relief	PEO/HPMC/PEG	Controlled release and abuse-deterrent
	Opana ER®	Endo Pharmaceuticals	Oxymorphone HCl	Pain relief	PEO/HPMC/PEG [b]	Controlled release
	Belsomra® *(2014, US)*	Merck	Suvorexant	Insomnia	PVPVA	Amorphous dispersion
	Viekirax® *(2014, EU)*/ Technivie® *(2015, US)*	AbbVie	Ombitasvir, paritaprevir, and ritonavir	Hepatitis C virus	PVPVA/Vitamin E polyethylene glycol succinate	Amorphous dispersion (3 separate ASDs)
	Viekira pak® *(2014, US)*	AbbVie	Ombitasvir, paritaprevir, ritonavir, and dasabuvir	Hepatitis C virus	PVPVA	Amorphous dispersion (3 separate ASDs of ombitasvir, paritaprevir, and ritonavir)

Pharmaceutical form	Commercial name	Owner	Drug(s)	Therapeutic Indication	Polymer	HME purpose
	Venclyxto® *(2016, EU)* Venclexta® *(2016, US)*	AbbVie	Venetoclax	Chronic lymphocytic leukemia	PVPVA/Polysorbate 80/Colloidal Silicon Dioxide	Amorphous dispersion
	Maviret® *(2017, EU)* Mavyret *(2017, US)*	AbbVie	Glecaprevir/Pibrentasvir	Hepatitis C virus	PVPVA/Vitamin E polyethylene glycol succinate	Amorphous dispersion

[a]Two additional discreet arm implants are under development by Titan Pharmaceuticals (preclinical phase): ropinirole for the treatment of Parkison's disease and T_3 hormone for hypothyroidism through ProNeura™ drug delivery platform.

[b]Polymers present in the formulation of the drug product likely used for the preparation of the extrudate.

Abbreviations: EU, Europe; US, United States of America; HPC, Hydroxypropyl cellulose; PLGA, Poly(lactic-co-glycolic acid); EVA, Ethylene-vinyl acetate; PVP, Polyvinylpyrrolidone; PVPVA, copovidone; HPMC, Hydroxypropyl methylcellulose; PEG, Polyethylene glycol; PEO, Polyethylene oxide; HPMCAS, Hydroxypropyl methylcellulose acetate succinate.

Lately, there have been new product submissions both to the FDA and to the European Medicines Agency (EMA). In 2016, a new implant for the treatment of opioid dependence, containing buprenorphine, was approved by the FDA. Probuphine® is a 6-month treatment for opioid dependence, the first to be approved, and the only one so far. It consists of 4 subcutaneous implants of 26 mm each, placed in the underside of the upper arm, which provides a continuous and steady release of low-dose buprenorphine [65]. In October 2018, FDA also approved Annovera® (segesterone acetate and ethinyl estradiol vaginal system), a combined hormonal contraceptive that marked the first time a vaginal ring that can be re-used for one year [66].

In what concerns oral dosage forms, novel products have also been approved. Belsomra® (suvorexant), an orexin receptor antagonist, and the first of its class, was approved in 2014 by FDA [67]. It is an ASD prepared by HME to maximize BA. The team has selected to extrude the compound with a pH-independent solubility polymer, copovidone (PVPVA) [68], and observed that the hardness of the tablets was related to disintegration, dissolution, and absorption [28]. Viekirax® (Europe, EU)/Technivie® (United States of America, US), approved in 2014 by EMA and in 2015 by FDA, is also a very interesting product from the technical point of view as all three drugs are individually converted into amorphous materials by HME to enhance their BA. Only then the individual extrudates are combined, tableted, and coated [64]. Venetoclax, approved as Venclyxto® in the EU and as Venclexta® in the US for the treatment of chronic lymphocytic leukemia, is also manufactured by HME as a solid dispersion due to the very poor water solubility [69]. Mixtures of drug and PVPVA with surfactants (Aerosil and Tween) were extruded to enhance its absorption, and the formulation was then patented [70], demonstrating improved BA when manufactured by HME. More recently, both EMA and FDA approved Maviret® (EU) / Mavyret® (US) for the treatment of chronic hepatitis C. Both drugs, glecaprevir and pibrentasvir, are poorly water-soluble and they are also individually formulated as ASDs to increase the apparent aqueous solubility and obtain adequate *in vivo* absorption [71].

To our knowledge, there are already two ophthalmic inserts, four implants, and two vaginal rings approved so far, and many more are under development. However, the focus is still in the oral administration, where HME is mostly applied to manufacture ASDs, and the aim is to overcome the poor solubility and to promote absorption *in vivo*. Lessons learned from the last approvals are that simple formulations can be used and manufactured by HME to solve several formulation and delivery issues. This is sometimes the only chance that challenging drugs have to be taken to patients, with the desired delivery, the adequate dose, and a suitable safety profile.

3. An Elementary Roadmap for HME Product Development

3.1. Principles of HME

In HME, the components are transformed by heat and mechanical stress into a new material of constant shape and density [26, 37]. This process involves compacting, blending, and dispersing a mixture of excipients and drug substance (DS) by two rotating screws through the heated barrel [72]. At the end of the barrel, there is a die, dictating the shape of the extruded system [2]. The theory behind HME technology (Figure 1.3) can be summarized step-by-step as follows [2, 37, 39]: feeding through a hopper, mixing and kneading, flowing, venting, extrusion from the die, and downstream processing.

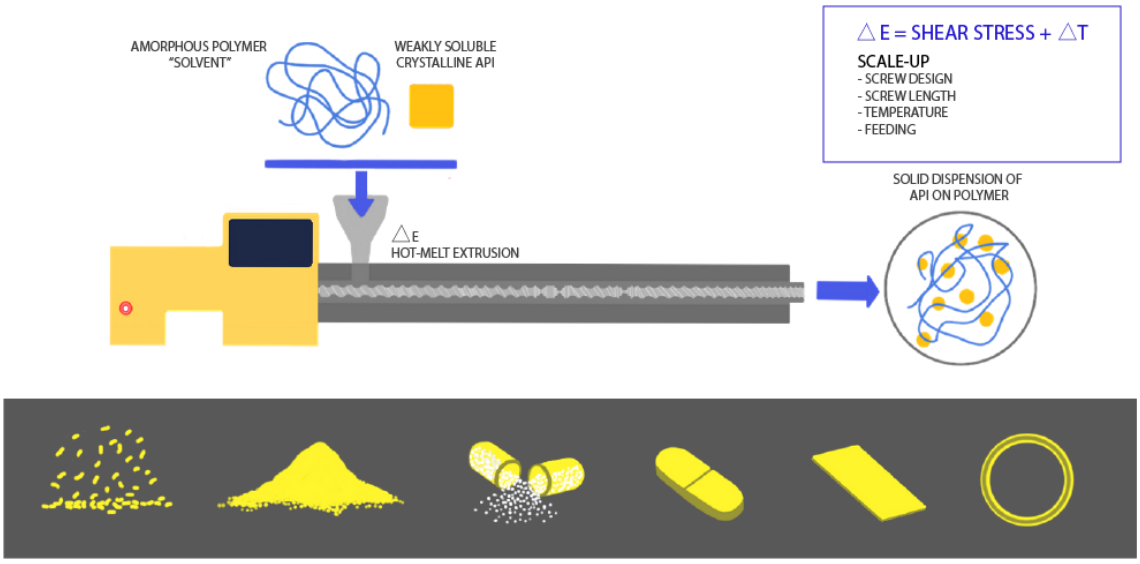

Figure 1.3. HME as an efficient processing method for solid dispersions and possible obtainable pharmaceutical forms: flakes, powder, pellets, tablets, films, and two-layered forms through co-extrusion.

HME works under high temperatures to soften the blend, and the different barrel sections are demarcated with specific temperatures [40]. After feeding, the material is conveyed by the rotating screws while it is melted, mixed, suffers kneading and dispersion. Mixing is a crucial step during HME and may be classified as distributive or dispersive. Distributive mixing is related to drug

homogeneity within the blend, whereas dispersive mixing means particle size reduction and molecular distribution [37]. Overall, HME aims to produce an intimately blended end product, the extrudate, where all the materials are mixed to the molecular level. Twin-screw extrusion offers several benefits over single-screw and is preferred in pharmaceutical processes. It provides an intense mixing of the components (high kneading and dispersing capability), easier feeding, a lower potential to overheat, and shorter residence time [29, 72].

Over the past 20 years, extruders' manufacturers worked in meeting the particular requirements of the pharmaceutical industry. The core unit and principles are similar to extruders used for plastics, but the main requirement is to follow the current Good Manufacturing Practices (cGMP). Individual parts of the extruder must be built from a special type of stainless steel to avoid reactions or adsorption with the formulation. There are also FDA approved lubricating oils that should be used, as well as water-cooled tubing [37, 72]. This technology is still under implementation in the pharmaceutical industry, specifically in adjusting documentation on cleaning, specifications, and validations [37].

3.2. Polymers in HME

The carrier is usually made from meltable substances, either polymeric (more common) or non-polymeric (like lipids). After the HME process, they function as drug depots or release retardants [29, 37]. Essential prerequisites are their thermal stability and thermoplastic behavior. Nonetheless, due to the usually short residence time, most thermolabile drugs are not excluded from HME processing [73]. Polymeric carriers must be thermoplastic and thermally stable. Other relevant characteristics include suitable glass transition temperature (T_g) or melting point (T_m) (usually in the range of 50 to 180°C), low hygroscopicity, and low toxicity since large amounts are required. The preferred carriers are the ones with high miscibility with the compound because a higher drug load may be achieved. Characteristics like lipophilicity and hydrogen bonding groups are also requisites for high solubilization [74]. Polymeric materials can be biodegradable or non-biodegradable, from natural or synthetic sources.

Natural polymers are valuable sources for pharmaceutical and biomedical applications. However, their degradation is usually based on enzymes at a hardly predictable rate. Moreover, they can cause immunological side effects due to their inherent biological activity [40]. Table 1.3 summarizes the characteristics of the most common natural polymers tested in HME processes.

Table 1.3. Examples of natural polymers and derivatives applied in HME.

Natural polymers	Characteristics	Processing temperatures	Comments	Ref.
Cellulose derivatives				
Hydroxypropyl cellulose (HPC) 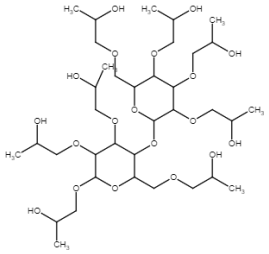	Non-ionic, water-soluble, pH independent dissolution. Hydrogen bond-donors ideal to stabilize amorphous drugs with H-bond acceptors.	Depends on its MW. Range from 120 to 200°C.	Cellulose derivatives are used instead of cellulose to improve its properties, namely poor water solubility and thermoplastic characteristics. Excellent biocompatibility.	[75-77]
Hydroxypropyl methylcellulose (HPMC) 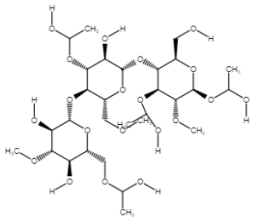	Non-ionic, water-soluble. Variety of grades depending on MW and hydroxypropyl and methyl substitution. Hydrogen bond-donors ideal to stabilize amorphous drugs with H-bond acceptors.	Depends on its MW. T_g varies from 139 to 173°C.	The release of drugs is tailored by changing its MW.	[76, 77]
Hypromellose acetate succinate (HPMCAS) 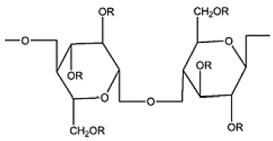 R = H, CH_3, $CH_2CH(OH)CH_3$, $COCH_3$, $COCH_2CH_2COOH$, $CH_2CH(CH_3)OCOCH3$, $CH_2CH(CH_3)OCOCH_2CH_2COOH$	Different grades depending on the extent of substitution of acetyl and succinoyl groups.	T_g varies from 120 to 135°C, depending on the grade. It degrades at 200°C.	Solubility is pH-dependent. Potentially incompatible with drugs with hydroxyl groups [78].	[79, 80]
Others				
Starch 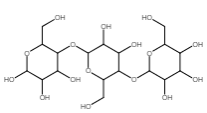 Amylose 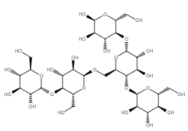 Amylopectin	Constituted by amylose and amylopectin.	-	-	[46, 81]

Natural polymers	Characteristics	Processing temperatures	Comments	Ref.
Chitosan 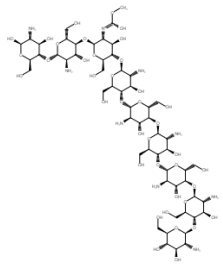	Linear hydrophilic polysaccharide. Used as a carrier and as a solubility enhancer.	T_g at 203°C.	Biocompatible, biodegradable, non-toxic. High MW chitosans may be applied as release retardants and low MW as release enhancers.	[82]
Xanthan gum 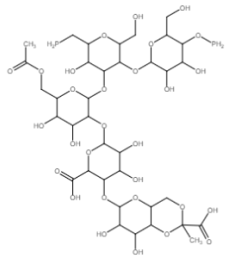	Heteropolysaccharide consisting of glucuronic acid, mannose, and β-D-Glucose.	-	Controlled-release applications.	[82, 83]

Abbreviations: MW, Molecular weight.

Synthetic polymers were developed to modulate physicochemical properties, which will ultimately control the products' performance. The necessity for using biodegradable excipients was identified by advancements in tissue engineering, gene therapy, and controlled release of drugs [40]. The goal of these materials is to perform a predetermined task, as drug release, through their slow degradation. Therefore, biodegradable polymers should be biocompatible (free of endotoxins, non-toxic, carcinogenic, immunogenic, or inflammatory) and have adequate mechanical, physicochemical, and thermal behavior. Moreover, if required by the dosage form, they should present resistance to sterilization methods and suitable degradation kinetics [40]. Table 1.4 summarizes the characteristics and uses of the most common synthetic biodegradable polymers. Processing temperatures are not mentioned as they depend heavily on the structure of the specific polymer.

Table 1.4. Examples of synthetic biodegradable polymers applied in HME.

Chemical family	E.g.	Characteristics	Polymer Degradation/ Drug release	Comments	Ref.
Aliphatic polyesters 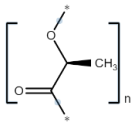 Poly(lactic acid) 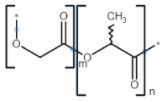 Poly(lactide-co-glycolide)	*Polymers* Poly(lactic acid): PLA Poly(glycolic acid) Poly(ε-caprolactone) *Copolymers* Poly(lactic-co-glycolic acid): PLGA ε-caprolactone and L, D-lactide or glycolide	It can be developed from various monomers and synthetic routes, resulting in polymers of variable MW and degradation kinetics. The main degradation pathway is the chain cleavage by hydrolysis.	Degradation mainly by bulk erosion, usually non-linear or discontinuous (drug release is difficult to predict). During degradation, an acidic environment may be formed.	The most extensively investigated synthetic polymers. The chemical stability of the drug may be affected.	[56, 84, 85]
Poly (orthoesters): POE's 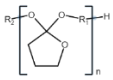 POE I 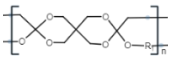 POE II 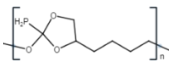 POE III  POE IV	Four different families: POE I – IV.	Highly hydrophobic. Degradation by hydrolysis of the polymer main chain. It forms carboxylic acid-based fragments. An acidic environment may be formed.	The hydrophobic polymer erosion occurs at the surface. Minor bulk erosion also occurs.	The water concentration in the bulk is lower than in aliphatic polyesters.	[86, 87]
Polyurethanes (PU's) 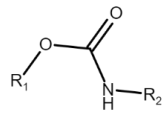 General chemical formula of PU's	Poly(ester urethanes)	Multiblock copolymers formed by a reaction between polyols (polyethers or polyesters) and di-isocyanate. Composed of soft and hard segments aimed at controlling thermoplastic and elastic behavior. Good	Most types are considered non-biodegradable due to the long-time required for degradation, but there are biodegradable PU. PU's are known as susceptible to hydrolysis (aliphatic ester linkage). They may present bulk or surface degradation	Non-biodegradable. PU's are not usually applied for drug release. PUs may also suffer mechanical degradation in highly stressed areas.	[88-90]

Chemical family	E.g.	Characteristics	Polymer Degradation/ Drug release	Comments	Ref.
		biological performances, mechanical properties, and processability.	depending on their hydrophilicity.		
Polyanhydrides 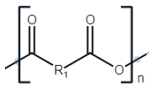 General chemical formula of polyanhydrides	-	Copolymers of dimers of sebacic and erucic acids.	Hydrophobic in nature. Degradation of the backbone by hydrolysis occurs mainly on the surface. Degradation initiates with water uptake, hydrolysis at the surface, and finally water penetration and slow erosion of the matrix.	These polymers were specially designed for drug delivery within a specific time.	[40, 91, 92]

Abbreviations: MW, Molecular weight.

Non-biodegradable polymers have been applied in very different systems, from oral formulations to transdermal films, implants, and scaffolds for tissue engineering. Physicochemical properties (as aqueous solubility, viscosity, or T_m/T_g) command the choice of a specific polymer. Table 1.5 presents an overview of the most common synthetic non-biodegradable polymers with applications reported in HME processes.

Table 1.5. Examples of synthetic non-biodegradable polymers applied in HME.

Chemical family	E.g.	Characteristics	Comments	Ref.
Polyvinyl lactam polymers 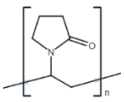 Poly (vinylpyrrolidone) 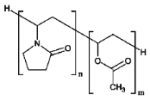 Copovidone	Poly(vinylpyrrolidone): PVP Copovidone Soluplus® (SLP)	Highly soluble in water. - PVP: Synthesized by polymerization of N-vinylpyrrolidone. Different grades vary in degree of polymerization, expressed as *K* values. Wide range of MW (2500-1 250 000 Da), which impacts T_g (from 72-177°C). The backbone contains proton acceptors, which can interact with H-donor groups for enhanced physical stability. High	Used as binders or solubility-enhancers.	[93-96]

Chemical family	E.g.	Characteristics	Comments	Ref.
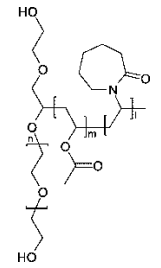 Soluplus®		MW grades (above K25) are very viscous and cannot be processed below their degradation temperatures. - Copovidone: block copolymer of vinylpyrrolidone and vinyl acetate in a 3:2 ratio. Available in one grade with *K* of 28. MW around 55 000 Da and T_g of 101°C. Lower T_g and hygroscopicity compared to PVP, being preferred for stability and smooth processing. - SLP: Polyvinyl caprolactam-polyvinyl acetate-polyethylene glycol graft copolymer. MW of 118 000Da and low T_g (70°C).		
Ethylene co-vinyl acetate (EVA) 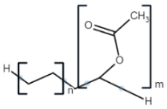	-	The water-insoluble copolymer of ethylene and vinyl acetate. It is possible to adjust the hydrophobicity of this polymer by changing the ethylene: vinyl acetate ratio, tailoring the release kinetics.	Widely used in sustained-release tablets and intra-vaginal rings.	[97, 98]
Acrylic polymers (poly (acrylic acid)) 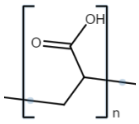	Polyacrylic acid (Carbomer or Carbopol®) Copolymers from esters of acrylic and methacrylic acid (Eudragit®)	Water-soluble polymers. T_g varies from 40°C to 160°C, depending on its MW and branching.	Due to the anionic nature, the drug release may be pH-dependent.	[99, 100]
Poly(ethylene glycol) (PEG), Poly(ethylene oxide) (PEO) and their copolymers 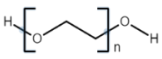 PEG 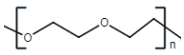 PEO	-	Repeating unit: -[CH_2CH_2O]- The difference between PEG and PEO is the number of hydroxyl groups at the end of the polymer chain, where PEG has two, and PEO has only one. PEO may be synthesized with up to 5 000 000 Da and PEG up to 40 000 Da. High aqueous solubility and low viscosity. PEG: T_g of -17°C for MW 6000; T_m of 37-63°C. PEO: T_g of -57 to -50°C; T_m of 62-67°C.	Used as solubility-enhancers for polymeric aliphatic polyesters. Used as solubility-enhancers or plasticizers in formulations.	[101-103]

Abbreviations: MW, Molecular weight.

3.3. Formulation development

The majority of excipients used in HME products are also applied for common solid forms. They may be matrix carriers, bulking agents, release modifying agents, thermal lubricants, antioxidants, or others. The selection of the excipients conveys specific characteristics to the HME-based formulation [29]. One of the specificities of this type of formulations is the relatively high amount of polymers, sometimes higher than the approved quantities in the Inactive Ingredient Database from the FDA. In some cases, toxicological studies may be required.

Drug properties may be either positive or harmful to the HME formulation and process. At the beginning of the development, a thorough drug characterization must be performed, including thermal, chemical, and physical properties [72]. Some drug characteristics are relevant for a quick assessment of the feasibility of amorphous formulations and the suitability of HME as the processing technology. For instance, drugs with very high T_m (> 250°C), thermal instability, or high melt viscosity, are usually not recommended for the HME process. Other characteristics are usually considered, namely the number of hydrogen acceptors or donors to establish intermolecular interactions with the polymer, the solubility in different solvents (aqueous and organic), solubility in biorelevant media, the T_m and T_g (its ratio is preferred below 1.3 [39]), logP, particle size distribution, among others.

For the development of any solid dispersion, the pre-formulation is a critical stage. The selection of processing conditions is highly influenced by the degradation of the materials and rheological properties of the blend. Drug and carrier properties should be deeply evaluated, as drug solubility in different solvents, drug solubility in polymeric solutions, T_m of the drug, T_g of polymer, drug-polymer miscibility, melt viscosity, and thermal stability of the blend [39]. The selection of potential carriers relies on the drug miscibility in the polymeric matrix, polymer physical properties, the stability of the composition, and other prerequisites of final dosage forms. Additionally, functional excipients as stabilizers, surfactants, antioxidants, plasticizers (usually added to reduce T_g and melt viscosity, smoothing the extrusion process), diluents, release modifiers, and processing aids can also be included in the HME formulation [29, 37].

The drug and the polymeric carriers may suffer chemical transformations during HME processes [72]. Solvolysis and oxidation are two common mechanisms for the degradation of drugs. Nonetheless, solvolysis is rarely an issue, as HME is a solvent-free process [72]. Oxidation has been described due to peroxides remaining after the polymer synthesis or on polymer oxidation. For instance, excessive temperatures needed for under-plasticized cellulose-based polymers (as Hydroxypropyl cellulose, HPC) may lead to polymer oxidation [37]. Antioxidants should be

considered if oxidative degradation of drugs or carriers is likely to occur. According to Lang *et al.,* mechanisms of chemical degradation may be classified into main or side-chain reactions [31]. The main chain reactions include cross-linking and scissions of the polymer backbone [48, 104], whereas side-chain comprehend cyclization and elimination [31]. Examples of polymer degradation during thermal treatment in HME have been reviewed [31] and are summarized in Table 1.6. Another common risk for HME-based formulations is drug-polymer interactions, often triggered by thermal and mechanical energy that accelerate these reactions. Some of these incompatibility cases are well described in the literature [105, 106].

Table 1.6. Mechanisms of polymer chemical degradation and examples [31].

	Main-chain reactions	
Chain scission	Poly(ethylene oxide) (PEO) [48, 107, 108]	Lack of thermal stability since the C–O bonds of the main chain are less stable than C–C bonds.
	Poly(lactic acid) (PLA) [109, 110]	Ester bonds are prone to reactions such as hydrolysis.
	Cellulose derivatives [111, 112]	The high viscosity and low chain flexibility turn these compounds susceptible to high mechanical stress. Main-chain scission was observed in amylopectin and Hydroxypropyl methylcellulose (HPMC).
Cross-linking	Polyurethanes (PU's) [113]	High extrusion temperatures (>200°C) led to cross-linking and oxidation.
	Side-chain reactions	
Side-chain elimination	Hypromellose acetate succinate (HPMCAS) [78]	Hydrolysis produces acetic and succinic acid. These degradation products can react with the drug to form process-related impurities.
	Poly(vinyl alcohol) (PVOH) [114]	During HME of partially hydrolyzed PVOH[a], high temperatures and mechanical energy may induce side-chain elimination, which produces acetic acid that triggers additional degradation. The hydroxyl groups in PVOH can also undergo nucleophilic addition reactions.
Side-chain cyclization	Eudragit® E[b] Eudragit® L[c] and S[d] Eudragit® L30D[e] [115, 116]	Formation of cyclic anhydrides when exposed to temperatures above 170°C by intramolecular ester condensation.
	Carbopol® (polyacrylic acid) [116]	Anhydride is formed when processed at 100°C.

[a] PVOH is manufactured through the hydrolysis of polyvinyl acetate. Partially hydrolyzed PVOH contains acetate groups on side chains. Fully hydrolyzed PVOH is more resistant to chemical degradation; [b] poly(butyl methacrylate, (2-dimethylaminoethyl) methacrylate, methyl methacrylate) 1:2:1; [c] poly(methacrylic acid, methyl methacrylate) 1:1; [d] poly(methacrylic acid, methyl methacrylate) 1:2; [e] poly(methacrylic acid, ethyl acrylate) 1:1.

3.3.1. Theoretical considerations on the physical stability

The stability of HME products has been demonstrated to be related to the characteristics of carriers, the physical state of the compound, packaging materials, and storage conditions. Although HME formulations usually have good long-term stability [37], amorphous compositions are metastable and tend in nature to the most thermodynamically favored state through recrystallization [31]. This is one of the most common problems observed with ASDs, in which the drug reverts into the crystalline form on storage.

The storage of ASDs 50°C below T_g is commonly accepted to decrease the risk of recrystallization, owing to reduced molecular mobility [117]. Nonetheless, molecular mobility still occurs below this point due to β-relaxations, and 50°C may not be enough taking into account typical storage time for pharmaceuticals [118]. Therefore, the characterization of the β-relaxation is crucial since amorphous products are usually stored at temperatures where relaxation is driven mainly by the β-process (below T_g). This characterization is typically performed with calorimetry (Differential scanning calorimetry (DSC) or isothermal microcalorimetry) or dielectric spectroscopy [118].

Two main approaches are generally considered to increase the physical stability of amorphous formulations, as reviewed by Baghel and colleagues [119] and first by Janssens and Mooter [120]. In one, polymers kinetically stabilize the amorphous systems through the reduction of the molecular mobility, “freezing” the drug and blocking any molecular movement. The addition of polycarbophil, Poly(vinylpyrrolidone) (PVP) K25, or hypromellose (HPMC) may be used as crystallization inhibitors [37]. On the other, molecular mobility is reduced by intermolecular interactions, which provide stability through the decrease of the thermodynamic energy of the system. These interactions are typically van der Waals, H-bonding, hydrophobic, electrostatic, and rarely ionic. Although weak, its sum is often enough to stabilize solid dispersions.

A number of equations were developed to predict molecular mobility. The three most commonly used are the Arrhenius equation, the Kohlrausch-Williams-Watts (KWW) equation, and the Adam-Gibbs (AG) equation. The Arrhenius equation may be applied to crystallization data to estimate the long-term physical stability of ASDs [121]. Zhu *et al.* managed to measure the impact of moisture and polymers on the recrystallization of ritonavir, which was well described by the parameters of the Arrhenius model. The model seemed feasible for estimating the long-term physical stability based on short-term data generated under accelerated conditions [121]. Bhardwaj *et al.* also correlated physical strength to molecular mobility in itraconazole in the amorphous form. The group identified β-relaxations responsible for its physical instability, which exhibited Arrhenius behavior, temperature-dependent over the entire experimental temperature [122]. Miyanishi and

his group evaluated the recrystallization of a nifedipine ASD, showing that the solid dispersion would need to be stored at -20°C to maintain its performance for at least three years [123]. Despite the wide use of this equation, the Arrhenius model is not always accurate. Amorphous polymers act as strong glasses exhibiting (near) Arrhenius behavior, and most of the small drugs act as fragile glasses which deviate significantly from the Arrhenius behavior [124]. In these cases, fragility parameters are preferred through the KWW or the AG equations.

The KWW equation links the "relaxation recovery enthalpy" to the average relaxation time constant (τ) and a stretch parameter (β) [120, 125]. The KWW equation has been mainly applied in single-component compositions [126, 127], and some complex systems [128]. However, the predictive capability for physical stability was demonstrated to be somewhat limited, as in studies performed with celecoxib [129, 130]. Its performance is usually acceptable for single-component systems but often fails when multicomponent systems are evaluated due to the increased complexity. Although still widely used, the predictive ability of the KWW equation is considered nowadays limited [124]. To overcome some of the handicaps of the KWW equation, the non-linear AG equation was proposed [120]. Mao *et al.* outlined a straightforward method based on DSC to assess the relaxation time [131]. The AG equation has been successfully used for the calculation of relaxation times and correlation with the physical stability of ASDs. Literature reports studies on indomethacin [132], salicin, felodipine and nifedipine [133], indomethacin, felodipine, griseofulvin, citric acid, ketoconazole and nifedipine [131], and even mixtures of phenobarbital and nifedipine in a PVP matrix [134]. What is still to be clarified is how these concepts may be related to a multicomponent system, in complex formulations. Although there was a clear improvement over the KWW equation, the AG theory did not always predict the physical stability of ASD accurately, as in the simvastatin case [135]. Clear limitations of the AG equation are that the relaxation process is not exponential in nature, and other entropic contributions besides configurational are not taken into account. Nonetheless, there seems that either calculated from KWW or AG approaches, the stability may still be predicted appropriately, at least qualitatively [124].

3.3.2. Theoretical considerations on drug-polymer miscibility/solubility

It is known that solutes and solvents are miscible only within specific percentage ranges, which also applies to the case of drugs and polymers [31]. A single-phase ASD system is usually preferred due to improved physical stability compared to a multi-phase system [31, 136]. Moreover, a low percentage of hydrophilic polymers in drug-rich phases decrease the release rate of poorly-soluble

compounds [31]. High drug-polymer miscibility is needed to lower the risk of recrystallization, and there are several approaches to evaluate properly this issue.

The Gordon-Taylor equation is used to predict the T_g of amorphous dispersions [137]. Deviations from the theoretical T_g are usually an indication of intermolecular interactions within the components. A positive deviation generally suggests that the number and strength may be greater than in the physical mixture due to, for instance, H-bonding, and a negative deviation is generally a sign of loss of interactions after mixing [138]. Several studies report the use of the Gordon-Taylor (or Fox) equation to predict the miscibility of drug-polymer compositions. For instance, Nair *et al.* determined the influence of interactions on the T_g of various drug-PVP blends, namely propranolol hydrochloride, acetaminophen, griseofulvin, naproxen, carbamazepine, or salicylamide [138]. Moreover, molecular interactions based on the deviation between experimental and theoretical T_g within four drug-amino acid systems were recently studied [139]. Another interesting study by Rask *et al.* reported increasing positive deviations with increasing copovidone ratios, suggesting strong interactions [140]. In another study, various grades of HPMC were used to produce ASDs of itraconazole by HME, and the theoretical T_g was compared with the experimental results [141].

Miscibility may also be predicted based on the calculation of the three-dimensional solubility Hansen parameters (δ). Compounds with comparable δ values are probably miscible [142]. Precisely, three Hansen parameters are calculated for each molecule, measured in $MPa^{0.5}$: the energy from dispersion forces between molecules (δ_d); the energy from the dipolar intermolecular force between molecules (δ_p); and the energy from hydrogen bonds between molecules (δ_h). Then, the total δ is calculated through the combination of solubility parameters. Group contribution methods may be applied, like the one by Hoftyzer and Van Krevelen [26], or the more recently developed by Just and Sievert [143]. The literature considers a cut-off value for the difference in δ of less than 7 $MPa^{0.5}$ for good miscibility [31, 39, 142, 144]. This method is widely applied for ASDs. Forster *et al*. evaluated two model drugs and some excipients to predict the formation of glassy solutions. Miscibility was determined experimentally by DSC and thermomicroscopy, and the experimental results met the Hanssen predictions [144]. Another study by Baghel *et al*., with dipyridamole and cinnarizine, predicted successfully the miscibility of binary mixtures tested [145]. Carbamazepine and Soluplus (SLP) miscibility was correctly estimated based on Hansen parameters by Djuris *et al.* [146]. Zhang and colleagues selected the proper carriers for HME for the drug baicalein also using the described method [147]. Although widely applied, this approach presents limitations, and for systems involving long-range interactions (such as ionic) or highly directional (as H-bonds), this approach may not work. Moreover, it is based on a pure chemical approach and does not consider crystal lattice energy [26, 124, 145]. Yoo *et al.* studied a multicomponent

amorphous system that showed ASD formation, regardless of the Hansen results [148]. In another study, the predicted Hansen parameters demonstrated a poor correlation with the experimental results [138]. Hence, in compositions with strong interactions, miscibility will probably be rated too low if assessed by the Hansen approach.

The Melting Point Depression (MPD) theory is also applied to predict miscibility. The basic principle is that the melting point of a drug decreases if it is miscible with a carrier, as it becomes a thermodynamically favorable phenomenon. The polymer that reduces the melting point the most is the more probable to be miscible with the drug [149]. Therefore, the theory of Flory-Huggins was adopted to evaluate drug-polymer solubility through the calculation of the interaction parameter (χ) [150]. Several successful examples are available from the literature. Marsac *et al*. estimated the χ from MPD data for two compounds, nifedipine and felodipine, when blended with PVP K-12, and the theoretical results were in accordance with the experimental data [151]. Also, Tian *et al.* determined the χ for felodipine with SLP and hypromellose acetate succinate (HPMCAS) using the MPD method, demonstrating limited miscibility [152]. The miscibility of carbamazepine and SLP was successfully estimated based on the Flory-Huggins theory by Djuris *et al.* [146], and Yang *et al.* used a theoretical model based on the MPD to successfully predict the solubility of paracetamol in poly(ethylene oxide) (PEO) [149]. To apply the MPD method, both the compound and the polymer need to be chemically stable over the studied range of temperature [26] and enough molecular interactions are required for the depression in the T_m be perceived in the DSC. Besides, this method is more suitable for systems where the drug has a T_m significantly higher than the T_g of the polymer [124]. However, the most significant handicap is that the calculation of χ is linear only at low percentages of polymer and, therefore, best applied to high drug loading systems [124].

Phase diagrams are another valuable tool for the development of ASDs. They are built with the Flory-Huggins theory and the link between χ and temperature [31]. It generates a curve between unstable and metastable regions, called spinodal [153]. Several examples may be found in the literature [145, 152, 154-156]. For instance, Thakral and Thakral investigated the miscibility of Poly(ethylene glycol) (PEG) 6000 with 83 drugs [154]. Baghel *et al.* presented a phase diagram of four systems, considered to provide a reasonable estimation of physical stability [145]. Li and colleagues constructed a phase diagram for the blend of felodipine and Eudragit® EPO and concluded that these diagrams are useful also to select processing temperature for HME manufacturing to ensure complete miscibility [155]. Phase diagrams of albendazole-polymer compositions were also used to assess the feasibility of HME and spray drying [156]. Phase diagrams are temperature dependent, and the miscibility of the drug-polymer system may change with slight variations in the product temperature [124].

3.4. HME process development

The HME process has been demonstrated as crucial to guarantee the Critical Quality Attributes (CQAs) of the drug product. For the first extrusion tests, the definition of general processing conditions is needed. These conditions rely on the physicochemical characteristics of drug and excipients and the phases to be considered. One of the two regimes may be chosen: miscibility or solubilization regime [157]. In the miscibility concept, the extrusion temperature is higher than the T_m, which requires a screw design able to provide higher distributive mixing to spread the two liquids. Here, residence time and shear stress are less significant for the efficacy of mixing. When considering the later, where the extrusion temperature is lower than the T_m, higher specific energy input and aggressive screw designs are needed to guarantee enough shear and residence time. However, as shown by Maddineni *et al.,* excessively harsh designs may result in unnecessary impurities [158]. The choice of screw design may become easier when the polymer melt viscosity is known. The modular design of the screws permits different configurations through the use of forwarding or reverse conveying elements, kneading blocks, and other structures (Figure 1.4) [72]. Moreover, when dealing with thermo-sensitive materials, reducing the residence time, or lowering the processing temperatures should be considered [159]. In summary, through the careful analysis of the collected data, it is possible to select the initial process parameters probably very close to the final or optimal.

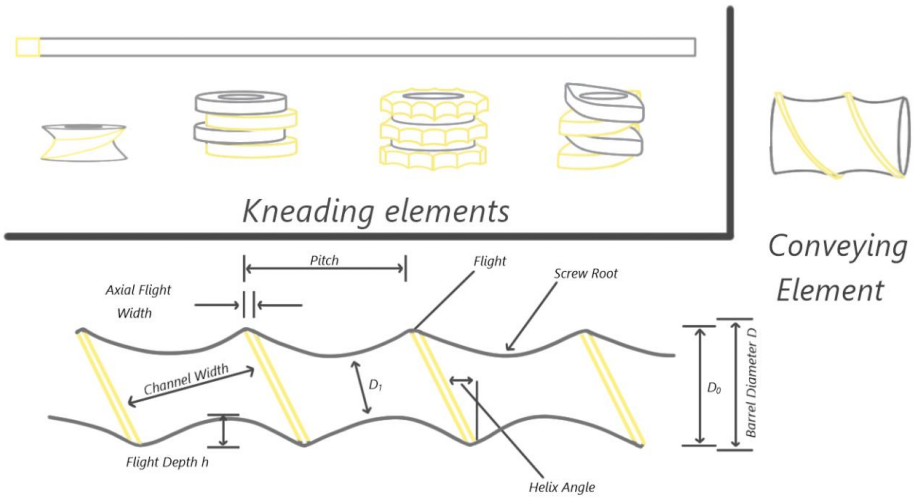

Figure 1.4. General characteristics of screws and details of screw elements. Di is the inner diameter of the screw and Do is the outer diameter.

The next stage is focused on assessing the manufacturability, solubility, and stability of prepared ASDs. It should focus on processing temperatures, screw speed, melt pressure, and motor load. Most HME systems provide measurements in real-time for these parameters, which are used to rank order performance. The first evaluation is purely visual, considering the presence of crystallinity when the extrudate is not seen as a transparent glass [160]. This evaluation should be supported by polarized light microscopy (PLM), complemented by other analytical technologies, such as DSC. Pressure and motor load are always evaluated in every extrusion test, but its study and optimization through processing parameters are usually performed later, along with selecting the prototype. The extrudate is then milled, and its performance is deeply characterized. Typical attributes evaluated in this stage are dissolution rate, chemical degradation, solid-state and physical stability, where ideal systems will have no change during storage. In case the compound is a BCS class IV, an in-depth characterization may be necessary, where testing in animal models is especially recommended [27, 153]. Results from each issue (manufacturability, solubility, and physicochemical stability) allow the selection of the preferred system. In general, solubility is considered primacy. The next topic for evaluation is physical stability, as options still exist for enhancing physical resilience, for instance, through restrictive storage conditions. Lastly, manufacturability is assessed. Excessive motor loads or high levels of impurities may be further improved with slight changes in formulation or process parameters.

3.5. Formulation of finished dosage forms

Molten materials are conveyed to the downstream equipment for final dosage form preparation. This may involve milling, pelletization, calendaring, or tableting/encapsulation (Figure 1.5) [29, 40, 161]. Cooling the extrudate may be performed with air, nitrogen, on conveyors, rolls, or even with water. Optimizing the cooling rate is of foremost importance to obtain the required amorphicity. Rapid cooling would form a relatively low crystallinity level (being an amorphous or molecularly dispersed product), whereas slow cooling would result in crystal growth [40]. The shape of the extrudate is molded by the die. Circular dies are the most common and are used for pellets and granules. Films and patches require flat dies and annular dies are dedicated to tubing and co-extrusion. The molten blend can also be used in injection molding [37], which can result in a tablet or a capsule shape, or into customized designs, as adhesives, vaginal tablets or rings, eye inserts, or others. All of this can be performed in a single continuous process, which can potentially decrease overall costs during production.

The most common downstream processing for oral administration is milling, to be finally converted into dosage forms like granulates, tablets, or capsules. The particle size of granules impacts the process capability. However, especially when poorly soluble compounds are concerned, it has an important impact on bioperformance, as generally speeds up the drug release rate. Therefore, it is an important parameter to understand and control. For certain extrudate compositions (for instance, cellulose-based), milling can be challenging. The selection of the type of milling technique depends on the material characteristics and the target mean size and size distribution of the resultant powder. For extrusion materials, hammer or pin mills are usually preferred (impact mills). The final size distribution is generally smaller with pin mills (15 - 30 µm) than when using hammer mills (20 - 60 µm) [162]. For solid pharmaceutics, like tablets and capsules, the materials flow is crucial, and fine particles are usually avoided. Therefore, a granulation step is, in some cases, added to the process as this range of particle sizes is relatively low to ensure a predictable powder flow.

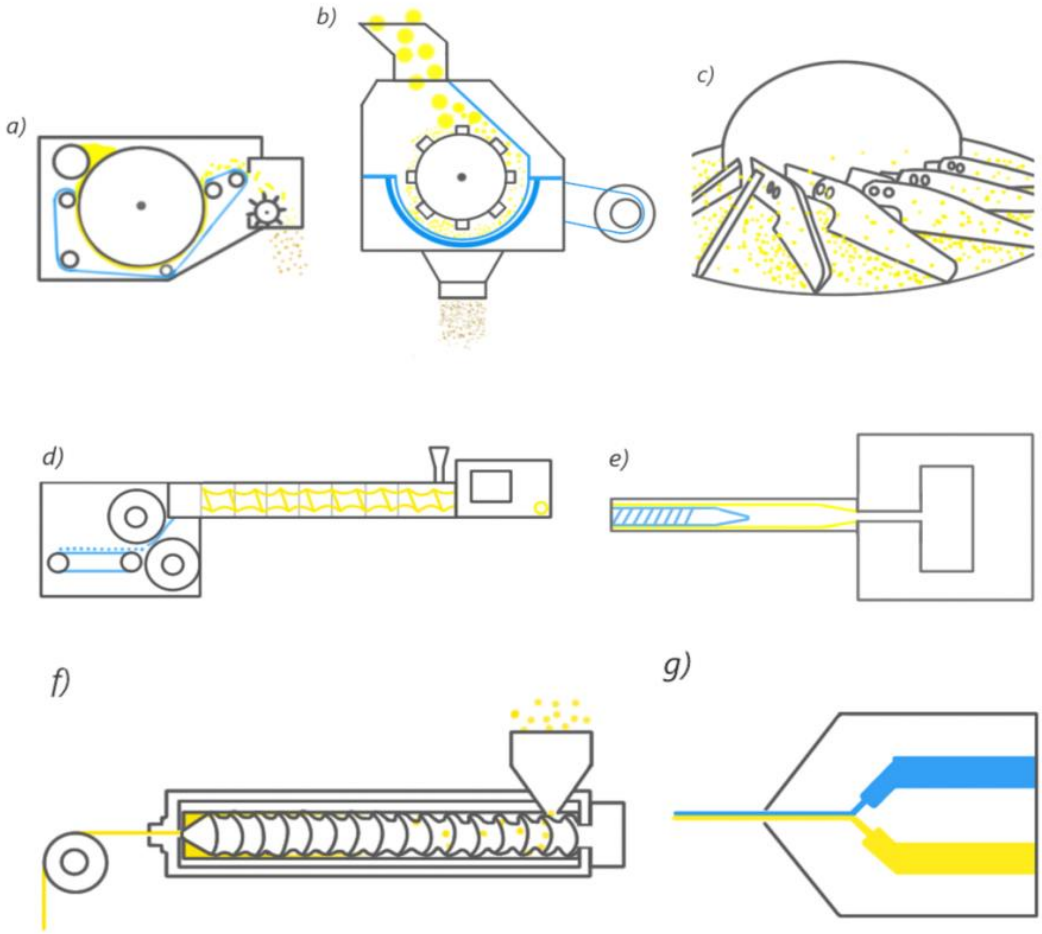

Figure 1.5. Downstream processing equipments: a) cooling calender; b) mill; c) pelletizer; d) shaping calender; e) injection molding; f) film extrusion; g) co-extrusion.

However, the disintegration time may become too long if the milled extrudate is filled directly into capsules or compressed into tablets. This is because polymers have high binding and gelling properties, and they are present at high levels in the formulation, which leads to the formation of non-dispersible lumps when in contact with water [163]. In such cases, water-insoluble excipients, *spacers* amongst polymeric ASD particles, should be used. Best results were found with microcrystalline cellulose (MCC) and crospovidone, but inorganic excipients as dicalcium phosphate may be used [164]. Another strategy is to use highly soluble ingredients to promote the formation of a porous system when in contact with water, triggering a faster drug release from the extruded matrix, using, for instance, mannitol or lactose. Typically, final dosage forms containing ASDs require disintegrant amounts of 5 to 20%, higher than usual. Crospovidone or another disintegrant with limited swelling performance is recommended to avoid the formation of gelified lumps when in contact with water.

Changes in the mechanical properties of the components during extrusion make ASDs less compressible than physical mixtures [163]. Molecular mobility is deferred due to the low free volume during extrusion, which leads to a compact product and prevents a further decrease in density during compression [165]. Therefore, extragranular excipients with suitable compactibility are essential to achieve a tablet with adequate pharmacotechnical properties, namely hardness, friability, and disintegration time. Sufficient lubrication is also crucial to avoid mechanical problems during compression processes, as picking and sticking.

3.6. Scale-up

Process scale-up is part of product development and enables large-scale and commercial production, assuring drug product CQAs simultaneously [31]. There is not much published information about HME scale-up, but some reports have proposed a number of models. The upscale of continuous processes is considered more straightforward than batch processes. Using the same equipment and process parameters, scape up is assured by longer running times [29, 166]. However, moving to a larger extruder demands a complete characterization of the process and end product to guarantee that it has not changed.

For this purpose, several scale-up models have been tried over the years. Carley and McKelvey presented in 1953 the first scale-up method, based on an adiabatic concept [167], later recovered

by Nakatani [168]. The influence of heat transfer in an HME scale-up was reported by Schenkel, Maddock, and Chung [169]. Others extended previous laws to a whole non-isothermal and non-Newtonian situation [170] or tried to relate the effects of processing conditions (throughput rate and screw speed) on different scales [171]. New scale-up rules were later developed and published by Bigio and Wang [172].

Methodologies had evolved until today. The geometric similarity between extruders is considered crucial to ensure the scale-to-scale production of HME materials with similar properties [166]. This is referred not only to the likeness of screw design (similar conveying, distributive and dispersive sections) but also to the screw geometry itself, as it can have implications on shear stress input and residence times [173]. When the extruders at both scales are geometrically similar, scale-up should be relatively straightforward [166]. Simple relationships between processing parameters may be used to provide a target throughput at a larger scale. The main HME process scale-up theories are known as the Volumetric Scale-up, the Heat Transfer Scale-up, and the Power Scale-up, widely discussed in the literature [28, 160]. For instance, a volumetric approach was used to upscale an HME process from laboratory to clinical scale [174], with minimum consumption of drug during the whole study.

Nonetheless, heat and mass transfer restrictions may happen, mainly when the difference between scales is too wide. When confronted with these limitations, adjustments are needed to maintain the CQAs. The specific energy, residence time, and product temperature are the most important factors to keep steady [173]. This may be accomplished by regulating HME process parameters, at this stage mainly by the feed rate (based on calculated throughput). The screw speed, the product temperature, and screw design should only be adjusted if calculations led to excessive motor torque [160], or if differences in CQAs arise due to decreased heat and mass transfer at the larger scale [173]. However, since kneading elements are usually required for the production of ASDs, screw configuration changes should not be the first approach and must be considered carefully.

4. An Industry perspective of HME Product Development

4.1. Pharmaceutical Development of HME-based formulations

Pharmaceutical development aims to provide robust knowledge through the application of systematic approaches that allow designing a quality product and its manufacturing process consistently. The complete understanding of the formulation and process is consolidated in the 3.2.P.2 section of the Common Technical Document (CTD) and then used to submit a new drug application to the competent authorities. The information and knowledge collected from development and production should provide the scientific understanding to support a design space, drug product specifications, and process controls [175].

In HME-based drug products, a robust pre-formulation assessment is the key to successful development. A step-by-step approach, starting with the thermodynamic evaluation of several systems, followed by a polymer screening test coupled with multivariate statistical analysis, is useful to rapidly identify the most promising HME systems. This is the way to avoid wasting time, money, and effort in failed compositions.

4.1.1. Thermodynamic predictions and considerations

The selection of a suitable carrier mainly depends on the solubility/miscibility of the drug-polymer system, polymer physicochemical properties, stability, and pre-requisites of final dosage forms. Therefore, the physical and chemical properties of drugs and possible carriers should be carefully evaluated before starting the development of HME-based formulations.

The miscibility of drug and carriers is usually one of the first issues to evaluate. This is essential to guarantee adequate drug load and chemical interactions between the components, which is valuable to optimize process parameters and product performance on dissolution [176]. However, there is no established procedure to select excipients for HME to date [177]. Several methods have been described to predict miscibility with the carrier, usually applying thermodynamic predictions in an attempt to guide formulation development rationally. Predicting miscibility is a difficult task, and the results are crucial [28] on the course of the development work. Some of the more common approaches include the prediction of T_g of the blend through the Gordon-Taylor equation [178] (or

the simplified form by Fox [179]), the calculation of the Hansen solubility parameters [180], the Flory-Huggins theory and the calculation of the interaction parameter (χ) [150], and also the construction of phase diagrams [31] (Figure 1.6). A review of thermodynamic and computational methods has been recently published by DeBoyace and Wildfong [181].

The Gordon-Taylor (or Fox) equation [137, 164] is a commonly used approach to predict the miscibility of drug-polymer blends in the pharmaceutical industry setting, as reflected in publications from Novartis [182], Merck [183], AbbVie [184], Johnson & Johnson [185], and Lundbeck [186]. One of the most recent examples is from J&J, where the Gordon-Taylor equation was applied in the assessment of the impact of the molecular structure of sorafenib and its fluorinated form, regorafenib, in interactions and consequent miscibility with polymers. A positive deviation of T_g from the prediction of the sorafenib formulation as opposed to regorafenib one was an indication of stronger interactions, lately confirmed by Nuclear Magnetic Resonance (NMR) and computational methods [185]. Another example was published by Lehmkemper *et al.*, where the Gordon-Taylor equation was used to model the T_g of ASDs of acetaminophen and naproxen, both manufactured by HME. The calculations were in line with experimental results for naproxen, but a negative deviation was observed for acetaminophen, which indicated weak interactions with the polymer. The results were validated by stability studies until 18 months [184].

In what concerns the Hansen solubility parameters (δ) [142, 164, 187], group contribution methods are often used to estimate δ, to avoid time-consuming tests and potentially inaccurate results. These methods are easy to use [181], and there are already some well-known approaches, like those by Hoy [188] or Hoftyzer and Van Krevelen [180]. The calculation of solubility parameters and its application to ASDs, both in academia and in the pharmaceutical industry, is still one of the most applied approaches due to its relative simplicity. There are even attempts to improve group contribution parameters and to develop new values based on solids, as the method published by Just and Sievert [143], verified with ASDs manufactured by HME and film casting. A number of publications describe the use of solubility parameters in an industry setting, namely by AstraZeneca [189], Merck [190], Sandoz [191], GlaxoSmithKline [144], ACG Pharma [192], Aizant [25, 193], Hoffmann-La-Roche [194], Boehringer-Ingelheim [174], and many others [195-198]. Wlodarski *et al.* reported the use of δ for the prediction of miscibility between itraconazole and two polymers, polyvinyl alcohol (PVOH) and PVPVA [190]. A work in collaboration with Aizant recommended using δ as part of a systematic approach to design solid dispersions and applied it to the development of a cilostazol ASD [25]. Pawar and co-workers developed an ASD of efavirenz by HME, where two polymers were selected based on the prediction of miscibility through the Hansen parameters [192]. Although δ can be useful for the fast screening of potential carriers, inadequacies in theory

often lead to the exclusion of good candidates and require additional experimental work to confirm the interpretations. This was verified and published by AstraZeneca, where 54 drug-polymer combinations were experimentally assessed for miscibility, and its results compared to δ results. The predicted δ did not match the experimental data, and some reasons were pointed out as the negligence of intermolecular interactions [189].

These weaknesses have led to the development of more complex methods, as the calculation of Flory-Huggins interaction parameter (χ), usually through the application of MPD theory [150]. This method is also used by the pharmaceutical industry and is probably the most popular approach, with research work published by Johnson & Johnson [199], Amgen [200], Bayer [201], Genentech [202], AbbVie [184, 203], Bristol-Myers Squibb [136, 204, 205], AstraZeneca [189], Lundbeck [140, 186, 206], Boehringer-Ingelheim [207], Dow and Dispersion Technologies [208, 209], Hoffmann-La Roche [210, 211], Abbott [212], Merck [213], Pfizer [150], Aizant [193], and others [214, 215]. In 2018, lapatinib has been formulated both by rotary evaporation and HME, and the polymers were selected based on several thermodynamic assessments, including the Flory-Huggins equation [200], and Rask *et al*. reported the solubility of 4 drugs in 3 different polymers determined and extrapolated to room temperature through the Flory-Huggins model. The authors also presented an interesting decision tree for the selection of the most suitable thermal method to determine the Flory-Huggins model based on the physicochemical characteristics of both the drug and the carrier [199]. Similar findings have been found by Chen *et al.*, where the solubility of a poorly water-soluble drug in different polymers through the Flory-Huggins interaction parameter was assessed, and the results matched well the experimental data [201]. Earlier, the assessment of acetaminophen and naproxen solubility in polymeric excipients as povidone and copovidone, calculated with three models including the Flory-Huggins, has been published by Lehmkemper and co-workers. The results were in line with the experimental solubility data, however, the Flory-Huggins method underestimated the acetaminophen miscibility on stability [184]. The characterization of molecular interactions by ^{13}C NMR and Fourier-transform infrared spectroscopy (FTIR) enabled the understanding of ketoconazole-polymer systems release, which was commanded by the polymer dissolution rate, intermolecular interactions, and mixture homogeneity. The interaction parameter between the drug and four polymers was applied to predict miscibility, and the results matched the experimental data [204].

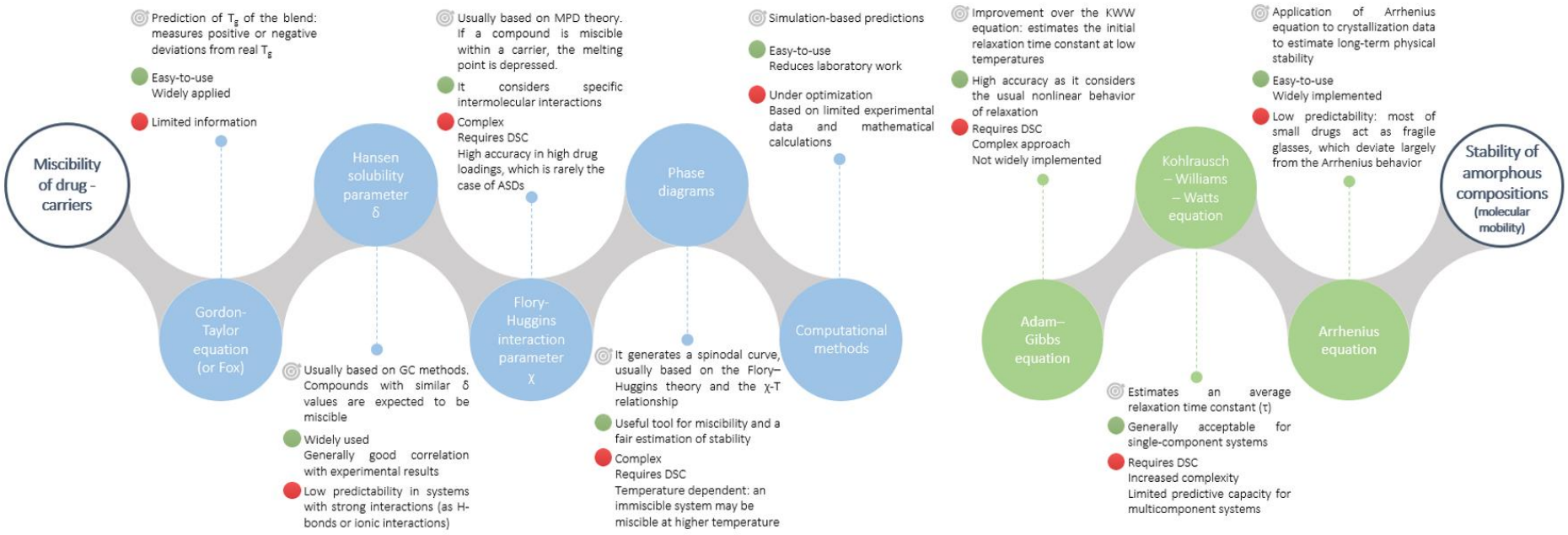

Figure 1.6. Thermodynamic assessment of amorphous compositions: applications, advantages, and limitations. Abbreviations: T_g, Glass transition temperature; GC, Group Contribution; MPD, Melting Point Depression; DSC, Differential Scanning Calorimetry; ASDs, Amorphous Solid Dispersions; KWW, Kohlrausch-Williams-Watts.

The MPD method was also used to predict drug miscibility of a model drug in different polymers. SLP was the selected polymer, supported by the optimized stabilization capacity [203]. Although largely used by the pharmaceutical industry, χ failed to predict miscibility in a recent study from AstraZeneca, where 54 drug-polymer combinations were assessed for miscibility [189]. Most of the publications to date, both from academia and pharmaceutical industry, describe the use of thermodynamic models like the Flory-Huggins method, although they were never intended to be applied to systems with strong interactions such as H-bonds [216]. Recent models that permit intermolecular interactions are undoubtedly needed to guide ASDs development.

Another common tool within the industry is the construction of phase diagrams, which is most of the times based on the Flory-Huggins theory [31]. Phase diagrams depict the relationship between the free energy of blending and composition, usually considering drug load [124]. The use of phase diagrams to predict miscibility of acetaminophen and naproxen ASDs have been reported, however, the compositions were modeled not by the Flory-Huggins theory, but through the Perturbed-Chain Statistical Associating Fluid Theory and by the Kwei equation [217]. Gumaste and co-workers published a prediction of miscibility based on ternary phase diagrams of itraconazole-polymer-surfactant, identifying the blend HPMCAS - poloxamer 188 as an optimal surface-active carrier system for ASDs [218]. The use of phase diagrams has also been described by many other pharmaceutical companies, such as AstraZeneca [152, 219], Hoffmann-La Roche [211], and Johnson & Johnson [220]. New miscibility prediction methods are being developed, such as the MemFis system by Evonik [221], but the predictions of miscibility are in general based on limited experimental data and mathematical calculations, presenting inherent limitations.

The stability of the amorphous compositions is known to be influenced by the miscibility of the drug within the carriers [177]. To predict physical stability, which is closely linked with molecular mobility, a number of thermodynamic equations are used, as the Arrhenius [121], the KWW [120], and the widely used AG equation [120, 222] (Figure 1.6). Despite its recognized utility to the ASDs area and physical stability, these equations are not widely implemented by the pharmaceutical industry in routine product developments. The Arrhenius and the KWW models cannot always predict the shelf-life of the product accurately [124]. Although considered complex for routine application, Graeser *et al.* applied the AG equation to calculate values of relaxation time (τ) of 14 different drugs analyzed through DSC. Through DSC and a Matlab software script developed by the authors, a 5-step method to calculate τ through the AG equation was described [223]. However, the same group also found that below T_g, which is the common storage temperature for pharmaceuticals, τ may not correlate with the experimental physical stability, indicating poor prediction-ability of this parameter [224].

Despite their complexity and even some inaccuracy, these approaches are slowly being taken by development teams. However, there is still the need for a more complete approach combining, for instance, experimental results, thermodynamics theory, and computational simulations [177], to finally be able to overcome the barriers of the development of ASDs.

4.1.2. Screening approaches and multivariate statistical analysis of results

A systematization of a rational approach to design solid dispersions is crucial for a successful, fast, and low-cost development, which avoids that promising formulations are prematurely eliminated from experimental studies. Ideally, strategies should be efficient enough for assessing a large number of binary and ternary – or with a higher-order – combinations (e.g. drug/polymer/surfactant), to identify systems with synergistic interactions promptly, for subsequent in-depth experimental study.

The most common approaches for screening excipients for HME formulations are based on solvent evaporation methods, DSC analysis, Hot Stage Microscopy (HSM), and melt-based methods. Solvent evaporation methods are probably the most common in the industry setting, due to its simplicity [218] and low cost [225]. Some studies have been published, describing ways of automating and miniaturizing the screening of excipients in a high-throughput manner, for instance by Teva [218], Catalent [226], Aizant [25], Hoffmann-La Roche [225], Merck [227], and others [228]. In particular, Gumaste and co-workers reported the film casting technique to determine the miscibility of ternary systems (polymer-drug-surfactant) [218].

DSC studies, HSM, or melt-based methods have the advantage of applying heat, which can be beneficial when the manufacturing process under study is HME. For instance, Kyerematen *et al*., combined DSC and a mathematical algorithm to construct complete solubility curves of drug-polymer systems, which was verified with ASDs of two model drugs, naproxen, and ibuprofen [229], whereas work from Boehringer-Ingelheim scientists described the use of HSM to evaluate mixtures of drug-polymer with or without surfactants or pH-modifiers. The HSM analysis showed that the drug was utterly miscible in PVPVA at 1:2 or 1:3 ratio around 195°C and in povidone only at 1:3 at around 200°C, but in cellulose-based polymers, the drug was only partially miscible even at higher temperatures. This method allowed the identification of one or two-phase systems that led to a fast scale-up to clinical batches [174]. More recently, Auch and co-workers noticed discrepancies between a solvent-based screening method and experimental results of ASDs, and therefore took the challenge of developing a new method using heat, a melt-based approach [230]. Enose and his group published a different approach designated as hot-melt mixing [231], and a miniaturized

extrusion device (MinEx) used for formulation screening has been developed by Hoffmann-La Roche [232].

There are a few reports from the pharmaceutical industry, as by Hoffmann-La Roche [225], Aizant [25], AbbVie [229], Boehringer-Ingelheim [174, 233] and Piramal [231] that present a proposal for a systematic approach for the identification of promising compositions for HME. In general, the thermodynamic evaluation is recommended and associated with screening techniques. A comprehensive overview of various miniaturized assays can be found in Shah *et al.* [234]. Moreover, new methods are still being developed, as the recently published thermal analysis by structural characterization (TASC) [235]. New approaches are still expected in the next couple of years.

Based on the literature and our own experience in the development of HME-based products, a proposal for a structured screening approach is presented in Figure 1.7. This methodology reflects usual techniques, based on physicochemical principles and thermodynamic assessment of the drug and the polymer, to maximize success rates and reduce risks. One of the main advantages is including the assessment of physical stability at early stages during product development.

This approach is divided into five stages. During the first stage, an in-depth evaluation of the physicochemical properties of both the drug and potential polymers is performed. Then, in the second stage, excipients are assessed through solubility parameters, prediction of T_g, and interaction between the components. This preliminary evaluation may be complemented with experimental tests by calorimetry, where the T_g may be confirmed (and the potential for interactions inferred through comparison with the theoretical value), the depression of T_m evaluated, and eventually, the interaction parameter determined. As an outcome, excipients with a high probability of miscibility and chemical interaction are taken to the next stage (third), where an experimental screening of carriers is proposed in a high-throughput and miniaturization manner. The solvent evaporation method is probably the most widely used approach, and is therefore proposed, but applied not only to the assessment of miscibility and solubility enhancement but also to a preliminary experimental evaluation of physical stability. In the later, thin films in glass slides are subjected to a short stability study and evaluated by PLM for birefringence. This evaluation may be complemented with other non-destructive techniques for the detection of crystallinity, like X-ray diffraction or Raman spectroscopy. In the fourth stage, all analytical results obtained from the initial assessment and the screening phase experiments are collected and assessed. Due to the massive load of results, namely from the HTS, one usually needs to apply statistical analysis, multivariate approaches such as the Principal Components Analysis (PCA) method. This is used to identify with confidence (statistical confidence) the most promising systems and drug loads that

will be subjected to small-scale HME tests (fifth stage). The fifth stage is the confirmation, where the focus is the dissolution (in non-sink conditions) and the potential for interactions, assessed both by DSC and spectroscopy. At the end of this process, one or two promising prototypes should be identified.

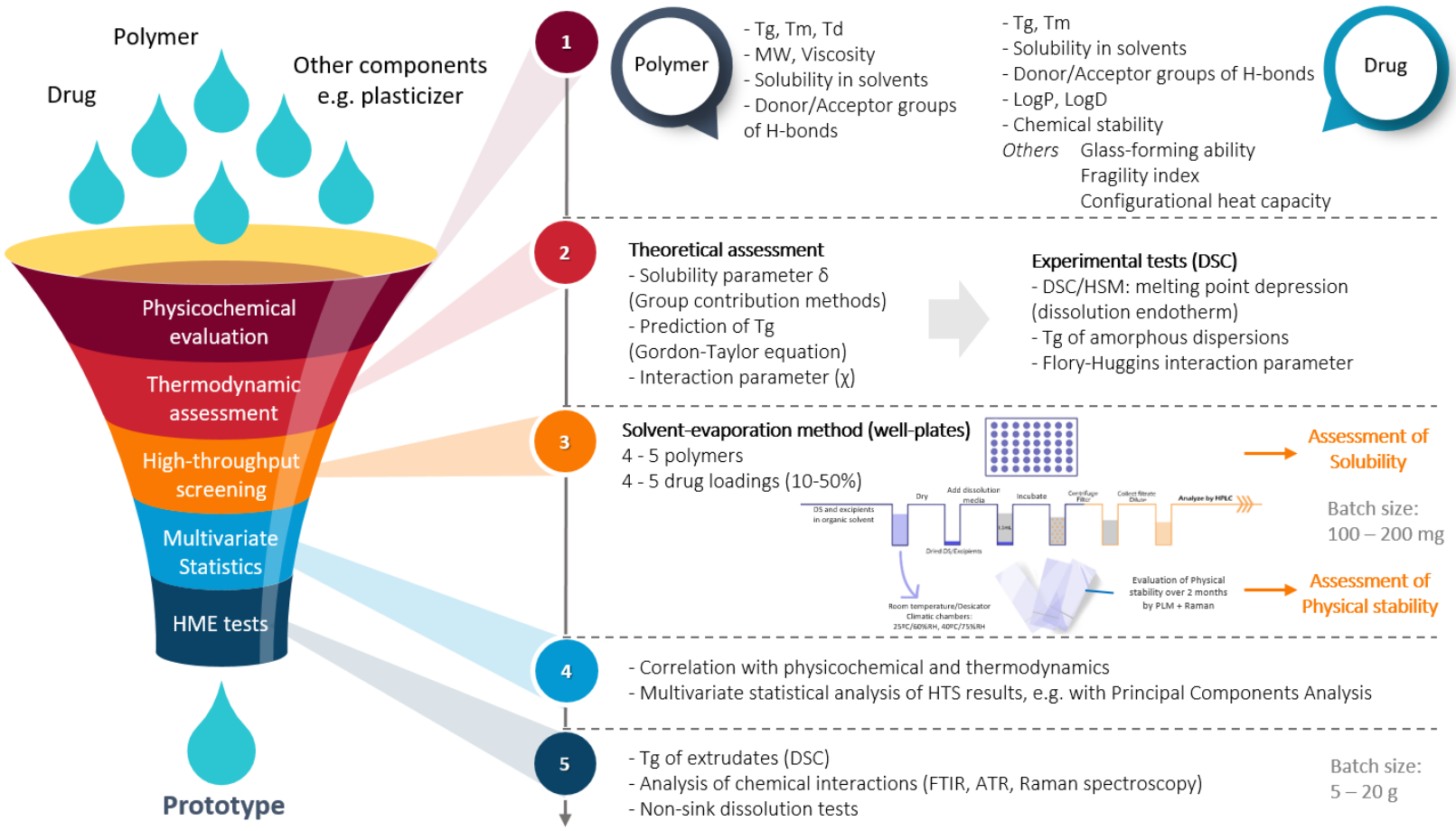

Figure 1.7. A structured approach to the development of ASDs, divided into five stages. 1, Physicochemical evaluation: in-depth evaluation of physicochemical properties of the drug and potential carriers; 2, Thermodynamic assessment: preliminary thermodynamic assessment of potential compositions, which may be supported by experimental calorimetry tests; 3, High-throughput screening: experimental screening of carriers by a miniaturized solvent-evaporation technique for solubility assessment. Thin films are evaluated by PLM under stability for physical stability; 4, Multivariate statistics: data analysis and identification of the most promising systems and drug loads through multivariate statistical analysis such as the Principal Components Analysis; 5, HME tests: small-scale HME tests, focused on the dissolution (in non-sink conditions) and the potential for interactions. Abbreviations: T_m, melting temperature; T_g, glass transition temperature; T_d, degradation temperature; MW, molecular weight; DSC, differential scanning calorimetry; HSM, hot-stage microscopy; PLM, polarized light microscopy; HTS, high-throughput screening; HME, Hot-melt extrusion; FTIR, Fourier-transform infrared spectroscopy; ATR, Attenuated total reflectance.

4.1.3. HME tests: from first extrusions to process optimization (prototype)

Several works published by the pharmaceutical industry describe extrusion tests, namely the selection of promising formulations, preliminary extrusion tests, process development, and, in some papers, even process optimization. Most of them come from the past 2 years, which is a clear indication of the relevance of HME in the pharmaceutical industry. Companies such as Amgen [200, 236], Bayer [45], Amneal [237], Merck [238, 239], Hoffmann-La Roche[232], AbbVie [240, 241], Novartis and Genentech [242], Dow [73], Boehringer Ingelheim [174], Thermo Fisher Scientific in collaboration with BASF [243], Evonik [244], Thermo Fisher Scientific [245], Novartis [35, 246, 247] have active research in the HME field. In their work with lapatinib, Hu and co-workers showed that both material attributes (as drug loading and solid-state) and process parameters (as extrusion temperature) affect manufacturability and solubility significantly [200]. A dual-polymeric system was developed by Hormann *et al.*, using nimodipine as a model drug, and it was found that the shear stress was the most relevant factor for the performance of the ASD [45]. An interesting application of HME has been described by Gajera *et al.* to dry an aqueous nanosuspension. Process parameters as feed rate, temperature, and screw speed were studied, and the statistical analysis revealed that the first two factors are significant and affect the performance of the end product [237]. Comparison of drug incorporation in an ASD both by HME and spray drying was reported by Zhang and co-workers [238]. Novartis scientists reported a HME-injection molding prototype of griseofulvin, where critical process parameters (CPPs) of the downstream processing step were carefully studied [242]. A highly sensitive platform based on torasemide was showed to enhance HME process understanding, namely the dynamic environment inside the extruder and the thermal and hydrolytic effects caused by the process [240]. The thermally sensitive drug gliclazide was studied by HME, through the optimization of screw design, machine setup, temperature, and screw speed [73].

Indeed, in addition to the formulation, the process is crucial for the quality attributes of HME products. This is why the HME process development is performed carefully, step-by-step, and usually in three main stages: the preliminary extrusion tests, process development, and process optimization. This reflects the usual procedure applied by the industry, intending to avoid wasting time, money, and effort in failed candidates. A summary is depicted in Figure 1.8.

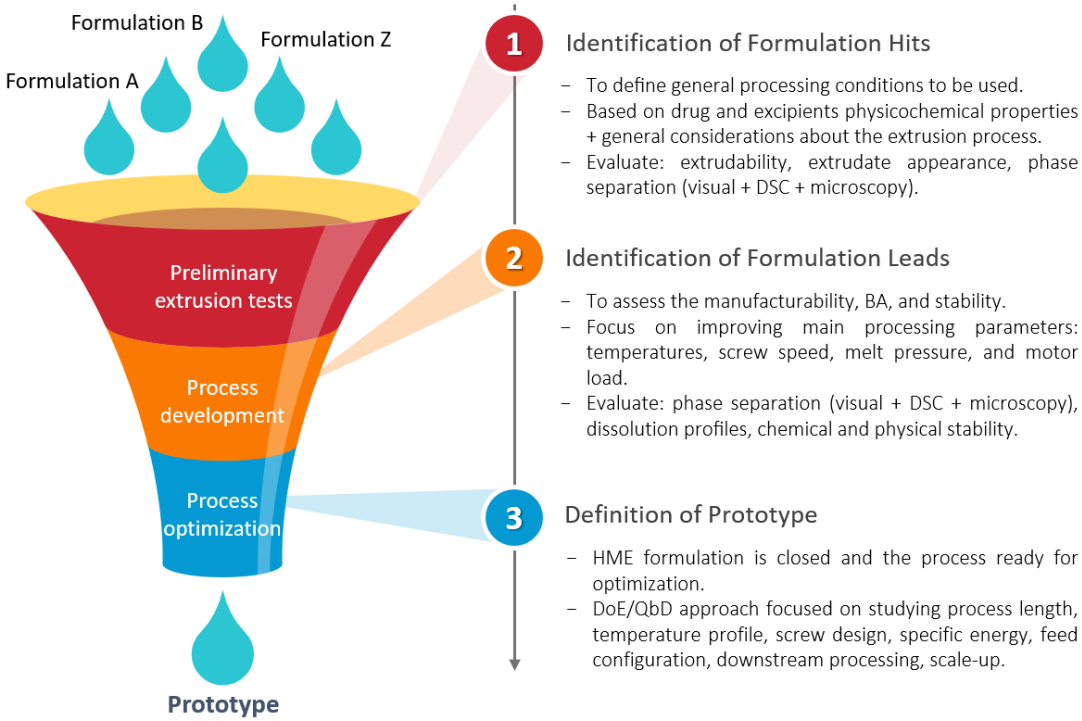

Figure 1.8. Flowchart for the development of HME-based formulations divided into 3 main stages. 1- Preliminary extrusion tests: to define general processing parameters; 2 - Process development: to assess extrudability, *in vitro / in vivo* release, and physical stability; 3 - Process optimization: based on QbD concepts. Abbreviations: DSC, Differential Scanning Calorimetry; BA, bioavailability; HME, Hot-melt extrusion; DoE, Design of Experiments; QbD, Quality by Design.

For the first extrusion tests, which is no more than a preliminary assessment of extrusion feasibility, the aim is to define general processing conditions to be used. These conditions are based on drug and excipients physicochemical properties and also some considerations about the extrusion process, for instance, solid phases to be considered [27]. Recommended process temperatures of different polymers and approaches for the thermal processing of challenging formulations have been recently reviewed by LaFountaine *et al*. [248] and should be considered by formulation scientists.

The next stage is dedicated to further developing the process. The selection of optimal processing parameters depends on the chemical stability of all the ingredients, as well as the physical and chemical properties of the blend, namely the T_m of the drug, T_g of the carrier, processing temperature, drug miscibility within the polymer, and melt viscosity [39]. It includes a set of experiments to assess the manufacturability, BA, and stability of ASDs prepared by HME. Following extrusion, the product is milled for further evaluation: drug dissolution profiles, chemical, and physical stability, where ideal compositions will have no recrystallization on storage. Testing in animal models is recommended to support the choice of the prototype [27, 153]. Results from each

topic (manufacturability, BA, and stability) contribute to the overall ranking of the systems. In general, BA is considered a priority as it is usually the most critical issue [27].

When the lead formulation and rough process are identified, the HME formulation is closed and the process can be optimized. The main HME process parameters recommended for evaluation are process length, temperature profile, screw design, specific energy, feeding configuration, downstream processing, and the impact of upscale [27, 160]. Process development requires careful analysis of the influence of not only each variable but also interactions between variables, as they influence product critical attributes [27]. A statistical experimental design approach (design of experiments, DoE) should support the development work, managing experimental data, and decoupling multivariate interactions [249]. A comprehensive review of physicochemical parameters to be studied when designing and optimizing an HME process was published in 2018 by Censi *et al.* [176], where different analytical techniques are described and its utility located within HME products development.

4.2. Product and Process Understanding through QbD

The concept of QbD was established to promote a better understanding of pharmaceutical products and manufacturing processes not only at any phase of the development cycle but also during commercial production and is promoted by regulatory authorities, namely the FDA and EMA [250, 251]. According to the International Council for Harmonisation (ICH) Q8 (R2), "quality cannot be tested into a product but must be incorporated by design" [175]. Essential elements of the pharmaceutical development are the Quality Target Product Profile (QTPP), the CQAs, the Critical Material Attributes (CMAs), and the CPPs (Figure 1.9) [251-253].

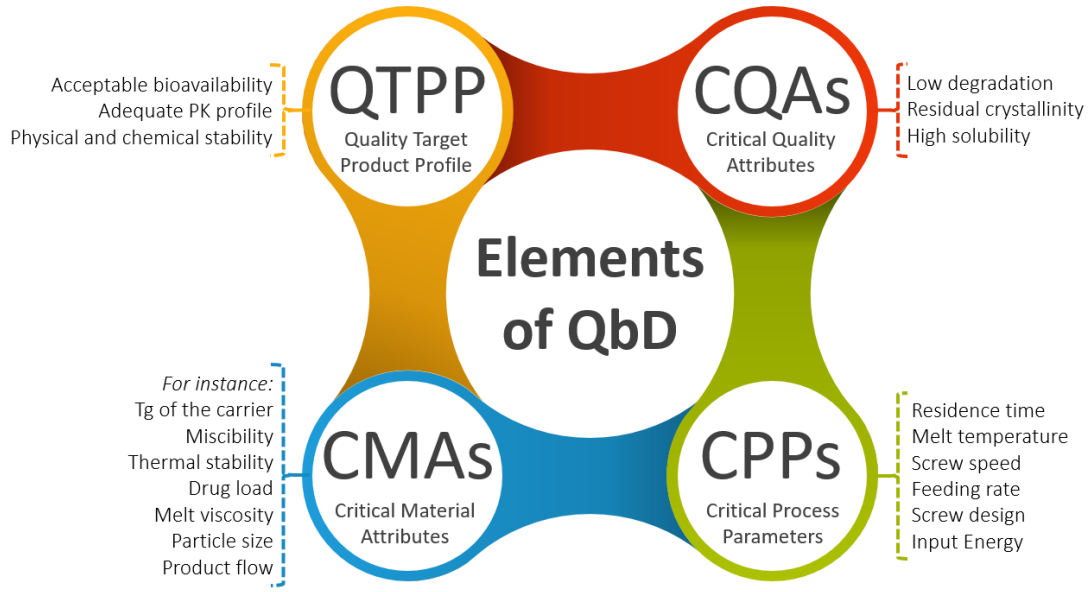

Figure 1.9. Elements of QbD with examples adapted for HME products. Abbreviations: QTPP, Quality Target Product Profile; PK, Pharmacokinetics; CQAs, Critical Quality Attributes; CMAs, Critical Material Attributes; T_g, glass transition temperature; CPPs, Critical Process Parameters.

Typical QTPPs for amorphous products are acceptable BA and pharmacokinetic (PK) profile, mainly when BCS class II or IV are concerned, and adequate stability, both physical and chemical, to have a minimum shelf-life of 2 years. To achieve these goals, CQAs require an in-depth study throughout the development process, namely acceptable levels of degradation, acceptable crystallinity (residual), suitable solubility, and dissolution rates. For drug and excipients, CMAs may include T_m, T_g of the carrier, miscibility, thermal stability, drug load, melt viscosity, particle size, product flow, among others, which is highly variable from product-to-product. The CPPs in the extruder may be considered to be residence time, melt temperature, screw speed, feeding rate, screw design, and an energy component that can be defined as shear stress, or specific energy input [245, 254]. These CPPs are not easily defined during extrusion, because shear, temperature and time are distributional in nature. Therefore, they should be managed based on controllable parameters, such as screw design, screw speed, process temperatures, and feed rate [254]. Moreover, it is important to keep in mind that environmental conditions may also have a role, namely the relative humidity (RH) in hygroscopic formulations and the room temperature for the cooling rate [255] when cooling is performed in a conveyor belt. The difference between QbD for a new product and generic products only exists in the first step of the process: the definition of the QTPP. For a New Drug Approval (NDA), the target profile is still not defined while for an Abbreviated New Drug Approval (ANDA) product, the QTPP is known and established by the reference product [256].

4.2.1. Steps and tools for QbD implementation in HME products

A complete QbD study involves a very well-defined roadmap [250, 255]. In summary, firstly the QTPP must be set, based on scientific knowledge and its relevance *in vivo*. Then, the formulation and the manufacturing process are studied to ensure the predefined profile (CQAs). In this stage, one should determine which are the material attributes or the process parameters that are critical (CMAs/CPPs) or significant sources of variability, which is performed through risk assessment methodologies [252]. Once they are set, a DoE should be applied to link CMAs and CPPs to CQAs and get enough information on how these factors impact QTPP [253]. This leads to the study and definition of the Design Space, which means determining the real values that can be applied during product manufacturing and lead consistently to the desired quality profile [251, 255, 257]. A complete QbD still includes a control strategy and continuous monitoring and improvement [252, 253]. This is the general roadmap for a QbD-based development, but a 9-step example applied to HME is provided in Figure 1.10.

Figure 1.10. 9-step QbD roadmap applied to HME: from the definition of QTPP to the product and process continuous monitoring and improvement. Abbreviations: QTPP, Quality Target Product Profile; BA, bioavailability; PK, Pharmacokinetics; CQAs, Critical Quality Attributes; CMAs, Critical Material Attributes; CPPs, Critical Process Parameters; DoE, Design of Experiments.

Both formulation and processing conditions may be considered critical (critical material or process parameters) and govern drug product CQAs [175]. Several studies have described the relationship between formulation and process parameters using QbD and rational approaches [155, 193, 258, 259]. Although the primary aim of preliminary studies is to develop a formulation and preparation process subjected to further optimization, CPPs should be identified from the early beginnings [27, 39].

To correctly implement QbD during product development, it is crucial to know three important tools, the risk assessment, the DoE, and the Process Analytical Technologies (PATs). Risk assessments at the beginning and throughout the HME product development process are crucial to success, as recommended by the QbD philosophy and the ICH Q8(R2). Probably the most common tools are the construction of Ishikawa diagrams and the Failure Mode and Effects Analysis (FMEA) [252]. Risks in the Ishikawa diagram are included in categories, while in the FMEA the failure modes that have the greatest chance of causing product failure are identified and translated into a ranking [252]. Fishbone diagrams are useful as a starting point as they provide an overview of the system. Some examples of Ishikawa diagrams applied to HME processes have been published [29, 192, 242, 244, 252, 255, 257], and also an example of an FMEA [244]. An example applied to the initial risk assessment of an HME product is depicted in Figure 1.11. This preliminary approach should be complemented with a more detailed risk assessment tool, as the FMEA or the Risk Estimation Matrix (REM).

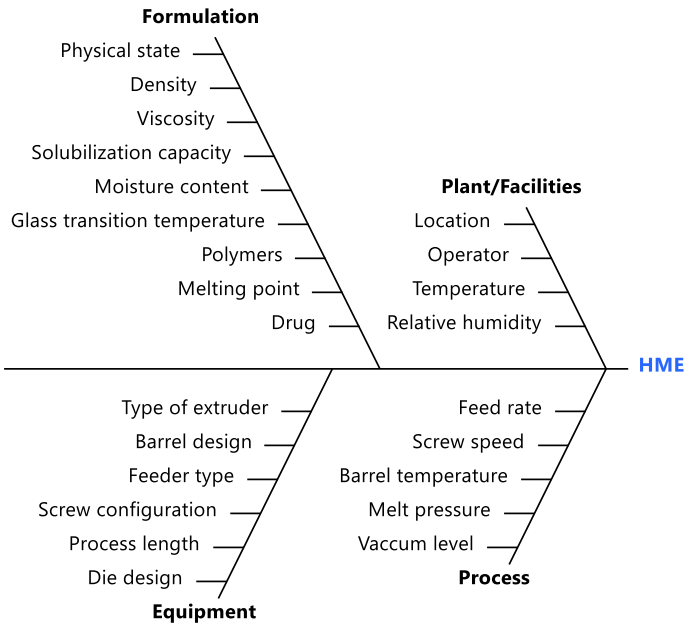

Figure 1.11. Fishbone diagram for an HME process based on ICH Q8(R2) recommendations.

The REM is especially useful for identifying factors for DoE studies and design space estimation, as it only considers the severity and the probability of occurrence, excluding the detection parameter of FMEA. This is the main advantage of REM, as no parameters are excluded from the DoE because of easy detection. It is the tool used by the FDA in their examples of pharmaceutical development report for ANDA submissions [260, 261]. As far as we know, no such example for HME is available in the literature, and Table 1.7 depicts an initial risk assessment based on REM of an HME process applied to the manufacturing of an ASD. The REM was created through a semi-quantitative analysis, where each process parameter was ranked as high, medium, or low-risk considering the severity and the probability of occurrence of the impact on the CQAs. Parameters identified as high risk should be further evaluated through a DoE. The risk ranking was performed on the assumptions of a cGMP environment and room conditions, both in manufacturing and storage, and the use of conventional equipment in a pharmaceutical facility, such as bin blenders, twin-screw extruders, and mills equipped with hammers or knives.

Table 1.7. Risk Estimation Matrix example of an initial risk assessment of the manufacturing process for an amorphous solid dispersion manufactured by HME. Each critical process parameter was qualitatively ranked as high, medium, or low-risk level considering the probability of occurrence and the severity of the impact on the CQAs.

Risk Estimation Matrix													
Process steps	**Room**	**Blending**			**Hot-melt extrusion**					**Cooling**	**Milling**		**Storage**
Process Parameters / CQAs	Temperature and RH	Order of Addition	Mixer Speed	Blending Time	Feed rate	Process temperature	Screw speed	Screw design	Residence time	Belt speed	Sieve Size	Sieve speed	Temperature and RH
Assay	Low	Low	Low	Med	Med	High	High	Med	High	Low	Med	Med	Low
Content Uniformity	Low	Low	Low	High	Med	Med	High	Med	Med	Low	Med	Med	Low
Dissolution	High	Low	Low	Low	High	High	High	High	High	Med	High	High	High
Degradation Products	Low	Low	Low	Low	High	High	High	High	High	Low	Low	Med	Med

Abbreviations: CQAs, Critical Quality Attributes; RH, Relative Humidity; High, high risk; Med, Medium risk; Low, low risk.

Since the institution of the QbD initiative, one of the most useful tools for the identification of design space is DoE. Indeed, DoE is the most effective approach to acquiring a good understanding of the process [160, 166, 255]. The adoption of statistical techniques based on desirability approaches and the evaluation of the optimization ability of statistical models has been widely used and has shown to be crucial for a successful product development [262, 263]. Several DoE studies have been published for ASDs, and some factors described to have a primary role for the physical stability of the formulation, such as drug load, polymer type, and physicochemical characteristics such as MW (molecular weight) [257, 264]. For instance, Pawar and his group developed an efavirenz HME formulation based on a QbD approach, where the combination of HPMCAS and SLP with 30% of the drug was optimized based on mathematical modeling [265]. Other studies have also highlighted the influence of process parameters, including screw speed, temperature, feeding rate, and screw design on product quality [160, 266-270]. It is important to note that in all the studies, involving DoE and statistical analysis, the dissolution rate is the most commonly defined dependent variable, which confirms and emphasizes the importance of this response for ASDs [255, 257]. In some cases, physical stability was also included in the statistical analysis, using both formulation and process as factors [264]. Typical QbD designs for pharmaceuticals were recently reviewed by Mishra *et al*. [251]. Moreover, a complete and practical review on DoE was published by Sandoz scientists, where the focus was current practices within the pharmaceutical industry, namely development strategies, typical experimental designs, and modeling methodologies [271].

Another important tool of QbD is PATs, which have been the focus of both regulators and the pharmaceutical industry. Along with the well-known ICH guidelines Q8 (R2), Q9, Q10, and Q11 [175, 272-274] emphasizing QbD and continuous manufacturing, FDA also issued the "PAT - A Framework for Innovative Pharmaceutical Manufacturing and Quality Assurance" guideline [275], regarded as the core of this concept [166]. PAT has been applied in HME to improve control and real-time analysis [39]. Rheology and several spectroscopic techniques, such as optical, ultrasonic, electrical, UV-VIS, Raman, and infrared, have been applied for HME production [37, 40, 276, 277]. Applications of PAT comprise the identification of polymorphic forms, characterization of solid-states (crystalline/amorphous), detection of degradation products, determination of water content, uniformity of drug, among others, via on-line, in-line, or at-line measurements of the CQAs [27, 278, 279]. PAT tools and their application in HME processes have been thoroughly reviewed [28, 280], but reports of PAT real applications in the pharmaceutical industry are still limited [39]. Besides, alternative techniques have demonstrated adequate capacity to control low amounts of crystallinity, such as terahertz, dielectric, NMR, and ultrasonic spectroscopies. These techniques were not used in HME so far, but they are likely to be applied in the future [28, 281]. This is still an

emerging issue for HME, with new publications each month [276, 282, 283]. A review was published in 2017 in collaboration with AbbVie, where the use of well-established and emerging PATs is assessed for the manufacturing of ASD by HME, with a focus on industrial manufacturing [281].

4.2.2. Design Space of an HME-product

HME fits well within QbD principles, namely defining a design space. By ICH Q8(R2), a design space is the "multidimensional combination and interaction of input variables (e.g., material attributes) and process parameters that have been demonstrated to provide assurance of quality", i.e. meeting the CQAs. For industries, the establishment of design space is a real advantage, since it is not considered a regulatory change provided they work within it [29, 255]. CPPs of HME processes may be readily determined, as the manufacturing at steady-state allows multiple sequential testing with minimal material losses. The knowledge of the overall process goals, the aims of each unit operation (e.g., feeding, conveying, blending, kneading, melting) and their relationship should be carefully evaluated to build the design space [254].

Several examples of QbD strategies for HME products published by the pharmaceutical industry are available, for instance by ACG Pharma [192], Amneal [237], Ashland [284], Novartis and Genentech [242], Foster Delivery Sciences [285], BASF in collaboration with ThermoFisher Scientific [243], Dr. Reddy's [286], Grünenthal [269], Boehringer Ingelheim [163], Evonik [244], Nektar Therapeutics and Mallinckrodt [158, 287], ThermoFisher Scientific [245], Merck [288], and others [289]. A Box-Behnken factorial DoE approach was reported by Pawar *et al.*, in which efavirenz was combined with SLP or copovidone, in three different drug loadings. Solubility and dissolution rate were studied through the effect of variables like polymer ratio, screw speed, and temperature, and the design space is provided [192]. The effect of HME process parameters on product performance of an amorphous nanosuspension was also studied by a Box-Behnken DoE [237]. In another work, a simplex centroid mixture design was applied to develop an optimized formulation of itraconazole processed by HME. Three different polymers were combined with the drug at 25% of drug load, and after modeling the best formulation was determined [284]. Desai *et al.* studied the impact of CPPs of the downstream processing step, namely injection pressure and solidification temperature of an HME-injection molding formulation. Risk assessment and other QbD concepts as CQAs and CPPs were applied, however, the authors provide no statistical analysis [242]. Other statistical methods to reach a design space have been also described in the literature, such as mixture designs [163, 289], central composite design [243, 269], retrospective analysis [269], Plackett-Burman

screening design [244], response surface design [244, 287], and response surface fraction factorial design [245].

As well noted by Debevec *et al.*, there is no uniform way of developing a design space for the pharmaceutical development of different dosage forms and regulatory guidance is still vague. Even though different strategies are acceptable, they must be based on sound science, risk management, adequate planning of experiences, and statistical data analysis [271].

5. Regulatory evaluation of HME-based products

In this era of building QbD, the pharmaceutical industry is entirely regulated, governed by several authorities and regulatory bodies. ASDs are complex formulations, where science is vital to guarantee product quality, not only regarding degradation but also in what concerns polymer science, physicochemical and thermodynamic concepts, physical stability, and process control. In this regard, possible questions/issues from the dossier reviewer's perspective may arise and are listed hereafter (Table 1.8). These questions should be taken into account not only during dossier compilation but addressed during product development.

Table 1.8. Possible questions from the reviewer's perspective focused on ASD issues. Adapted from [290].

Topic	Issue	Comments
Product Design and Understanding	Justification of the need for ASD formulation to achieve QTPP targets	-
	Use of appropriate biopharmaceutics tools (e.g., discriminating dissolution methods) to screen formulations	Discriminating capability can be demonstrated by conducting dissolution on ASD formulation with a spiked crystalline drug. Absorption modeling may be considered to determine the extent of phase change that can cause clinical BA failure.
	Justification for the selection of critical excipients including physical and chemical compatibility: polymer/additives selection and justification	To be considered: ▪ Miscibility with drug, ▪ Phase behavior under heat and humidity stress: phase separation, ▪ Phase behavior during dissolution: supersaturation behavior, ▪ Process considerations: e.g., HME vs. spray drying. Prototype formulation stability is not similar to excipient compatibility. Chemical compatibility should be carefully used.
	Justification of container closure system choice proposed by the applicant	Prove adequate protection to assure adequate product performance throughout the shelf life.
	Stability data to guarantee that the drug product will be physical and chemically stable	ICH stability conditions do not capture *in use* behavior. Demonstration of product performance under simulated *in use* condition is recommended:

Topic	Issue	Comments
	throughout the shelf life and *in use*.	▪ Induction seal broken; daily open and close, ▪ Potential transient exposure to high humidity (e.g., bathroom or kitchen storage, high humidity seasons), ▪ Decreased or no moisture protection until the container is exhausted.
	Physicochemical characterization of drug	E.g.: Phase behavior of crystalline and amorphous forms, the effect of humidity and heat stress.
	CMAs of drug	E.g.: ▪ Polymorphism, ▪ Crystalline vs amorphous behavior, ▪ Hygroscopicity, ▪ Thermal behavior (T_m and T_g), ▪ Solubility, ▪ Impurities, ▪ Residual solvents.
	CMAs of excipients	E.g.: ▪ Polymers: T_m, T_g, hygroscopicity, MW, viscosity, the effect of the substitution, amphiphilic/non-amphiphilic. ▪ Surfactants: hydrophilic-lipophilic balance, peroxide/aldehydes level.
	Justification for the drug loading limit	Selected drug load should be well below the limit of failure.
	Demonstration of scale up to commercial scale, Assurance that the product manufactured at the commercial scale has the same performance as the one used in pivotal studies, Verification of design space at a commercial scale when established at a lower scale	-
	Potential for continuous manufacturing	Including PATs implementation.
Control Strategy	Demonstrated and validated appropriate PAT methods for real-time product release	-
	Conventional methods for detecting crystallization during routine manufacture and lifecycle control (e.g., XRPD, dissolution, Raman, DSC, microscopy).	Product development might benefit from more advanced methods, e.g., spectroscopy (NMR, terahertz). The development of methods to detect crystallization should be done during product development. Method validation should demonstrate that it is suitable for use.

Topic	Issue	Comments
General regulatory considerations	ASD information, as an intermediate, should be included in the drug product section of eCTD	-
	Holding time studies should be carefully performed and justified	-
	Date of drug product manufacture: recommended to be the date of ASD addition to the final drug product	-
	Size/shape constrictions for generic tablets and capsules	For the US market [291].
	Comply with the Inactive Ingredient Database limits (maximum potency per dosage unit)	Otherwise, toxicological studies are required. For the US market.
Human use	Requirements for new excipients	A comprehensive evaluation of pharmacology, including carcinogenicity and chronic toxicity, is mandatory. Need to be recognized as GRAS.
	Requirements for GMP Manufacturing	Cleaning and validation requirements. All surfaces that come in direct contact with the materials or finished product must be nonreactive, nonabsorptive, and nonadditive.

Abbreviations: ASD, Amorphous solid dispersions; QTPP, Quality Target Product Profile; BA, bioavailability; HME, Hot-melt extrusion; ICH, International Council for Harmonisation; T_m, melting temperature; T_g, glass transition temperature; MW, molecular weight; CMAs, Critical Material Attributes; PATs, Process Analytical Technologies; XRPD, X-Ray Powder Diffraction; DSC, Differential Scanning Calorimetry; NMR, Nuclear Magnetic Resonance; eCTD, electronic Common Technical Document; GMP, Good Manufacturing Practices; GRAS, generally recognized as safe.

The need for an ASD formulation, a complex composition, to achieve the QTPP should be appropriately justified, and this should be performed through a patient-centric perspective: to improve BA, physical stability, decrease the drug burden or improve the overall safety profile of the drug product. The usage of appropriate biopharmaceutical tools is also of foremost importance for this type of formulations. Usually, dissolution tests are applied, but they need to be demonstrated as discriminative and capable of detecting small amounts of drug crystallization. It is recommended to complement dissolution with solid-state characterization, most commonly X-Ray Powder Diffraction (XRPD), but DSC may also be applied and, more recently, Raman spectroscopy [174, 176, 255]. Owing to the high impact on drug release and BA, this should be assessed not only during formulations screening but also throughout the whole product and process development, as well as in pre-stability and ICH stability studies.

The selection of critical excipients should also be appropriately justified, namely in what concerns the impact on the physical stability and chemical compatibility with the drug. Similarly, the container closure system needs to be evaluated through stability studies but also *in use*. Usually, a new shelf-life after opening High-density polyethylene (HDPE) bottles is defined, due to the impact of moisture on product physical stability. Concerning CMAs, both the drug and the excipients require extensive evaluation in terms of polymorphism, thermal behavior, and hygroscopicity, but the impact of moisture should be particularly evaluated. Moisture causes a decrease in the overall blend T_g [292], which may lead to increased molecular mobility and eventually recrystallization.

The batch upscale also needs to be carefully monitored and the end product fully characterized, due to the high impact of process parameters on the ASD physicochemical properties. The product manufactured at the commercial scale must have the same performance as the one used in pivotal studies. Therefore, if the design space is established at a laboratory or pilot scale, it should be verified at the commercial scale to assure quality performance throughout the product lifecycle.

A control strategy for the entire process, encompassing input material controls, process monitoring and controls, design spaces around individual or multiple unit operations, and/or final product specification should also be established. PAT tools may be incorporated into the control strategy for real-time monitoring and control of the process. If used, PATs need to be studied, demonstrated, and validated for the intended purpose.

For the CTD, detailed data on the ASD as an intermediate should be included in the drug product section and characterized almost as an end product. The extrusion process should also be considered within hold-time studies, for instance from extrusion to downstream processing and from processed extrudate to final blending.

In what concerns inactive ingredients, only the ones generally recognized as safe (GRAS) are listed in the FDA's inactive ingredient database, have a compendial monograph, or documented human use at specific levels. To ensure that all new excipients are safe for use in humans, a comprehensive evaluation of pharmacology, including carcinogenicity and chronic toxicity, is mandatory [293]. This is especially relevant to HME-based formulations because the amount of polymers is typically much higher than the present in conventional dosage forms, where they are used as binders or as film-forming agents in coatings.

Finally, and common to other processes, all extruders used for pharmaceutical HME processes must also comply with the cleaning and validation requirements of the GMPs, and all surfaces that come in direct contact with the materials or finished product must be nonreactive, non-absorptive, and non-additive [294].

5.1. Case studies of recent approvals

In this section, the latest approvals of ASD manufactured by HME are analyzed as case studies within the QbD paradigm.

5.1.1. Belsomra® (Merck, 2014)

Belsomra® was developed by Merck and was approved in 2014 in the US [67], and also in Japan [295]. It is an ASD prepared by HME to maximize BA, as a BCS class II compound [61]. The team has selected to extrude the compound with a pH-independent solubility polymer, copovidone [68], and to coat and pack in aluminum blisters, to protect from light and moisture. The product development followed full QbD principles, from the compound synthesis to product development and manufacturing. In the drug synthesis, DoE and statistical analysis were applied for a complete understanding of the process, namely identification of QTPP and CQAs, risk assessment, and DoE to understand the impact of CMAs and CPPs on the product performance. Moreover, the design space was identified and the proposed ranges further confirmed (Proven Acceptable Ranges, PARs) by worst-case-scenario experiments. DS specifications, in most cases, were established based on multi-factor DoE and design space. A complete control strategy was presented, with raw materials specifications, in-process controls (IPCs), and release specifications [296].

The development of the drug product was also based on QbD principles, and design spaces were proposed for several unit operations [296]. For instance, CQAs were defined through risk assessment and are listed as, among others, content uniformity, assay, degradation products, physical form, stability, and dissolution. The discriminating ability of the dissolution method was proven towards several CPPs. It is the same method and specification for all the strengths, and similarity between them was proven, indicating that the lower and the higher strengths have similar performance. Drug release, as one of the most critical CQAs, was used as a response parameter to support the design space of the product. A multiple level C *in vitro-in vivo* correlation (IVIVC) model was developed to support the proposed dissolution acceptance criterion and even to establish IPCs [297]. This correlation was published, and the authors stated that a clear relationship between dissolution, disintegration, and C_{max} exists [28, 61]. The IVIVC was validated for C_{max} for specific dissolution time points and tablet disintegration time. Then, tablet hardness was linked to dissolution to provide adequate ranges, which allowed the establishment of a clinically relevant

IPC. This study sheds light on IVIVC as a complementary tool to QbD, namely to support the establishment of clinically relevant controls [61].

5.1.2. Viekirax® /Technivie® (AbbVie, 2015)

Viekirax® (EU)/Technivie® (US) is a fixed-combination tablet, developed by AbbVie and approved in 2014 by EMA, and in 2015 by FDA. All three drugs are individually converted into amorphous materials by HME to enhance their BA. Only then the individual extrudates are combined, tableted, and coated [64]. Tablets are packed in aluminum blisters (US) or Polyvinylchloride/Polyethylene/Polychlorotrifluoroethylene (PVC/PE/PCTFE) – Alu blisters (EU) for maximum water vapor and oxygen protection. The development was focused on optimizing the three solid dispersions, individually. During the first steps of formulation development, ombitasvir and paritaprevir solid dispersions were manufactured by spray drying, but a solvent-free process was preferred. Moreover, *in vivo* studies comparing spray drying to HME showed that both C_{max} and AUC from the HME formulations were substantially higher. Ritonavir followed the path of Norvir®, keeping the same manufacturing process (HME) and extrudate composition [64]. During HME, the three drugs are converted from the crystalline to the amorphous state, with no recrystallization on storage [64, 298, 299].

There is not much available information on the development of this product. To our knowledge, there is no additional literature besides the published by EMA and FDA during product review [64, 298, 299]. They applied risk assessments, and other QbD concepts as QTPP and CQAs definition, the study of CPPs and CMAs through DoE, data modeling, and statistical analysis (no details available) [298]. A final risk assessment and a control strategy is referred to, both for the control of drugs synthesis and the manufacturing of the final product [64]. The release of the finished product includes typical parameters for an ASD, for instance, degradation products, solid-state form, water content, and dissolution [64, 298]. The discriminating power of the dissolution method was proven, and specification criteria thoroughly discussed between the applicant and the agency [298]. Although this method does not meet sink conditions, it does provide sensitivity to crystallinity.

5.1.3. Venclyxto®/ Venclexta® (AbbVie, 2016)

Venetoclax was developed by AbbVie in collaboration with Genentech and Roche and was approved as Venclyxto® in the EU and as Venclexta® in the US, both in 2016. It is also manufactured by HME as a solid dispersion due to the very poor water solubility of this compound [69]. Mixtures

of drug and copovidone with surfactants were extruded to enhance BA [70]. It is available in HDPE bottles and unit-dose PVC/PE/PCTFE aluminum foil blisters, which demonstrated to provide adequate protection from oxygen and moisture to avoid chemical degradation or recrystallization of the product [69]. The development of this product also followed QbD principles, from the synthesis of the compound to the development of the drug product. A systematic approach was taken during the development of the DS: identification of the potential drug CQAs that could affect drug product QTPP, identification of CMAs and CPPs through prior knowledge, DoE, and use of process understanding and risk management to establish the control strategy. The development of the manufacturing process was based on a combination of univariate studies, DoE, and kinetic modeling, but no design space has been claimed by the applicant [69, 300].

The focus of formulation development was set on BA, storage stability, and manufacturability. The development of the finished product contains QbD elements too, similar to the previously described for the drug, with no request for design space approval. The development was based on experience with similar products, published literature, DoE, and material characterization. It ends with the updated risk assessment, where low risks were rated for all parameters, and the control strategy, where CPPs and IPCs for the extrusion were determined to ensure a homogeneous blend and adequate dissolution. Besides, target parameters and PARs were specified for each CPP [69]. The release specification includes appropriate tests for an ASD, including water content, dissolution, and degradation products [69, 301], from which dissolution and water content were considered the most critical. The dissolution recommended for quality control is a reciprocating cylinder (United States Pharmacopeia, USP apparatus 3) with 250 mL de phosphate buffer pH 6.8 with 0.4% sodium dodecyl sulfate (SDS), considered biorelevant. This method has demonstrated a discriminating capacity to changes in the crystalline venetoclax content of tablets, and this is why solid state analysis of venetoclax tablets is not performed [69]. After a discussion with the agency, a strength-dependent multi-point dissolution acceptance criteria was established [301]. The three strengths have different dissolution profiles as the release is governed by erosion, however available *in vivo* studies did not indicate a relevant difference in BA [69]. To understand the mechanisms of drug absorption in humans, a Physiologically Based Pharmacokinetic (PBPK) model was developed by AbbVie, verified with fed and fasted clinical studies, as well as clinical drug interaction studies [302]. This study demonstrated how innovative tools, as PBPK models, may be applied and be part of product development, in a clear trend to turn the development of pharmaceutical products more and more patient-centered.

5.1.4. Maviret®/Mavyret® (AbbVie, 2017)

The latest approval of an HME-based ASD, to our knowledge, is a fixed-drug combination of glecaprevir and pibrentasvir, also developed by AbbVie, and approved under the names Maviret® by EMA or Mavyret® by FDA. Both drugs are poorly water-soluble, and they are also individually formulated as ASDs to increase solubility and to enhance BA [71]. The individual extrudates are milled, compressed into bilayer tablets, and coated with an esthetic film. Tablets are packed into blister cards of PVC/PE/PCTFE-aluminum, to protect from moisture. There is not much available information on the development of this product. To our knowledge, there is no additional literature besides the published by EMA and FDA during product review [71, 303, 304]. The synthesis process of both drugs is well described and controlled, including CPPs with proper ranges to ensure a product with consistent quality. An adequate control strategy was also provided to authorities [71], but a complete QbD study was not mentioned.

In what concerns the formulation development, the focus was the enhancement of BA and physical stability. It started with the development of the individual solid dispersions as first-in-humans tablets, used in early phases of clinical development [304]. A full QbD approach was taken to develop the tablet formulation and manufacturing process, although the applicant did not claim a design space. The QTPP was defined, as well as the product CQAs. Then, systematic evaluation and optimization of the manufacturing process, namely the relationship between CMAs and CPPs with the product performance, were carried out using DoE, statistical analysis, and mathematical modeling. For instance, several particle sizes of both drugs were evaluated and an appropriate specification set. The control strategy was then defined and the risk assessment updated to demonstrate that the risks were mitigated. The release specification includes appropriate tests for an ASD, like degradation products, water content, and dissolution [71]. The dissolution method demonstrated the capacity of discriminating specific changes in formulation or process parameters. The applicant used a two-stage numerical deconvolution approach to establish an IVIVC, but it was not successful, although a relationship between *in vitro* and *in vivo* data was noticed. A two-point specification was set for both drugs due to the slow release from tablets [303]. It is not mentioned if the dissolution method can detect drug crystallinity, but full amorphicity is controlled after extrusion [71]. Besides, the effect of different tablet manipulations (namely splitting, crushing, or grinding) on the BA of the two compounds was assessed in phase 1 clinical trial. Splitting tablets demonstrated no relevant impact on BA, but crushing or grinding is not recommended [305]. This study is also part of QbD, as it enhances the knowledge on the product behavior, apart from guiding the adequate administration to patients.

6. Conclusion

HME is not yet a common technique to manufacture new DDS, and few products have reached the market so far. This trend is clearly being shifted as more and more HME products are finally getting into the pipeline of pharmaceutical companies, which is also translated by the high number of publications found in this field. Technical and scientific challenges of amorphous forms and the intrinsic complexity of these developments request the collaboration of specialists from industry and academia. This reflects the science and the dedication needed for successful ASDs development. Moreover, the increasing number of recent publications from pharma is quite high, demonstrating a stronger trend in sharing work and scientific achievements.

Other techniques have been used in the industrial setting for the amorphization of practically insoluble drugs, including spray drying, freeze drying, and supercritical fluid drying. However, HME is the only solvent-free technology, easily upscalable, fast, which allows a continuous process and with a small footprint. HME has also some disadvantages: it works under high temperatures (which may lead to the rejection of thermolabile compounds), it requires downstream processing most of the times and also the input of a high amount of energy. Moreover, the number of polymers with thermoplastic characteristics approved for pharmaceutical application is admittedly low and it still presents unique challenges due to the metastable nature of ASDs. Specifically for ASDs, the impact of process parameters on the product quality is crucial, and small variations in the feeding rate, local temperature, screw speed, resident time, or cooling rate, may lead to an end-product with slightly different internal microstructure. As we are referring to ASDs, this may lead to an entire batch failure due to a dramatic change in the dissolution behavior. Indeed, a complete understanding of the complex relationship interplay between process and product parameters must be dominated to ensure quality and consistency.

As an attractive alternative to other processes, the interest in HME rapidly grown and several companies are now specialized in HME as a new delivery technology and have developed a significant (and recent) intellectual property. This is one of the issues related to the widespread product development using HME, as the number of patented technology platforms is rising very fast, and specific uses may be then blocked.

The aim of this work was to look at how to develop and submit new products to regulatory authorities. There is no established approach, even after decades of working with solid dispersions. Based on a thorough literature research focused on reports from the pharmaceutical industry and the experience of our group, a systematic step-by-step approach for the development of HME products was proposed. Common thermodynamic assessments were reviewed and illustrated with proven application examples from the industry. However, further developments are still expected in the next couple of years. The success of the future developments lies in not giving up the research on the applicability of thermodynamics and other predictive methods as replacements for the current strategies. Useful and practical methods, rather than heavy and unfeasible ones, able to rapidly guide formulation scientists towards the right formulation will certainly be beneficial.

As a core in product development, the QbD paradigm applied to HME was discussed, including steps and tools for its implementation and a risk assessment based on REM that can support regulatory dossiers. Moreover, possible questions from reviewers were listed, which reflect the technical and scientific specificities of this type of formulations. HME has unique adaptability to QbD and PAT tools, recognized by the FDA. The construction of design spaces for HME products was also reviewed and supported by case studies of the latest approvals within the QbD paradigm. The usefulness of design space in the pharmaceutical industry will certainly lead to further research and new publications, as there is yet no uniform method. New thoughts, discussions, and guidance from regulatory agencies in what concerns expectations on design space submissions would be valuable for formulation scientists.

The QbD philosophy is considered very useful for pharmaceutical development, and the primary proof is their application by all the recent approvals discussed in this work. In all the dossiers, QbD elements and steps as the definition of QTPP, identification of CQAs, risk assessment for identification of critical parameters or attributes, process and product understanding by DoE, data analysis, and modeling were carefully applied throughout the product development. In any case, the developments are more and more science-based, as requested by the QbD paradigm, and development decisions, the definition of controls, specifications, and even IPCs are more patient-centered and focused on what is clinically relevant. HME will continue to be highly explored and investigated since simple formulations can be used to solve complex delivery issues. Moreover, as lipophilicity is the trend of new therapeutic compounds, the use of enabling formulations will be highly sought in the forthcoming years. HME will undoubtedly be a leading technology in this new paradigm, as a novel solution to poor BA and drug delivery through innovative platforms.

CHAPTER II. FIVE-STAGE APPROACH FOR A SYSTEMATIC SCREENING AND DEVELOPMENT OF ETRAVIRINE AMORPHOUS SOLID DISPERSIONS BY HOT-MELT EXTRUSION

Abstract

This study aimed to develop a fast, effective, and material sparing screening method to design amorphous solid dispersions of etravirine, leading to improved solubility, and stability. A systematic step-by-step approach was followed by combining theoretical calculations with high-throughput screening and software-assisted multivariate statistical analysis. The thermodynamic miscibility and interaction of the drug in several polymers were predicted using Hansen solubility parameters. The selected polymers were evaluated in a high-throughput manner, with solvent evaporation. Binary compositions were evaluated by their solubilization capacity and physical stability over 2 months. JMP® 14.0 was used for multivariate statistical analysis using Principal Components Analysis. In general, a good correlation was found between the results of theoretical predictions, high-throughput screening, and the HME. PVP-based formulations were shown to be easily extrudable, with low degradation and complete amorphicity. The drug release rate was improved more than two times, and the manufactured system demonstrated to be stable physical and chemically. The unexpected stability at 40°C / 75% RH was correlated with the presence of molecular interactions characterized by Raman spectroscopy. A fast and effective screening technique to develop stable amorphous solid dispersions for a poorly soluble drug was successfully applied to etravirine. The given method is easy to use, requires a low amount of drug, and is fairly accurate in predicting the amorphization of the drug when formulated.

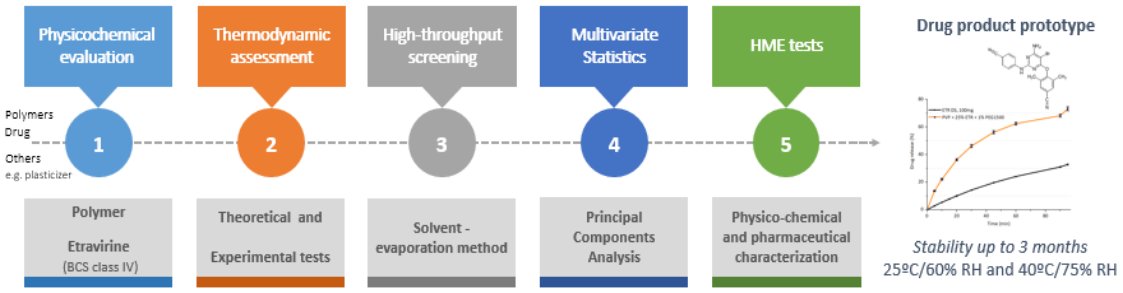

Figure 2.1. Graphical abstract of chapter II. A systematic step-by-step approach for the development of an etravirine solid dispersion by HME.

The results presented in this chapter were published in Simões MF, Pereira A, Cardoso S, Cadonau S, Werner K, Pinto RMA, Simões S. Five-Stage Approach for a Systematic Screening and Development of Etravirine Amorphous Solid Dispersions by Hot-Melt Extrusion. Mol Pharm. 2020 Feb 3;17(2):554-568. doi: 10.1021/acs.molpharmaceut.9b00996.

My contribution to this work was performing thermodynamic predictions, designing and performing the systematic screening of promising formulations, the HME laboratory tests, characterization by PLM, and interpretation of thermal analysis, XRPD, and Raman spectroscopy results, and statistical analysis. The analytical characterization by HPLC and UPLC was performed by the analytical development team of Bluepharma, thermal analysis, and XRPD characterization was conducted at UCQfarma (Faculty of Pharmacy of the University of Coimbra), and Raman spectroscopy by Rui Fausto and coworkers in the Department of Chemistry of the University of Coimbra.

This chapter is not an integral copy of the published work.

1. Introduction

In the last three decades, the use of HTS methodology generated a large number of new drug candidates with poor aqueous solubility, generally classified as class II or IV as per BCS [27, 63]. The poor aqueous solubility and dissolution rate of class II and IV molecules are rate-limiting steps for absorption, which generally leads to low BA and their failure as drug candidates. To overcome solubility issues and increase the likeliness of low solubility drugs as viable options for further drug development, diverse approaches have been employed, such as drug-polymer solid solutions/dispersions (amorphous systems) [25, 26, 119]. Although thoroughly used as synonyms, a solid solution is not a solid dispersion. The drug may be molecularly dispersed within the matrix (i.e., a solution), or exists in small clusters of a crystalline or amorphous phase (i.e., a solid dispersion). However, drugs and excipients are miscible over a limited range, and a true solid solution is in practice not always clearly distinct from an amorphous dispersion. The term ASD is therefore broadly applied in these cases.

The application of ASDs using hydrophilic polymers has been proved to be effective in improving the dissolution performance of poorly water-soluble drugs [25, 26]. These systems often lead to an improvement of BA by increasing its surface area, as given by the well-known Noyes-Whitney equation [27, 306]. A comprehensive understanding of a solid dispersion structure, particularly the existing physical form of a drug in the carrier matrix is required to predict the stability, solubility and hence the BA of the solid dispersion [307]. ASDs are a result of a kinetic entrapment of the drug in its amorphous state. Although these types of systems exhibit an increased rate of dissolution due to high thermodynamic activity, they have also the potential to revert to the more stable crystalline form [39]. This is the main issue associated with ASDs: the physical instability on aging in the form of phase separation which can affect the dissolution performance [33, 34, 36, 37, 40].

Etravirine (Figure 2.2), chemically designated as 4-[[6-amino-5-bromo-2-[(4-cyanophenyl) amino]-4-pyrimidinyl] oxy]-3,5dimethylbenzonitrile and hereafter named as ETR, is a second-generation nonnucleoside reverse transcriptase inhibitor (NNRTI) which acts by blocking the viral reverse transcriptase enzyme. By preventing the enzyme from converting its genetic material (RNA) into proviral DNA, it prevents the incorporation of the viral genome into the human host cell [308].

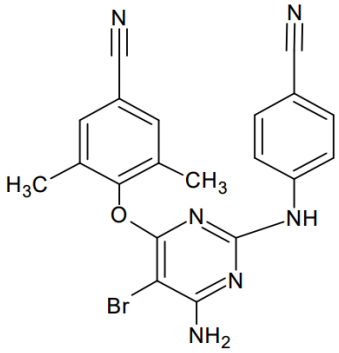

Figure 2.2. Chemical structure of ETR.

ETR is marketed under the name Intelence®, both in EU and in the US by Janssen Pharmaceuticals, Inc., and is indicated for the treatment of HIV-1 infection in treatment-experienced patients 6 years of age and older with viral strains resistant to an NNRTI and other antiretroviral agents. The physicochemical properties of ETR are undoubtedly challenging concerning formulation and BA as indicated in Table 2.1. The crystalline drug, available as needle-shaped (Figure 2.3), is classified as a BCS class IV compound.

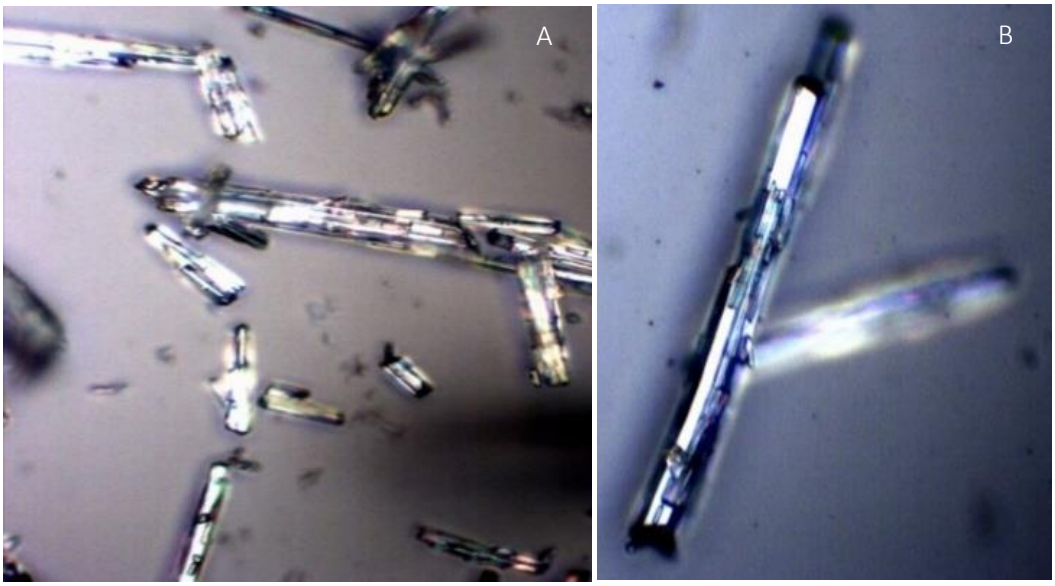

Figure 2.3. Crystalline ETR: typical needle-shaped particles from two different batches, A and B. Observed through polarized light microscopy, objective 50x.

Table 2.1. Physicochemical and solubility properties of ETR [309-311].

Characteristic	Value
Molecular weight	435.28 g/mol
Molecular formula	$C_{20}H_{15}BrN_6O$
Melting point	260°C, followed by immediate decomposition
Polar Surface Area	120.64 $Å^2$
Log P	> 5
pKa (base)	< 3
BCS class	IV
Solubility in aqueous media	< 1 mg/mL Practically insoluble in water over a wide pH range
Solubility in Polyethylene glycol 400	Soluble
N, N-dimethylformamide and tetrahydrofuran	Freely soluble
Molar Volume	275.7 ± 5.0 cm^3

The clinical use of ETR depends on formulation strategies that allow a suitable BA, and currently, spray drying is the process in use by Janssen to manufacture oral dosage forms of ETR. Other formulation strategies have been reported in the literature to enhance the drug release and thus the BA of ETR. Weuts and colleagues suggested a three-part strategy to predict the formulation-ability of ASDs of ETR, that includes an assessment of the amorphous form, a study of binary cast films and the evaluation of a mixture of the drug and polymer processed in a manner relevant to the intended final dosage form [309]. Later, Ramesh *et al*. prepared ASDs of ETR using both HME and spray drying, and faster and high drug release was found in the ASDs prepared by HME with SLP in the ratio of 1:3, which is justified by the fourfold increase in the ETR solubility when dispersed in this polymer [312]. The same group also prepared ASDs of ETR by solvent evaporation technique. One of the prepared formulations comprising ETR, poloxamer P407, and SDS (1:2:1) has shown enhanced solubility of about ninefold and a significant improvement in drug release rate, as well as BA in male Wistar rats [313]. More recently, the drug release characteristics of ASDs of ETR prepared by spray drying, in dichloromethane, were evaluated in three different dissolution media [314].

The search for an optimal polymer screening methodology to speed up the development of ASDs is still a trending topic and a lot of work has been published lately [25, 229-232, 234, 235, 315]. Recently our group published a keynote review where a strategy that combines theoretical calculations, HTS, and software assisted-multivariate statistical analysis is applied for systematic step-by-step development of feasible HME-based solid dispersions, with adequate dissolution, stability and BA [316]. In this study, the described approach is applied to ETR in the development of an ASD, manufactured by HME (Figure 2.4). The screening of several polymers was performed

by a high-throughput solvent evaporation technique, both for solubilization capacity and physical stability. The most promising systems were selected for HME tests. The HME systems were characterized and the influence of drug physical state on the dissolution performance was evaluated accordingly. To our knowledge, this is the first study that correlates rational polymer identification and selection based on thermodynamics, with a fast forward HTS technique, characterization, and stability of solid dispersions of ETR prepared by HME.

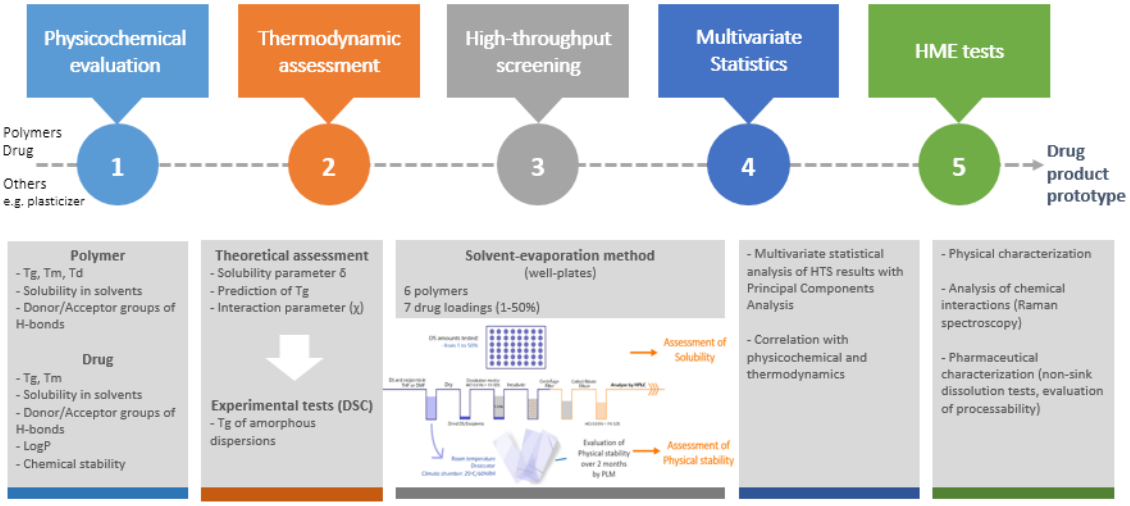

Figure 2.4. A step-by-step approach for the development of ETR solid dispersion by HME. Adapted from [316] to the ETR case study. Abbreviations: DSC, Differential Scanning Calorimetry; PLM, Polarized Light Microscopy; HTS, High-throughput screening.

2. Experimental section

2.1. Materials

ETR and impurity 1 standard were supplied by Midas Pharma. PVPVA, brand name Kollidon® VA64, and PVP of grade K12, brand name Kollidon® 12PF, were obtained from BASF (Ludwigshafen, Germany). HPMC grade E5 was obtained from the Dow Chemicals (Redmond, WA), and HPMCAS grade MF, brand name AQOAT®, was kindly donated by Shin-Etsu (Totowa, NJ). PEG grade 1500 was acquired from Clariant (Muttenz, Switzerland).

2.2. Methods

2.2.1. Systematic Identification of ASD Components

2.2.1.1. Calculation of Solubility Parameters

The Hansen solubility parameters, δ [142, 164], of drug and polymers were calculated from their chemical structures using the van Krevelen and Hoftyzer group contribution method [180]. For each molecule, three Hansen parameters were calculated: the energy from dispersion forces between molecules (Equation 2.1, δ_d); the energy from the dipolar intermolecular force between molecules (Equation 2.2, δ_p); and the energy from hydrogen bonds between molecules (Equation 2.3, δ_h).

Equation 2.1. $\delta_d = \frac{\sum F_{di}}{V}$

Equation 2.2. $\delta_p = \frac{\sqrt{\sum F_{pi}^2}}{V}$

Equation 2.3. $\delta_h = \sqrt{\frac{\sum E_{hi}^2}{V}}$

where F_{di}, F_{pi}, and E_{hi} are the group contributions for different components (dispersion forces, polar interactions, and hydrogen bonding, respectively) of structural groups that are reported in the literature at 25°C [180], and V the molar volume.

The total solubility parameter (Equation 2.4, δ_t), generally measured in $MPa^{0.5}$, was then determined through the combination of solubility parameters, as follows:

Equation 2.4. $\delta_{total} = \sqrt{{\delta_d}^2 + {\delta_p}^2 + {\delta_h}^2}$

For a system without specific interactions, the χ (Flory-Huggins drug-polymer interaction parameter) may be determined from the solubility parameters of those two components [211, 317]. The relationship between χ and the solubility parameter is given by Equation 2.5 [180]:

Equation 2.5. $\chi = \frac{V_{site}}{RT}(\delta_{drug} - \delta_{polymer})^2$

where V_{site} is the hypothetical lattice volume, R is the gas constant, T is the absolute temperature, and δ are the solubility parameters of the drug and the polymer, respectively.

2.2.1.2. Prediction of T_g of the ASD through the Gordon-Taylor equation

For a given molecule, the T_g of the overall formulation can be modulated by selecting different polymers. The T_g of a miscible blend (drug and polymer) is given by the Gordon–Taylor equation (Equation 2.6) [178]), or the simplified form by Fox (Equation 2.7) [179]):

Equation 2.6. $Tg = \frac{w_1 Tg_1 + K w_2 Tg_2}{w_1 + K w_2}$

Equation 2.7. $\frac{1}{Tg} = \frac{w_1}{Tg_1} + \frac{w_2}{Tg_2}$

where T_g, T_{g1}, and T_{g2} are the glass transition temperatures of the blend and the two different components, respectively; w represents the weight fraction; and the value of K is calculated from the Simha–Boyer rule (Equation 2.8), where ρ indicates the true density of the component [318]:

Equation 2.8. $K \approx \frac{\rho_1 Tg_1}{\rho_2 Tg_2}$

2.2.2. High-throughput screening of carriers

2.2.2.1. Design of screening of binary systems

The study was designed to allow a set of screening assays in high-throughput nature, miniaturization (material sparing, small sample size), and prompt response, and encompassed 6 different polymers and drug in 7 charge levels, ranging from 1% to 50%. ETR and a panel of 6 polymers were dissolved in tetrahydrofuran (THF) or N, N-dimethylformamide (DMF), solutions

of 10% Polymer + ETR, and dispensed into the wells of a 48-well plate (n=2). The preferred solvent was THF for rapid drying. DMF was used when the polymer was not soluble in THF, which was the case of PEG, HPMC, and HPMCAS. The solvent was then evaporated.

2.2.2.2. Solubilization capacity (HPLC)

Following solvent evaporation, the neat formulations were incubated at 37°C for 1 h with standard dissolution media (1.5 mL of HCl 0.01N + 1% SDS). The solubilization capacity of the excipients for the compound was determined by High Performance Liquid Chromatography (HPLC). The content of ETR (%) in each formulation was calculated against an external standard solution at 100% of the theoretical target concentration. The analytical column used was Zorbax SB-Phenyl (150 x 4.6 mm; 3.5 µm) and was operated at 30°C with a flow rate of 1.0 mL/min and UV detection at 325 nm. The mobile phase used was a mixture of MeOH: H_2O (90:10, % v/v), in the isocratic mode. The injection volume was 5 µL and the run time defined was 3 min (retention time of ETR was 2.25 min). Data was integrated using Empower® software.

2.2.2.3. Physical stability

Evaluated by PLM using Motic® BA310MET-T (Motic Europe, S.L.U., Barcelone, Spain) for 2 months, under exposure to room temperature, desiccator and 25°C/ 60% RH. Glass slides were examined directly for birefringence with reflected polarized light. Crystalline structures were evaluated qualitatively on a scale from 1 to 5 in terms of both crystals size and quantity. The plasticizing capacity of the produced films was also confirmed by PLM (Figure 2.5).

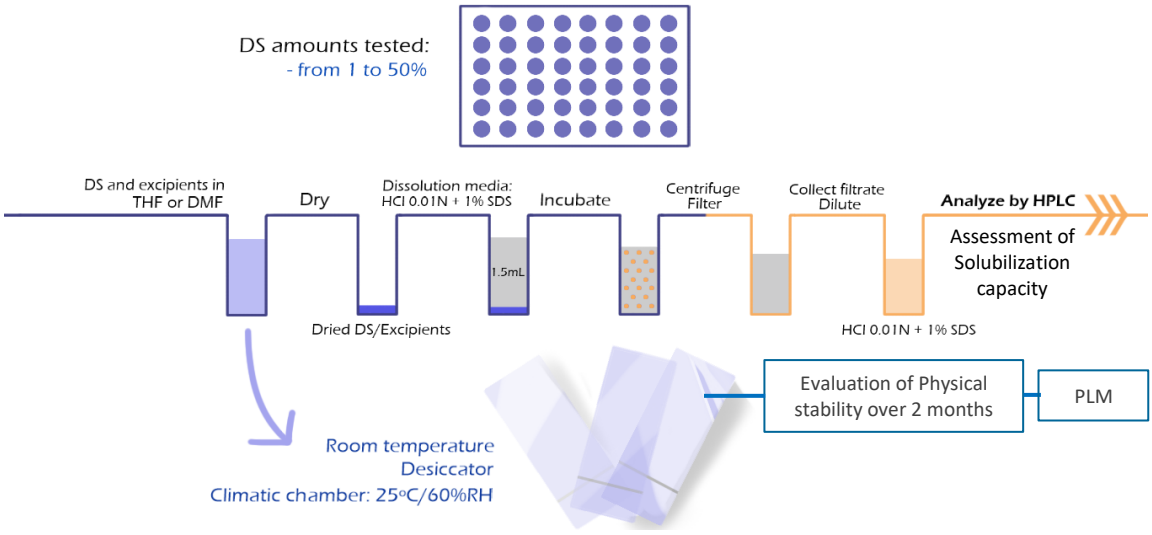

Figure 2.5. High-throughput screening of polymers for HME formulation development by solvent evaporation technique. Abbreviations: DS, Drug substance; THF, Tetrahydrofuran; DMF, Dimethylformamide; SDS, Sodium dodecyl sulfate; HPLC, High performance liquid chromatography; PLM, Polarized Light Microscopy; RH, Relative humidity.

2.2.3. HME at Laboratory Scale

HME was performed using a corotating twin-screw extruder Thermo Scientific® HAAKE MiniLab II (Thermo Scientific, UK). Temperature and screw speed were optimized based on extrudate appearance, extrudability, torque, and ease of manual feeding. The powder blends were added manually in small amounts. Screening formulations of ETR with PVP, PVPVA, and SLP were prepared with a ratio of 1:3 (w/w), using batch sizes of 5 g. Selected formulation (PVP k-12 + 1% PEG 1500 + 25% ETR) was prepared at 25 g scale. A round die with a diameter of 2 mm was attached to the extruder. The screw is conical with conveying elements only. All the glassy material exiting the extruder was cooled in a conveyor belt to room temperature and then ground at 20 000 rpm in IKA® M20 to a fine powder. This powder was finally collected to glass bottles and stored in a desiccator to keep it moisture free.

2.2.4. Analytical Methods for Characterization of Solid Dispersions

2.2.4.1. In vitro dissolution test (HPLC)

In vitro drug release behavior of solid dispersions in capsules was performed using Apparatus II (USP paddle apparatus) with a rotation speed of 75 rpm. A non-sink dissolution method was chosen to assess the performance of ASDs as well as crystalline dosage forms. Dissolutions tests

of samples (pure ETR and HME formulations) containing the equivalent to 100 mg of ETR were performed in 900 mL of HCl 0.01N + 1% SDS medium at the temperature of 37.0 ± 0.5°C in two phases: phase 1 was 500 mL of degassed 0.01 N HCl for 10 min and, in phase 2, 400 mL of 2.25% SDS in 0.01 N HCl was added. At a predetermined sampling schedule, 8 mL of solution was withdrawn and filtered through online tip filters at first and then with 0.45 µm filter, previously tested. The amount of drug released was quantified by the HPLC method, against an external standard solution at 100% of the theoretical concentration.

The analytical method used a mixture of MeOH: H_2O (90:10, % v/v) as mobile phase, in the isocratic mode. The analytical column used was Zorbax SB-Phenyl (150 x 4.6 mm; 3.5 µm) and was operated at 30°C with a flow rate of 1.0 mL/min and UV detection at 325 nm. The injection volume was 5 µL and the run time was 3 min. The data were integrated using Empower® software. The dissolution method was pre-validated in terms of selectivity, linearity, system precision and filtration, and samples stability, according to ICH guidelines, to demonstrate that it was suitable for its intended purpose.

2.2.4.2. Quantification of Assay (UPLC)

For assay determination, an Ultra Performance Liquid Chromatography (UPLC) method was developed and pre-validated. A UPLC method operates at higher pressures with improved analyte separation and detection, lower mobile phase consumption, and shorter run times when compared with the HPLC method. An Aqquity UPLC HSS PFP (50 x 2.1 mm; 1.8 µm) analytical column was used at 40°C, with a flow rate of 0.3 mL/min and UV detection at 325 nm. The injection volume was 5 µL with a run time of 2 min. A mixture of MeOH: H_2O (80:20, % v/v) was used as a mobile phase and as a solvent.

2.2.4.3. Quantification of Related Substances (HPLC)

A gradient HPLC method was used for quantification of related substances in drug product using a Zorbax SB-C18 (150 x 4.6 mm; 3.5 µm) at 30°C. The flow rate was 1.0 mL/min and UV detection at 303 nm. The injection volume was 10 µL and the run time was 35 min. Ammonium acetate buffer at pH 6 was used as mobile phase A and a mixture of MeOH: Acetonitrile (50:50, % v/v) was used as mobile phase B. The solvent used was methanol. For the development of this method, known related substances from ETR and degraded samples were used to predict

the retention time of each peak in the chromatogram and to ensure the best separation of each impurity.

2.2.4.4. Polarized Light Microscopy

Representative fragments of unmilled extrudate were examined directly for birefringence with polarized reflected light using Motic® BA310MET-T (Motic Europe, S.L.U., Barcelone, Spain).

2.2.4.5. Thermal Analysis (DSC and TGA)

DSC was performed in a Pyris® 6 (Perkin Elmer, Massachusetts, US). Data analysis was done using Pyris® thermal analysis software (Perkin Elmer, Massachusetts, US). Samples of 2-4 mg were weighed and placed in aluminum crimped pans. Samples were equilibrated at 25°C for 1 min and then heated on a heating rate of 10°C/min from 25 to 300°C.

Modulated temperature DSC (mDSC) was performed in a Q100 (TA Instruments, New Castle, Delaware). Samples of 8-10 mg were weighed and placed in aluminum crimped pans. mDSC analysis was performed using a heating rate of 5°C/min, from 25°C to 300°C, amplitude ± 1°C, and a period of 60 seconds. For each sample, measurements were performed in duplicate.

Thermogravimetric analysis (TGA) was performed on a TGA 4000® system (Perkin Elmer, Massachusetts, US). Samples were placed in open aluminum pans and heated from room temperature to 900°C at 10°C/min under a nitrogen atmosphere (20 mL/min).

2.2.4.6. X-Ray Powder Diffraction

XRPD analysis was performed at ambient temperature using a MiniFlex 600 (Rigaku, Tokyo, Japan). The pattern was collected from scans within the range 3.0°-50.0° at 2θ with a step size of 0.02° (2θ) and time per step of 1.0 s. Extrudates were pre-milled at 20 000 rpm in IKA M20 to a fine powder before the tests, transferred into sample holders with a zero background, and placed onto a spinner stage. The X-ray source used was Cu Kα (1.54 Å) with a voltage of 40 kV and a current of 15 mA, using a high-speed silicon strip detector (D/teX Ultra).

2.2.4.7. *Raman spectroscopy*

Raman spectroscopy was performed using a Horiba® LabRAM HR Evolution, coupled to a confocal Olympus® microscope (HORIBA France SAS, France). The focusing spot for this technique is around 1 µm, with a collection time of 30 seconds for characterization after extrusion and 50 seconds for characterization under stability. Each spectrum was collected 30 times. The laser irradiation was performed at 633 nm wavelength, with a power of 17 mW and a 50x magnification objective was used to focus on every sample. The spectra were collected in a wavenumber range of 50-2500 cm^{-1}.

2.2.5. Stability study

A stability study was performed where milled extrudates (free powder) were stored in glass amber bottles of 30 mL at 25°C / 60% RH and 40°C / 75% RH, for 1 and 3 months, in ICH climatic chambers. No desiccant was used in this study. Samples were analyzed for assay, related substances, and *in vitro* dissolution, and recrystallization was evaluated by XRPD. A representative fragment of unmilled extrudates was also stored at the same conditions and examined directly for birefringence by PLM.

2.2.6. Statistical analysis

Performed using the commercial software package JMP® 14.0 from SAS Institute, Inc.

3. Results and discussion

3.1. Systematic Identification of ASD Components

The selection of the optimal polymer/carrier is crucial to enable the development of a bioavailable and stable ASD. The ideal polymer should readily dissolve the API in its matrix to form an ASD without causing degradation and be easily extrudable at the applied processing conditions [174]. A preliminary selection of polymers was based on a drug solubility characterization in organic and aqueous solvents. Polymers with a high solubilization capacity are particularly suitable because large quantities of drugs can be dissolved. Some features like hydrophilicity, hydrogen bonding acceptors or donors, and amide groups are basic prerequisites for a high solubilization capacity. The first step was to characterize ETR solubility in detail, aiming to support the selection of polymers to proceed with the development. The quantification of the solubilized drug was determined semi-quantitatively (weighing and mixing until precipitation was visually detected). Table 2.2 displays the results of drug solubility studies.

Table 2.2. Physicochemical drug solubility in different solvents. Quantification by the semi-quantitative method.

Solvent	Drug content (mg/mL)
Dimethyl sulfoxide	> 200 mg/mL
N-Methyl-2-pyrrolidone	> 200 mg/mL
Dimethylacetamide	> 200 mg/mL
Tetrahydrofuran	> 200 mg/mL
Dimethylformamide	>200 mg/mL
Polyethylenoglycol 400	40 mg/mL
Acetone	30 mg/mL
Ethyl acetate	10.5 mg/mL
Dichloromethane	6.6 mg/mL
Acetonitrile	2.86 mg/mL
Methanol	2.2 mg/mL
Ethanol	0.83 mg/mL
Propylene glycol	< 0.8mg/mL
Tert. Butylmethylether	0.59 mg/mL

Solvent	Drug content (mg/mL)
Glycerine	< 0.50 mg/mL
Toluene	< 0.53 mg/mL
Propanol	< 0.48 mg/mL
Fed state simulating intestinal fluid pH 5.0	< 0.40 mg/mL
N-Heptane	Insoluble
Purified water	Insoluble

The rule *Similia similibus solvuntur* ("like dissolves like") applies, i.e. two materials with similar solubility parameters are expected to be miscible [319]. These results allowed the selection of 6 polymers to be tested in the subsequent stage: SLP, PVPVA, PVP, HPMC, HPMCAS, and PEG.

3.1.1. Prediction of Drug-Polymer Miscibility

The thermodynamic miscibility between ETR and the identified polymers was investigated by first calculating the Hansen solubility parameters, which was based on van Krevelen and Hoftyzer group contribution (Equation 2.4). Despite their known limitations [26, 124, 145], the calculation of solubility parameters and its application to ASDs is still one of the most applied approaches due to its relative simplicity. Group contribution methods are often used to avoid time-consuming tests and potentially inaccurate results [181]. The δ for each component, the difference between drug and each polymer ($\Delta\delta$), and the interaction parameter (χ) are provided in Table 2.3. Additional details of these calculations are provided in Appendix I, A. Calculation of Solubility Parameters. It is known from the literature that a difference in solubility parameter of less than 7 $MPa^{0.5}$ indicates good miscibility, whereas if the difference is above 10 $MPa^{0.5}$, the system is expected to be immiscible [31, 39].

Table 2.3. The estimated solubility parameter of ETR and HME polymers using the Hansen group contribution theory.

Compound / Polymer	Solubility Parameter δ ($MPa^{0.5}$)	$\Delta\delta = \delta_{ETR} - \delta_{POL}$ ($MPa^{0.5}$)	Interaction parameter[a] χ
ETR	27.86	-	-
PEG	21.25	6.61	4.86
PVP	27.19	0.67	0.049
PVPVA	25.26	2.60	0.752
SLP [b]	21	7	5

Compound / Polymer	Solubility Parameter δ (MPa$^{0.5}$)	$\Delta\delta = \delta_{ETR} - \delta_{POL}$ (MPa$^{0.5}$)	Interaction parameter[a] χ
HPMC	27.28	0.58	0.037
HPMCAS	24.63	3.22	1.16

δ_{ETR}, solubility parameter of ETR; δ_{POL}, solubility parameter of polymer; $\Delta\delta$, solubility parameter difference between ETR and polymers.

[a]The molar volume of small molecule drug was chosen as the hypothetical lattice volume (V_{site}).

[b]To determine the solubility parameters for SLP, which is composed of polyvinyl caprolactam: polyvinyl acetate: polyethylene glycol at a ratio of 57:30:13, the weighed average number of the three monomers was calculated.

From the presented results, ETR has a solubility parameter (27.86 MPa$^{0.5}$) closer to PVP (27.19 MPa$^{0.5}$) and HPMC (27.28 MPa$^{0.5}$) whereas PEG and SLP have the most different results, 21.25 and 21.30 MPa$^{0.5}$, respectively. However, the difference between the solubility parameter of ETR and each polymer is lower than 7.0 MPa$^{0.5}$, indicating good miscibility for all systems.

The value of χ refers to the square of the difference in solubility parameters that were calculated from the values of group contributions at 25°C, following Equation 2.5. From this equation, it can be concluded that the interaction parameter will approach zero if the solubility parameter of the drug and the polymer are similar. A small value of χ leads to a small magnitude of enthalpy of mixing and a more negative free energy, favoring the mixing [31], i.e. a closer value of χ to zero suggests greater interaction between the drug and the polymer [180]. According to the results in Table 2.3, the miscibility between ETR and each polymer is likely to follow the order: HPMC = PVP > PVPVA> HPMCAS > SLP = PEG. Here, SLP and PEG are theoretically suggested to have the lowest solubility capacity to dissolve ETR and produce a solid solution.

3.1.2. Prediction of T_g of the ASD through Gordon-Taylor equation

It is well known that the T_g is related to the physical stability of amorphous systems. The following table presents the results of calculated T_g based on the Gordon-Taylor equation (Equation 2.6) as well as on the simplified form by Fox (Equation 2.7). Based on these equations, polymers with higher T_g may help to improve the T_g of the entire system.

Table 2.4. Prediction of T_g of the ASD through Gordon-Taylor equation, considering a mixture of ETR and polymer of 1:3.

Compound / Polymer [a]	T_g (°C) [b]	ΔT_g (°C) = T_{gETR} - T_{gPOL}	K [c] (Simha-Boyer rule)	T_g (°C) of the blend – Gordon-Taylor equation [d]	T_g (°C) of the blend - Fox equation[e]
ETR	100.85 (Data from Ref. [309])	-	-	-	-
PVP K12	90	11	1.4	92	92
PVPVA	101	0	1.29	101	101
SLP	70	31	2.0	74	76
HPMC	178	-77	0.72	153	149
HPMCAS-MG	130	-29	0.915	122	121

[a] PEG was not evaluated due to its crystalline nature.

[b] T_g of polymers was extracted from suppliers' technical datasheet.

[c] Calculated following Equation 2.8.

[d] Calculated following Equation 2.6.

[e] Calculated following Equation 2.7.

The T_g values of the five amorphous polymers are between 70 to 178. The ΔT_g values between ETR and the polymers are relatively low, except for HPMC. Since the T_g value indicates the temperature above which the polymer chains become flexible, more interactions are expected to occur in the HME process if the components have similar T_g values. On this ground, PVPVA is considered one of the most promising polymers for interacting with ETR, and HPMC the least probable.

Hancock *et al*. proposed the 'T_g – 50°C' rule, where at the temperature 50°C lower than T_g, molecular mobility might be negligible and the amorphous solids are considered to be stable enough over a period of years [117]. The Gordon-Taylor and the Fox equations demonstrated that all the systems should have negligible molecular mobility at least until 25°C, which is the usual storage restriction for ASDs, as the lowest calculated T_g was around 75°C. This effect relies on the assumption of complete miscibility between the drug and the polymer(s) [31]. Although the 'T_g - 50 rule' ignores the β-relaxation and relies on several assumptions, it is still considered guidance for determining the storage temperature and predicting physical stability.

Indeed HPMC seems to present divergent results. On one side, it should provide the highest blend T_g, which favors physical stability. On the other side, polymer-drug interactions are known to be difficult to establish, due to the large difference between individual T_g values. Experimental results were deemed to clarify the usefulness of HPMC as a carrier for ETR.

Based on the theoretical calculations, systems comprising HPMC, PVP, and PVPVA are promising to yield miscible systems with ETR. The greater tendency for interactions due to similar T_g is expected

for systems with PVPVA while, on the contrary, discrepant T_g of HPMC should afford systems with a low tendency to interact with ETR. PVP K12 is predicted to provide enough stability for the intended purpose, as well as SLP. Due to the low melting point of PEG (around 55°C), this polymer was only considered as a negative control, as rapid crystallization of ETR is expected in this composition. Therefore, these six polymers proceeded to the next stage, where they were evaluated experimentally in terms of ETR solubility and physical stability to rank order performance. Besides, ETR may be able to establish hydrogen bonds and Van der Waals interactions with these polymers, since it presents two hydrogen bond donors and seven acceptors, as shown in Figure 2.2.

3.1.3. High-throughput screening of carriers

A solvent evaporation technique [231] was employed to prepare small films in 48-well plates of different combinations of polymers and ETR, to narrow down on a few polymer-drug combinations. The experiments were evaluated in what concerns solubilization capacity, measured by HPLC, as well as physical stability over 2 months, assessed by PLM. High drug loads and high surface area of thin films in contact with ambient humidity leads to a lack of thermodynamic equilibrium, which promotes rapid drug recrystallization and the fast failure of unsuccessful systems. Therefore, this method was selected to readily select promising systems by promoting the failure of doomed compositions.

3.1.4. Solubilization capacity

The screening of polymers by solvent evaporation yielded the following solubility results obtained by HPLC (Figure 2.6). The solubility and miscibility of the drug in the polymer are directly related to the stabilization of an amorphous drug against crystallization. In general, higher solubility among the same drug loading is related to increased amorphicity of ETR in the binary mixture, although the solubilizing capacity of different polymers may also contribute to the observed results.

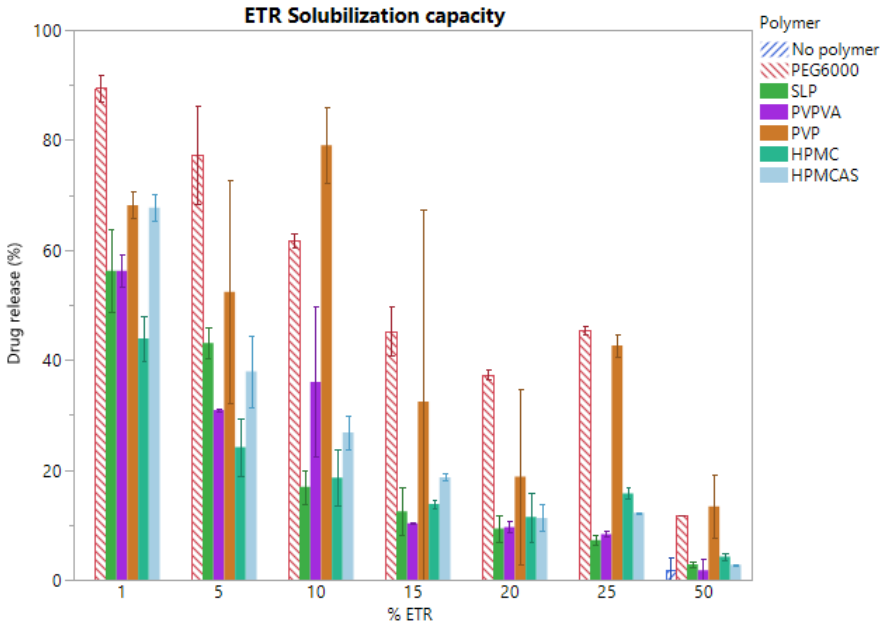

Figure 2.6. Assay result by HPLC of the screening of polymers. Error bars represent standard deviation. Drug release from polymeric blends decreases drastically with higher drug loadings. PVP is clearly distinguished by higher drug release in all drug loadings when compared to the remaining binary compositions.

To gather a deeper understanding of the relationship between drug solubilization from the binary mixtures, excipient type, and drug load, the studied responses were applied to JMP® 14.0. The distribution platform was used, which illustrates the distribution of several individual variables using histograms and simple statistics (Figure 2.7). A drug release higher than 30% was considered acceptable. Low RSD is preferred, but due to the low scale of the experiment, high RSD is accepted and not considered relevant at this stage of the investigation.

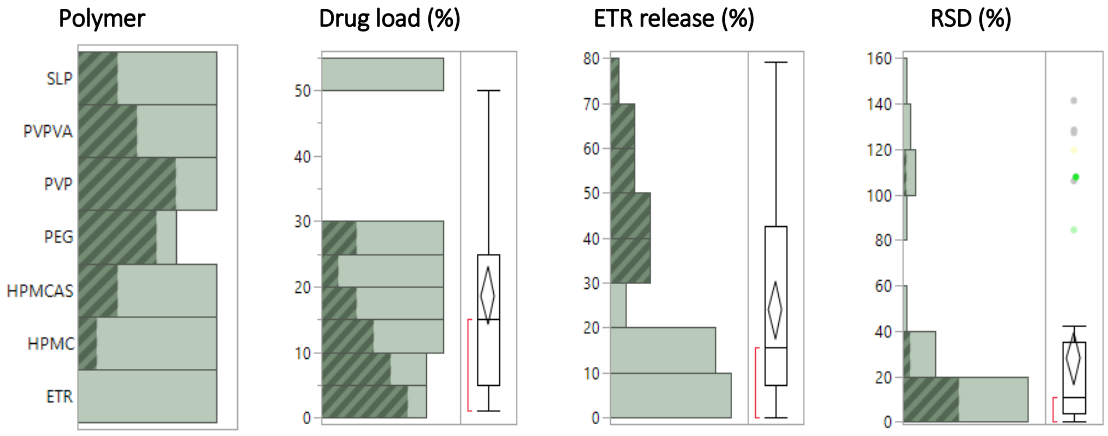

Figure 2.7. Histograms showing the distribution of the obtained data. Drug release higher than 30% is highlighted and was obtained with PEG > PVP > PVPVA > SLP > HPMCAS > HPMC.

The analysis of the above histograms demonstrated that to have a drug release higher than 30%, drug load should not be as high as 50%. An acceptable drug release is obtained with all the tested polymers, but mainly with PEG, followed by PVP > PVPVA > SLP > HPMCAS > HPMC.

3.1.5. Physical stability

The physical evaluation of the binary systems over time was performed by PLM and the results are portrayed in Appendix I, B. High-throughput screening – Physical stability evaluation. Some PLM pictures are presented below, where Figure 2.8 exemplifies cracks in solid films and Figure 2.9 detected birefringence in glass slides of different binary compositions. The distribution platform of JMP® 14.0 was also used to assess the physical stability. However, to analyze the amount of data generated, a multivariate statistic was applied, namely PCA, where the level of crystallization, time, and drug load (variables) were analyzed by storage condition. The aim was to compare the evolution of each binary composition to a hypothetically perfect system, where no crystallization was seen throughout the stability time, no matter the condition it was exposed to. Usually, PCA is applied as a dimension-reduction technique but, in this case, a different application was given, as it was applied as a means to measure the distance to the ideal amorphous system. The higher the distance, the worst the composition is in what concerns physical stability.

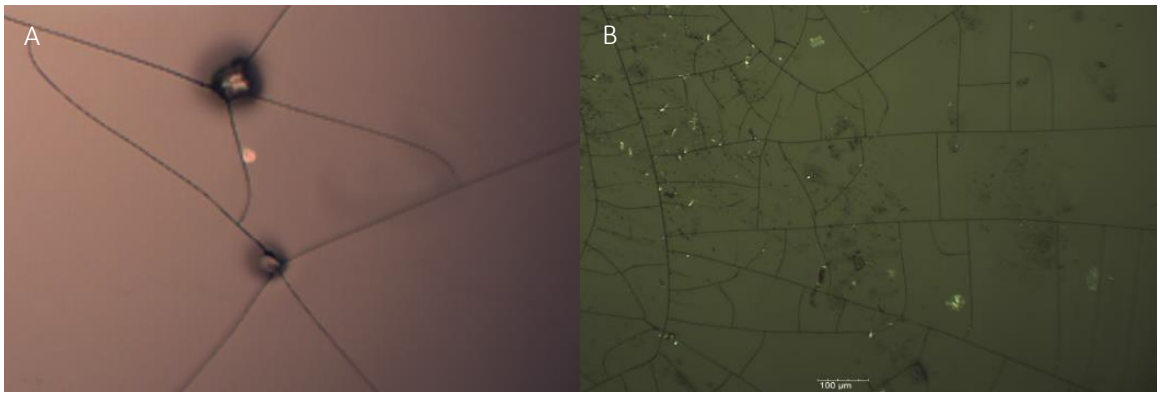

Figure 2.8. Lack of plasticizing capacity detected by polarized light microscopy. A, Sample PVPVA + 50% drug after 4 days of storage in the desiccator, objective 10x; B, Sample PVP + 50% drug after 17 days of storage at 25°C/ 60% RH, objective 10x.

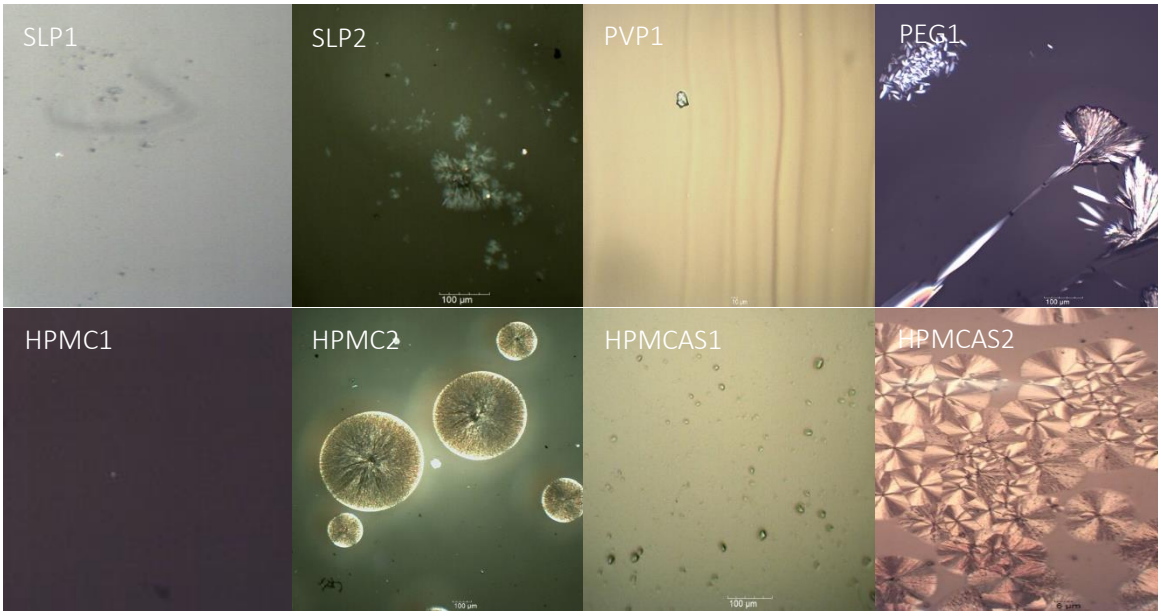

Figure 2.9. Birefringence of some binary compositions detected by polarized light microscopy. SLP1: Sample SLP + 1% ETR at T0 with no crystals detected, objective 50x; SLP2: Sample SLP + 50% ETR after 7 days of storage in the 25°C/ 60% RH climatic chamber, objective 10x; PVP1: Sample PVP + 25% ETR after 4 days of storage at room temperature with no crystals detected, objective 10x; PEG1: Sample PEG + 50% ETR at T0, objective 5x; HPMC1: Sample HPMC + 30% ETR at T0 with no crystals detected, objective 10x; HPMC2: Sample HPMC + 50% ETR after 7 days of storage in the 25°C/ 60% RH climatic chamber, objective 5x; HPMCAS1: Sample HPMCAS + 20% ETR after 4 days of storage in the 25°C/ 60% RH climatic chamber with no crystals detected, objective 10x; HPMCAS2: Sample HPMCAS + 50% ETR at T0, objective 10x.

The following graphs (Figure 2.10) portray the score and loading plots for each condition. Each composition is marked in a different color, and the perfect system is marked with an X. The score plot graphs each component's calculated values in relation to the other, adjusting each value for the mean and standard deviation. The loadings plot depicts the unrotated loading matrix between the variables (level of crystallization, time, % ETR), and the principal components. The closer the value is to 1, the greater the effect of the component on the variable. Two principal components were generated with statistical significance (p <0.0001, calculated through the Bartlett Test), which explain almost the total results variability in the three performed analysis, namely 94.9% for the storage at 25°C / 60% RH, and 94.8% and 94.0% for the room temperature and the desiccator, respectively.

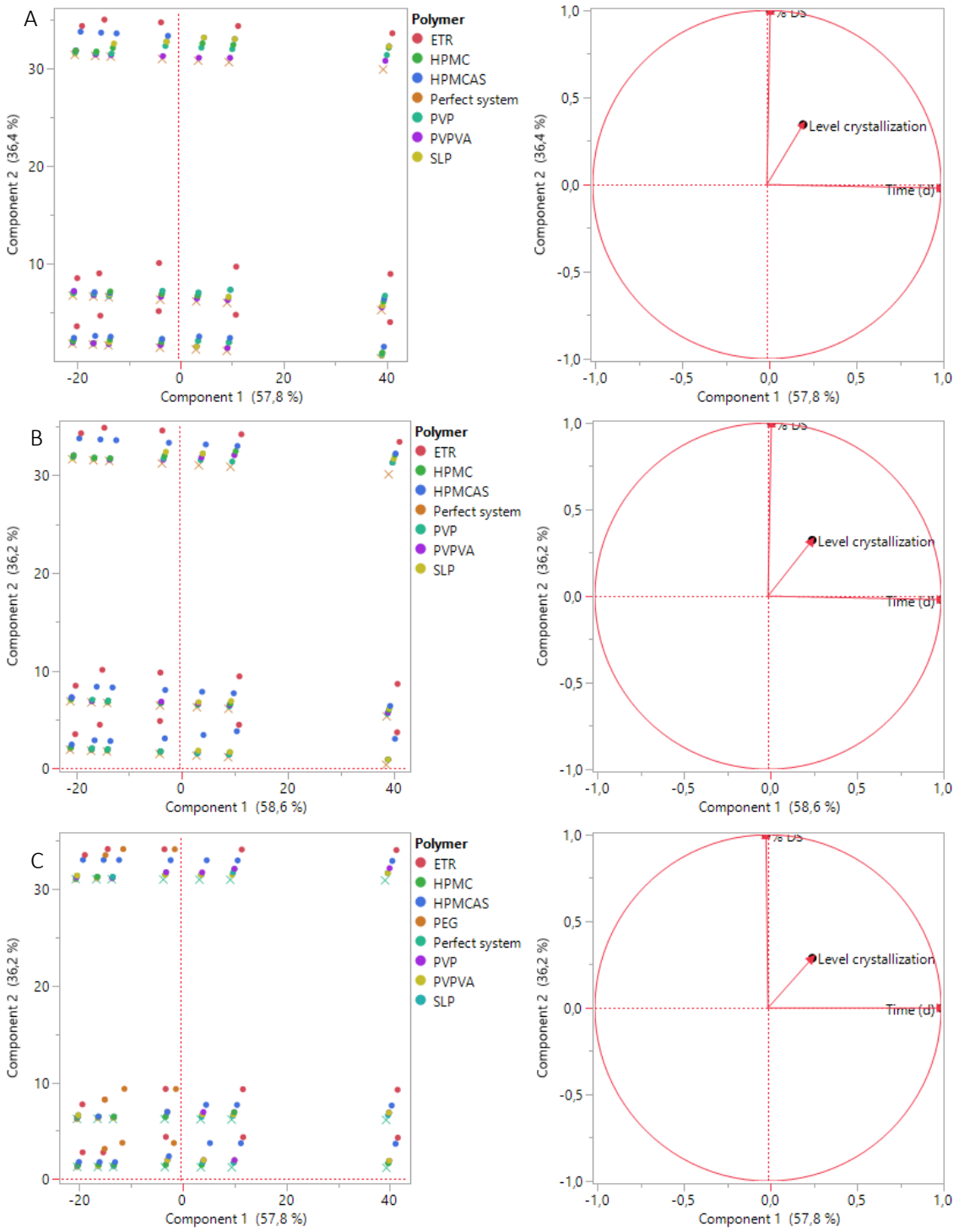

Figure 2.10. JMP® 14.0-assisted PCA performed by storage condition. Only drug loadings > 20% are depicted. A, Systems exposed to 25°C / 60% RH; B, Systems exposed to room temperature; C, Systems exposed to desiccator. The score plot (left) and the loadings plot (right) are depicted. The score plot graphs each component's calculated values in relation to the other, adjusting each value for the mean and standard deviation. The loadings plot depicts the unrotated loading matrix between the variables (level of crystallization, time, % DS) and the components (1 and 2). The closer the value is to 1, the greater the effect of the component on the variable. Two principal components were generated with statistical significance (p <0.0001, Bartlett Test), which explain 94.9% of the variability of the results for condition A, and 94.8% and 94.0% for condition B and C, respectively. The perfect system for each binary composition is marked in x.

When looking at the score plots, it is possible to observe the deviation from the hypothetical perfect system with no crystallization (marked with an X) of each binary composition. This deviation was quantified based on the Euclidean distance, which was calculated per system. Then, a weighted mean value of the distance was calculated to rank order performance. The weighted mean was preferred over arithmetic mean to lend higher importance to systems with higher drug loadings. This was performed by condition, to check discrepancies in systems' behavior by temperature or humidity. Table 2.5 portrays an overview of these calculations and the resultant rank order.

Table 2.5. Calculation of the Euclidean distance from the perfect system based on PCA results and rank order performance of binary systems tested in the HTS. Absolute values represent the deviation from the perfect system (scored 0).

System | Condition	25°C / 60% RH	Room temperature	Desiccator
ETR	3.7	3.6	3.4
HPMC	0.84	0.57	0.52
HPMCAS	1.3	1.6	1.5
PVP	0.67	0.44	0.62
PVPVA	0.34	0.42	0.51
SLP	0.70	0.52	0.39
Rank order performance	**PVPVA**	**PVPVA**	**SLP**
	PVP	**PVP**	**PVPVA**
	SLP	**SLP**	**HPMC**
	HPMC	HPMC	PVP
	HPMCAS	HPMCAS	HPMCAS
	ETR	ETR	ETR

HPMC seems also to be quite stable in lower room humidity. Predictions of blend T_g of HPMC compositions presented divergent results. On one hand, it should provide the highest blend T_g, which favors physical stability. On the other, the large difference of T_g value from ETR hampers the formation of polymer-drug interactions. Experimental results were deemed, and they corroborated the lack of stability. These results also suggest that ΔT_g may contribute to predict the success of HME solid dispersions, as demonstrated with the case of HPMC and already defended by Liu and colleagues [320].

Based on Euclidean distance calculations of PCA results, the top 3 in terms of physical stability become evident: PVPVA, PVP, and SLP. At this stage, PVP and PVPVA were selected to proceed to extrusion studies. This is in line with major conclusions from the prediction of drug-polymer miscibility and binary systems T_g, where PVP and PVPVA were considered the most promising

systems. SLP was predicted by Gordon-Taylor calculations to provide enough stability, but not miscibility with ETR, and this was in line with the experimental results. However, due to the unexpectedly positive stability results, probably due to interactions established as hydrogen bonding, SLP was also included in the extrusion tests.

3.2. HME at Laboratory Scale

Before HME tests, TGA and DSC were used to evaluate the thermal stability of ETR during the heating process (Figure 2.11). ETR is thermally stable up to 260°C. Mass loss or degradation of ETR was observed right after its T_m (256°C) indicating the extrusion temperature should never reach this temperature. This working temperature is quite high and was never applied during extrusion.

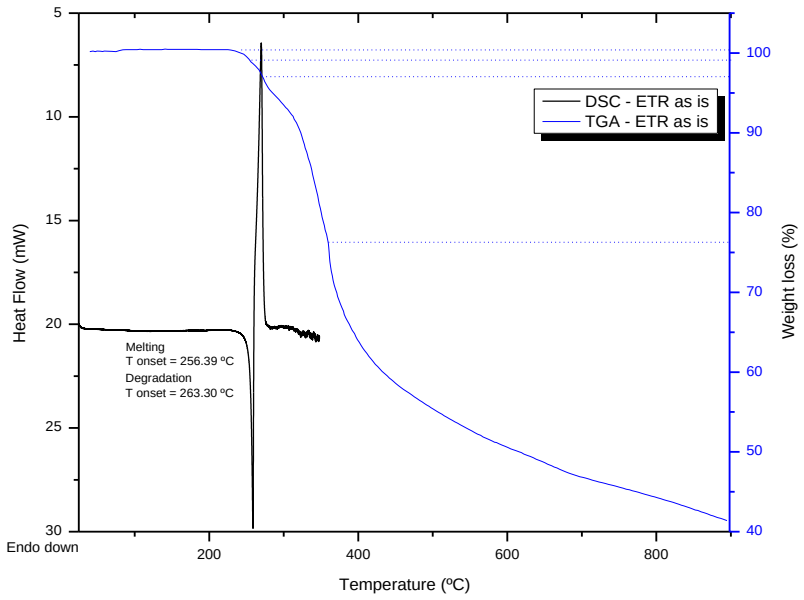

Figure 2.11. Black line: DSC thermogram of pure ETR. Equipment: Pyris 6 (Perkin Elmer). Aluminum capsules. Method: from 25°C to 300°C at 10°C/min, after 1 min at 25°C (equilibrium). Blue line: Thermogravimetric analysis of ETR. Equipment: TGA 4000 System (Perkin Elmer). Method: from 25°C to 900°C at 10°C/ min.

The selected systems were subjected to HME to assess important pharmaceutical properties: extrudability (processability) and drug release on dissolution. A drug load of 25% was selected, due to the results of the HTS tests, where an acceptable drug release was obtained at loadings lower than 30%. The details of the HME process and the appearance of corresponding extrudates are summarized in Table 2.6. The predicted T_g of the systems was taken as a starting point for selecting

process temperatures, and HME parameters were then optimized to decrease molten viscosity, torque, and residence time, to lead to the better extrudate appearance (clear and transparent), and the smoothest process. A 1% of PEG 1500 was added to the PVP and PVPVA formulations to improve extrudability. The appearance of the PVP system was improved, but not in the PVPVA composition, where the dark color was even exacerbated. In the SLP binary system, extrusion was smooth and no plasticizer was needed.

Table 2.6. Formulations, extrusion parameters, appearance, and extrudability.

Description	Screw speed (rpm)	Tempera-ture (°C)	Torque (Ncm)	ΔP (bar)	Appearance
PVP k-12 + 25% ETR	320	165	60	1	Transparent yellow. Hard to feed. 
PVP k-12 + 1% PEG1500 + 25% ETR	270	167	70	1	Transparent yellow. Smooth extrusion. 
PVPVA + 25% ETR	180	150	90	1	Dark brown, opaque. Hard to feed. 
PVPVA + 1% PEG1500 + 25% ETR	270	177	80	1	Dark extrudate, opaque. 
SLP + 25% ETR	265	160	90	1	White, opaque. Smooth process. 

3.3. Characterization of Solid Dispersions

3.3.1. Assay and purity testing

The extrusion of PVP k-12 compositions led to acceptable ETR content in the manufactured extrudates, as well as an acceptable level of impurities (Table 2.7). Only the amorphous compositions were characterized. The assay level at 95% reflects the small batch size, where drug losses occur easily and should be improved during upscale.

Table 2.7. Analytical results of extrusion tests. The assay was determined considering the percentage of ETR loaded in the extrudate.

Description	Assay (%) ± RSD	Imp 1 (%)	Higher unknown (%)	Total Impurities (%)
PVPk-12 + 25%ETR	94.68 ± 0.36	0.17	0.03 (RRT=0.48)	0.42
PVP k-12 + 1% PEG1500 + 25% ETR	94.97 ± 0.94	0.35	0.04 (RRT=0.49)	0.65
PVPVA + 25% ETR + 1% PEG 1500	61.64 ± 0.25	19.33	0.22 (RRT=0.81)	20.34

With PVPVA the content of ETR decreased drastically, along with an astonishing rise in impurities detected by HPLC. The most relevant impurity in these binary systems was impurity 1 (Figure 2.12), related to thermal degradation (data from internal forced degradation studies performed in-house, available in Appendix I, C. Forced degradation study).

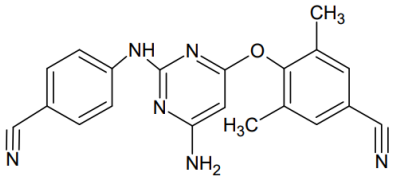

Figure 2.12. Impurity 1 of ETR: 4-(6-amino-2-(4-cyanophenyl amino) pyrimidine-4-yl oxy) -3,5-dimethyl benzonitrile.

It has been reported that in HME the decomposition of drugs may occur at temperatures much lower than the predicted by DSC/TGA of the pure compound because the crystalline drug dissolves into the molten polymer and is transformed into amorphous. Besides, the energy that comes from the intensive mixing and high screw speed and torque also contributed to the decrease in the onset degradation temperature [320]. To confirm this, DSC studies were conducted on a physical mixture of PVPVA and ETR (system with 20% of loading). The high formation of impurity 1 in PVPVA systems after extrusion is seen through DSC analysis. At the beginning of the ETR melting process, degradation occurs rapidly. Degradation was observed at approximately 225°C, which is 38°C lower than the onset degradation temperature of pure ETR (Figure 2.13A). It is supposed that interaction between excipient and drug may occur, leading to the fast degradation of ETR, triggered by the high energy provided during extrusion (shear stress and temperature). An underlying mechanism of Friedel-Crafts acylation may be one of the explanations (acylation of one of the aromatic rings

with an acyl group from PVPVA molecule). This might be the reason for high unknown impurities and may occur even at relatively low temperatures.

As shown in Table 2.6 and Table 2.7, PVPVA compositions (with and without plasticizer) demonstrated extensive drug degradation. In what concerns SLP, ETR crystalline particles were obtained as extrudates were white opaque. This phenomenon indicates the poor miscibility of ETR and SLP, which was already predicted with the Hansen solubility parameters. Therefore, the binary systems with PVP k-12 seem to be the most promising to enhance ETR solubility.

3.3.2. Differential Scanning Calorimetry

DSC profiles of ETR, polymer, and the solid dispersion of PVP k-12 are shown in Figure 2.13B. DSC results seem to indicate that there is a crystalline drug within the analyzed sample. However, the presence of a T_m during heating in the DSC study is, in this case, not a proof of crystalline content in the extrudates as ETR recrystallized on heating. The evidence of recrystallization is not observed in standard DSC but detected using mDSC in stability samples (3 months) (refer to stability results and discussion). Moreover, although it would be useful to know the crystalline content of the sample, this is not possible to determine as ETR immediately decomposes along with melting, which limits the correlation with intermolecular interactions within the systems [185, 321, 322]. Other analytical techniques were necessary to clarify the solid-state of ETR in the solid dispersions and XRPD analysis was used.

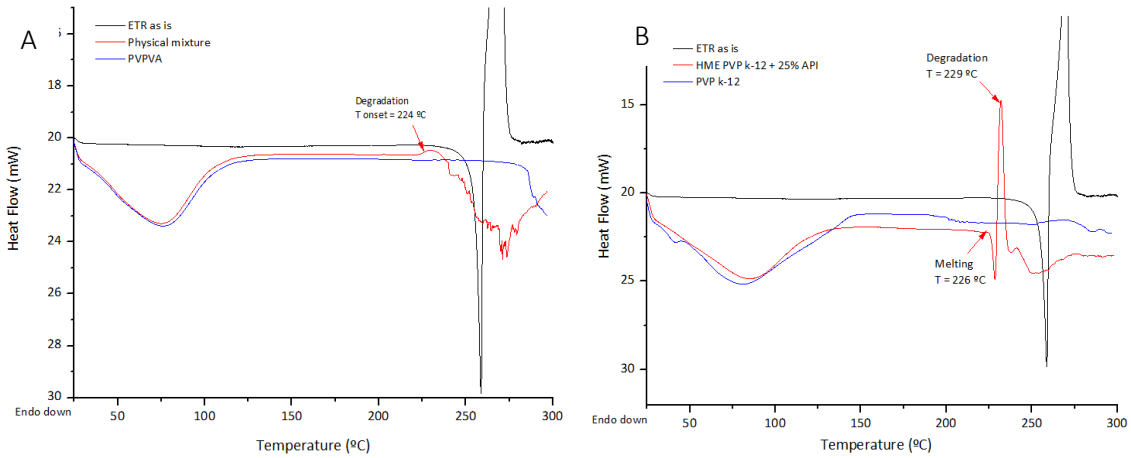

Figure 2.13. DSC thermograms. Equipment: Pyris 6 (Perkin Elmer). Aluminum capsules. Method: from 25°C to 300°C at 10°C/min after 1 min at 25°C (equilibrium). A: ETR, placebo, and physical mixture of PVPVA system. Blue line: PVPVA. Red line: physical mixture of PVPVA and ETR. Black line: pure ETR. B: ETR, placebo, and extrudates of PVP k-12 + 25% ETR. Blue line: PVP k-12. Red line: PVP + 25% ETR. Black line: pure ETR.

3.3.3. X-Ray Powder Diffraction

The typical halo of the XRPD pattern of amorphous materials was observed on the PVP k-12 binary system. A similar XRPD pattern was found in the PVP + 25% ETR + 1 % PEG1500 system, however, it is observed the presence of very small crystalline peaks, attributed to ETR (Figure 2.14B). SLP binary composition, as expected, was crystalline, with the same polymorphic form as the plain drug (form I), as depicted in Figure 2.14A. This result is explained by the immiscibility of ETR within the carrier. In the specific case of ETR solid dispersions, it is clear that XRPD should be used for amorphicity evaluation, instead of thermal analysis (DSC).

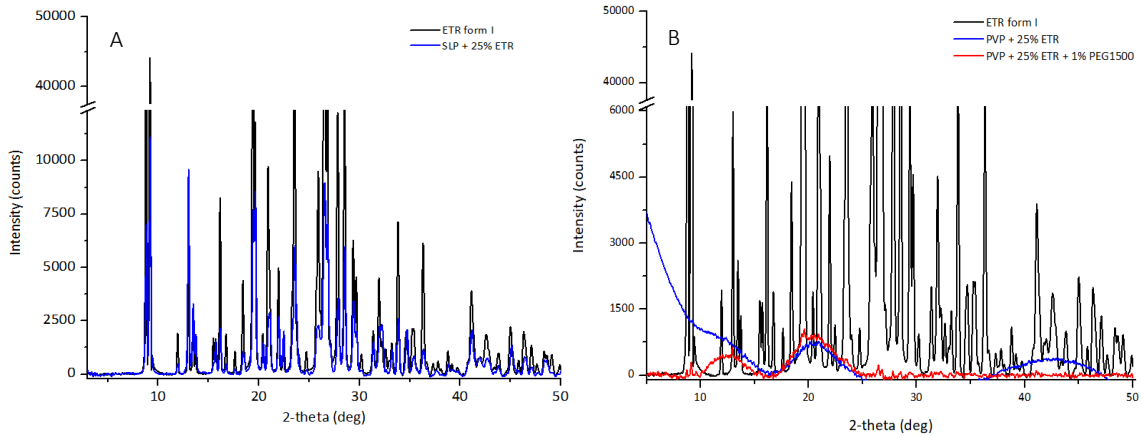

Figure 2.14. XRPD patterns of A: overlay of crystalline Form I of ETR and SLP binary system; B: overlay of crystalline form I of ETR and PVP formulations manufactured by HME.

3.3.4. Raman spectroscopy

To gain more insight into the physicochemical behavior of the manufactured systems, Raman analysis was performed and demonstrated different spectra between the crystalline and the amorphous form, where sharp absorption peaks were substituted by broad and wide bands. The Raman spectra of pure ETR and two formulations, SLP + 25% ETR and PVP + 1% PEG1500 + 25% ETR, are depicted in Figure 2.15. Four sections where the different solid-state forms demonstrate the greatest divergence were highlighted.

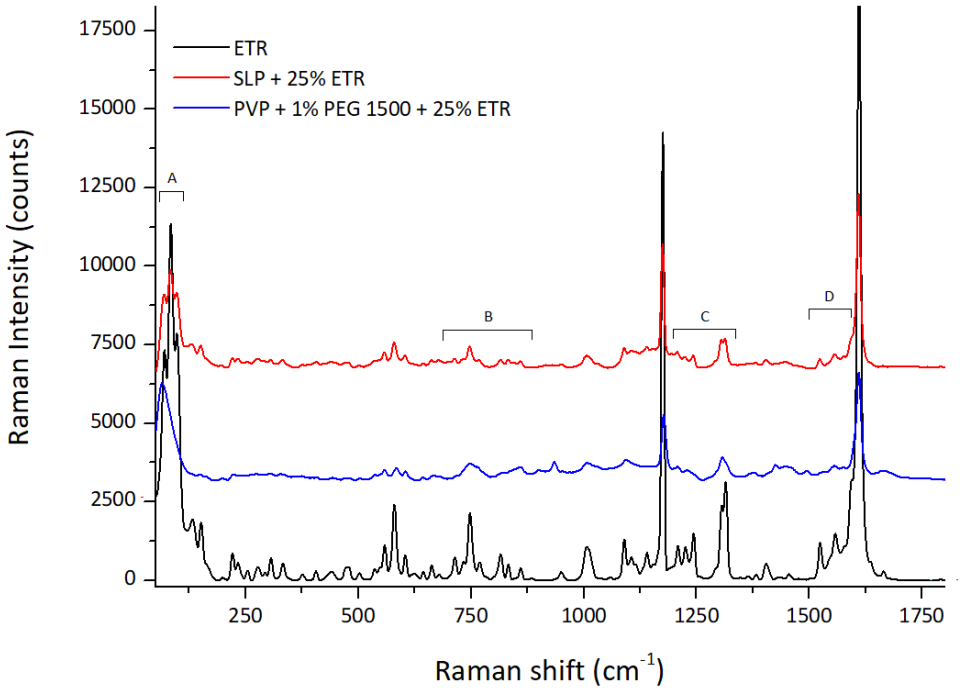

Figure 2.15. Raman spectra of crystalline Form I of ETR, SLP binary system, and PVP composition from 50 to 1800 cm^{-1}. The spectra were recorded in the 50-2500 cm^{-1} wavenumber range, during 30 seconds with 30 accumulations, with excitation at 633 nm. Regions with the greatest divergence were highlighted.

It was demonstrated that Raman has a high potential to distinguish the solid-state forms of ETR, with several regions identified with the potential to discriminate between amorphous and crystalline forms. Crystalline ETR in the SLP binary system (SLP + 25% ETR) was detected as sharp peaks below 100 cm^{-1}, and at around 850, 1200, 1300, and 1600 cm^{-1}. This spectrum exhibits a perfect match to the crystalline drug, indicating the same polymorphic form and probably no interactions between ETR and SLP in the extrudate. In the PVP composition (PVP + 1% PEG 1500 + 25% ETR), straight peaks were replaced by weak and broad bands at the highlighted sections of the spectrum, which indicate that ETR form I is converted into fully amorphous by HME. These conclusions are in line with previous publications with Infrared characterization of crystalline and amorphous ETR [309, 323].

Any deviations in the Raman shift or shapes of these bands may reflect an interaction between the drug and the polymer. As referred above, in the PVP composition several sharp peaks were replaced by weak and broad bands, and this may be related to the amorphous solid-state form, or reflect the existence of weak intermolecular interactions as Van der Waals, electrostatic or hydrophobic. Besides, the sharp peak of plain ETR at 2225 cm^{-1} was replaced by a broader and shifted band to 2221 cm^{-1} in the PVP composition (Figure 2.16), which may also represent the formation of a weak interaction affecting the CN groups of ETR. Although weak, these dipolar

intermolecular interactions may enhance the miscibility of ETR within PVP and, through the inhibition of molecular mobility to some extent, stabilize the system and improve the physical stability of extrudates. There is no clear evidence of such interactions with SLP, as the spectrum was very similar to the plain drug.

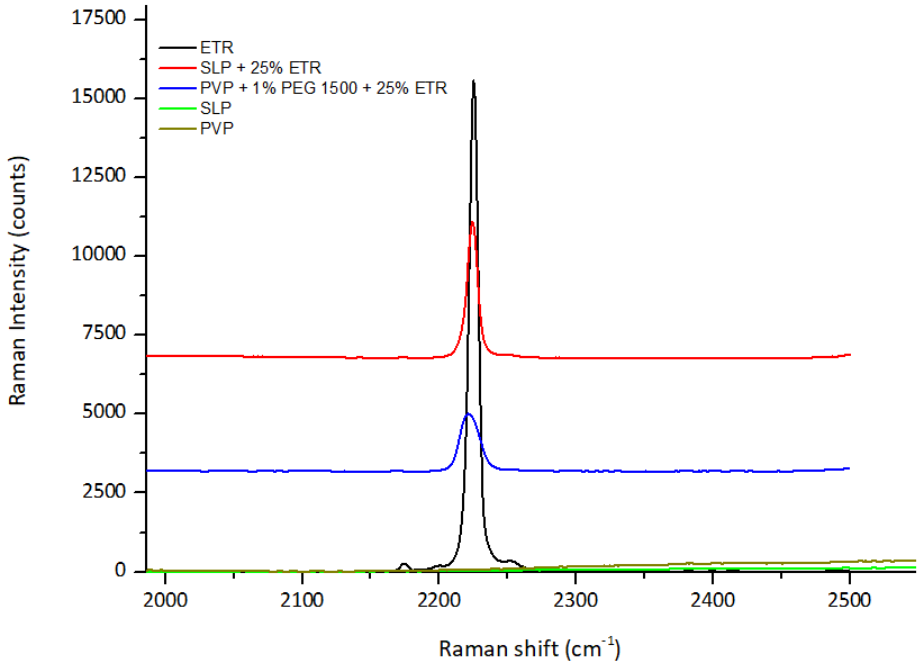

Figure 2.16. Raman spectra of crystalline Form I of ETR, polymers SLP and PVP, and solid dispersions of SLP and PVP. A shift of 2225 cm^{-1} peak of ETR is observed to 2221 cm^{-1} in the PVP formulation, which may be related to an intermolecular interaction affecting the CN groups of ETR.

3.3.5. *In vitro* dissolution test

Figure 2.17 portrays the dissolution curves of pure ETR (crystalline drug) and prepared HME compositions at 25% drug loading, one with SLP and the others with PVP. PVP systems were characterized by XRPD and Raman spectroscopy as fully amorphous and SLP as crystalline. A significant enhancement in the dissolution rate was observed for PVP solid dispersion prepared by HME compared with the crystalline ETR. More specifically, PVP enabled the release of more than two times higher than the crystalline drug. Furthermore, the addition of PEG1500 was crucial not only as a plasticizer but also as a solubility-enhancer.

Despite being fully amorphous, the dissolution rates of these preparations were still not complete. The dissolution behavior of the polymers themselves and the porosity of the granules may explain the obtained behavior [306]. Generally, HME formulated products have low porosity and thus drug

release kinetics are mainly determined by the dissolution of the polymeric matrix. This is even more noticeable in the case of low drug loadings, which is often the case of ASDs. The hydration and dissolution speeds of a polymer are dependent on the MW and other polymer physicochemical characteristics like hydrophilicity [324]. Moreover, it is quite common to have large bolus without any porosity, which cannot generate a very fast drug release. This is known as the lumping effect, due to the high binding and gelling properties of polymers, which may lead to incomplete release.

SLP is well-known for its good aqueous solubility and the release rate of ETR was in this case improved when comparing to the crystalline form, despite being a crystalline suspension. This was probably caused by the hydrophilic polymer that promotes solubilization by wetting the surface of the hydrophobic drug. This is in line with previous work in the field of ASDs suggesting that release rates of many systems are determined by the dissolution of the polymeric carrier and not by the drug itself [26, 325-327].

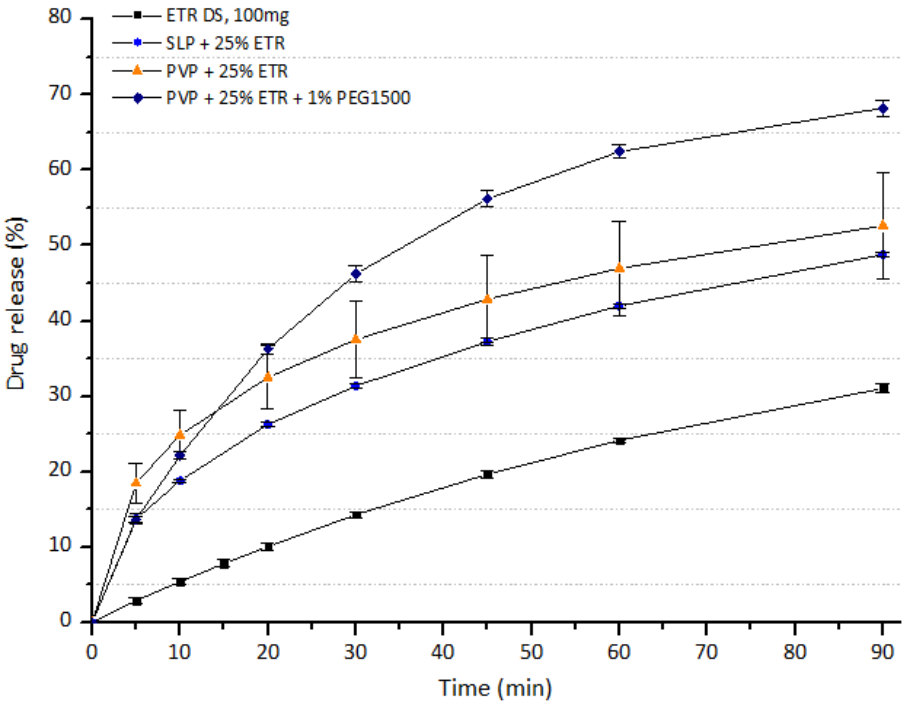

Figure 2.17. Dissolution profiles of pure ETR and 25% drug-loaded HME formulations with PVP k-12 and SLP (PVP systems were characterized as amorphous and SLP crystalline). Error bars represent standard deviation.

3.4. Stability study

Physical and chemical stability of extrudates of PVP k-12 + 1% PEG 1500 + 25% ETR was evaluated by determination of assay and related substances, *in vitro* dissolution test, DSC (including modulated temperature), XRPD, Raman spectroscopy and PLM, and the results are summarized in Table 2.8. The product seems to be chemically stable as no substantial decrease in ETR assay or change of the impurity profile was detected after 3 months of storage at 25°C / 60% RH and 40°C/ 75% RH. The slight decrease in ETR assay is attributed to moisture adsorption, as powder lumping was reported, and already expected. Based on XRPD (Figure 2.18) and Raman (Figure 2.19), no recrystallization of ETR was observed after 3 months of storage even when stored at 40°C / 75% RH. The apparent stability at such a high temperature and humidity is quite surprising taking into account the predicted T_g by the Gordon-Taylor equation, but probably explained by the detected bonding between ETR and carrier in Raman spectroscopy [31, 124, 145]. The broader and shifted band to 2221 cm^{-1} in the PVP compositions was kept along the stability time when exposed to 25°C/ 60% RH. However, after 3 months at 40°C / 75% RH, the detected deviation decreased, which may be related to a molecular structural rearrangement perhaps leading to the recrystallization in the upcoming months (Figure 2.20).

Table 2.8. Analytical results of milled extrudates of formulation PVP k-12 + 1% PEG 1500 + 25% ETR under stability.

Time points		**0**	**1 month**		**3 months**	
Storage condition		**-**	**25°C/60%RH**	**40°C/75%RH**	**25°C/60%RH**	**40°C/75%RH**
Appearance		Loose powder	Loose powder	Loose powder with small lumps	Loose powder	Loose powder with small lumps
Assay (%) ± RSD		94.97 ± 0.94	95.63 ± 0.52	94.43 ± 0.07	93.53 ± 0.70	92.73 ± 1.16
Related substances	Imp 1 (%)	0.34	0.31	0.31	0.30	0.29
	Total (%)	0.65	0.55	0.55	0.55	0.57
***In vitro* release** (Q(90 min)) (%) ± RSD		68.23 ± 1.55	54.13 ± 1.03	53.62 ± 6.53	52.31 ± 2.96	56.43 ± 0.09
Polymorphic form		Amorphous [a, b]	Amorphous [a, c]	Amorphous [a, c]	Amorphous [a, c, e]	Amorphous [a, d, e]

[a] analyzed by XRPD and Raman spectroscopy; [b] PLM shows no crystallization; [c] PLM shows very slightly crystalline structures, likely attributed to PEG1500; [d] PLM shows crystalline structures, likely attributed to PEG1500; [e] analyzed by DSC and modulated temperature DSC.
Abbreviations: Imp, Impurity; RH, relative humidity.

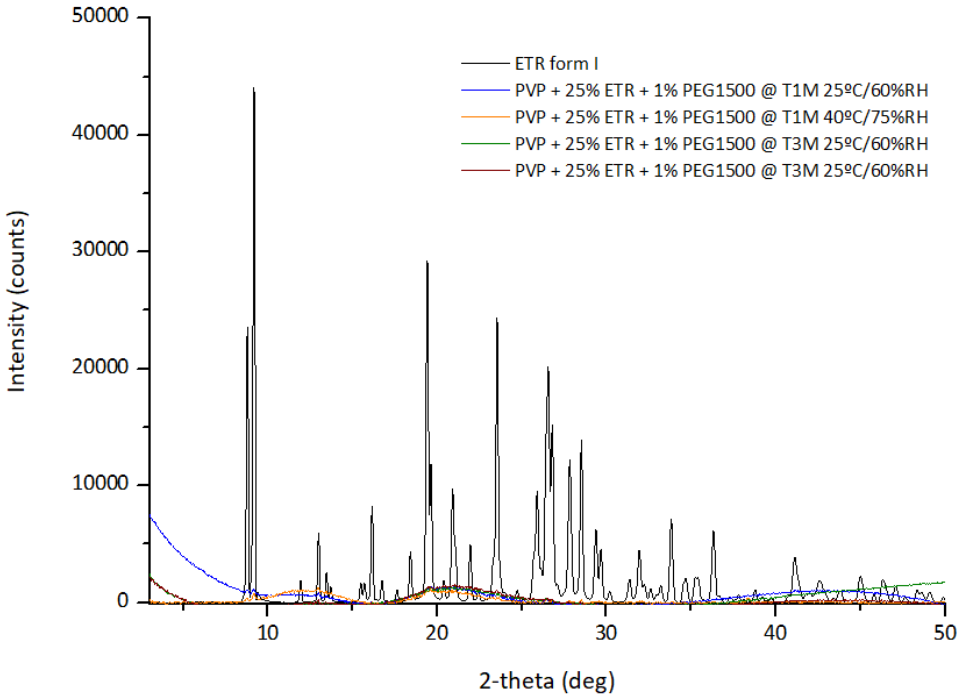

Figure 2.18. XRPD patterns of crystalline Form I of ETR and PVP formulation manufactured by HME after 1 and 3 months of stability stored at 25°C / 60% RH and 40°C / 75% RH.

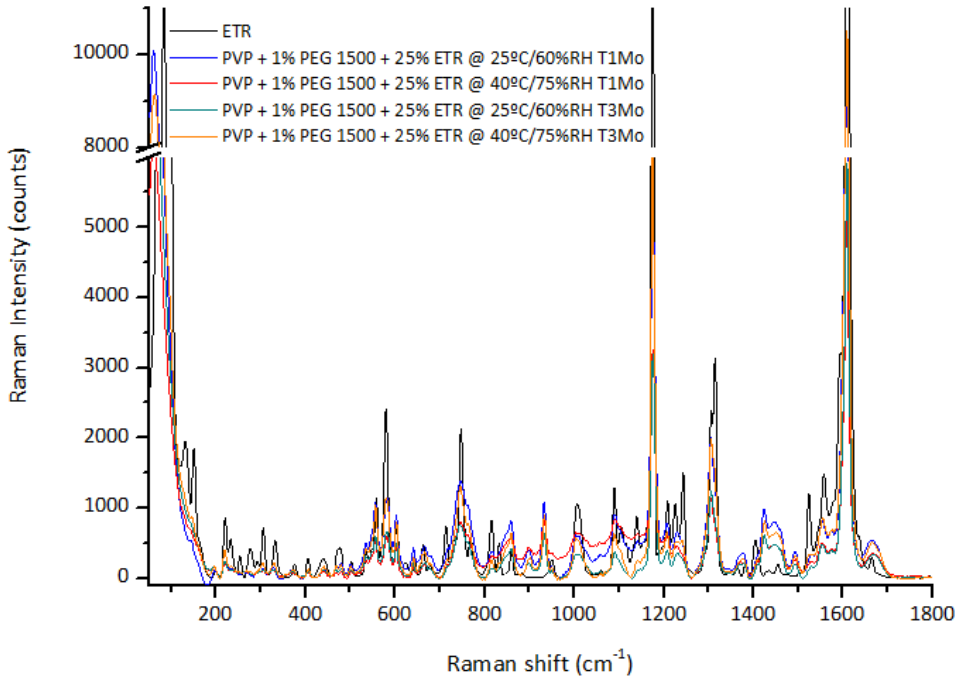

Figure 2.19. Raman spectra of crystalline Form I of ETR, and PVP composition under stability at 25°C / 60% RH and 40°C / 75% RH, from 50 to 1800 cm^{-1}. The spectra were recorded in the 50-2500 cm^{-1} wavenumber range, during 50 seconds with 30 accumulations, with excitation at 633 nm.

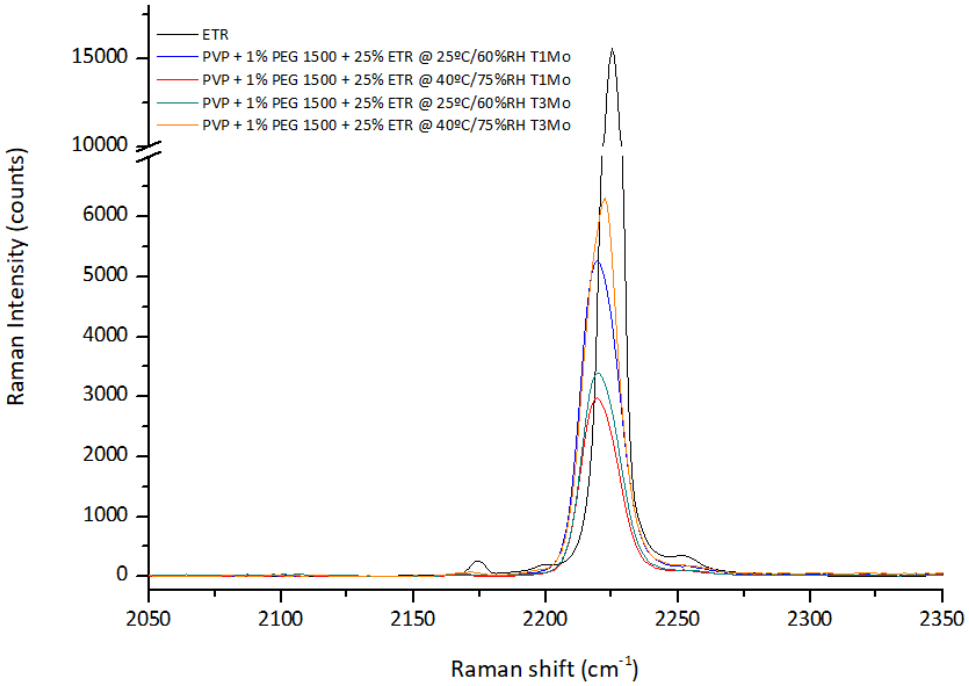

Figure 2.20. Raman spectra of crystalline Form I of ETR and solid dispersions of PVP after 1 and 3 months of stability, exposed to 25°C / 60% RH and 40°C / 75% RH. A shift of 2225 cm^{-1} peak of ETR is observed to 2221 cm^{-1} in the PVP formulation, which may be related to an intermolecular interaction. After 3 months exposed to 40°C / 75% RH, the detected deviation is decreasing which may be related to a structural rearrangement probably leading to drug crystallization.

DSC characterization was also performed to confirm the results and eliminate the possibility of phase separation (Figure 2.21). A similar result to T0 was obtained with the standard DSC method, where the melting of the ETR drug is observed. This is usually an indication of phase separation, which is not corroborated by the XRPD and Raman spectroscopy results. To gain more insight into these stability samples, mDSC experiments were performed, and the results are depicted in Figure 2.22. Indeed, there is evidence of crystallization, after 200°C, with a maximum of 216°C, as observed in the total heat flow and non-reversing heat flow curves. This event is followed by melting and drug decomposition. There is also an endothermic event from 50 to 130°C, related to the elimination of residual moisture. This is common to both 25°C / 60% RH and 40°C / 75% RH, suggesting similar behavior. The detection of the recrystallization event explains the observed melting of ETR before decomposition, which along with XRPD and Raman spectroscopy results are strong evidence of a fully amorphous system.

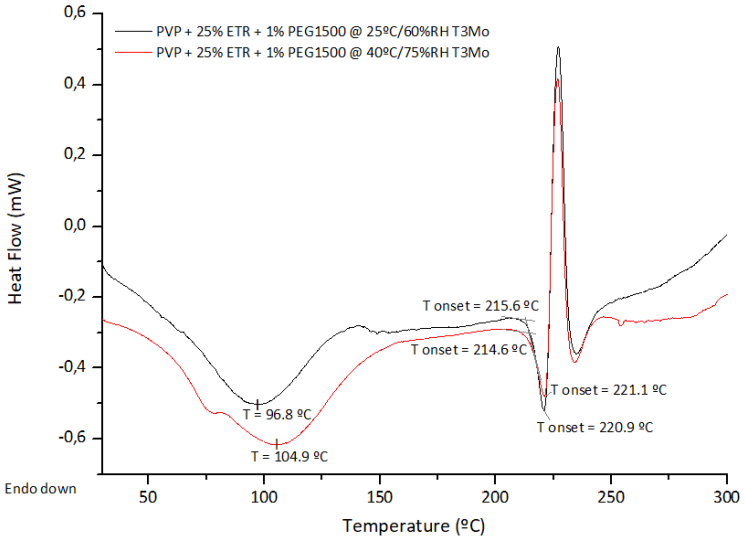

Figure 2.21. DSC of PVP systems prepared by HME after 3 months of stability stored at 25°C / 60% RH and 40°C / 75% RH.

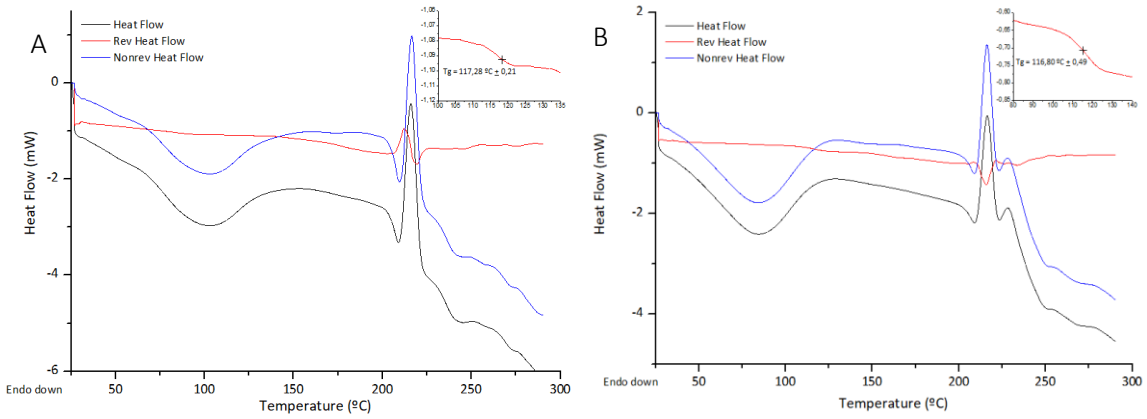

Figure 2.22. mDSC of PVP systems prepared by HME after 3 months of stability stored at 25°C/60%RH (A) and 40°C/75%RH (B). Drug crystallization is detected after 200°C, followed by melting and decomposition. The graph insets highlight the glass transition temperature detected at approximately 117°C.

An additional relevant result is that the systems' T_g was detected with this method, at approximately 117°C, for both stability conditions. The original T_g at T0 was probably higher, as we observed moisture adsorption over stability. Despite that, the experimental T_g is still well above the predicted value from the Gordon-Taylor equation (92°C), and this is a clear confirmation of intermolecular interactions between the drug and the polymers, as the one detected in Raman spectra of these systems.

However, the drug release decreased from the T0 to the stability results (Figure 2.23). No further decrease was noticed over stability, namely from 1 to 3 months, under exposure to both room

conditions. As no drug crystallization was detected, this decrease of about 10 to 15% may be related to polymer chain rearrangement, namely to secondary relaxations (β-relaxations, molecular mobility of polymeric side chains) that have an important role in ASD stability at temperatures below T_g. This may be more relevant taking into account the probable uptake of water by the polymeric system, as indirectly indicated by the decrease of the assay, without significant formation of impurities, and the observation of powder lumps.

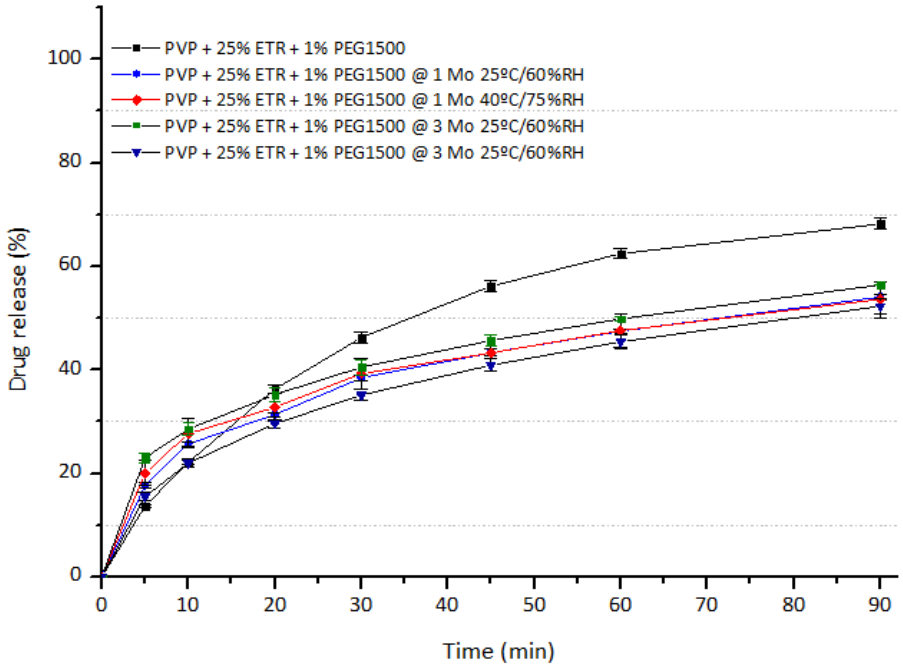

Figure 2.23. Dissolution profiles of 25% drug-loaded HME formulation with PVP k-12 after 1 and 3 months of stability at 25°C / 60% RH and 40°C / 75% RH. Error bars represent standard deviation.

These results are related to milled extrudate only, where loose powder, with far higher surface area than the final form (tablets), was exposed to room conditions. Polymers are typically very hygroscopic and no protection from moisture was applied in these experiments, for instance through the use of silica canisters. Additional excipients for tableting are still to be included in the formulation, where moisture scavengers may be considered, as well as surfactants to enhance the drug release rate. Therefore, we consider the results very suitable for further development of an HME-based ETR formulation.

4. Conclusion

In conclusion, a systematic step-by-step approach towards the development of a formulation of ETR, with improved solubility and promising stability, is reported. The development was performed in three successive steps to optimize the development of ETR ASDs: thermodynamic evaluation, experimental assessment by HTS, and finally manufacturing of selected formulations by HME. Overall, the predicted miscibility and interaction between ETR and each polymer agreed with the experimental results. PVP was found to have the greatest miscibility with ETR leading to a fully ASD, even after storage over 3 months at 40°C / 75% RH. These findings demonstrate the complex interplay between miscibility and performance, but also highlights the importance of physicochemical-based predictions, successfully applied to ETR.

The selected formulation is quite simple (a ternary composition) and its production was considered easy and straightforward, which is crucial for industrial technology implementation. The ETR solid dispersion demonstrated more than two times of improvement in the drug release when compared to the crystalline drug. XRPD and Raman spectroscopy were key to characterize it as essentially amorphous. Raman spectroscopy was demonstrated to be especially useful to control the solid-state of ETR, as different sections of the spectra were identified with the potential to discriminate between amorphous and crystalline forms. Besides, a weak interaction affecting the CN groups of ETR was also detected in the solid dispersions. There was no evidence of such interactions with SLP, as the Raman spectrum was very similar to ETR, and this may also be related to its low potential for miscibility with ETR. Besides, this dipolar intermolecular interaction may be responsible for the stability at such a high temperature and humidity as 40°C / 75% RH, which is quite surprising taking into account that the theoretical T_g, calculated without considering the high impact of moisture, was very close to the limit set by the 'T_g – 50°C' rule. It was also shown to be useful in detecting structural rearrangements, probably leading to drug recrystallization shortly, as the deviation decreased along the stability time when exposed to 40°C / 75% RH, moving closer to the typical crystalline Raman shift. mDSC experiments were able to determine the real T_g, well above the predicted value, and a clear confirmation of the existence of intermolecular interactions within the system. No drug crystallization was detected by Raman spectroscopy and XRPD, and the decrease in the *in vitro* dissolution profile was then attributed to a polymeric chain rearrangement, probably β-relaxations, even more prominent taking into account the water uptake by the system. This was

not detected previously by the Raman spectroscopy. Secondary relaxations are typically very weak and translated into very smooth changes in the position or shape of spectroscopy bands, which may not be detectable in mixtures of complex materials. Taken together, these results are promising for a successful solid dispersion of ETR, prepared by HME. The next steps include formulation studies, where additional excipients will be included, as well as the optimization of the HME process parameters.

CHAPTER III. ENHANCED SOLID-STATE STABILITY OF AMORPHOUS IBRUTINIB FORMULATIONS PREPARED BY HOT-MELT EXTRUSION

Abstract

One of the applications of Hot-melt extrusion is the stabilization of amorphous drugs through its incorporation into polymeric blends in the form of ASDs. In this study, HME was applied to solve a real problem in the development of an ibrutinib product, stabilizing the amorphous form. A systematic approach was followed by combining theoretical calculations, high-throughput screening focused on physical stability, and Principal Components Analysis. The HTS enabled the evaluation of 33 formulations for physical stability and the PCA was key to select four promising systems. The low relevance of drug loading on the drug crystallization supported the HME tests with a very high drug load of 50%. Milled extrudates were characterized and demonstrated to be fully amorphous. The thermal analysis detected a glass transition temperature much higher than the predicted values. Along with several weak intermolecular interactions detected in Raman spectroscopy, a dipolar interaction involving the α, β unsaturated ketone was also noticed. The additive effect of these intermolecular interactions changed markedly the performance of the ASDs. The physical strength of the prepared systems was corroborated by stability studies until 6 months at long-term and accelerated conditions.

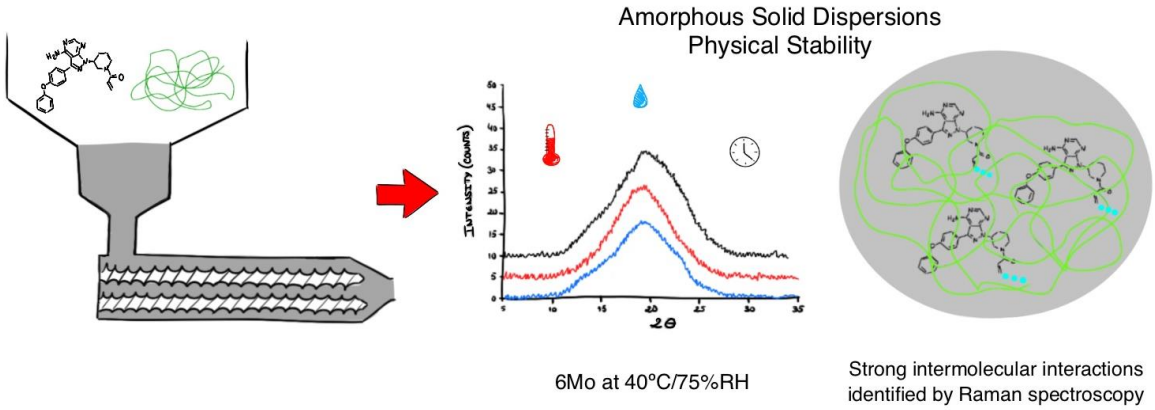

Figure 3.1. Graphical abstract of chapter III. The stabilization of an amorphous drug through its incorporation into polymeric blends in the form of ASDs.

The results presented in this chapter were published in Simões MF, Nogueira BA, Tabanez AM, Fausto R, Pinto RMA, Simões S. Enhanced solid-state stability of amorphous ibrutinib formulations prepared by hot-melt extrusion. Int J Pharm. 2020 Apr 15;579:119156. doi: 10.1016/j.ijpharm.2020.119156.

My contribution to this work was performing thermodynamic predictions, designing and performing the systematic screening of promising compositions, the preparation of the solid dispersions, its characterization by PLM, interpretation of thermal analysis, XRPD and Raman spectroscopy results, conducting and managing the stability study, and statistical analysis. Thermal analysis was conducted at the Chemical Process Engineering and Forest Products Research Centre (CIEPQPF), XRPD characterization was performed at the Centre for Physics of the University of Coimbra (CFisUC), Polarized Light Thermal Microscopy and Raman spectroscopy in the Department of Chemistry of the University of Coimbra, by Rui Fausto and co-workers.

This chapter is not an integral copy of the published work.

1. Introduction

The poor water solubility of BCS class II and IV molecules are the rate-limiting steps for absorption, which generally leads to low BA and their failure as therapeutic agents [328, 329]. The amorphization of crystalline drugs is often seen as a solution to this problem, due to the enhanced apparent solubility caused by the disruption of the crystal lattice and its high energy state [330-332]. Although these forms exhibit an increased rate of dissolution due to high thermodynamic activity, they have also a potential to revert to the more stable crystalline form [333, 334]. This is the main issue associated with the amorphous state: the physical instability on aging in the form of phase separation and recrystallization, which can eventually affect the dissolution [32-34] and lead to the therapy failure. This justifies at least partially, why there are only a few amorphous drugs and formulations in the market [36, 40]. Thus, improved strategies for the stabilization of amorphous compounds in pharmaceutical development are still needed.

HME has been revealed as a successful technology for a large spectrum of applications in the pharmaceutical industry. One of the most recently reported applications of HME is the stabilization of amorphous drugs through its incorporation into polymer blends in the form of ASDs [28]. Despite the promising performance of HME to enhance the physical stability of amorphous compounds, there are only a few studies reporting this application [35, 335]. Solid dispersions are systems where one component is dispersed in a carrier (usually polymeric), and where the whole system is solid [32-34, 36, 37]. These systems can increase the physical stability of drugs through fundamentally two main approaches, as reviewed by Janssens and Mooter [120] and by Baghel and colleagues [119]. In one, polymeric carriers with T_g can kinetically stabilize amorphous systems by reducing molecular mobility and thus ‘‘freezing’’ the amorphous drug in a metastable state. The other is related to intermolecular bonds, which decrease the molecular mobility of the compound within the polymeric matrix and provide stability to the composition [28, 120], through the decrease of the overall thermodynamic energy. These interactions are weak, as H-bonding, van der Waals, electrostatic, ionic, or hydrophobic, but enough to stabilize ASDs.

Preliminary formulation tests with the amorphous form of ibrutinib, hereafter known as IBR, failed to demonstrate physical stability and recrystallized only after 1 month of stability at 40°C / 75% RH. Therefore, there was the need to physically stabilize this drug, and, as part of our ongoing program where HME is applied to drug product development [93, 316], a new formulation strategy was

pursued, where polymers were combined with this compound by HME. A very recent study was published by Xu and colleagues [336] reporting enhanced solubility and physical stability of a coamorphous solid form of IBR and saccharin. However, as there is no guidance available for coamorphous forms to date, and even the co-crystals are still under implementation in pharmaceutical R&D units, a polymeric formulation strategy would be preferred to mitigate risks and increase the chance of getting to patients [337]. To our knowledge, there is no other published strategy to enhance the physical stability of amorphous IBR.

IBR (Figure 3.2) is chemically designated as 1-[(3R)-3-[4-amino-3-(4-phenoxyphenyl)-1*H*-pyrazolo[3,4-d]pyrimidin-1-yl]-1-piperidinyl]-2-propen-1-one, and is an inhibitor of Bruton's tyrosine kinase through the formation of a covalent bond with a cysteine residue in the active site, relevant in B cells. It is available in the market under the brand name Imbruvica®, both in EU and the US by Janssen, for the treatment of B cell diseases, such as Mantle Cell Lymphoma, Chronic Lymphocytic Leukemia/Small Lymphocytic Lymphoma, Waldenström's Macroglobulinemia, Marginal Zone Lymphoma, and Chronic Graft versus Host Disease [338]. A summary of the physicochemical characteristics of IBR is presented in Table 3.1.

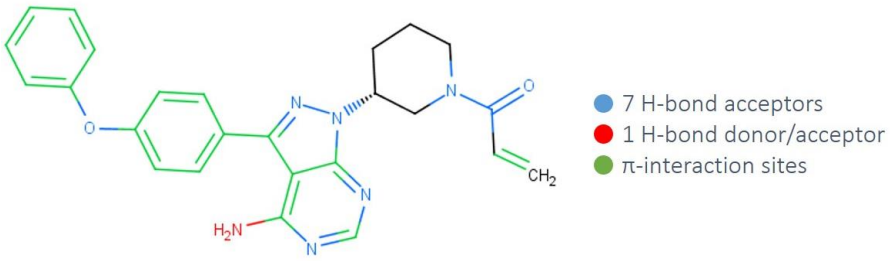

Figure 3.2. Chemical structure of IBR. Potential interaction sites are highlighted.

Table 3.1. Physicochemical properties of IBR [339, 340].

Characteristic	Value
Molecular weight	440.51 g/mol
Molecular formula	$C_{25}H_{24}N_6O_2$
Melting point	152.2 ± 0.37°C (form I, experimental data)
Glass transition temperature	79.1 ± 0.4°C (amorphous, experimental data)
Polar Surface Area	99.2 Å^2
Log P	3.97
pKa (base)	3.74
BCS class	II
Solubility	0.003 mg/mL in water
	Practically insoluble in water
	Freely soluble in N, N-dimethylformamide
Molar Volume	327.5±7.0 cm^3

Our study initiated by thermal characterization of amorphous IBR to assess the viability of the proposed strategy. A comprehensive thermodynamic evaluation of the drug and possible carriers to predict polymer-drug miscibility was then performed, followed by an HTS focused on physical stability. Physical stability was evaluated by both Raman spectroscopy and PLM. After the selection of the most promising systems, HME tests were performed and the extrudates characterized. Stability studies focused on the physical stability of milled extrudates prepared by HME were carried out for 6 months.

2. Experimental section

2.1. Materials

Amorphous and crystalline IBR were acquired from a GMP-approved drug supplier. PVPVA brand name Kollidon® VA64, PVP of grade K12 (brand name Kollidon® 12PF), and Polyvinyl caprolactam-polyvinyl acetate-polyethylene glycol graft copolymer (brand name Soluplus®, SLP) were obtained from BASF (Ludwigshafen, Germany). HPMCAS grade MF (brand name AQOAT®) was kindly donated by Shin-Etsu (Totowa, NJ), and PVOH, brand name Parteck® MXP, was obtained from Merck Millipore (Darmstadt, Germany). PEG grade 6000 (PEG6000) was acquired from Clariant (Hoechst) (Muttenz, Switzerland), and Poloxamer 407micro (P407), brand name Kolliphor® P407, was also obtained from BASF (Ludwigshafen, Germany).

2.2. Methods

2.2.1. Thermal analysis

mDSC analysis was performed in a Q100 (TA Instruments, New Castle, Delaware). Samples of 2-4 mg were weighed and placed in aluminum crimped pans. mDSC analysis was performed using a heating rate of 5°C/min, from 0°C to 220°C, amplitude ± 0.80°C and a period of 60 s. Nitrogen purge gas was used with a flow rate of 50 mL/min. Calibration was performed using indium and tin. For each sample, measurements were performed at least in duplicate. TGA was performed on a TG Q500 (TA Instruments, New Castle, Delaware). Samples were placed in platinum pans and heated from 25°C to 220°C at 5°C/min under a nitrogen atmosphere (60 mL/min).

2.2.2. Polarized Light Thermal Microscopy

Polarized Light Thermal Microscopy (PLTM) images were obtained through the combination of polarized light and wave compensators, a hot stage DSC600 (Linkam Scientific Instruments Ltd. Surrey, UK) with a magnification power of 200x, attached to a Leica® DMRB microscope (Leica Microsystems GmbH, Germany), and a Sony® CCD-IRIS/RGB video camera. The evaluation of

images was performed with Linkam Real-Time Video Measurement System software. Drug and HME samples were heated to 250°C at a rate of 10°C/min and, subsequently, let gradually cool until room temperature.

2.2.3. Raman spectroscopy

All spectra were recorded with the Horiba® LabRAM HR Evolution, coupled to a confocal Olympus® microscope (HORIBA France SAS, France). Individual Raman spectra from various random points of the samples were collected and averaged. The focusing spot for this technique is around 1 µm, with a collection time between 5 and 60 seconds. Each spectrum was collected from 5 to 50 times and averaged. The laser irradiation was performed at 633 nm wavelength, with a power of 17 mW and a 50x magnification objective was used to focus on every sample. The spectra were collected in a wavenumber range of 50-1800 cm^{-1}.

2.2.4. Variable Temperature Raman spectroscopy

The Raman spectroscopy was carried out using the same spectrometer, irradiation source conditions and microscope described above. A 10x magnification objective, with a laser spot around 1000 µm was used to analyze the largest possible sample area. Samples were placed in a hot stage THMS 600 (Linkam Scientific Instruments Ltd. Surrey, UK), controlled by a T95-PE Linkpad controlling unit, heated up to 170°C at a rate of 10°C/min, and gradually let to cool until room temperature. For IBR samples, the collection time was 10 seconds and each spectrum was collected 10 times, with a delay time of 250 seconds; for HME systems, 5 seconds and 15 times, with 320 seconds of delay. Raman spectra were recorded at 10°C intervals, in a wavenumber range of 50-1800 cm^{-1}.

2.2.5. Calculation of Solubility Parameters

The thermodynamic solubility/miscibility of IBR in each polymeric carrier was assessed using Hansen solubility parameters δ [142], calculated from their chemical structures using the van Krevelen and Hoftyzer contribution group method [180]. For each molecule, the energy from dispersion forces between molecules (δ_d); the energy from dipolar intermolecular forces between molecules (δ_p); and the energy from hydrogen bonds between molecules (δ_h) were calculated. The total solubility parameter (δ_t) was then determined following Equation 3.9.

Equation 3.9. $\delta_t = \sqrt{{\delta_d}^2 + {\delta_p}^2 + {\delta_h}^2}$

2.2.6. Prediction of T_g through the Gordon-Taylor equation

The T_g of a miscible blend (drug and polymer) is given by the Gordon–Taylor equation (Equation 3.10) [178]), or the simplified form by Fox (Equation 3.11) [179]):

Equation 3.10. $Tg = \frac{w_1 Tg_1 + K w_2 Tg_2}{w_1 + K w_2}$

Equation 3.11. $\frac{1}{Tg} = \frac{w_1}{Tg_1} + \frac{w_2}{Tg_2}$

where T_g, T_{g1}, and T_{g2} are the glass transition temperatures of the blend and the two different components, respectively; *w* represents the weight fraction; *K* is calculated from the Simha–Boyer rule (Equation 3.12), where ρ indicates the true density of the component [318]:

Equation 3.12. $K \approx \frac{\rho_1 Tg_1}{\rho_2 Tg_2}$

2.2.7. Design of binary system studies

Solvent evaporation technique [93] was applied to prepare small films in microscopic slides of different combinations of polymers and IBR, to narrow down on a few polymer-drug combinations. The study was designed to allow a set of screening assays in high-throughput nature, miniaturization (material sparing, small sample size), and prompt response, and encompassed 8 different polymers and drug in 5 charge levels, ranging from 10% to 50%. IBR and a panel of eight polymers were dissolved in THF or DMF (solutions of 10% polymer + drug) and dispensed onto microscopic slides. The solvent was then evaporated. The experiments were evaluated in what concerns physical stability over 2 months, under exposure to 60°C (oven), 40°C / 75% RH, 25°C/ 60% RH, and room temperature in the desiccator, and assessed by PLM and Raman spectroscopy.

2.2.8. Polarized Light Microscopy

Glass slides were examined directly for birefringence with polarized reflected light by Motic® BA310MET-T equipped with Moticam 5 (both by Motic Europe, S.L.U.). Crystalline structures were evaluated qualitatively, a scale from 1 to 5 in terms of both crystals size and quantity.

2.2.9. Preparation of ASDs

HME was performed using a co-rotating twin-screw extruder Thermo Scientific® HAAKE MiniLab II (Thermo Scientific, UK). Temperature and screw speed were optimized based on extrudate appearance, extrudability, and torque, using batch sizes of 10 g. The powder blends were added manually in small amounts. A round die with a diameter of 2 mm was attached to the extruder. The screw is conical with conveying elements only. All the glassy material was cooled in a conveyor belt and ground at 20 000 rpm in IKA® M20 to a fine powder. This powder was collected to glass bottles and stored in a desiccator.

2.2.10. X-Ray Powder Diffraction

XRPD analysis was performed at ambient temperature using a Bruker® D8 powder diffractometer (Bruker Corporation, Massachusetts, US), in a Bragg-Brentano geometry (reflection geometry), equipped with a Ni monochromator and LYNXEYE TE energy-dispersive detector. The X-ray source used was Cu $K\alpha^{1/2}$ (1.54 Å) with λ_1=154.056 pm and λ_2=154.439 pm. Spectra were collected from scans within the range 5.0° - 35.0° at 2θ with a step size of 0.02° (2θ) and time per step of 0.5 s.

2.2.11. Stability studies

ASDs were stored in closed glass bottles of 30 mL at defined conditions (two climatic chambers, 25°C / 60% RH, and 40°C / 75% RH) and investigated from time to time concerning crystallization (1, 3, 6 months) by XRPD. Raman spectroscopy was also performed at 6 months of stability. To evaluate by PLM, unmilled samples were preferred.

2.2.12. Statistical analysis

Performed using the commercial software package JMP® 14.0 from SAS Institute, Inc.

3. Results and discussion

3.1. Solid-state characterization of Ibrutinib

3.1.1. Thermal analysis

TGA and mDSC were used to evaluate the thermal stability of amorphous IBR during a heating process (Figure 3.3A). There is an endothermic event in the 15-70°C region, probably due to the loss of volatile components, which was also detected in the TGA (mass loss of approximately 0.6%). This likely represents water and residual solvents, also reported at the same level by the drug manufacturer. Moreover, the T_g of amorphous IBR was detected as 79.1 ± 0.4°C, as observed in the reversing heat flow curve. An exothermic event in the region 100-175°C is related to a solid-solid transition from the amorphous to a crystalline phase, as no loss of mass was detected in the TGA. No other significant enthalpy changes are visible in the studied range of temperature and, therefore, no degradation of amorphous IBR was observed in the mDSC or the TGA. IBR is thermally stable at least up to 220°C. This working temperature is quite high and was never applied during IBR extrusion. The crystalline IBR is characterized by an endothermic event at 152.2 ± 0.37°C (onset), which corresponds to the melting point, as suggested by the reverse heat flow curve (Figure 3.3B). This is immediately followed by an exothermic signal between 160 and 200°C, which is related to material decomposition with a loss of mass of 0.4% reported in the TGA.

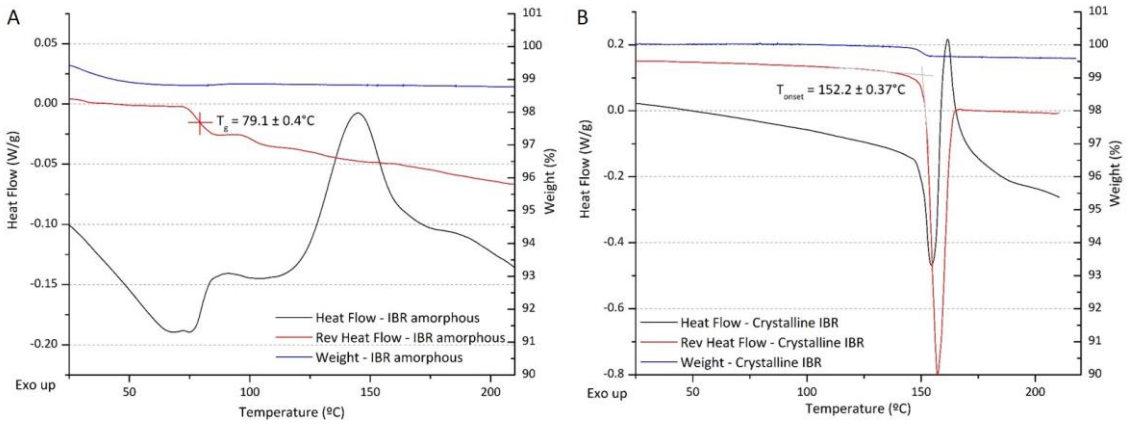

Figure 3.3. Modulated temperature differential scanning calorimetry and thermogravimetric analysis of IBR. A: amorphous; B: crystalline. Black line: Total heat flow; Red line: reversing heat flow. Equipment: Q100 (TA Instruments). Aluminum capsules. Method: from 0°C to 220°C at 5°C/min, amplitude ± 0.80°C and a period of 60 s. Blue line: Thermogravimetric analysis of IBR. Equipment: TG Q500 (TA Instruments). Method: from 25°C to 220°C at 5°C/min.

The amorphous drug was also characterized by PLTM, where the amorphous sample was heated up to 250°C and then cooled gradually until room temperature. The results are portrayed in Figure 3.4. It is possible to conclude that at 90°C the sample already has visible morphologic changes, compatible with a glass transition, more pronounced the higher the temperature as it evolves towards a less viscous state. The recrystallization is visible from 115°C and became more evident until 150°C. At 157°C, the whole sample is molten, i.e. both the crystalline and the amorphous form. No changes were observed above this temperature and, after cooling, the sample returns to the initial amorphous state. These results are in agreement with the mDSC. The slight differences in the reported temperatures are essentially due to the method (the modulated heating rate at 5°C/min or non-modulated at 10°C/min) and sample quantity. Moreover, mDSC experiments were performed under inert atmosphere and hermetically sealed pan, which did not happen in the case of PLTM. Also proven by the PLTM experiment, no further relevant thermal event is detected in the amorphous IBR.

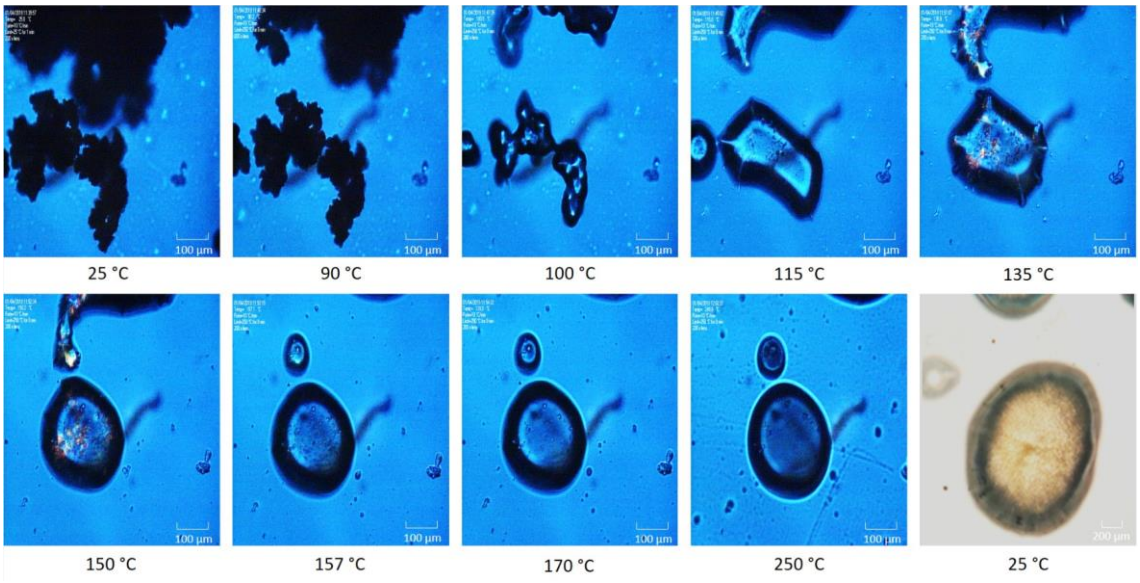

Figure 3.4. Polarized light thermal microscopy images collected in the IBR heating process from 25 to 170°C at a rate of 10°C/min, and magnification of 200x.

3.1.2. Raman spectroscopy

The Raman analysis demonstrated different spectra between the crystalline IBR and the amorphous form, with marked differences throughout the whole spectra, and in particular in the spectral regions where the most intense bands are observed, i.e., below 150 cm^{-1}, between 700

and 800 cm^{-1}, and between 1400 and 1650 cm^{-1}. Relatively pronounced frequency shifts are also perceived for the bands appearing at 1471 and 1557 cm^{-1} in the spectrum of the crystalline material, which are observed at respectively 1476 and 1564 cm^{-1} in the spectrum of the amorphous material (Figure 3.5). The three spectral sections where the amorphous material demonstrates the greatest divergence from the crystalline form are highlighted in the figure. These changes in the Raman spectra are caused by the destruction of the crystal lattice, as well as by the disorganized molecular orientation [341]. Raman spectroscopy can control the solid-state of IBR, with several regions identified and marked differences between the amorphous and crystalline forms, as also reported by Zvoníček and his group [342].

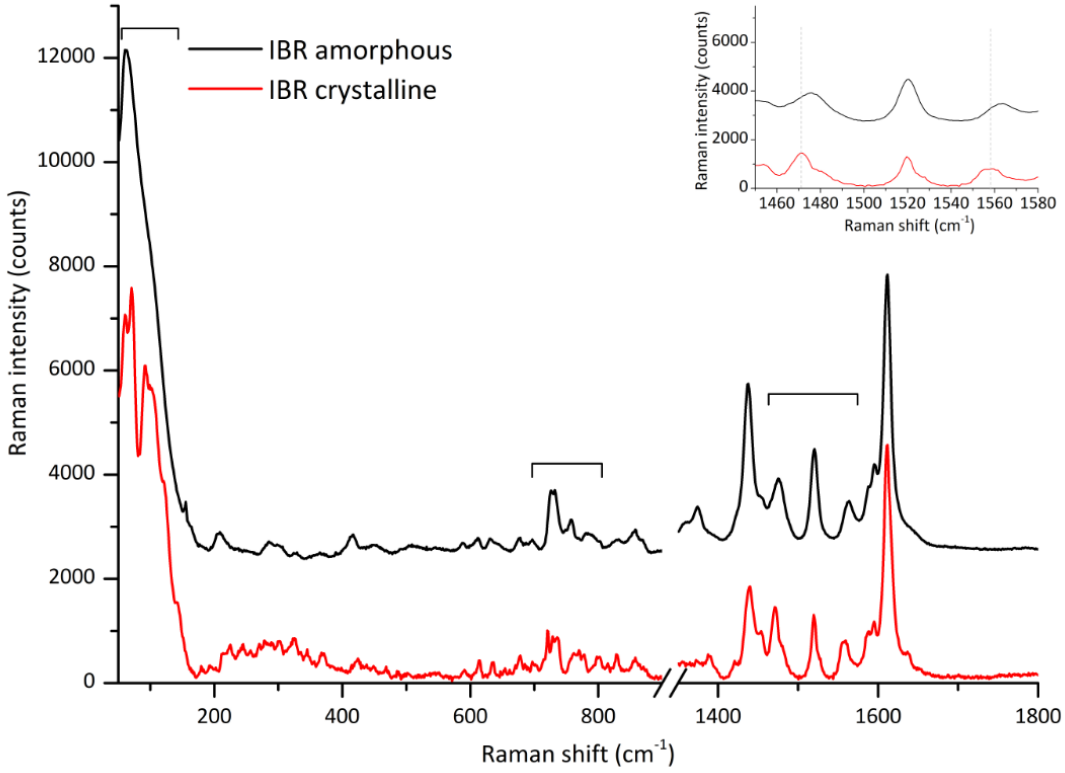

Figure 3.5. Raman spectra of crystalline and amorphous IBR. The spectra were recorded in the 50-1800 cm^{-1} wavenumber range, during 20 seconds with 20 accumulations, and excitation at 633 nm. The highlighted areas correspond to where most pronounced differences were detected. The graph inset depicts the spectra zone from 1450 to 1580 cm^{-1}, where band shifts are highlighted by the vertical red dashed lines (see text for discussion).

3.1.3. Variable Temperature Raman spectroscopy

The Raman spectra were collected at different temperatures on heating to verify the potential for structural changes. IBR amorphous sample was heated up to 170°C (well above T_g and other thermal events) and then cooled until RT. The results are portrayed in Figure 3.6. Visible changes are noticed with temperature, in particular in the intensity of Raman peaks, for instance in the

relative intensities of the bands at 1436 and 1476 cm^{-1}. Moreover, shifts of the 1476 and 1564 cm^{-1} bands to 1469 and 1557 cm^{-1} respectively, are observed when heated above 120°C, as well as changes in the area below 150 cm^{-1}, denoting clear solid-state changes compatible to conversion from amorphous to the crystalline phase. This is related to the drug recrystallization as it matches the typical bands of crystalline IBR (compare the spectra shown in Figure 3.6 with the reference spectra for the amorphous and crystalline IBR presented in Figure 3.5), expected due to what was already observed in the PLTM and reported in the mDSC experiment. Importantly, the Raman spectra of IBR before the experiment and after re-cooling are very similar, excluding drug degradation or structural changes on heating, and supporting mDSC and PLTM conclusions.

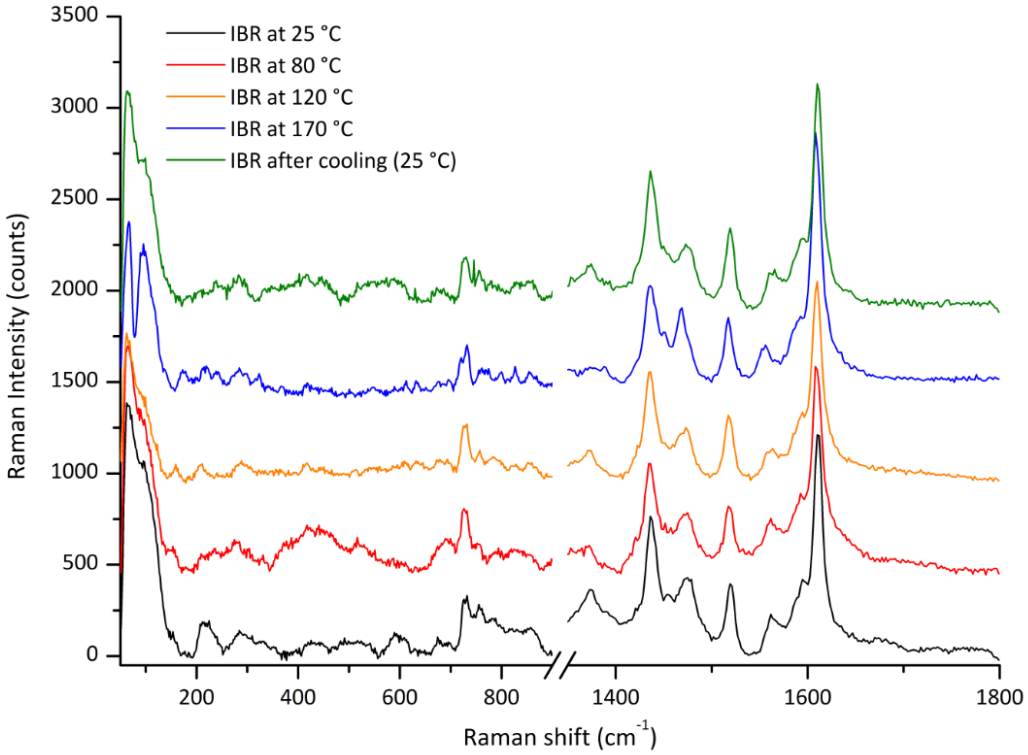

Figure 3.6. Raman spectra of amorphous IBR with thermal analysis (25, 80, 120, 170, and 25°C (after cooling)). The spectra were recorded in the 50-1800 cm^{-1} wavenumber range, during 20 seconds with 20 accumulations, and excitation at 633 nm.

3.2. Prediction of Drug-Polymer Miscibility

Van Krevelen and Hoftyzer group contribution method was used to calculate the Hansen solubility parameters (Equation 3.9). Eight structurally different polymers were considered at this stage. To determine the solubility parameters for SLP, which is composed of polyvinyl caprolactam: polyvinyl

acetate: PEG at a ratio of 57:30:13, the average number of the three monomers was calculated. The δ for each component and the difference between the drug and each polymer ($\Delta\delta$) are provided in Table 3.2. It is known from the literature that a difference in solubility parameter of less than 7 $MPa^{0.5}$ indicates good miscibility, whereas if the difference is above 10 $MPa^{0.5}$, the system is expected to be immiscible [31, 39, 142, 144].

Table 3.2. Estimated solubility parameter of the drug and HME polymers using Hansen parameters.

Compound / Polymer	Solubility Parameter δ ($MPa^{0.5}$)	$\Delta\delta = \delta_{drug} - \delta_{POL}$ ($MPa^{0.5}$)
IBR	23.62	-
PEG	21.25	2.37
PVP	27.19	3.57
PVPVA	25.26	1.64
SLP	21.03	2.59
HPMC	27.28	3.66
HPC	29.71	6.10
HPMCAS	24.63	1.02
PVOH	32.52	8.90

Δ_{drug} solubility parameter of the drug; δ_{POL} solubility parameter of the polymer; $\Delta\delta$ solubility parameter difference between the drug and polymers.

IBR has a solubility parameter (23.62 $MPa^{0.5}$) closer to HPMCAS, as well as to PEG, PVPVA, and SLP, whereas HPC and PVOH had the most different results, very close or higher than the recommended cut-off limit of 7.0 $MPa^{0.5}$, predicting poor miscibility. According to the results in Table 3.2, the miscibility between IBR and each polymer is likely to follow the order: HPMCAS > PVPVA > PEG > SLP > PVP > HPMC > HPC > PVOH. Here, PVOH is suggested to have the lowest solubility capacity to dissolve IBR and to produce a solid solution. However, it is important to keep in mind that the miscibility estimated by this approach is likely to be an underestimation [31, 124] for complex systems involving long-range orders (such as ionic) or highly directional (as hydrogen bonding) [26, 124, 145, 307]. In this work, HPMCAS, PVPVA, PEG, SLP, PVP, and HPMC were identified as the polymers with the highest potential to be miscible with IBR. PVPVA, SLP, PVP, and HPMC are usual carriers for HME immediate-release formulations, whereas PEG is preferred as a solubility-enhancer or plasticizer, and HPMCAS as a release-modifying agent or stabilizer.

3.3. Prediction of T_g of the ASD through Gordon-Taylor equation

It is well known that the T_g is related to the physical stability of amorphous systems [28, 117, 120]. Table 3.3 presents the results of calculated T_g based on the Gordon-Taylor equation (Equation 3.10) as well as on the simplified form by Fox (Equation 3.11).

Table 3.3. Prediction of T_g of the ASD through the Gordon-Taylor and Fox equations, considering a mixture of IBR and polymer of 1:1.

Compound/ Polymer [a]	T_g (°C) [b]	ΔT_g (°C) = T_{gIBR} - T_{gPOL}	Blend T_g (°C) - Gordon-Taylor equation	Blend T_g (°C) - Fox equation
IBR	79.1 [c]	-	-	-
PVP K12	90	-10.9	84.2	84.2
PVPVA	101	-21.9	89.1	88.7
SLP	70	9.1	73.9	74.3
HPMC	178	-98.9	110.5	109.5
HPC	0	79.10	0.0	0.0
HPMCAS - MG	130	-50.9	98.1	98.4

[a]PEG was not evaluated due to its crystalline nature. PVOH was also not considered in this evaluation due to being semi-crystalline. [b]T_g values of polymers were extracted from suppliers' technical datasheet. [c]Determined experimentally by mDSC.

Overall, all the compositions should have neglected molecular mobility at least until 25°C, which is the usual storage restriction for pharmaceuticals, as the lowest predicted T_g was around 75°C (following the 'T_g – 50°C' rule proposed by Hancock *et al.*) [117, 343]. It is important to keep in mind that these conclusions rely on the assumption of complete miscibility between the drug and the polymer(s) [31] and that it ignores the β-relaxation and potential intermolecular interactions. However, it is still considered guidance for determining the storage temperature and predicting the physical stability of amorphous systems.

The T_g values of the amorphous polymers are very different, from 0 to 178°C. In terms of blend T_g predicted by the Gordon-Taylor equation, HPMC should provide the lowest molecular mobility, followed by HPMCAS, but very high processing temperatures are needed to extrude these pure compositions. The ΔT_g values between the drug and the polymers are quite low for PVP, SLP, and PVPVA, but not for the cellulose-based polymers. Since the T_g value indicates the temperature above which the polymer chains become flexible, more interactions are expected to occur in the HME process if the components have similar T_g values [320]. On this ground, SLP, PVPVA, and PVP should be the most promising polymers for interacting with IBR and are considered for testing by HME. Five combinations (IBR with PVP k12, PVPVA, SLP, SLP + HPMCAS, and HPMC) were selected

to proceed to the next stage, where they were evaluated experimentally in terms of physical stability to rank order performance. A binary combination with PEG was also considered as a negative control for physical stability, due to its high molecular mobility at room temperature.

3.4. High-throughput screening of carriers

Solvent-evaporation is usually applied to verify the solubility enhancement of ASDs. In this study, solvent evaporation [93] was employed to study physical stability over 2 months, assessed both by PLM and Raman spectroscopy, used as a validation of PLM observations. Small films of different combinations of polymers and IBR were prepared in microscope slides and analyzed to narrow down on a few polymer-drug combinations (Figure 3.7). High drug loads and high surface area of thin films in contact with ambient humidity lead to a lack of thermodynamic equilibrium, which promotes rapid drug crystallization and the fast failure of unstable systems. With this method, it is possible to readily select promising systems by promoting the failure of doomed compositions. The study design and detailed results may be found in Appendix II, A. High-throughput screening – Physical stability evaluation.

In total, 33 systems were stored in four different conditions and evaluated over two months, where at least five evaluations per system by PLM/Raman were performed. This led to a total of around 600 results to handle. To analyze this amount of data, a multivariate statistic was applied, namely, PCA, where the level of crystallization, time, and drug load (variables) were analyzed by storage condition. The aim was to compare the evolution of each binary composition against a hypothetically perfect system, where no crystallization would be seen throughout the stability time, no matter the condition it was exposed to. PCA is usually applied as a dimension-reduction technique, but in this case, a different application was considered, as it was applied as a means to measure the distance to the ideal amorphous system. The higher the distance, the worst the composition would be in what concerns physical stability.

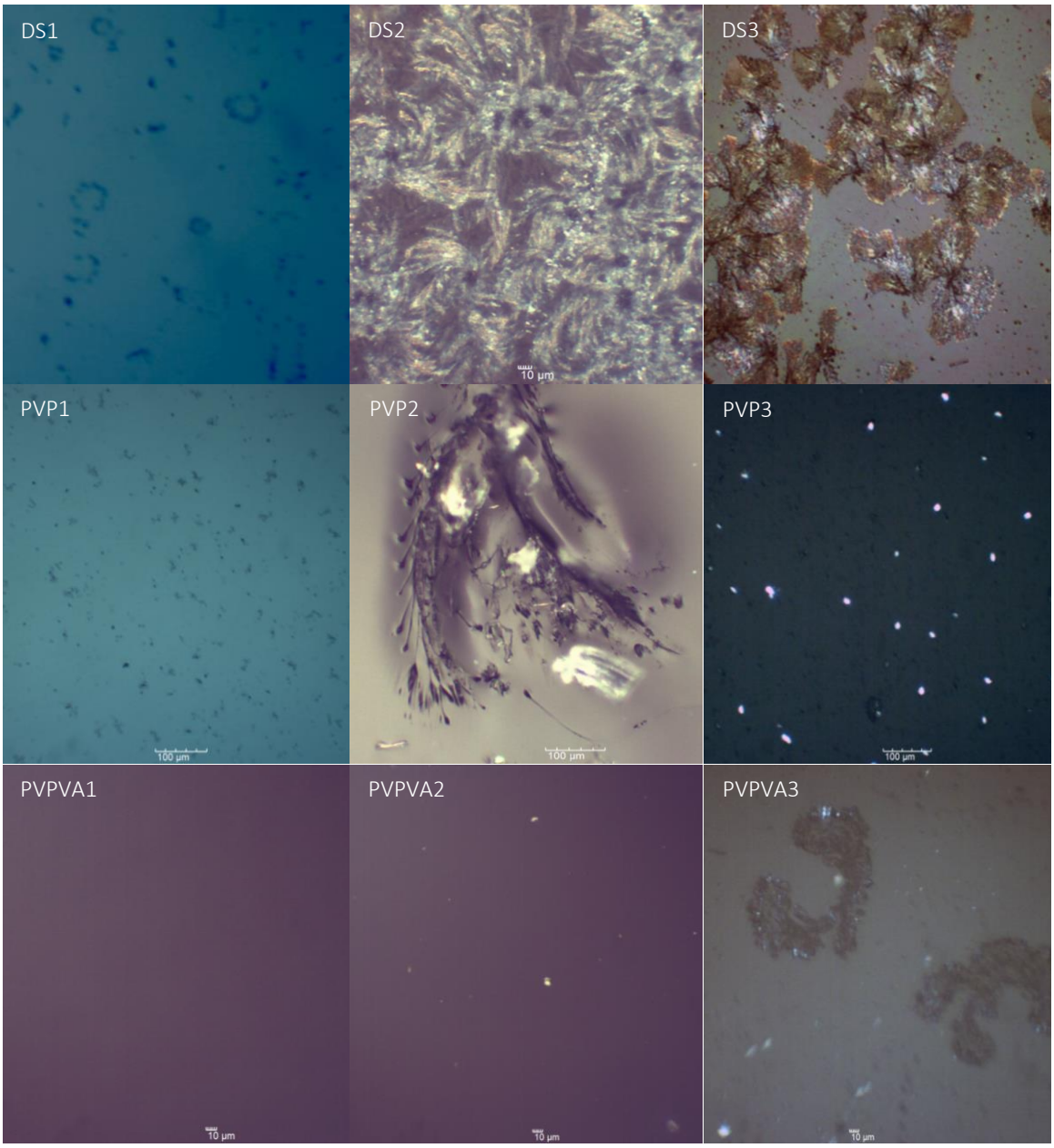

Figure 3.7. Birefringence of some binary compositions detected by PLM. DS1: sample pure drug (40%) at T0 with no crystals detected; DS2: sample pure drug (50%) after 6 days of storage at 60°C; DS3: sample pure drug (30%) after 1 month of storage at 60°C; PVP1: Sample PVP + 50% drug at T0 with no crystals detected; PVP2: Sample PVP + 50% drug after 3 days of storage at 60°C; PVP3: Sample PVP + 50% drug at 25°C / 60% RH after 2 weeks; PVPVA1: sample PVPVA + 30% drug after 6 days of storage at 60°C with no crystallization detected; PVPVA2: sample PVPVA + 50% drug after 6 days of storage at 60°C; PVPVA3: sample PVPVA + 40% drug after 1 month of storage at 25°C / 60% RH.

The following graphs (Figure 3.8) portray score and loading plots for the conditions under study, namely 60°C, 25°C / 60% RH, 40°C / 75% RH, and room temperature. Each composition is marked in a different color, and the perfect system is marked with an X. The score plot graphs each component's calculated values in relation to the other, adjusting each value for the mean and standard deviation. The loading plot depicts the unrotated loading matrix between the variables

(level of crystallization, time, % DS), and the principal components. The closer the value is to 1, the greater the effect of the component on the variable. Two principal components were generated with statistical significance ($p < 0.0001$, calculated through the Bartlett Test), which explain almost the total results variability in the performed analysis, namely 86.1% for the storage at 60°C (oven), 96.0% for the 40°C / 75% RH, 98.6% for 25°C / 60% RH and 99.2% for the storage at room temperature (Table 3.4).

Table 3.4. Eigenvalues table with results of the Bartlett test.

Condition	Component	Eigenvalue	Percent (%)	Cumulative Percent (%)	Prob > ChiSq[a]
60°C (oven)	1	124.27	47.0	86.1	< 0.0001
	2	103.60	39.1		< 0.0001
40°C / 75% RH	1	461.30	68.3	96.0	< 0.0001
	2	186.60	27.6		< 0.0001
25°C / 60% RH	1	454.12	69.9	98.6	< 0.0001
	2	186.34	28.7		< 0.0001
Room	1	454.03	70.4	99.2	< 0.0001
temperature	2	185.50	28.8		< 0.0001

[a] *p* value for the Bartlett test. This test evaluates if the data correlation is of random origin. If the null hypothesis is rejected, it means that the correlation of the data is linked with the determined eigenvalue.

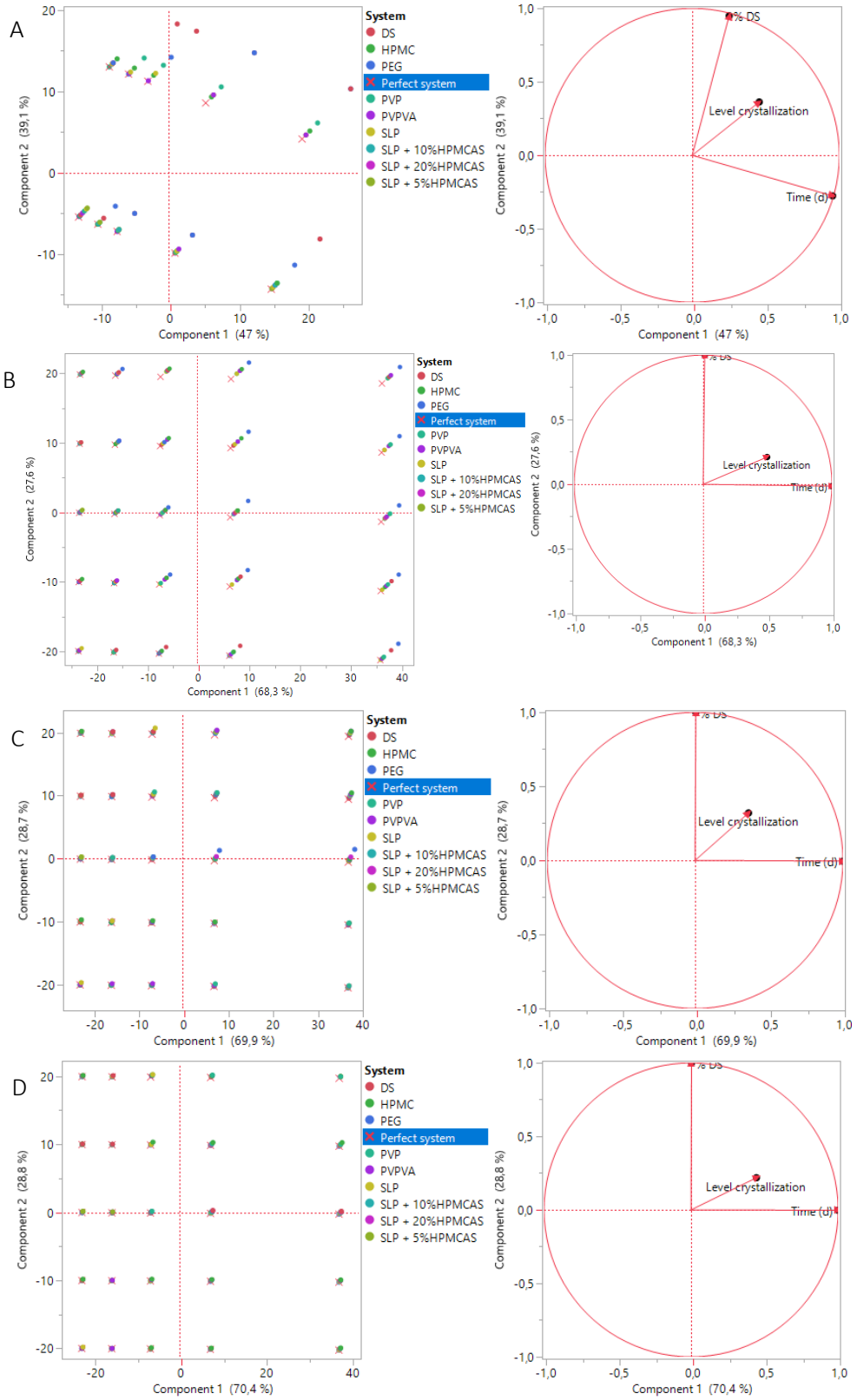

Figure 3.8. JMP® 14.0-assisted PCA performed for the storage at A, 60°C; B, 40°C / 75% RH; C, 25°C / 60% RH; D, Room temperature. The score plot (left) and the loading plot (right) are depicted. The closer the PC value is to 1, the greater the effect of the component on the variable. Two principal components were generated with statistical significance ($p < 0.0001$, Bartlett Test), which explain almost the total results variability. The perfect system for each binary composition is marked in x.

When looking at the score plots, it is possible to observe the deviation from the hypothetical perfect system with no crystallization (marked with an X) of each binary composition. This is more evident in systems with high temperature and humidity, as in 60°C or 40°C / 75% RH conditions, where the birefringence becomes evident in the PLM. This deviation was quantified based on the Euclidean distance, which was calculated per system. Then, a weighted mean value of the distance was calculated to rank order performance. The weighted mean was preferred over an arithmetic one to lend higher importance to higher loadings. This was performed by condition, to check discrepancies in systems' behavior by temperature or humidity. Figure 3.9 portrays an overview of these results.

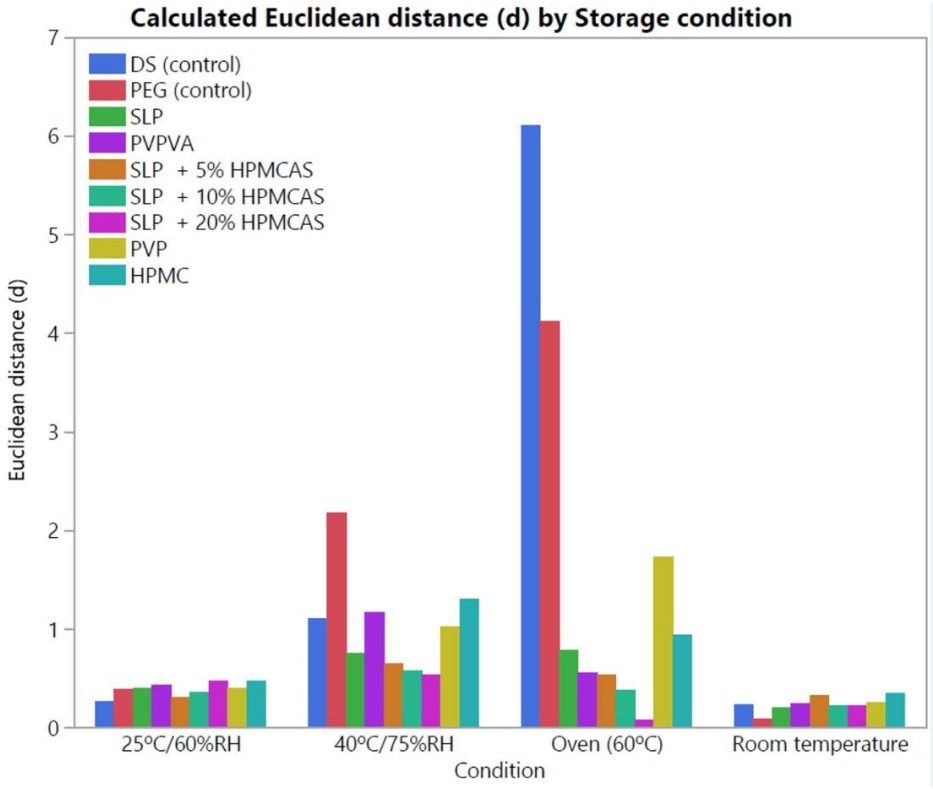

Figure 3.9. Euclidean distance from the perfect system based on PCA results.

It is clear that the storage at high temperature and humidity lead to more discriminant results, as the oven and the climatic chamber 40°C / 75% RH led to a generally higher distance from the perfect system. Although all the systems seem to be stable at low temperature and humidity, storage at 25°C / 60% RH and room temperature are not discriminative after 2 months. PVP-based systems seem not to provide stability when exposed to high temperatures, which is expected due to increased chain mobility, whereas for PVPVA the humidity seems to be key, as the 40°C / 75% RH triggered higher crystallization than in the oven (60°C, dry – approximately 8% RH). HPMC

compositions seem to be one of the least stables, probably due to the lack of intermolecular interactions (very discrepant T_g from IBR, as seen in Table 3.3). In what concerns SLP-based compositions, it seems that it is an adequate polymer for physical stabilization, mainly if HPMCAS is added as a stabilizer. A level of 20% of HPMCAS seems to be beneficial for IBR stabilization, mainly protecting against the effect of heat in the molecular mobility of polymers. This effect is not that clear in high humidity (40°C / 75% RH), where water causes a drastic decrease of T_g of HPMCAS, leading to increased chain mobility freedom.

To conclude on the effect of individual factors such as temperature, humidity, drug load, and time on crystallization, an additional multivariate statistical analysis was performed. Each polymeric composition was assessed again through PCA, to identify what is the underlying cause of crystallization for each system and, ultimately, what should we avoid to have a stable product. This may be observed by the loading plots depicting the variables (level of crystallization, time, temperature, humidity, and drug load) and the components (1 and 2). The details of this analysis, results, and additional conclusions may be found in Appendix II, B. HTS test: PCA analysis per system. It was concluded that humidity is the most important factor that triggers IBR crystallization and, surprisingly, drug load seems not to be relevant for the physical stability of an ASD of IBR. Therefore, a high drug load of 50% was selected to proceed to extrusion tests with the following systems: SLP, SLP + 20% HPMCAS, PVPVA, and PVP.

3.5. HME tests

The selected systems were subjected to HME to assess extrudability and physical state. The results of the extrusion of different formulations and the appearance of extrudates are detailed in Table 3.5. HME parameters were optimized to lead to the best appearance (clear and transparent), and the smoothest process. High temperatures were needed to extrude these systems, which was quite unexpected due to the predicted T_g. Moreover, all the systems required a plasticizer, which type and amount were selected based on the manufacturability of the system. The three binary systems were easily extrudable and led to yellowish and cloudy systems. This appearance is due to the high drug loading, not completely miscible, leading to amorphous IBR suspensions.

Table 3.5. Formulations, extrusion parameters, appearance, and extrudability.

Description	Speed (rpm)	Temperature (°C)	Torque (Ncm)	ΔP (bar)	Appearance
SLP + 50% IBR + 10% PEG6000	120	200	45	1	Yellowish and cloudy. Smooth extrusion.
SLP + 50% IBR + HPMCAS	Not extrudable. HPMCAS loads from 20% to 5% were investigated, but extrusion was not possible considering 50% of drug loading.				
PVPVA + 50% IBR + 15% P407	250	205	55	2	Yellowish and opaque. Smooth extrusion.
PVP k-12 + 50% IBR + 10% PEG6000	260	195	50	1	Yellowish and opaque. Smooth extrusion.

3.6. Characterization of the ASDs manufactured by HME

3.6.1. X-Ray Powder Diffraction

A halo was observed in all the systems studied, which is the typical XRPD spectrum of amorphous materials (Figure 3.10). In two of the systems, two small crystalline peaks seem to be emerging, but they are not related to the crystalline drug. Instead, they represent the crystalline plasticizers (PEG6000 or P407), with 2θ peaks observed at 19 and 23°, as described in the literature [344, 345]. Both components are known as fast re-crystallizers [346]. These peaks were not detected in the SLP composition due to the complete miscibility of PEG within the formulation and in all the systems IBR was considered fully amorphous as no relevant crystalline peaks were detected.

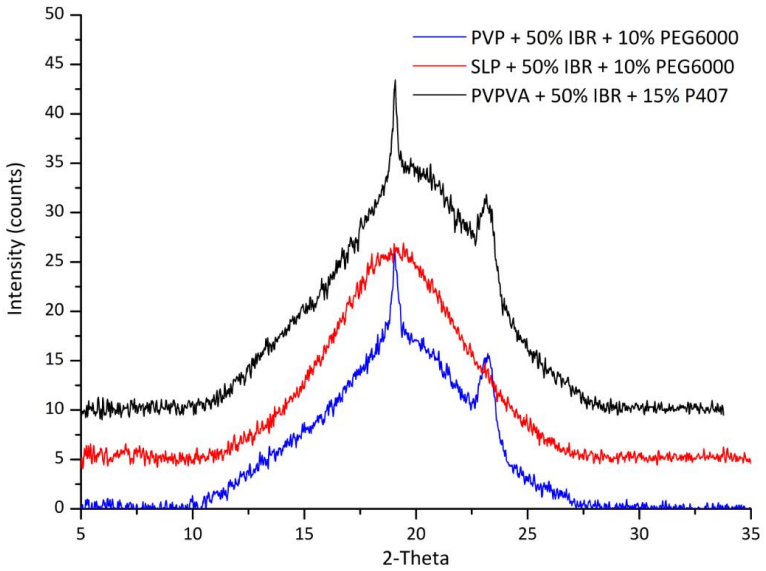

Figure 3.10. Overlay of XRPD patterns of solid dispersions manufactured by HME: SLP + 50% IBR + 10% PEG6000, PVPVA + 50% IBR + 15% P407, PVP + 50% IBR + 10% PEG6000.

3.6.2. Polarized Light Microscopy

The surface of unmilled extrudates was characterized by PLM. As depicted in Figure 3.11, all the systems display birefringence, but not similar to a typical crystallization pattern. Therefore, and also supported by the XRPD results, the observed mesh is related to the used plasticizers, which are clearly and homogenously dispersed within the matrix.

Figure 3.11. PLM images of solid dispersions manufactured by HME: A, SLP + 50% IBR + 10% PEG6000; B, PVPVA + 50% IBR + 15% P40; and C, PVP + 50% IBR + 10% PEG6000. The scale bars of PLM represent 100 µm.

3.6.3. Raman spectroscopy

The Raman spectra of IBR and the three ASDs manufactured by HME, SLP + 50% IBR + 10% PEG6000, PVPVA + 50% IBR + 15% P407, and PVP + 50% IBR + 10% PEG6000, are depicted in Figure 3.12. The three sections where the different solid-state forms demonstrate the greatest divergence from the crystalline form are highlighted and were already discussed in the drug characterization section. In general and besides the observation of the characteristic Raman bands of amorphous IBR, broadening of the bands is observed in the ASDs, which corroborate with a fully amorphous dispersion of IBR.

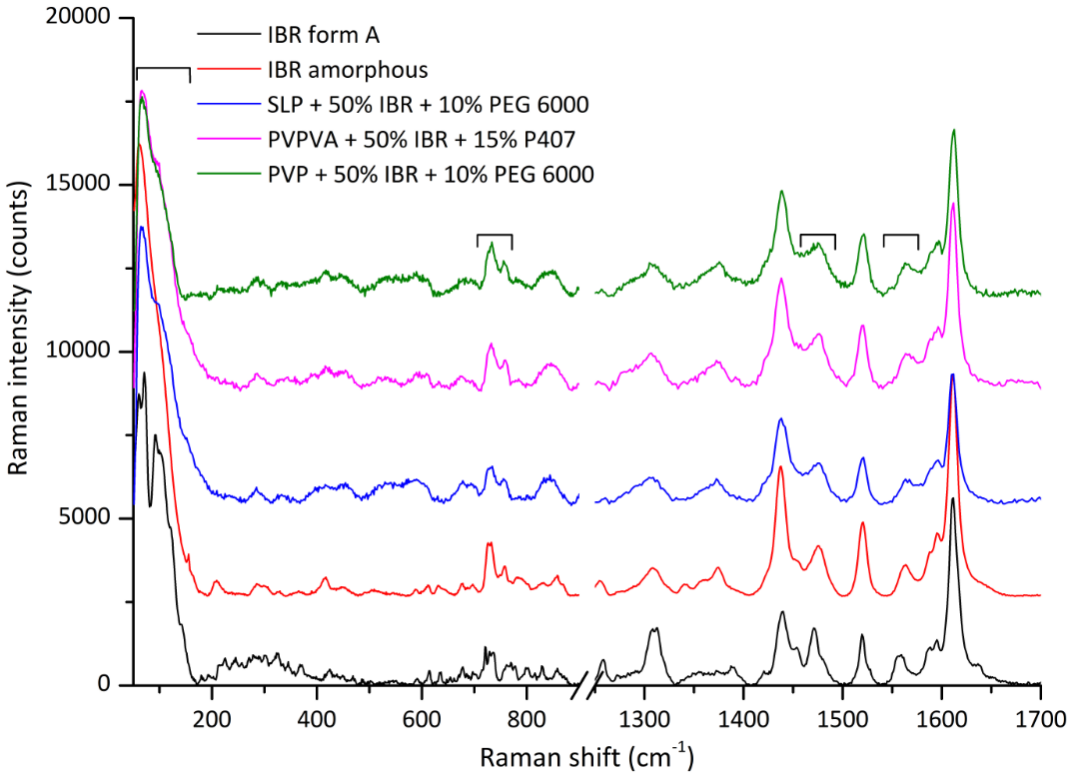

Figure 3.12. Raman spectra of crystalline and amorphous IBR, SLP, PVPVA, and PVP compositions. The spectra were recorded in the 50-1800 cm^{-1} wavenumber range, during 20 s with 20 accumulations, with the delay time of 1500 s and excitation at 633 nm. The highlighted areas correspond to where most pronounced differences from the crystalline structure were detected.

The broader bands obtained in the ASDs may also reflect a different local environment due to a tither binding with the polymer, due to the existence of weak intermolecular interactions [347], such as Van der Waals, electrostatic or hydrophobic. Therefore, possible interactions between drug and polymers in the extrudates were also investigated, as IBR has eight H-bond acceptors, one donor, and several moieties capable of establishing π-interactions (Figure 3.2) [342]. Changes in the Raman shift or shape of specific bands may indicate a drug-polymer interaction in these sites, as reflected in spectral features associated with C=O stretching at 1610 cm^{-1}, C=C aromatic ring chain vibrations at for instance 1475, 1587, and 2869 cm^{-1}, and C-H stretching modes of the alkene group at 2948 and 3066 cm^{-1}.

There are slight shifts in the position of specific peaks, as the 858 cm^{-1} shifted to 843 cm^{-1}, the 1254 cm^{-1} to 1260 cm^{-1} or the 1308 cm^{-1} moved to 1305 cm^{-1}, common to the three ASDs (Figure 3.13A). These may represent the formation of weak intermolecular interactions affecting the two aromatic rings, through Van der Waals or π interactions. Moreover, a decrease in the intensity of some bands was noticed between 1150 and 1650 cm^{-1}, specifically in the case of the band observed at 1164 cm^{-1}, assigned to the asymmetric stretching of the ether group, 1254 cm^{-1}, due to C-N stretching

modes, 1437 and 1520 cm^{-1}, related to C=C vibrations (aliphatic and aromatic), and 1610 cm^{-1}, assigned to the stretching of the C=O group (Figure 3.13A) [348]. These changes may also be related to the involvement of these molecular fragments in new Van der Waals or π interactions in the formulations. To investigate other possible interactions, Raman spectra until 4000 cm^{-1} of a representative composition was collected (SLP), and is depicted in Figure 3.13B. The most notable change is also a drastic decrease of the 3066 cm^{-1} peak, which is attributed to the C-H stretching of the vinylic hydrogens. These findings suggest a dipolar interaction with the α, β unsaturated ketone of IBR, stabilized by electronic resonance, which decreases the π character of the terminal C=C bond. This is corroborated by the simultaneous decrease of the frequency of the 1610 cm^{-1} band, attributed to the C=O. Noteworthy, the primary amine bands are usually of low intensity in Raman spectra, thus the H-bond interactions likely involving this function are not easily evidenced. Along with several weak interactions pointed out, this is likely the stronger interaction identified that enhanced significantly the physical stability of IBR through the inhibition of molecular mobility, and is the major effect responsible for its surprising behavior on extrusion.

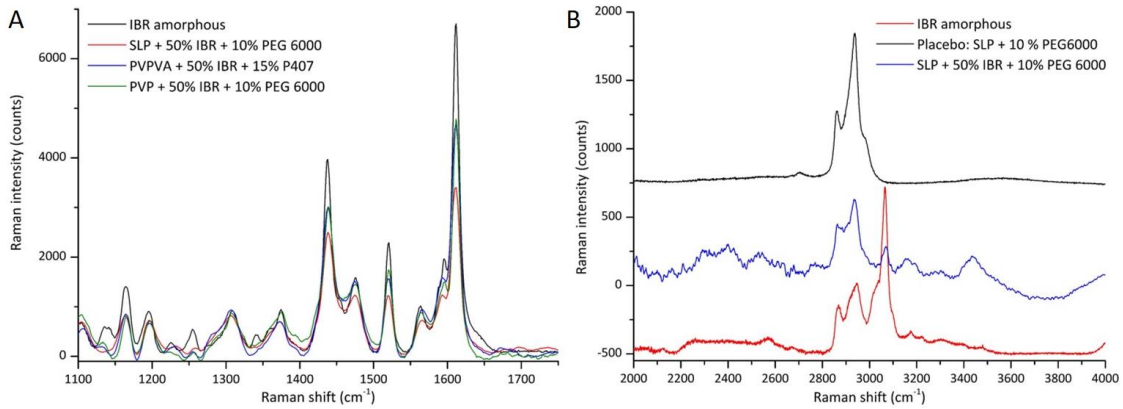

Figure 3.13. Detail of Raman spectra amorphous IBR, and SLP, PVPVA and PVP compositions. A, Detail of 1100-1750 cm^{-1}, where the decrease in the intensity of some bands was noticed, namely at 1164, 1254, 1437, 1520, and at 1610 cm^{-1}. B, Spectra of IBR, SLP system, and its placebo collected between 2000 and 4000 cm^{-1}, to highlight the decrease of the 3066 cm^{-1} peak in the system prepared by HME.

3.6.4. Thermal analysis

mDSC profiles of pure polymers and solid dispersions are depicted in Figure 3.14 (only reversing heat flow curves are represented, to simplify). PEG6000 and P407 were again detected as crystalline in the three systems, as an endothermic event is observed in the mDSC profile at the typical melting range of these materials (40 - 60°C). The T_gs were detected, both for the polymers and the solid dispersions. However, in the ASDs they are very weak, hardly detected and they were

not consistent in all measurements. This is also an indication that HME samples may be characterized as between amorphous dispersions and solid solutions, where each IBR molecule is completely dispersed and embedded in the polymer, with some minor dispersed amorphous clusters. Besides, no indication of drug degradation was detected in any of the three IBR compositions.

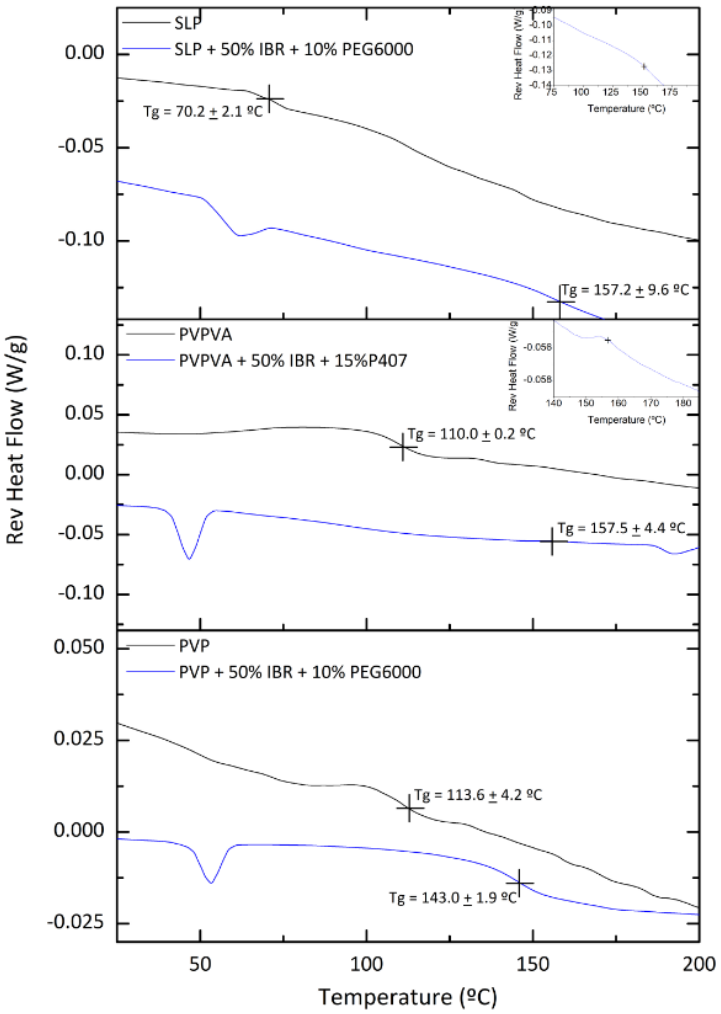

Figure 3.14. mDSC profiles for pure polymer and milled extrudates of SLP + 50% IBR + 10% PEG6000, PVPVA + 50% IBR + 15% P407, and PVP k12 + 50% IBR + 10% PEG6000. Method: From 0°C to 220°C at 5°C/min, amplitude ± 0.80°C and a period of 60 s. Blue lines: solid dispersions; Black lines: pure polymer. Details of glass transition detected for the SLP and PVPVA systems are depicted as insets.

mDSC results are in line with the observations from the PLM: the drug is dispersed within the polymer, and the plasticizer is at least partially crystalline. Another important conclusion from these measurements comes from the comparison of the theoretical T_g with the experimental values. As observed in Table 3.6, the experimental glass transitions are well above the predicted values, with

an increment of 83°C for the SLP system, 65°C for the PVPVA composition, and 50°C for the PVP dispersion. The high T_g of these systems should be the reason for the required high extrusion temperatures, much higher than expected. Besides, the theoretical predictions lack the plasticizer contribution, as well as residual moisture, which decreases the T_g and thereby increases the real difference between predicted and experimental values. Nevertheless, the real values are still well above the predictions, and this is another indication of very strong intermolecular interactions between the drug and the polymers.

Table 3.6. Prediction of T_g of milled extrudates through the Gordon-Taylor equation and comparison with experimental values.

Component	Experimental T_g (°C) of pure components	Calculated T_g (°C) of the blend[a] (1:1)	Experimental T_g (°C) of milled extrudates[b]	ΔT_g (°C)
IBR	79.1 ± 0.4	-	-	-
SLP	70.2 ± 2.1	74.1	157.16 ± 9.6	83.1
PVPVA	110.0 ± 0.2	92.6	157.52 ± 4.4	64.9
PVP K12	113.6 ± 4.2	93.3	142.97 ± 1.9	49.7

[a]Based on the Gordon-Taylor equation, using the experimental T_g of individual components. [b]Equipment: Q100 (TA Instruments). Aluminum capsules. Method: From 0°C to 220°C at 5°C/min, amplitude ±0.80°C, period of 60 s.

3.7. Stability studies

Accelerated and long-term stability studies were carried out to validate the thermodynamic predictions. The extruded ASDs were stored in ICH climatic chambers at 25°C / 60% RH (long-term conditions) and 40°C / 75% RH (accelerated stability study). Samples were investigated for recrystallization by XRPD and PLM imaging periodically, namely after 1, 3, and 6 months of storage in these conditions. Raman spectroscopy was also performed after 6 months of storage in all samples. The results, including XRPD, and Raman, are summarized in Table 3.7. PLM images are depicted in Figure 3.15.

Table 3.7. Analytical results of extrudates of IBR amorphous drug and ASDs manufactured by HME on stability.

Formulation	Storage	-	25°C/60%RH			40°C/75%RH		
	Time points (months)	0	1	3	6	1	3	6
Amorphous drug	Appearance	Loose	Loose	Loose	Loose	Lumps	Lumps	Lumps
	XRPD	A	-	-	A	A	C	C
	Raman	A	-	-	A	-		A
Preliminary IBR formulation	XRPD	A	A	A	C	C	C	C
SLP + 50% IBR + 10% PEG6000	Appearance	Loose	Loose	Loose	Loose	Loose	Loose	Loose
	XRPD	A	-	-	-	A*	A*	A*
	Raman	A	-	-	A	-	-	A
PVPVA + 50% IBR + 15% P407	Appearance	Loose	Loose	Loose	Loose	Loose	Loose	Loose
	XRPD	A*	-	-	-	A	A	A
	Raman	A	-	-	A	-	-	A
PVP + 50% IBR + 10% PEG6000	Appearance	Loose	Loose	Loose	Loose	Loose	Loose	Loose
	XRPD	A*	-	-	-	A*	A*	A*
	Raman	A	-	-	A	-	-	A

Abbreviations: A, amorphous; C, crystalline; – not performed.

*diffraction peaks at 19 and 23 2θ are found in XRPD pattern but attributed to PEG6000 or P407 [344, 345].

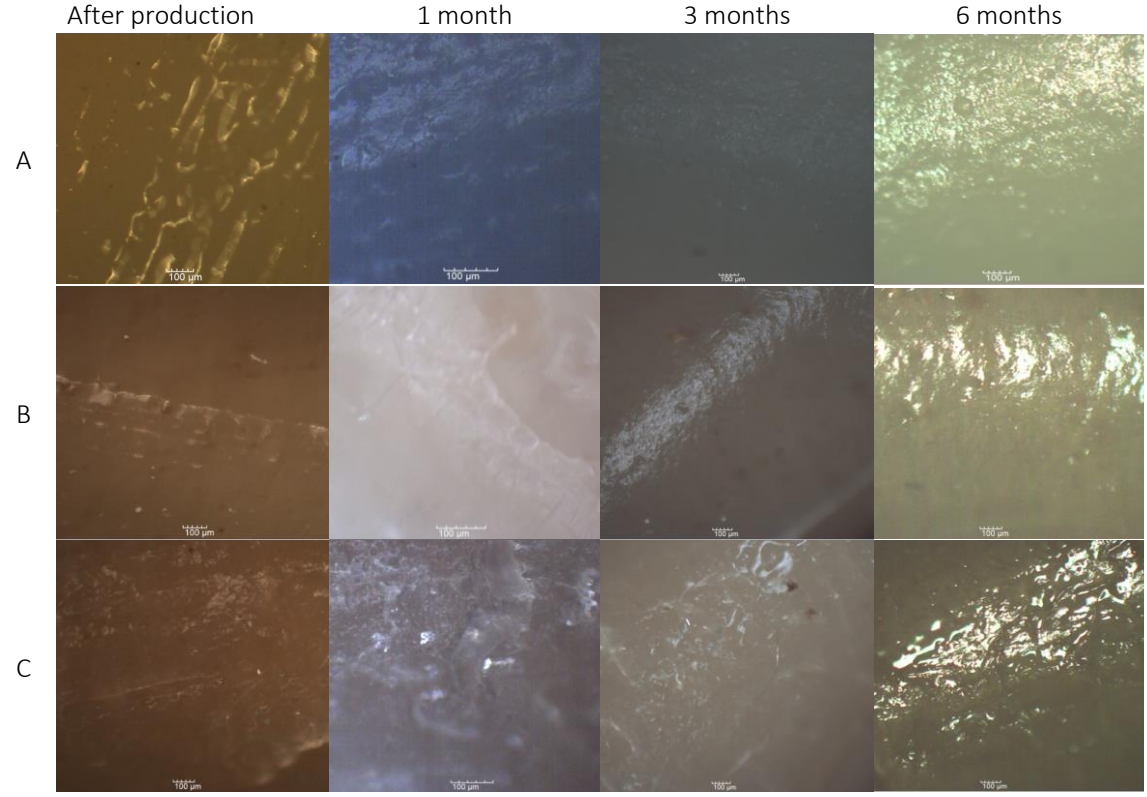

Figure 3.15. Examples of PLM images of extrudates prepared by HME under stability exposed to 40°C / 75% RH: A, SLP + 50% IBR + 10% PEG6000; B, PVPVA + 50% IBR + 15% P407; and C, PVP + 50% IBR + 10% PEG6000. The scale bars represent 100 µm.

Birefringence was still detected from the very early in the stability study, mainly in the 40°C / 75% RH storage condition. In some cases, typical shapes and growing patterns of crystal nuclei allow to infer on the birefringence source, but in this case, it was not possible to discriminate if it was caused by the drug or by any of the excipients. XRPD and Raman spectroscopy were key to clarify the observations.

The IBR drug samples crystallized right after 3 months at 40°C / 75% RH, as demonstrated by XRPD (Figure 3.16), whereas at 25°C / 60% RH the drug was kept in the amorphous form during the whole stability study, as observed in the Raman spectra, as well as in the XRPD diffractogram. When formulated (preliminary IBR formulation), the physical stability of IBR was lower and IBR crystallized only after one month at 40°C / 75% RH, and after 6 months at 25°C / 60% RH. This demonstrates, indeed, the need for a stabilization strategy of amorphous IBR. When included in any of the three HME systems, no recrystallization of IBR was observed whatever the storage condition was, even at 40°C / 75% RH. The samples exhibit two identifiable XRPD peaks at 19 and 23 2θ, but they do not match the patterns of IBR in 2θ. They are attributed to crystalline PEG6000 and P407, as reported [344, 345]. They were used in the formulations as plasticizers, and these peaks occurred already after preparation.

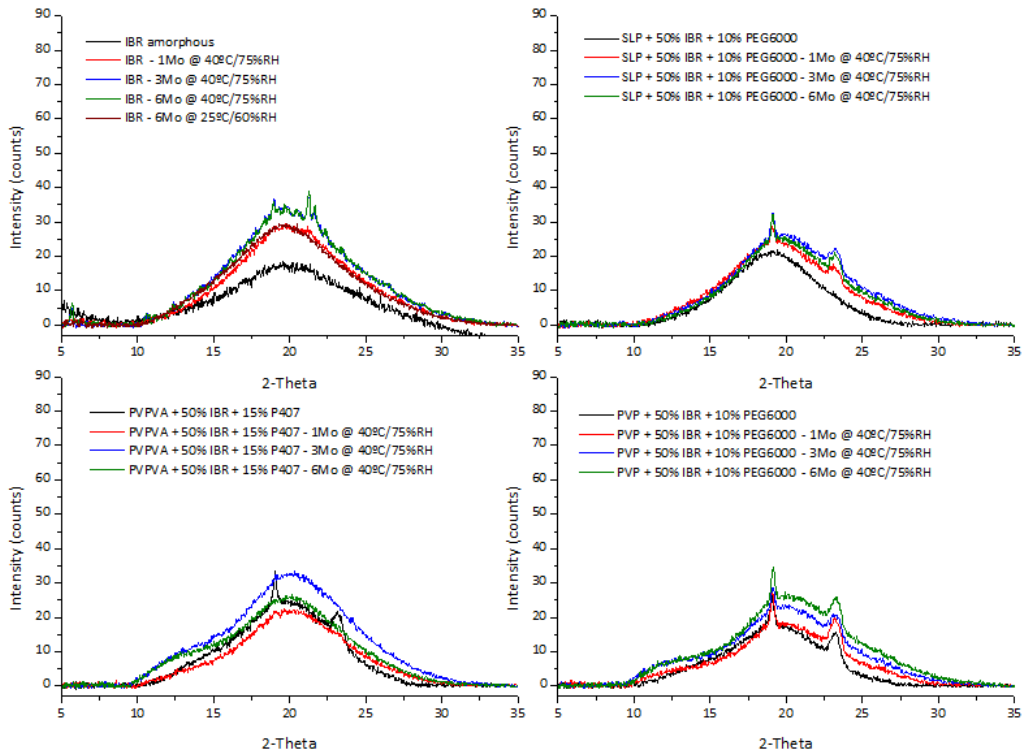

Figure 3.16. XRPD patterns of IBR amorphous drug (control) and solid dispersions prepared by HME under stability: SLP + 50% IBR + 10% PEG6000, PVPVA + 50% IBR + 15% P407, PVP + 50% IBR + 10% PEG6000.

The Raman spectra were initially collected and they provided support to assess the physical state of IBR during the stability tests. The Raman spectroscopy characterized all samples as amorphous, both drug and polymeric systems, at T0, and 6 months (Figure 3.17). The typical amorphous IBR Raman shifts and band shapes were detected, and the residual crystallinity of IBR when exposed to 40°C / 75% RH was not detected. It seems that, in this case, XRPD can detect crystalline traces sooner than Raman. Besides a complementary technique for structural characterization, another important contribution of Raman spectroscopy is the ability to detect chemical changes over time. For the PVPVA and PVP systems, the Raman spectra are quite similar to the amorphous drug and T0. However, there are three newly identified bands in the SLP system when exposed to 40°C / 75% RH, detected at 634, 984, and 1731 cm^{-1}, highlighted in Figure 3.17 with *. These bands were not present neither at T0 nor at 6 months in the 25°C / 60% RH chamber. They are attributed to the chemical degradation of the SLP system, where a storage restriction is needed.

Raman spectroscopy was also used to verify changes and intermolecular interactions over time, in stressed conditions at various humidity and temperature conditions. All the reported deviations of Raman shift at T0 and attributed to intermolecular interactions were maintained over time, for the three systems under study. Besides, in the SLP composition, the 1437 cm^{-1} peak was also shifted to 1445 cm^{-1}. This may be a reflection of the reported minor chemical degradation, but can also be attributed to C=C vibrations, triggered by the typical moisture uptake of these systems in such high humidity conditions.

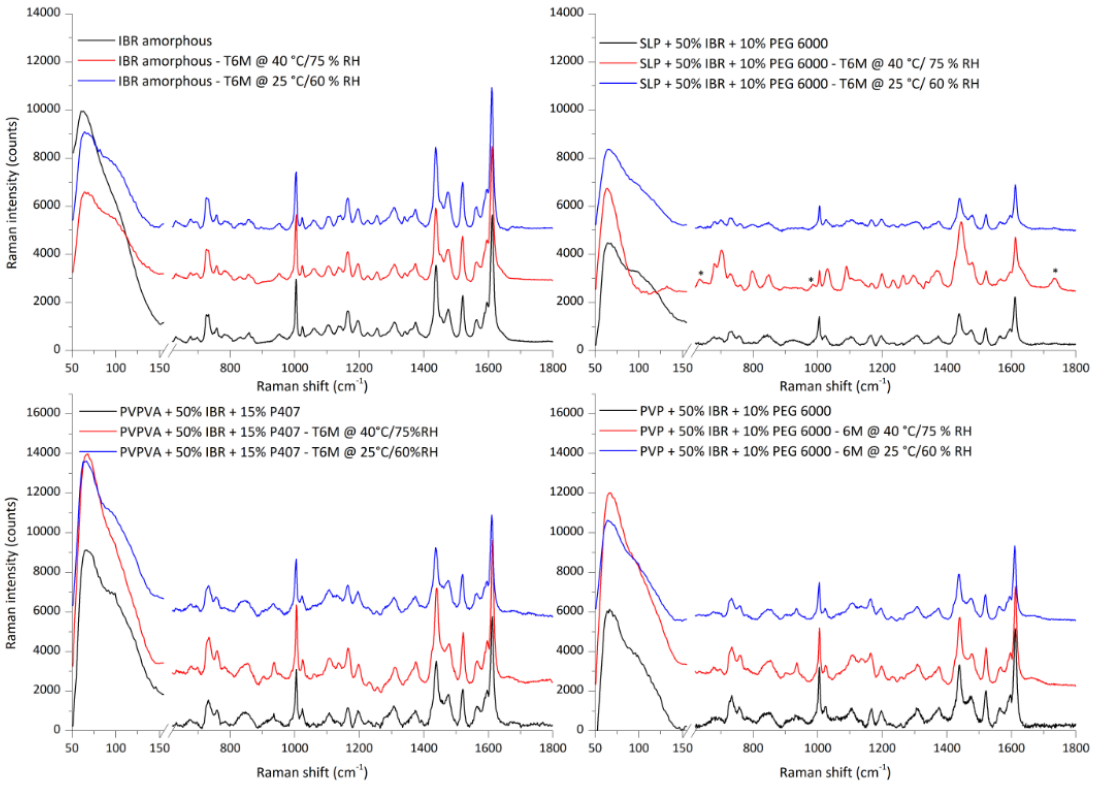

Figure 3.17. Raman spectra amorphous IBR, SLP, PVPVA, and PVP compositions after 6 months of stability exposed to 40°C / 75% RH and 25°C / 60% RH. The spectra were recorded in the 50-1800 cm^{-1} wavenumber range, during 20 seconds with 20 accumulations, with the delay time of 1500 s and excitation at 633 nm. A * marks new bands identified in the SLP system after 6 months of storage at 40°C / 75% RH.

4. Conclusion

In this study, a real technical hurdle was resolved, the thermodynamic instability of the amorphous IBR. The study initiated with a full characterization of IBR by thermal analysis coupled with Raman spectroscopy, which was essential to exclude the possibility of drug degradation with heat or other transformations that require enthalpy changes during HME processing. Then theoretical thermodynamic predictions were performed, namely miscibility based on the Hansen solubility parameters and the T_g with the Gordon-Taylor equation. Selected polymers were subjected to a complete HTS focused on physical stability, where PLM was complemented with Raman spectroscopy to select the most promising systems. Multivariate statistics were key to extract useful conclusions from the HTS, namely the relevance of humidity in triggering IBR crystallization and the low importance of drug load. The latest was surprising taking into account the typical behavior of amorphous systems and the well-known correlation between thermodynamic stability and drug load.

Three systems were manufactured, all characterized as amorphous by thermal analysis, XRPD, and Raman spectroscopy. The HME process required high temperatures to process these systems, which was unexpected due to the predicted T_g by the Gordon-Taylor equation. The experimental T_gs were determined with mDSC, and they were well above the predicted values. It is known that this approach ignores potential intermolecular interactions, and was, indeed, an underestimation for these systems. Moreover, this was the reason for the required high extrusion temperatures and an indication of strong interactions between the drug and the polymers.

The Raman spectroscopy was used to investigate drug-polymer intermolecular interactions. There are shifts in the position of specific peaks, common to the three ASDs, and probably related to a weak interaction affecting the aromatic rings of IBR, through a Van der Waals or π interactions. Moreover, a decrease in the intensity of some bands between 1150 and 1650 cm^{-1} was noticed, assigned to the stretching of the ether group, C-N stretching, C=C vibrations, and to the stretching of the benzene groups, either caused by Van der Waals or π interactions. Amine groups do not commonly lead to intense signals in Raman spectroscopy, which are even less intense and broader when involved in hydrogen bonds, as observed in the pure IBR amorphous. Therefore, hydrogen bond interactions were not evidenced by Raman spectroscopy. Nevertheless, the decrease of the

3066 and 1610 cm^{-1} peaks was attributed to a strong intermolecular dipolar interaction, involving the α, β unsaturated ketone. All these interactions between amorphous IBR and the polymers justify the surprisingly high T_g of the prepared HME systems. The additive effect of these intermolecular interactions changed brutally the performance of the ASDs, observed latter in the stability studies.

Raman spectroscopy identified three new bands in the SLP system when exposed to 40°C / 75% RH, detected at 634, 984, and 1731 cm^{-1} and likely attributed to chemical degradation. Although physically stable, the SLP composition should require a storage restriction to avoid impurities, and this is considered for product development from the very early. Overall, all these compositions were determined to be amorphous until at least 6 months, both by XRPD and Raman spectroscopy, which indicated that the molecular mobility of the IBR compound in the prepared matrixes is slow enough to avoid crystallization, even when stored in accelerated conditions. It revealed the physical strength of these polymeric systems in the presence of high humidity and temperature, attributed to the described intermolecular interactions.

CHAPTER IV. NOVEL TECHNOLOGICAL PLATFORM FOR EXTENDED-RELEASE TABLETS BY COMBINING HOT-MELT EXTRUSION AND MUPS

Abstract

The aim of this study was the development of a drug delivery platform for the controlled-release of a highly soluble drug, a BCS class III compound with a very short half-life, for a once-daily administration. Hot-melt extrusion was considered a promising technology able to control the drug release rate and established among the pharmaceutical industry. Formulation development started with a screening of ingredients by HME, using a Thermo Scientific HAAKE MiniLab II. Different technological platforms were then evaluated to optimize dissolution kinetics. The prototype's selection was based on a statistical analysis using JMP® 14.0 (SAS Institute, Inc), through the Weibull function and Principal Components Analysis. Finally, the prototype was upscaled and fully characterized. The unusual selected technological platform is based on a Multi-Unit Particulate System (MUPS) of PVAC/PVOH, prepared by HME coupled with downstream compression in microtablets and finally into tablets. SEM and Raman mapping demonstrated that the microtablets are well defined and not damaged by the main compression step. The release profile led to near zero-order kinetics for 6 to 8 hours. A mechanistic understanding was obtained through the Weibull function and SEM of dissolution samples and revealed a combination of diffusion, erosion, and swelling. The prototype was demonstrated to have the intended target release kinetics and is an alternative to patented osmotic systems.

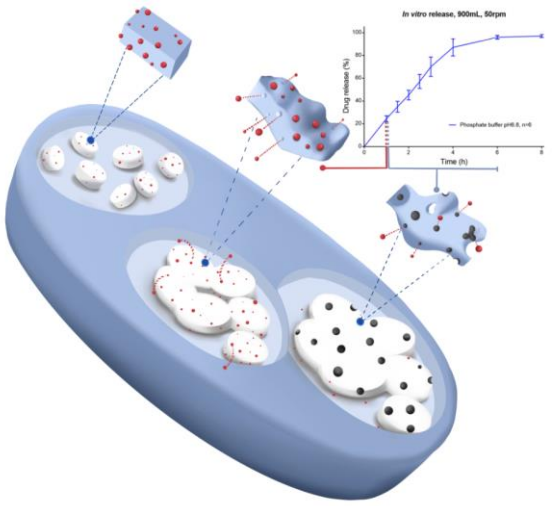

Figure 4.1. Graphical abstract of chapter IV. Mechanistic dissolution of the multi-unit particulate system (MUPS), characterized by swelling, diffusion, and erosion.

The results presented in this chapter will be published in Simões MF, Rocha-Gonçalves A, Pinto RMA, Simões S. Novel technological platform for extended-release tablets by combining hot-melt extrusion and MUPS. Submitted for publication.

My contribution to this work was designing and performing the systematic screening of polymers and technologies, its characterization by optical microscopy, interpretation of XRPD, SEM and Raman mapping results, conducting all the statistical analysis, modeling, and risk assessment. The analytical characterization by HPLC, UPLC and Karl-Fischer was performed by the analytical development team of Bluepharma, XRPD analysis was performed at the Centre for Physics of the University of Coimbra (CFisUC), Raman mapping in the Department of Chemistry of the University of Coimbra, by Rui Fausto and Andreia Tabanez, and SEM at Paralab, SA (Porto, Portugal).

This chapter is not an integral copy of the work submitted for publication.

1. Introduction

Extended-release (XR) formulations have been key to improve patient compliance for drugs suffering from a relatively short half-life and rapid elimination [349-351]. Apart from a straightforward dosing regimen and reduced administration frequency, benefits of XR formulations include lower off-time and higher tolerability. They lead to less plasma dose fluctuations and adverse events related to peak concentrations (C_{max}). Lack of patient adherence is commonly associated with poor treatment outcomes, leading to a higher hospital admission rate and even morbidity [349, 350]. By enhancing convenience and ease of use, adherence is improved, and this is commonly seen as one of the primary goals to ensure treatment efficacy.

The extended oral drug release of highly soluble compounds in low dosages is a well-known technological challenge for formulation scientists, even more when a constant release kinetics is sought [352]. A high solubility drug, from BCS class I or III, tends to dissolve in aqueous media or the gastrointestinal fluids rapidly. This means the release from the pharmaceutical form is fast, as well as its absorption *in vivo*, leading to a sharper peak in the blood concentration over time when compared with poorly soluble compounds. Decreasing the dissolution rate of this type of drug is challenging and often requires innovative technological approaches. This is even more demanding when a zero-order oral release is needed [353] to keep blood levels constant. Zero-order kinetics is described as a release at a constant rate for a specific time and not dependent on the initial drug concentration [354]. Typical technological solutions for zero-order, or near, in the industrial setting is based on osmotic systems [355-358] but requires dedicated technology. Additional approaches have also been described, as the combination of an hydrophilic matrix with an insoluble film coating [359] or the extruded-spheronized lipid pellets [360]. However, most of them are considered complex or time-consuming for industrial production, as the core-in-cup [361] or compression-coated doughnut tablets [362], floating tablets and beads [363, 364], coating mini-tablets in a fluidized bed chamber [365], or applying non-uniform drug distributions by fluid bed beads coating with insoluble polymers [366].

Therefore, alternative technological approaches for zero-order kinetics are needed. 3D printing has recently been described for zero-order release, using hot-melt extruded filaments by fused deposition modeling [367-370]. The use of HME for zero-order oral administration was also described in the last few years [371-375]. However, only one study reported the application in a

highly soluble compound [376]. In this study, Vervaet *et al.* prepared mini-matrices of metoprolol in ethylcellulose, which were not milled into powder before dissolution testing [376]. Diffusion and erosion of the extrudate dictated the release rate of metoprolol, as it typically occurs in solid implants where zero-order is also commonly observed.

This study aimed to develop a drug delivery platform for the controlled-release of a highly soluble drug, a BCS class III compound, with a very short half-life. The drug has a moderate permeability, explained by its medium diffusivity, and it has a low potential to inhibit the P-gp. The most permeable molecular microspecie (non-polar) occurs in pH environments between 2 and 8, which leads to an absolute bioavailability of immediate-release formulations of approximately 70%. The immediate-release formulation reaches peak plasma concentrations at 0.5 - 1 hours after oral administration, and the elimination half-life is about 3 hours, which requires two administrations daily. The goal is to have a once-daily formulation, improve patient convenience, and ultimately improve treatment compliance for a chronic condition. The drug under study is a small molecule highly soluble in HCl 0.1N, acetate buffer pH 4.5, phosphate buffer pH 6.8, and purified water[4]. It is a weak base with a pKa of about 5. An additional challenge for manufacturing was high-containment requirements to reduce the operator's exposure, as it is also considered a highly potent drug (Safebridge system band 4, corresponding to an occupational exposure limit, OEL < 1 µg/m^3).

Preliminary tablet formulations prepared by direct compression (DC) led to a very fast drug release, reaching the full release after 1 hour of the dissolution test[5]. Hydrophobic polymers such as ethylcellulose, polyvinyl acetate (PVAc), and different copolymers of acrylate and ammonium methacrylate were tested with no success. These preliminary formulation tests demonstrated the need for an intimate blend with a release-controlling component integrated into an XR technological platform. HME was considered as a technology able to modify the drug release rate of drugs and recommended to deal with high-potency compounds. In HME, the components are converted into a new material of constant shape and density by the effect of heat and mechanical stress [26, 37]. This process involves compacting, blending, and dispersing a mixture of excipients and DS by two rotating screws through the heated barrel [72, 316]. HME usually leads to high-

[4] Solubility data determined as preformulation work to this study (data not shown).

[5] Preliminary formulation development/initial screening was performed (data not shown).

density materials, with slow disintegration, or even promotes relatively strong intermolecular bonds between the formulation components.

Our study for the development of the XR platform for a highly soluble drug was designed in three sequential stages. Firstly, a screening of ingredients with the potential to control the release rate of this highly soluble compound by HME was performed. The selected components were included in the second stage, aimed at seeking the right shape of the dissolution curve. This means a near zero-order XR kinetics, for at least 8 hours of dissolution, with pH and food independent behavior. Therefore, they were included in different technologies well-known as able to modulate the release rate to the intended target profile. Finally, the prototype was selected, manufactured, and fully characterized from the physical, chemical, and pharmaceutical point of view. This pharmaceutical development work was performed in an industrial atmosphere and will be concluded with the preparation of a New Drug Application submitted to regulatory authorities for evaluation.

2. Experimental section

2.1. Materials

HPMC, brand name Affinisol® HPMC HME, grade 15LV and 4M was kindly donated by DuPont (Delaware, US). HPC (Klucel®) grades MF and EF and Ethylcellulose (EC, Aqualon®) grades N10 and N100 were obtained from Ashland (Covington, US). PVAc, brand name Kollidon® SR, PVPVA (Kollidon® VA64), SLP (brand name Soluplus®), and PVP grade K12 (brand name Kollidon® PF12), were obtained from BASF (Ludwigshafen, Germany). Two grades of insoluble Eudragit®, namely RL and RS PO (copolymers of acrylates and ammonium methacrylate), were also donated by Evonik (Darmstadt, Germany). PVOH (brand Parteck® MXP) and stearic acid vegetable grade (Parteck® LUB STA 50) were obtained from Merck KGaA (Darmstadt, Germany). For the dissolution experiments, 0.05M phosphate buffer pH 6.8 and HCl 0.1N were prepared. The phosphate buffer pH 6.8 was prepared as 1250 mL of 0.2M potassium dihydrogen phosphate R placed in a 5000 mL volumetric flask, 560.0 mL of NaOH 0.2M added and diluted to 5000 mL with water R. HCl 0.1N was prepared using 41.4 mL of fuming HCl 37% R added to a 5000 mL volumetric flask containing around 2000 mL of purified water and the remaining volume completed with water. The standard stock solution used for quantification was prepared in the corresponding dissolution media. All other chemicals were of analytical grade and were used as received. Also, the excipients and drug were of pharmaceutical grade. The BCS class III drug source cannot be disclosed for confidentiality reasons. Statistical and mathematical modeling was performed using JMP® Pro 14.0, from SAS Institute Inc. (North Carolina, USA).

2.2. Methods

2.2.1. Manufacturing of tablets

HME was performed using a co-rotating twin-screw extruder Thermo Scientific® HAAKE MiniLab II (Thermo Scientific, UK). Temperature and screw speed were optimized based on extrudate appearance, extrudability, and torque, using batch sizes of 15 g. The powder blends were added manually in small amounts. A round die with a diameter of 2 mm was attached to the extruder. The

screw is conical with conveying elements only. All the glassy material was cooled in a conveyor belt and ground at 20 000 rpm in IKA® M20 to a fine powder. The manufacturing process depended on the final pharmaceutical form: i) monolithic tablets (prepared by DC); ii) bilayer tablets (BiTABS); iii) multi-unit particulate systems (MUPS). For DC and BiTABS, the milled extrudate was blended with external excipients for 10 min in a cylindrical blender of 250 mL (Erweka® AR403, ERWEKA GmbH, Langen, Germany) and then lubricated for 3 min with magnesium stearate. For the BiTABS, a support layer was prepared by direct compression based on HPMC and glyceryl behenate. The final mixture was then tableted in a rotary bench press with eight stations (Ronchi FA, Officine Meccaniche F.lli Ronchi, Milano, Italy) in 10.8 mm oblong tablets. In MUPS, the mixture was tableted into 2 mm round microtablets of 8 mg using multi-tip punches (Ronchi FA). After blending with the external phase and lubrication, they were also tableted into 10.8 mm oblong tablets (Ronchi FA).

For the manufacturing of the prototype, the inner phase (BCS class III drug, PVAc, PVOH, and stearic acid as a plasticizer) was sieved through a 0.71mm net size and blended for 5 min at 6 rpm in a 250 mL bin before being subjected to HME. The extrusion process was performed at 173ºC and 150 rpm with manual feeding, and the process ran smoothly with a low measured torque of 24 N.cm. The extrudate was opaque, light yellow, with no change over the entire process. After cooling, milling at 20 000 rpm, and sieving, the material was blended with HPMC, lubricated, and tableted into 2 mm microtablets. They were then combined with MCC and lactose, and lubricated before the final tableting into 200 mg tablets at 70N in a rotatory tablet press.

2.2.2. *In vitro* dissolution tests

In vitro drug release tests were performed using Apparatus II (USP/NF paddle apparatus) with a rotation speed of 50 rpm (708-DS Dissolution Apparatus, Agilent Technologies Inc., California, USA). Dissolutions tests were performed in 900 mL of HCl 0.1N or 0.05M phosphate buffer pH 6.8 at a temperature of 37 ± 0.5°C for 8 hours. At predetermined sampling time points, 8 mL of solution was withdrawn and filtered through online tip filters (0.10 µm) at first and then with 0.45 µm syringe filters into the HPLC vial, with previously membrane compatibility tested, and immediately replaced with an equal volume of fresh dissolution medium, to guarantee sink conditions. The amount of drug released was quantified by the High-Performance Liquid Chromatography (HPLC) method against an external standard solution at 100% of the theoretical concentration. The analytical method used a mixture of triethylamine solution pH 3.5: acetonitrile (75:25, % v/v) as the mobile phase, in the isocratic mode. The column was YMC-Pack ODS-AM (150 x 4.6 mm; 5 µm) and

operated at 25 °C with a flow rate of 1.0 mL/min and UV detection at 285 nm. The injection volume was 20 µL, and the run time 4 min. Data were integrated using Empower® software. The dissolution method was subjected to a short validation program that included evaluation of selectivity, linearity, system precision, accuracy, filtration, and sample stability, according to ICH Q2(R1) guideline, to demonstrate that it was suitable for its intended purpose. The dissolution data represent an average of at least three tablets.

2.2.3. Assay and degradation products

A gradient Ultra Performance Liquid Chromatography (UPLC) method was used to quantify assay and related substances in drug product using a Kinetex C18 column (150 x 3.0 mm; 2.6 µm) at 33 ºC. The flow rate was 0.6 mL/min and UV detection at 280 nm. The injection volume was 4 µL, and the run time 30 minutes. Sodium perchlorate ($NaClO_4$) buffer 10mM at pH 2.5 was used as mobile phase A and acetonitrile gradient grade as mobile phase B in a gradient mode. The solvent used for sample preparation was a mixture of mobile phase A and B (80:20, % v/v). For the development of this method, known related substances from drug and forced degraded samples were used to predict each peak's retention time in the chromatogram and ensure the best separation of each impurity. The method was validated for an immediate-release formulation of this BCS class III drug, including selectivity, linearity, precision, accuracy, repeatability, filtration, and robustness. For the XR formulation, the UPLC method was subjected to a short validation program that included extraction tests and selectivity.

2.2.4. Water content

The water content was determined following method Ia (USP <921> / Ph. Eur. 2.5.12), direct titration by Karl-Fischer, using methanol R as solvent and Hydranal Composite 5K as titrant. The sample water was extracted from the tablets by the methanol and quantified by potentiometry, with a drift value of 20 µL/min. The procedure was performed in duplicate. The method was validated for the immediate-release formulation.

2.2.5. Scanning Electron Microscopy

The tablets were analyzed by Scanning Electron Microscopy (SEM) without any pre-treatment in a Phenom Pro-X SEM EDS (ThermoFisher Scientific®, Netherlands) with a standard sample holder.

Each tablet was cut into two equal parts. One of the pieces was fixed with Graphite colloidal Pelco® on aluminum pin. Finally, a flow of compressed air was used to remove any unbound material. For the dissolution study, tablets were removed from the dissolution apparatus at predetermined time intervals, water excess removed by vacuum filtration, and samples prepared for SEM as detailed above.

2.2.6. X-Ray Powder Diffraction

XRPD analysis was performed at ambient temperature using a Bruker® D8 powder diffractometer (Bruker Corporation, Massachusetts, USA), in a Bragg-Brentano geometry (reflection geometry), equipped with a Ni monochromator and LYNXEYE TE energy-dispersive detector. The X-ray source used was Cu $K\alpha^{1/2}$ (1.54 Å) with λ_1=154.056 pm and λ_2=154.439 pm. Spectra were collected from scans within the range 5.0° - 35.0° at 2θ with a step size of 0.02° (2θ) and time per step of 0.5 s.

2.2.7. Raman mapping

All spectra were recorded with the Horiba LabRAM HR Evolution, coupled to a confocal Olympus microscope (HORIBA France SAS, France). Individual Raman spectra from various random points of the samples were collected and averaged. The focusing spot was around 1 µm. For mapping, each spectrum was collected 5 times with a collection time of 8 seconds, and averaged. The laser irradiation was at 785 nm wavelength, with a power of 55 mV, and a 50x magnification objective was used. The spectra were collected in a wavenumber range of 450-1600 cm^{-1}.

2.2.8. Modeling of dissolution data

The dissolution data were fitted to several kinetic models as zero-order, first-order, Higuchi, Hixson-Crowell, Korsmeyer-Peppas, Weibull, Hopfenberg, and Gompertz equations [377, 378], by JMP® 14.0 from SAS Institute, Inc. Using non-linear modeling, the platform applies a least-squares loss function to fit the models, minimizing the sum of the loss function across the observations. The best model for each formulation was selected by analyzing the residual sum of squared errors (SSE) and the standard deviation of the residual error (root mean squared error, RMSE).

2.2.9. Multiple linear regression

The dataset for the Multiple Linear Regression (MLR) analysis in JMP® 14.0 consisted of the screening of polymers, using the formulation components and tablets hardness as factors, and dissolution results as response variables. The responses were defined as the drug release in phosphate buffer pH 6.8 in specified time points, namely 1, 2.5, and 6 hours. A Standard Least Squares method was used for data modeling, and the dataset contained 11 factors and 24 experiments, which were analyzed retrospectively. Only the main effects were considered. The responses were analyzed and fitted separately, and the model coefficients were estimated by the software. The regression models were simplified by the removal of statistically insignificant terms ($p > 0.05$). This procedure was applied to all responses that were deemed to be suitably described by the model. The models were evaluated through the coefficient of determination R^2, ANOVA, and the *p* value of the parameter estimates.

2.2.10. Artificial Neural Network modeling

The dataset used for this study comprised twelve input variables, from which ten were related to formulation components and two for the manufacturing process (downstream preparation method and tablets hardness). Details are provided in Appendix III, B. Dataset for the screening of technologies. Specialized predictive modeling of the obtained dataset was performed through Artificial Neural Networks (ANNs) using JMP® Pro 14.0, which implements a fully connected multi-layer perceptron (MLP) with one or two layers. Overfitting was minimized through a random *k*-fold validation of five. A different number of nodes (from 1 to 10) in one layer was tested by systematic trial and error until no significant improvement in the model parameters was obtained. The predictive ability of the models was assessed by different parameters, namely the R^2 of the ANOVA of the linear regression between actual and predicted values, the RMSE, the SSE, and the mean absolute difference (MAD). These parameters were computed as detailed in Equation 4.1, Equation 4.2, Equation 4.3, and Equation 4.4, respectively.

Equation 4.1. $$R^2 = \frac{\sum_{i=1}^{n}(Y_{i,p}-Y_{i,e})}{\sum_{i=1}^{n}(Y_{i,p}-Y_e)^2}$$

Equation 4.2. $$RMSE = \sqrt{\frac{\sum_{i=1}^{n}(Y_{i,e}-Y_{i,p})^2}{n}}$$

Equation 4.3. $$SSE = \sum_{i=1}^{n}(Y_{i,e} - Y_{i,p})^2$$

Equation 4.4. $$MAD = \frac{i}{n}\sum_{i=1}^{n}(Y_{i,e} - Y_{i,p})$$

where, n is the total number of experiments, $Y_{i,e}$ is the actual result of experiment i, $Y_{i,p}$ is the predicted result of experiment I, and Y_e the mean of actual determined values.

The optimum ANN architecture was determined as an MLP 12-7-3, where twelve input factors are related to three output responses (dissolution results in three time points, Q) by seven neurons in a single hidden layer. The activation functions are hyperbolic tangent (sigmoid). The architecture of the optimized MLP model is depicted in Figure 4.2.

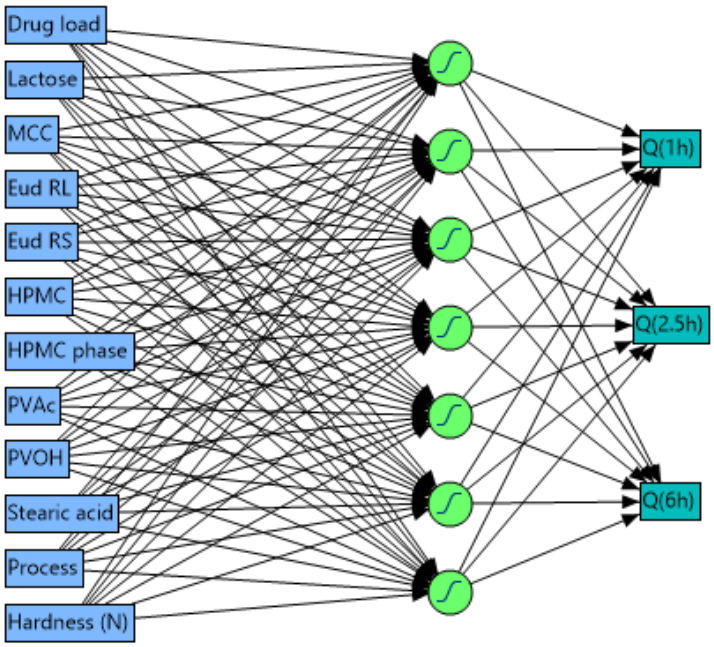

Figure 4.2. The network architecture of the ANN model, with eight hidden nodes in one layer, using sigmoid functions. Abbreviations: MCC, microcrystalline cellulose; Eud, Eudragit; HMPC, hypromellose; PVAc, polyvinyl acetate; PVOH, polyvinyl alcohol.

2.2.11. Comparison of dissolution profiles by Principal Components Analysis

Multivariate statistical analysis was performed on dissolution results to compare *in vitro* performance with the target profile. PCA on correlations was applied as a dimension-reduction technique. PCA simplified the complete dissolution data into two principal components, represented in the score plot.

2.2.12. Risk assessment

The QTPP was defined, reflecting the requirements of the product quality and behavior. The risk assessment started by listing all the factors that could affect the product quality in an Ishikawa diagram. Once the variables were identified, the next step was to rank them in terms of criticality. A REM was created through a semi-quantitative analysis. Each parameter was ranked as high, medium, or low-risk, considering the severity and probability of the impact on the CQAs. Parameters identified as high risk requires further evaluation experimentally.

3. Results and discussion

3.1. Definition of QTPP and CQAs

A patient-centered product profile describing the finished product's characteristics to ensure quality, safety, and efficacy are summarized in Table 4.1.

Table 4.1. Quality Target Product Profile for tablets of the BCS class III drug.

Attribute	Target Product Profile	Rationale
Dosage Form	Extended-release tablets	Commonly accepted solid oral dosage form. Extended-release aims at a once-daily administration.
Route of administration	Oral	The preferred route of administration.
Dosage Strength	Double from the immediate-release product.	From twice to once-daily administration.
Pharmacokinetics	Peak blood concentrations: 4-5 hours.	Once-daily administration.
Container closure system	HDPE bottles with desiccant and heat induction closure liners. Quantity of tablets/bottle: 30.	To maintain the full therapeutic capacity of drug product during shelf-life.

Abbreviations: HDPE, High-density Polyethylene.

To meet the QTPP, the formulation and the manufacturing process were analyzed and translated into CQAs (Table 4.2).

Table 4.2. Critical Quality Attributes for tablets of the BCS class III drug.

Quality Attributes of the Drug Product	Target Product Profile	Is this a CQA?	Rationale
Appearance	Oblong tablets with 10.8 mm	No	The appearance was not considered critical as it is not directly related to safety and efficacy.
Identification	Positive	No	Formulation and manufacturing process are unlikely to impact identity.
Polymorphism	Only one polymorphic form is known.	Yes	The possibility of a change of solid-state form during the manufacturing process should be assessed.
Drug content and uniformity	100% (95% - 105%)	Yes	Meet the compendial quality standard of product, meet product stability.
Dissolution	Extended drug release for at least 6 to 8 hours, in near zero-order kinetics.	Yes	The formulation and manufacturing process critically affect the drug release rate.
Degradation Products	Meet ICH Q3B(R2) limits. Reporting threshold: 0.1%	Yes	Must meet the compendial quality standards. Levels of ICH Q3B(R2) reporting and qualification threshold cannot be exceeded.
Residual Solvents	Meet ICH Q3C(R5) limits	No	Must meet the compendial quality standards. Levels of ICH Q3C(R5) cannot be exceeded.
Microbial Limits	Meet ICH Q4B(4C) limits	No	Formulation and manufacturing process unlikely to affect.

Abbreviations: CQA, Critical Quality Attributes; ICH, International Council for Harmonisation.

As an XR product, the dissolution profile was considered crucial to ensure a gradual drug release to the patient. In this case, a near zero-order kinetics was sought for approximately 8 hours of dissolution, with a pH and food independent release. Three time points of the dissolution profile were selected as the most discriminant, 1, 2.5, and 6 hours, with very well-defined limits. Mathematical modeling of drug release is one of the best methods to understand and predict *in vitro* and *in vivo* performance. Therefore, the target profile was modeled using JMP® Pro 14.0, and the Weibull function (Equation 4.5) led to the best fitting, with an SSE of 1578.4 and an RMSE of 4.9 (details available in Appendix III, A. Mathematic modeling of dissolution profiles).

Equation 4.5. $\frac{Q(t)}{Q0} = 1 - e^{(-b \times t^a)}$

Q represents the amount of drug released at time *t*, Q_0 is the initial amount of drug, and *a* and *b* are constants and represent a time scale parameter and a shape parameter, respectively [379]. The estimates of the model parameters are described in

Table 4.3. These values represent the target for the development of the test product.

Table 4.3. Parameters estimates of target dissolution kinetics and their upper and lower 95% confidence limits.

Parameter	Estimate	Standard error	Lower 95%	Upper 95%
Q_0	96.01	1.18	93.70	98.31
a	2.114	0.097	1.925	2.327
b	0.128	0.011	0.106	0.151

3.2. Screening of polymers

A total of 18 combinations of polymers for extended-release were tested by HME, including HPMC 4M and 15LV, HPC grades MF and EF, EC grades N100 and N10, PVP k12, SLP, PVPVA, PVAc, PVOH, and Eudragits RS and RL PO. These combinations were based on literature and previous experience with the referred components. For screening purposes, a total of 30% of XR components in the formulation was considered. All cellulose-based blends led to extensive drug degradation during extrusion, as very twisted, dark, and wrinkled extrudates were obtained (extrusion temperature 175°C). Although the drug was not incompatible with cellulose polymers[6], the energy from heat and shear stress in the extruder triggered an enormous degradation. These formulations were immediately discarded, and only eight compositions from the initial eighteen proceeded in the screening experiment. Extrudates were milled, blended with the external phase (HPMC and magnesium stearate), tableted, and the *in vitro* release in phosphate buffer pH 6.8 analyzed. These formulations consisted of blends of PVAc with PVOH, PVPVA, SLP, or PVP, and mixtures of Eudragit PO RS/RL. A 4% of stearic acid was added as a plasticizer in formulations containing a high level of PVOH or Eudragit to facilitate the extrusion process and lower the processing temperature to approximately 170 ºC and 155 ºC, respectively, depending on the specific composition.

This step consists of a screening experiment, which aims at identifying which factors are most influential. It was used as an exploratory analysis to identify main effects by identifying critical components that can control the release rate of this highly soluble drug formulated at a low load.

[6] Binary compatibility studies were performed (exposure of 1:1 binary mixtures to 25°C / 60% RH and 40°C / 75% RH for up to 2 months), data not shown.

The focus was the release in pH 6.8, as it reflects the main pH environment where the XR tablets are exposed *in vivo*. An MLR was fitted on the dataset for the selection of the promising XR components. The summary of the Least Squares fit is presented in Table 4.4, and the parameter estimates for the valid terms are summarized in Table 4.5.

Table 4.4. Summary of Least Square Fit for the three dissolution responses.

Responses	Summary of Fit		ANOVA	Lack of fit
	R^2	R^2 *Adjusted*	*p value*	*p value*
Q(1h)	0.976	0.969	< 0.0001	0.245
Q(2.5h)	0.963	0.953	< 0.0001	0.091
Q(6h)	0.971	0.963	< 0.0001	0.159

The treatment of the obtained responses led to significant and valid models for all responses. The magnitude of the coefficient gives an idea of the importance of that term in the estimation of the response, but they are not scaled nor centered and cannot be compared directly. The sorted effects allow this comparison by ranking the absolute values of the *t* ratio. Therefore, to control the release at 1h of *in vitro* dissolution test, PVAc, PVOH, Eudragit RL, or RS, and hardness seem important. At 2.5h and 6h of dissolution, Eudragit RL or RS, stearic acid as plasticizer, tablets hardness, and PVAc are statistically identified as relevant factors. Moreover, PVOH and stearic acid are identified as the components where increasing amounts trigger a significant delay in the dissolution rate. Therefore, the balance between the internal composition of the extrudate, namely PVOH, PVAc, and stearic acid, is crucial to achieve the target release kinetics.

Table 4.5. Summary of parameter estimates for the three models and individual *p* value.

Factor/Parameter[a]	Estimate/ Coefficients	Standard error	Sorted effects[b]	Prob>|*t*|
Q(1h)				
Intercept	-80.474	8.333	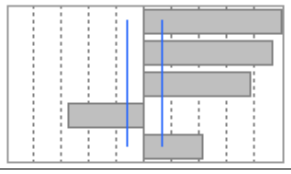	<0.0001
PVAc	1.282	0.079		<0.0001
Hardness	1.723	0.112		<0.0001
Eudragit RS	1.178	0.093		<0.0001
PVOH	-0.688	0.077		<0.0001
Eudragit RL	0.590	0.085		<0.0001
Q(2.5h)				
Intercept	-38.400	11.063	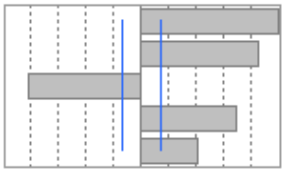	0.0027
Eudragit RS	1.681	0.116		<0.0001
Eudragit RL	1.281	0.102		<0.0001
Stearic acid	-7.313	0.616		<0.0001
Hardness	1.450	0.144		<0.0001
PVAc	0.676	0.112		<0.0001

Factor/Parameter[a]	Estimate/ Coefficients	Standard error	Sorted effects[b]	Prob>|*t*|
Q(6h)				
Intercept	-33.214	10.643		0.0059
Eudragit RS	1.988	0.112		<0.0001
Eudragit RL	1.680	0.099		<0.0001
Stearic acid	-7.509	0.593		<0.0001
Hardness	1.409	0.138		<0.0001
PVAc	0.740	0.108		<0.0001

[a] Other parameters evaluated included relative amount of other formulation components (HPMCAS, PVP k12, PVPVA, SLP, Lactose, and MCC). However, those showed not to impact with significance the dissolution profile at the selected time points. [b]Effects significance is organized from top to bottom by the absolute value of the *t* ratio. The blue lines represent the significance level of 0.05. The greater the effect in the dissolution rate (positive or negative), the higher the grey bar representing significance.

Although a high fitting was obtained with MLR, this exploratory analysis was not optimized or validated, and should not be used for response prediction but only to identify critical factors [380, 381] for the second stage of the prototype development. PVAc/PVOH and Eudragit-based compositions were selected as promising systems and included in different technologies to modulate the release rate to the intended target kinetics.

3.3. Screening of technologies

The next step was based on testing different downstream manufacturing processes for HME, namely standard compression (DC), microtablets in tablets (MUPS), and bilayer compression (BiTABS). Other parameters were also tested, namely the tablet size (reflected in the drug load), the quantities of the external phase (lactose, MCC, and HPMC), the need for stearic acid, and the hardness of the tablets. Two statistical DoE were planned, one for each polymer type (Eudragit or PVAc/PVOH), where the impact of varying concentrations of the external phase and the manufacturing process on the CQA dissolution were studied. A D-optimal design was selected, which is focused on reducing the prediction variance at the design points and allows different factor types. It is especially useful for screening designs, where the experiment's goal is to identify active factors. Eleven experiments were performed, taking into account the initial planned DoE, where three categorical and six continuous variables were studied. Eight additional tests were performed and added to the same table for a retrospective statistical evaluation, summing 19 formulation tests. The description of these tests is detailed in Appendix III, B. Dataset for the screening of technologies.

Very different release kinetics were obtained, as observed in Figure 4.3. Three compositions were not able to control the drug release rate, namely H, J, and K. These formulations were based on PVAc/PVOH prepared by DC or bilayer tableting. One of the compositions (K) even has HPMC in the external phase, with no success. Others demonstrate a drastic delay in the release rate, as compositions M, N, O, and P, which refers to PVAc/PVOH-based compositions in BiTABs or MUPS, where HPMC was added in the internal phase of the pharmaceutical system (the active layer or the microtablets). Another group is also seen, where the release is moderately controlled but tends to reach a low asymptote. It is the case of formulations A, B, E, and F, all Eudragit-based.

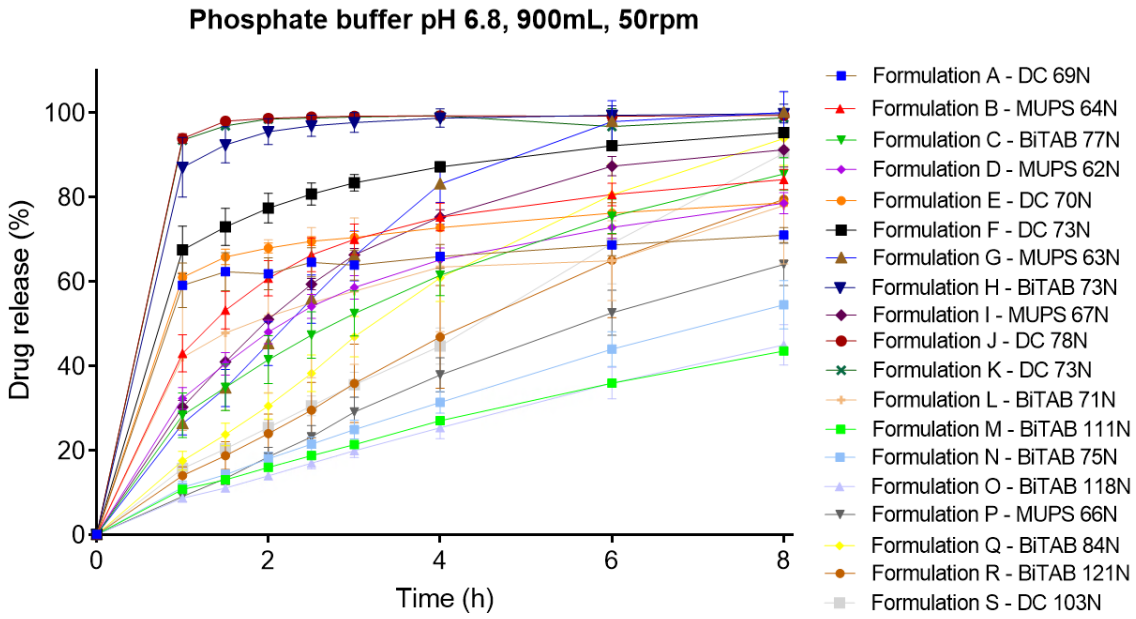

Figure 4.3. Dissolution profiles in phosphate buffer pH 6.8, 900 mL, paddles at 50 rpm, obtained in response to the screening of technologies. Error bars represent standard deviation.

Due to the high multicollinearity of the predictors and the presence of non-linear relationships of formulation and pharmaceutical processes, an ANN model was applied, in order to correlate formulation and process input factors with the dissolution responses. The ANN model was evaluated through the R^2 of the ANOVA of the linear regression between actual and predicted results, the RMSE, the SSE, and the MAD (Table 4.6). The prediction formulas demonstrated adequate prediction accuracy for all the responses. The results revealed better prediction accuracy for the Q(1h) and Q(2.5h) responses than for Q(6h). This is indicated by the lower R^2, both for training and validation datasets and higher RMSE, SSE, and MAD.

Table 4.6. Summary of the MLP model parameters.

Response	Q(1h)		Q(2.5h)		Q(6h)	
Dataset	*Training*	*Validation*	*Training*	*Validation*	*Training*	*Validation*
R^2	0.994	0.987	0.985	0.990	0.933	0.938
RMSE	3.996	1.680	4.374	2.607	6.084	5.429
SSE	878.17	36.68	1052.42	88.39	2036.02	383.15
MAD	2.228	1.385	2.785	1.922	4.091	3.546

Abbreviations: RMSE, root mean square error; SSE, sum of squared errors; MAD, mean absolute difference.

The overall prediction profiler was constructed with the prediction formulas. The prediction profiler demonstrates the effects of input variables on responses and is portrayed in Figure 4.4. From the curve slopes, one can understand which the most influential parameters are. It is observed that Eudragit RS has a higher impact on the dissolution kinetics than RL, which can be justified by its lower permeability. The addition of HPMC also seems to be relevant (amount and composition phase) as well as the PVAc/PVOH/stearic acid system. No doubt, the most relevant factors are the technology process and tablet hardness. A strict control of the compression force during tablets manufacturing seems to be required, but this is based on preliminary data on very short compression tests and additional data is required.

The prototype's selection started by identifying those whose release kinetics is described by the Weibull function, with an α value of 0.05. From the nineteen tested compositions, only nine showed the same release kinetics as the target profile, as detailed in Table 4.7.

Table 4.7. Parameter estimates for the Weibull function (Equation 4.5), by JMP® Pro 14.0 using a least-squares loss function and α of 0.05.

Formulation code	SSE	RMSE	Estimated Q_0 (std error)	Estimated a (std error)	Estimated b (std error)
A	Lack of fit	Lack of fit	-	-	-
B	1.117	0.431	85.65 (0.65)	0.804 (0.021)	0.702 (0.009)
C	Lack of fit	Lack of fit	-	-	-
D	1.488	0.498	84.25 (1.41)	0.814 (0.025)	0.480 (0.009)
E	Lack of fit	Lack of fit	-	-	-
F	0.207	0.186	109.31 (1.72)	0.369 (0.012)	0.955 (0.023)
G	33.93	2.378	104.50 (3.35)	1.307 (0.092)	0.242 (0.016)
H	0.119	0.141	99.70 (0.11)	0.590 (0.014)	2.062 (0.012)
I	1.467	0.495	95.03 (0.84)	1.045 (0.020)	0.375 (0.005)
J	0.118	0.140	99.17 (0.07)	0.955 (0.062)	2.924 (0.028)

Formulation code	SSE	RMSE	Estimated Q_0 (std error)	Estimated a (std error)	Estimated b (std error)
K	Lack of fit	Lack of fit	-	-	-
L	Lack of fit	Lack of fit	-	-	-
M	Lack of fit	Lack of fit	-	-	-
N	Lack of fit	Lack of fit	-	-	-
O	Lack of fit	Lack of fit	-	-	-
P	1.039	0.416	86.85 (4.16)	1.231 (0.03)	0.103 (0.004)
Q	9.035	1.227	119.51 (8.95)	1.164 (0.061)	0.138 (0.008)
R	Lack of fit	Lack of fit	-	-	-
S	Lack of fit	Lack of fit	-	-	-

Abbreviations: SSE, sum of squared errors; RMSE, root mean squared error.

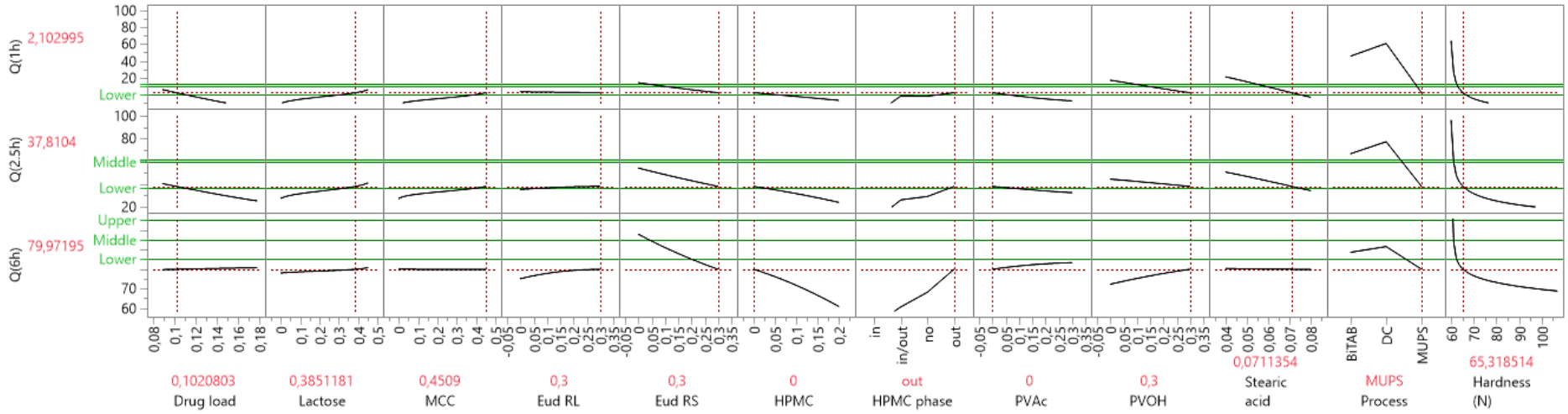

Figure 4.4. Prediction profiler originated from the neural network model (with JMP® Pro 14.0). The x-axis represents the factors (inputs) and the y-axis the predicted responses (outputs). Abbreviations: MCC, Microcrystalline cellulose; Eud, Eudragit®; HPMC, hypromellose; PVAc, Polyvinyl Acetate; PVOH, Polyvinyl Alcohol.

To select the most promising platform, all the compositions that were capable of being described by the Weibull function were analyzed by PCA on correlations, and the results are depicted in Figure 4.5. The aim was to reduce the dimensionality of the dataset, converting it into two principal components. The graphs portray score and loading plots, where each system and the target profile are marked. The score plot graphs the component's calculated values, and the loadings plot portrays the unrotated matrix between dissolution results and the principal components. Component 1 is composed of 80.5% of the dataset variance and is mostly represented by the results at 3 and 4 h, while component 2, representing 17% of the results' variance, is primarily explained by the extreme dissolution time points, 1 and 8h. Only two components are represented, both with statistical significance ($p < 0.0001$, Bartlett test), as they represent 97.5% of the variance of the results of the dissolution dataset. The most similar formulation with the target profile (marked with X) is marked in blue and corresponds to composition G.

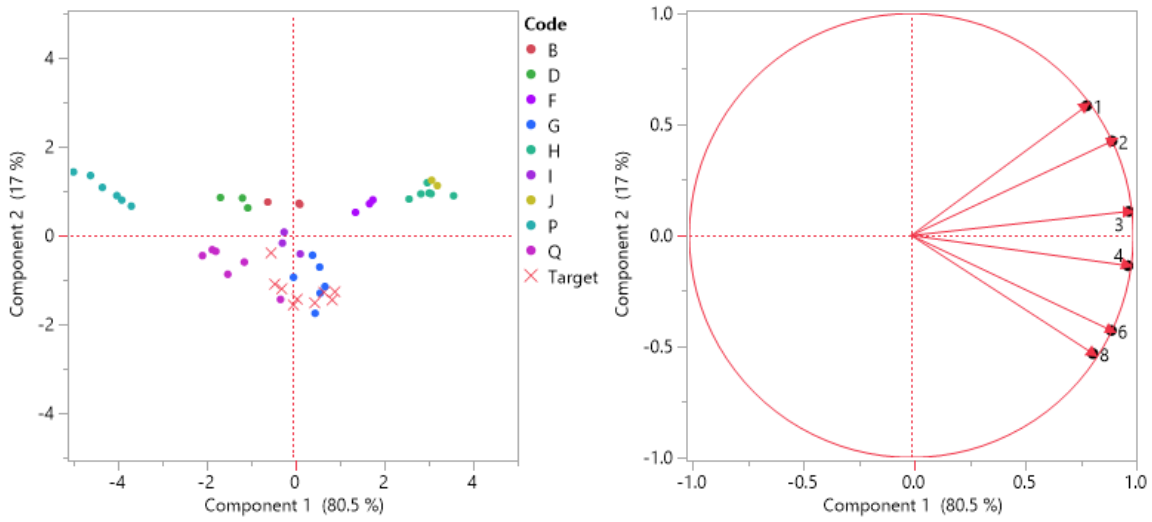

Figure 4.5. PCA statistics (with JMP® 14.0) performed on dissolution profiles, represented by score (left) and loadings (right) plots. The score plot graphs the component's calculated values, and the loadings plot portrays the unrotated matrix between *in vitro* release and the calculated principal components 1 and 2. The higher the value, the greater the impact on the dissolution variable timepoints (h), represented by the numbers in the loading plot. The Bartlett test determined two principal components as significant ($p < 0.0001$), explaining 97.5% of the results' variance. The target profile is marked in X.

3.4. Manufacturing of prototype and characterization

The selected formulation (G) comprehended an uncommon technological platform based on MUPS of PVAC/PVOH. The process was scaled-up to 100 g to confirm the robustness of the preparation method and fully characterize the performance of this composition (Figure 4.6).

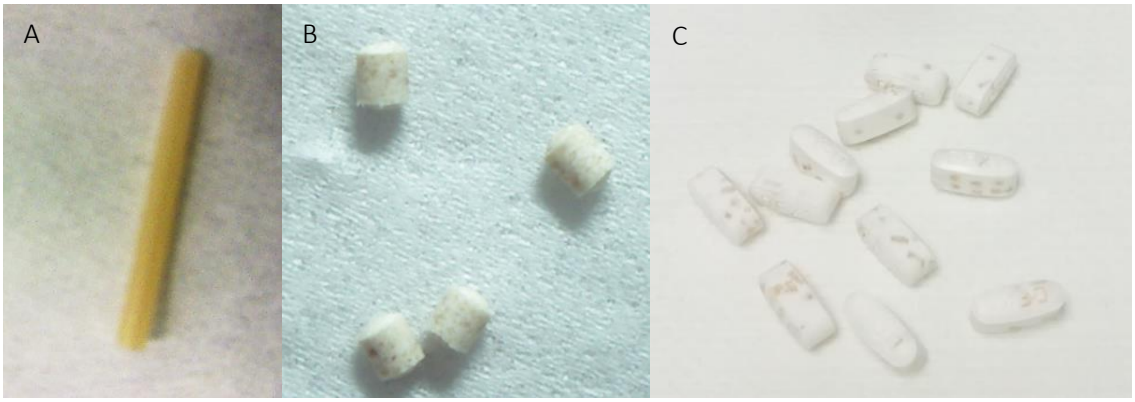

Figure 4.6. Macroscopic photographs of extrudate prepared by HME (A), microtablets of 2 mm (B), and MUPS (C).

3.4.1. Chemical characterization

The prototype composition led to acceptable drug content (102.20% with an RSD of 5.14%) and a low impurities level (0.25%) (Table 4.8). All unknown impurities were below 0.1%, the reporting threshold. The relatively high RSD of assay is not surprising as we are dosing 13.2 microtablets per tablet. Each microtablet has 1.35 mg of the drug, and 13 microtablets by tablet leads to a theoretical content of 99%, but 14 leads to 106%. Only two tablets were tested in the assay method, with individual results of 98.48% and 105.91%, probably explained by 13 and 14 microtablets per tablet, respectively. The water content was expectedly low (2.05%). Chromatograms are depicted in the Appendix III, C. Chromatograms from assay and degradation products UPLC analysis.

Table 4.8. Results of assay and degradation products analysis by ULPC and water content by the Karl-Fischer method.

Assay (%) ± RSD	Known impurity 1 (%)	Total impurities (%)	Water content (%)
102.20 ± 5.14%	0.25%	0.25%	2.05 ± 0.30 %

3.4.2. Surface characterization

To understand the structure of the prepared MUPS, cross-sections were observed by SEM. It was hard to obtain a smooth cut due to the presence of the microtablets and relatively high resistance to crushing. The microtablets are observed in the tablet with well-defined interfaces and not damaged by the main compression step (Figure 4.7A and B), which is crucial to control the release kinetics and avoid variability. The border between the microtablets and the external phase is observed, and the inner structure of the microtablets seems to be irregular and rough (Figure 4.7C and D).

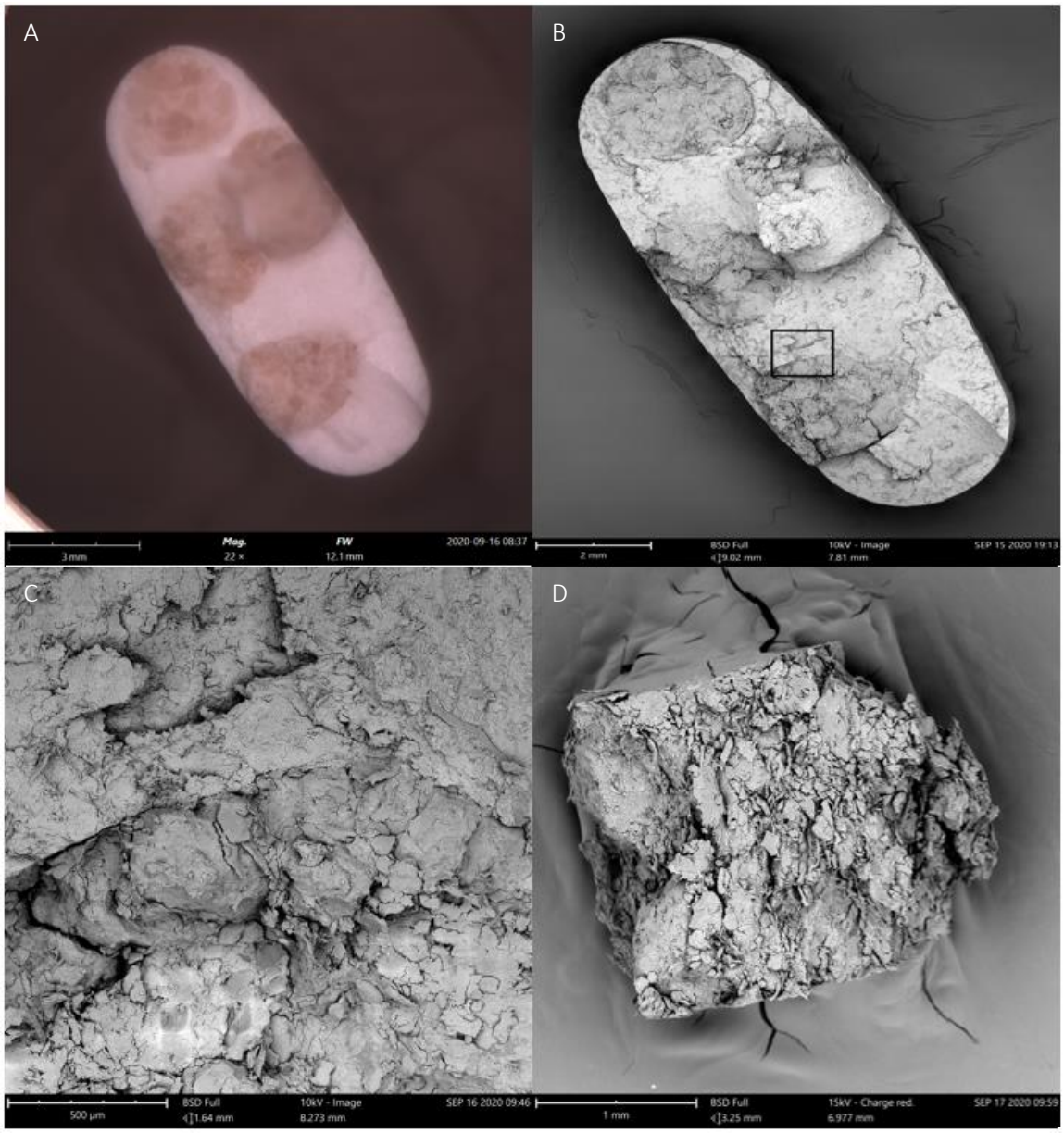

Figure 4.7. Optical (A) and SEM analysis of the prototype MUPS (B), a selected area between the borders of the two phases (C) as highlighted in B, and a microtablet (D).

3.4.3. Raman mapping

A Raman map was collected from an interface area between microtablets and the external phase, in a longitudinal cut of the MUPS, to confirm that the main compression did not damage the microtablets. This method was selected as complementary to SEM for this assessment due to their orthogonality. The results are portrayed in Figure 4.8. This analysis was complicated by the difficulty of obtaining a smooth cut to allow a proper collection of Raman spectra in well-focused areas and low spectrum noise. Microtablets seem to be intact, and a clear border is seen in the Raman mapping. Some drug residues are also detected in the external area, corresponding to loose powder and triggered by the cutting procedure.

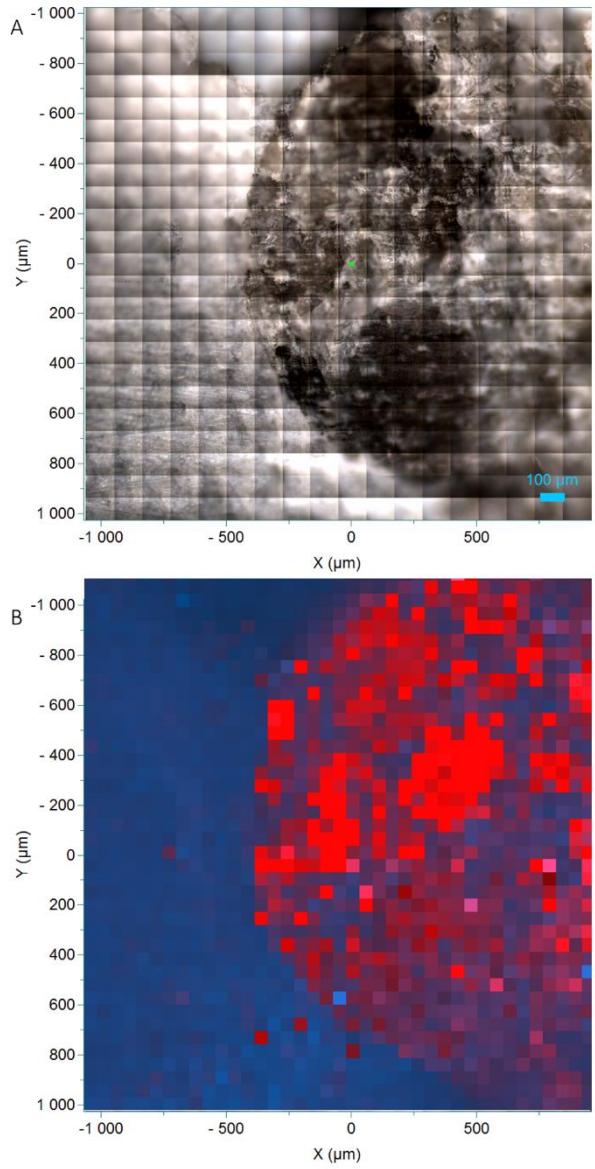

Figure 4.8. A, Microscopic image of the tablet longitudinal cut with a magnification of 50x. B, Raman mapping of an interface between microtablet and external phase, at 2 x 2 mm, acquired with the 785 nm laser, power of 55mV, collection time of 8 seconds and 5 times, and 50x magnification. The spectra were collected in a wavenumber range of 450 – 1600 cm^{-1}. Red is used for the drug and blue the formulation excipients.

3.4.4. X-Ray Powder Diffraction

The XRPD revealed that the drug is mostly amorphous in the prepared system (Figure 4.9), contrasting with the well-defined diffractogram of the crystalline drug. Although some residual peaks are detected in the microtablets and in the MUPS phases, a halo pattern is predominant, which is typical of amorphous systems. In this phase, only HPMC and magnesium stearate are added to the milled extrudate before tableting into microtablets. HPMC is an amorphous component [382, 383], and main peaks of magnesium stearate are typically at 5.5°, 9°, and 21-22° 2θ [384], also seen in the XRPD diffractogram (Figure 4.9). The detected peaks in the MUPS diffractogram are mostly due to the presence of the highly crystalline lactose monohydrate, with typical 2θ signals at 12.5°, 16.4°, the triplet at 19.1°, 19.5°, and 20.0°, and also 20.8°, 21.2°, 22.8°, 23.8°, 25.7°, and 27.5° [385-387].

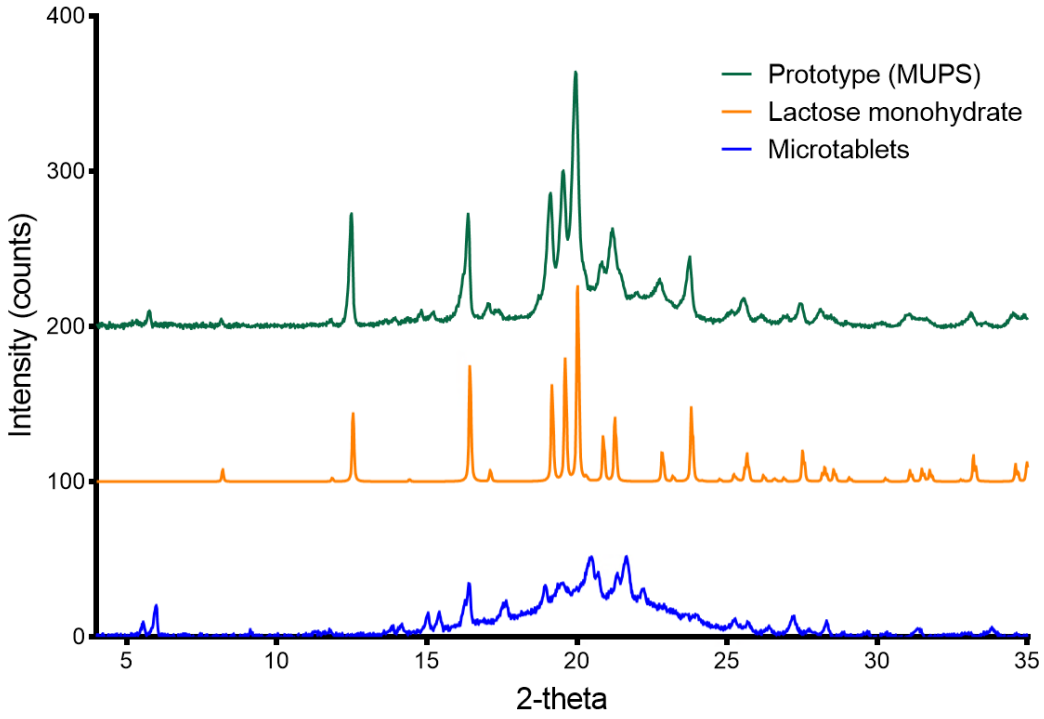

Figure 4.9. Overlay of XRPD patterns of lactose monohydrate, microtablets, and MUPS. The detected peaks in the MUPS diffractogram are mostly due to the presence of the highly crystalline lactose monohydrate.

The miscibility in the blend of PVOH/PVAc was somewhat expected based on the calculation of the Hansen solubility parameters, δ [142], which led to a value of 27 $MPa^{0.5}$ for the drug and 31 $MPa^{0.5}$ for the PVAc/PVOH blend (1:1) (data not shown). With an absolute difference of approximately 4

$MPa^{0.5}$ [31, 39], the drug was expected to be miscible with the polymeric blend and led to an ASD. Indeed, the opaque color of the extrudates was not a sign of a crystalline suspension in this case, as the HME-placebo had a similar appearance.

3.4.5. Drug release

Figure 4.10 portrays the dissolution curves of the selected prototype in two extreme pH conditions, HCl 0.1N and phosphate buffer pH 6.8, which intend to translate its behavior over the gastrointestinal tract. Both tests were performed using paddles at 50 rpm, as recommended by EMA and FDA for an optimal discriminatory ability and biopredictive power. The release in HCl 0.1N is approximately 20% faster than in pH 6.8, which is in line with the drug's higher solubility at low pH. However, the acid environment is transitory as it represents the stomach, where in fasting conditions it should last for approximately 20 min and in fed for 40 min [388, 389]. Therefore, the higher release in HCl 0.1N is not drastic and should not affect severely the product XR behavior. In phosphate buffer pH 6.8, a near zero-order XR kinetics is seen, reaching the asymptote after 6 hours of the dissolution test.

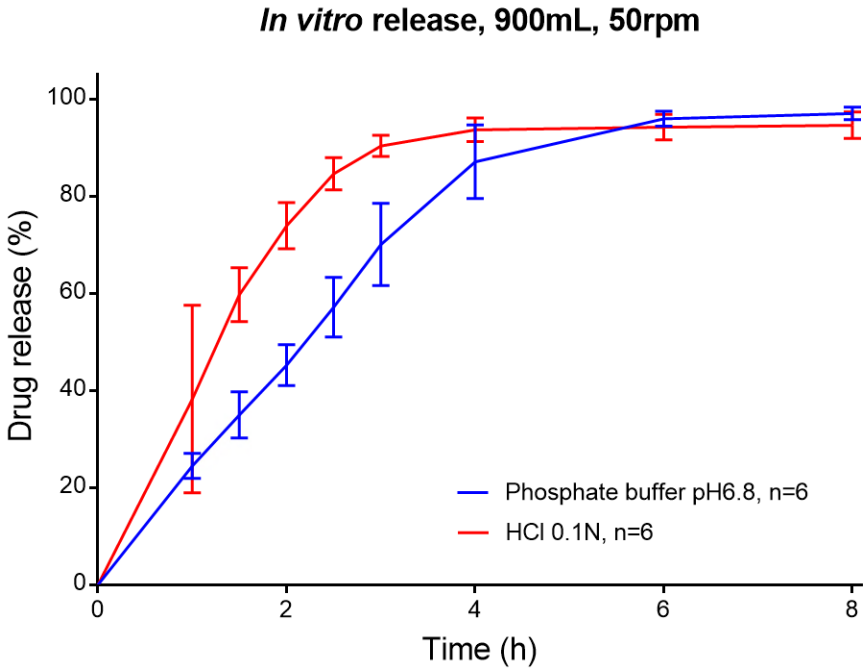

Figure 4.10. Dissolution profiles of the prototype formulation in phosphate buffer pH 6.8, 900 mL, paddles at 50rpm and HCl 0.1N, 900 mL, paddles at 50rpm, both n=6. Error bars represent standard deviation.

To better understand the mechanistic drug release behavior and determine its kinetics, the release profile was modeled using JMP® Pro 14.0. Among all the tested models (zero-order, first-order, Hixson-Crowell, Higuchi, Weibull, Korsmeyer-Peppas, Gompertz, and Hopfenberg equations), the Weibull function (Equation 4.5) led to the best fitting, with an SSE of 1341.7 and an RMSE of 5.1 (details available in Appendix III, A. Mathematic modeling of dissolution profiles). The estimates of the model parameters are described in Table 4.9. The Weibull model is empirical, not deduced from any kinetic fundament. It is often seen as multi-mechanistic, where the release parameters *a* and *b* are related to the system geometry (size and shape) [379, 390, 391]. The parameter *b* is often studied as a hint for kinetic analysis. It generally explains diffusional mechanisms and reflects the medium's disorder, i.e., higher *b* values are related to lower disorder. A *b* of 0.24 is a clue of a highly disordered space, with no specific release mechanism defined, and this is the case of the prepared prototype [379]. It may indicate the effect of combined mechanisms on the drug release. The random position and orientation of the microtablets in the MUPS may explain the disordered system geometry. Despite the complex conformation, the prototype exhibits similar release kinetics to the target profile, as both have low *b* values and approximate Q_0 and *a* parameters.

Table 4.9. Parameters estimates of prototype dissolution kinetics and their upper and lower 95% confidence limits.

Parameter	Target estimate and CI	Prototype estimate	Standard error	Lower 95%	Upper 95%
Q_0	96.005 [93.702 - 98.307]	98.889	1.960	95.297	103.085
a	2.114 [1.925 - 2.327]	1.496	0.086	1.328	1.674
b	0.128 [0.011 - 0.151]	0.235	0.0160	0.203	0.270

Abbreviation: CI, confidence interval.

As an empirical model, the Weibull function may describe but not characterize the release kinetics, even more, when low *b* values are obtained. Therefore, it often requires complementary release models or experiments to in-depth knowledge of the release mechanism.

In this case, the change in the MUPS surface topography was studied over the dissolution experiment by SEM. Tablets were removed from the dissolution apparatus at predetermined time intervals and water excess was removed by vacuum filtration for SEM analysis. The tablet disintegration was immediate, but that was not the case of microtablets, as at 1 h and 2.5 h of the dissolution experiment, they were still visible to the naked eye, and progressively eroded and

involved in a gelling cape. HPMC swelling was observed in SEM images as elongated microfibers and deformed structures because the excess water was removed. This is seen in Figure 4.11A-D, where swollen and gelling areas lead to agglomerated regions of different surface aspect and porosity. The microtablets were completely disintegrated at 6 h, and only granules were then observed (Figure 4.11E and F). They can be described as homogeneous in shape and size, but highly porous, which is perfect for drug diffusion. When comparing with Figure 4.7D from the intact MUPS, porosity was very low. The microtablets were observed to control the drug release rate, and the formation of gelling and micropores supported swelling, erosion, and diffusion as the main mechanisms responsible for the extended drug release from MUPS.

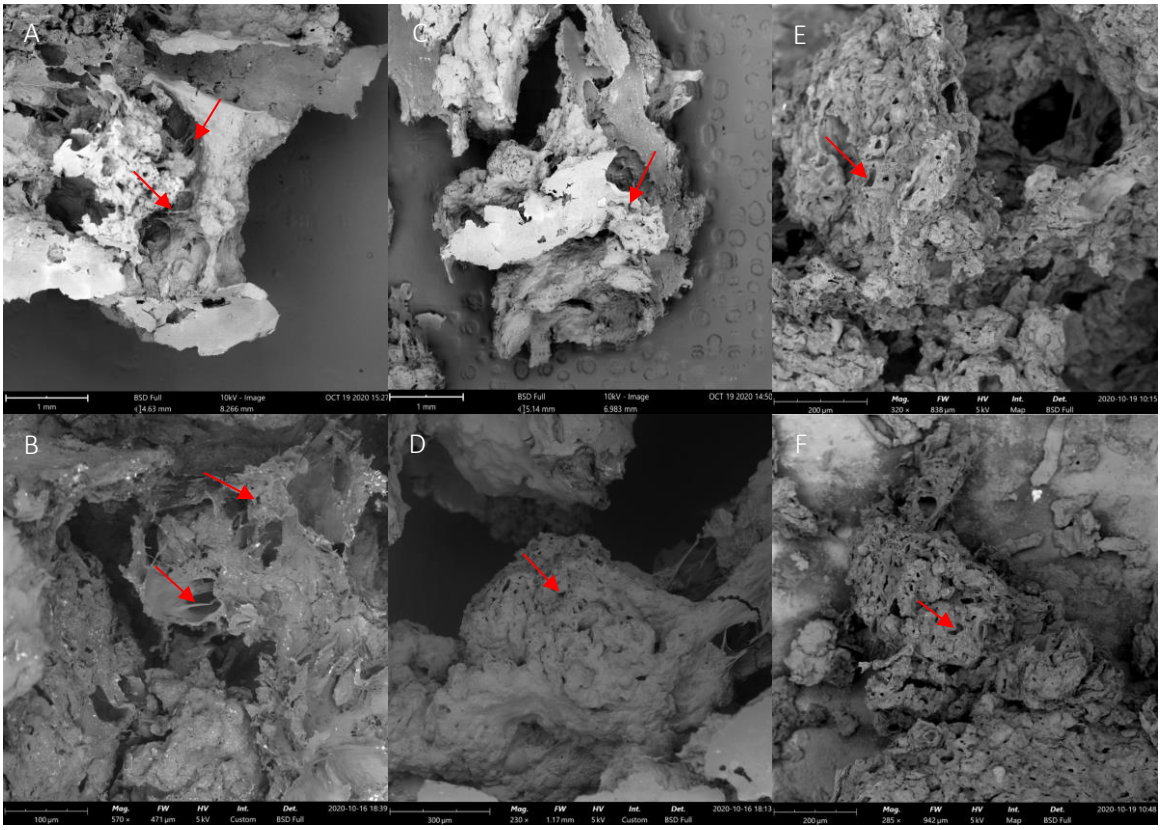

Figure 4.11. SEM of the *in vitro* dissolution test samples in phosphate buffer pH 6.8, 900 mL, paddles at 50rpm, at 1h (A and B), 2.5h (C and D), and 6h (E and F). Magnifications are detailed in each photomicrograph. The red arrows highlight the swelling phenomenon and micropores formed by matrix erosion.

3.5. Risk assessment

After the prototype definition, a risk assessment was carried out to identify critical factors during the preparation of this system for drug product CQAs. Table 4.10 depicts a summary of the initial

process risk assessment. Room conditions, namely the temperature and relative humidity, are controlled within strict limits for GMP manufacturing. Therefore, no significant impact is expected for the drug product. However, polymeric-based XR products are typically very hygroscopic, which may compromise the drug release rate, HME processability and degradation products. Sieving and pre-blending are the next steps in the preparation process. They are considered simple de-lumping and homogenization steps to enable a constant powder flow, blending, and dispersing into the extruder. The HME process is probably the most critical step, where process temperature, screw speed, feeding rate, and cooling as CPPs require an in-depth study. Extrudate milling speed and time may affect the material particle size, which may impact its chemical and physical stability, as well as dissolution. Then, the polymeric phase is blended with HPMC and magnesium stearate, where technical hurdles are not expected but must be confirmed, mainly for the content uniformity. The tableting into microtablets may also have a critical impact on the dissolution performance, but also in the solid-state (conversion promoted by the energy of compression), in degradation products (promoted by the energy and heat of compression), and in the content uniformity (for instance due to insufficient flow or uneven die filling).

The subsequent process steps are also considered crucial for the successful preparation of the product. Microtablets must be blended and homogenized with the external phase, which is clearly demanding due to the materials' discrepant sizes. The final compression follows, where chemical and physical stability must be controlled, but the focus is dissolution impacted by the compression force, and content uniformity, affected mainly by CPPs as the filling weight and the turret speed.

In summary, the HME process seems to be the most critical to ensure product quality and performance. Furthermore, the extrudate milling, the multi-tip compression, the blending with the external phase, and the final compression seem also to be critical to ensure the defined CQAs. Parameters identified as medium and high risks require further evaluation experimentally.

Table 4.10. Risk Estimation Matrix of the initial risk assessment of the manufacturing process. Each critical process parameter was qualitatively ranked as high, medium, or low-risk considering the probability of occurrence and the severity of the impact on the CQAs.

Risk Estimation Matrix																					
Process step	**Room conditions**	**Sieving of raw materials**	**Blending**		**Hot-melt extrusion**				**Milling**		**Sieving of milled extrudate**	**Blending**		**Multi tip tableting**			**Blending**			**Tableting**	
Process parameter /CQAs	Temperature and RH	Sieve size	Time	Rotation speed	Temperature	Screw speed	Feeding rate	Cooling method/speed	Speed	Time	Sieve size	Time	Rotation speed	Filling weight	Compression force	Turret speed	Time	Rotation speed	Filling weight	Compression force	Turret speed
Polymor-phism	Low	Low	Low	Low	High	High	Med	High	Med	Med	Low	Low	Low	Low	Med	Low	Low	Low	Low	Med	Low
Drug content and uniformity	Low	Low	Low	Low	Med	Med	High	Low	Low	Low	Low	Med	Med	Med	Low	Med	High	Med	Med	Low	Med
Dissolution	Med	Low	Low	Low	High	High	High	Med	High	High	Med	Low	Low	Low	High	Med	Low	Low	Med	High	Med
Degrada-tion Products	Low	Low	Low	Low	High	High	Med	Low	Med	Med	Low	Low	Low	Low	Med	Low	Low	Low	Low	Med	Low

Abbreviations: CQA, Critical Quality Attribute; RH, relative humidity; High, high risk; Med, Medium risk; Low, low risk.

4. Conclusion

This study led to the development of a new drug delivery platform for the controlled-release of a high solubility and a very short half-life drug, to improve patient compliance through a once-daily administration. This work was performed within a pharmaceutical industry development team, and the goal is to bring a new drug product to market. Preliminary tests demonstrated the need for an intimate blend with a release-controlling component, and HME was considered a promising technology. The study was initiated by the systematic screening of polymers and technological platforms. The support of mathematical modeling and statistical analysis was crucial to seek the right kinetics, i.e., the target shape of the dissolution profile, namely using the Weibull function and PCA. Then the prototype was scaled-up and thoroughly characterized.

Our new technological platform is not common as it is based on MUPS of PVAC/PVOH/drug, prepared by HME coupled with a downstream compression into microtablets of 2.0mm, and a further compression into 10.8mm tablets (MUPS). The smooth processing conditions, including low extrusion temperatures, led to an ASD with a very low degradation level. The assay was considered acceptable, and the variability expected. SEM and Raman mapping demonstrated that the microtablets are well defined and not damaged by the main compression. The release profile in phosphate buffer pH 6.8 led to a near zero-order XR kinetics for 6 to 8 hours. In HCl 0.1N, it seems to be approximately 20% faster, but it represents a transitory stage *in vivo* and is, therefore, considered sufficient to reach the target PK profile. The prototype was demonstrated to have the intended target release kinetics and is an alternative to patented osmotic systems.

For an in-depth understanding of the mechanistic drug release kinetics through this innovative platform, the release profile was modeled by the Weibull function. A highly disordered geometry was revealed, explained by the random microtablets arrangement in the MUPS. It led to an unspecific release mechanism, defined by a combination of diffusion, erosion, and swelling, corroborated by SEM analysis of dissolution samples. The next steps include the prototype optimization, both in terms of formulation and process, following QbD concepts, and *in vivo* PK study for proof-of-concept.

CHAPTER V. CONCLUSION

HME emerged as a novel technology for product development and represents a promising tool to enhance solubility and absorption, and improve stability of drugs. This technology has been used successfully for already approved products and many others under development, including medical devices. The interest of the pharmaceutical industry in HME is easily justified as a solvent-free, continuous, and cost-effective technology, creating robust processes for a variety of pharmaceutical forms, as oral solids, oral films, topical, ophthalmic inserts, and implants. The consistency and reproducibility of the continuous process is also a significant benefit of HME. Moreover, extrusion is suitable for high potency compounds, very common nowadays. The current advances in HME and the in-depth understanding of material science and process engineering enable pharmaceutical scientists to develop efficient and robust products and to solve complex problems of drug delivery.

The versatility of HME for the development and manufacturing was demonstrated in this thesis, where the main goal was to overcome formulation barriers in the pharmaceutical development path, tailoring formulation performance. The enhancement of solubility is the primary use of HME, but other approaches were exploited. Therefore, this technology was applied in three different scopes, namely in the solubility enhancement of a poorly-soluble compound, in the physical stabilization of an unstable amorphous drug, and the controlled release of a highly soluble drug.

The significant aspects of HME technology and its application in the preparation of solid dispersions were discussed, including critical molecular and thermodynamic factors governing the physicochemical properties of these systems. Some weaknesses, mostly chemical and physical instability, temper the use of amorphous drugs. The preparation of amorphous solid dispersions (ASDs) is currently the last but most effective strategy to stabilize those systems, and many factors must be taken into consideration when planning for this type of product development. A systematic step-by-step approach was presented, where thermodynamics, screening approaches, multivariate statistics, and process optimization were combined to increase the success of HME pharmaceutical development. The QbD concept was applied to HME, and steps and tools for its effective implementation were provided, including a risk assessment, highlighting critical points that can be useful in regulatory submissions. HME-based compositions were then developed to overcome formulation limitations and tailor challenging drug properties.

In the Etravirine case, a systematic step-by-step formulation screening approach was followed. The Hansen solubility parameters, the interaction parameter, and the prediction of T_g through the Gordon-Taylor equation were key to select promising polymers to be tested in the high-throughput screening (HTS), using solvent evaporation. After the evaluation of solubilization capacity and physical stability by PCA, the prototype was selected. The amorphous system led to an improvement of drug release of more than two times. The ASD proved to be physically and chemically stable for at least three months, when stored at long-term and accelerated conditions. The unexpected stability at 40°C / 75% RH was correlated with the presence of molecular interaction observed in the Raman spectrum.

HME was applied to improve the physical stability of an amorphous drug in the Ibrutinib case. The described systematic screening approach was used to identify promising compositions, but in this case, focusing on physical stability. Milled extrudates demonstrated to be fully amorphous, even with a very high drug load of 50%. The thermal analysis detected a glass transition temperature much higher than the predicted values, explained by intermolecular interactions detected in Raman spectroscopy. The additive effect of all the intermolecular interactions changed the performance of the ASDs markedly, and they demonstrated to be stable until, at least, six months at both long-term and accelerated conditions.

Finally, HME was applied to develop a drug delivery platform for the controlled-release of a highly soluble drug in a low drug load, a well-known technological challenge. HME was considered a promising technology not only to modulate drug release but also to deal with high potency compounds. After a screening of ingredients and technological platforms, the Weibull function and PCA were applied to select the most promising system. The unusual technological platform selected is based on a MUPS prepared by HME, coupled with downstream compression in microtablets and finally into tablets. The release profile matched the near zero-order kinetics for 6 to 8 hours. An in-depth understanding of the molecular mechanism by the Weibull function and SEM of dissolution samples revealed a combination of swelling, diffusion, and erosion.

Although successful results have been achieved, as discussed during these investigations, further effort and expertise are still required. In the three described cases, potential prototypes were exploited and defined. The next steps include the prototype optimization, both in terms of formulation and process, following QbD concepts and complemented with biorelevant *in vitro* evaluations for potential bioprediction and correlation with PK data. After the fine-tuning of formulations and manufacturing processes, scale-up must be evaluated, followed by a GMP manufacturing and *in vivo* PK studies for proof-of-concept. Process validation, pivotal

bioequivalence studies, and dossier filing will comprehend the last and decisive stages to reach the market.

The results described in this thesis contributed to the progress of formulation development strategies, to understand the relevance of the HME carriers in the product performance, considering different scopes. Moreover, this work also provided a better comprehension of the factors affecting the physical structure, stability, and drug release, where both immediate (and enhanced) or extended-release are aimed. Overall, this project also contributed to a deeper understanding of the complex solid-state science of drug products, considering the assurance of quality, safety, and efficacy.

Final remarks and Future perspectives

The development of new drug products, from drug discovery to product and clinical development, is a lengthy and costly process. Shorter development times get new therapies sooner to patients and benefit the developer financially, by reducing the time between investment and return. Moreover, accelerated clinical development programs approved for breakthrough therapies lessen the time available to optimize phase III and commercial manufacturing processes. Developers of all types of pharmaceutical products are always under pressure to decrease product development timespan, and often the formulation and process optimization is postponed to post-approval. Several examples of products where the first approved formulation is upgraded afterwards for a more bioavailable, physically and chemically stable, or even with simpler administration schemes, exist. The underlying reasons may be to avoid any further delays in entering the market after clinical development, or the lifecycle management strategy, creating new intellectual property and extending the investment return.

Therefore, there is an increased interest of both innovator and generic companies in alternative drug delivery technologies, able to overcome the current limitations of conventional drug products. The scope is generally the reformulation of already marketed drug products to improve efficacy, safety, or even patient compliance. Specifically, HME has been used to improve solubility, and therefore oral absorption of drugs, increasing the treatment efficacy or decreasing the recommended dosage, leading to less adverse events and improved safety. Furthermore, it was also used to enhance product stability or administration convenience, decreasing the number of tablets or capsules per day. HME emerged as a technology that shifted the entire paradigm of pharmaceutical industry research and manufacturing in this era of patient-centric formulations.

During the investigation described in this thesis, some techniques and technologies were evaluated and shown to be crucial for the development of this type of system. The thermodynamic evaluations were revealed as the key to identify the most promising HME systems rapidly. They allow a rapid assessment of the complex interplay between miscibility, solid-state, and performance, avoiding wasting time and efforts in doomed compositions. In this work, different approaches were applied, such as the calculation of the Hansen solubility parameters, the interaction parameter, or the prediction of the glass transition temperature through the Gordon-Taylor and Fox equations. The screening techniques selected to initiate product development were

also discussed as critical for a fast and effective massive evaluation of potential compositions. It is essential to apply a simple and easy-to-use method that requires low amounts of drug, and which adequacy and accuracy have been proved to predict the performance of the drug when formulated. Another significant contribution was from applying integrated characterization methods to improve the comprehension of the link between structure and property and its impact on product performance. This methodical approach was used throughout this investigation, combining PLM, XRPD, thermal (TG, DSC, and PLTM), and spectroscopy methods, like Raman. Others have been applied to complete the characterization, namely chromatography for content and degradation products, dissolution experiments in different conditions, and optical and scanning electron microscopy for surface and topographical understanding. The molecular mechanism behind drug dissolution was also assessed using SEM for surface analysis of dissolution samples, supporting the identified release kinetics experimentally. The evaluation of the intermolecular interactions promoted by the intimate blend of components during extrusion is also strategic in this type of formulations, answering questions and explaining unexpected results. Raman spectroscopy and DSC analysis were successfully applied in this regard. Finally, this thesis also proposed using specific statistical methods to guide formulation development and support major formulation decisions, from the standard Least Squares method to multivariate statistics as Principal Components, or advanced non-linear methodologies as the Artificial Neural Networks.

As a core in product development, the QbD paradigm was applied to HME throughout the research described in this thesis. QbD should be seen as an opportunity to gain a better understanding of pharmaceutical products and manufacturing processes and not only as a requirement of regulatory authorities. As different strategies and tools may be applied, the selection of an adequate tool should be based on the primary goal of the study and the product development phase. Risk assessment and DoE were cautiously used, but other methodologies were followed like the high-throughput screening, the in-depth solid-state characterization, the thermodynamic predictions, and the judicious statistical analysis. Although there is no uniform method for implementing QbD, developments are more and more science-based as requested by the QbD philosophy.

Additional studies could complement this research, namely applying PATs to optimize design, analysis, and control within the manufacturing processes following the QbD principles. Examples comprehend rheometric analysis or spectroscopy, like optical - Raman, UV-Vis, or infrared. Additionally, the rheological behavior during extrusion may be exploited. Other techniques for a better understanding of the developed systems' molecular arrangement may be used to determine low amounts of crystallinity and predict stability performance, for instance, through terahertz, dielectric, and ultrasonic spectroscopies, or through NMR or Atomic Force Microscopy.

Further research on predicting the *in vivo* performance of the developed systems would also provide a unique contribution to the comprehension of the performance after oral administration. Dissolution testing under biorelevant conditions, IVIVC, or PBPK modeling may be exploited and are considered critical to biopredict the behavior of solid dispersions and other types of enabling formulations. Dissolution testing is a powerful tool to fasten product developments and increase quality and performance when associated with IVIVC or PBPK modeling and QbD.

Some challenges came across during the execution of this work. Solid dispersions are considered complex, and there is a lack of knowledge on chemical-physics and thermodynamics of pharmaceutical systems among formulation development teams. These involve concepts adapted from other research areas like material science, thermodynamics, solid-state, polymers, and amorphous materials sciences, which are quite different from the standard oral solids development concepts. This adaptation is an ongoing process, with the contribution of specific research groups in the field, but has evolved considerably over the last decade. Being a new technology under implementation, it was also a challenge to have the support of experienced scientists in the field for fruitful discussions and rapid resolution of simple problems. Moreover, this type of development requires the consistent application of advanced characterization methods for physical and solid-state analysis, which are not widely implemented in pharmaceutical development groups. This was the perfect opportunity to strengthen partnerships between academia and the pharmaceutical industry and to promote knowledge translation to backing decisions with data analysis and science support.

The expertise required and the lack of regulatory guidance for developing such highly complex products make these developments starving for teamwork and multidisciplinary contributions. Moreover, new thoughts, discussions, and guidance from regulatory agencies, in what concerns expectations on the submission of solid dispersion products, would be valuable for formulation scientists.

As lipophilicity is the trend of new therapeutic compounds, enabling formulations will be highly pursued in the forthcoming years, and HME will undoubtedly be a leading technology in this new paradigm. FDA acknowledged the exceptional flexibility of HME to QbD concepts and PAT tools, both enabling real-time control to ensure the consistency of the end products. This feature is becoming more important and should place HME as a central technology in pharmaceutical manufacturing. The trend seems to be the specialization of companies and human resources, instead of generalized implementation, due to the several specificities of this technology discussed in this thesis, and applied to both developers and manufacturers.

You cannot get through a single day without having an impact on the world around you. What you do makes a difference, and you have to decide what kind of difference you want to make.

Jane Goodall
(Primatologist and Anthropologist, born in 1934)

APPENDIX I: ETRAVIRINE

A. Calculation of Solubility Parameters

The Hansen solubility parameters, δ, of drug and polymers were calculated from their chemical structures using the van Krevelen and Hoftyzer contribution group method [180]. For each molecule three Hansen parameters were calculated: the energy from dispersion forces between molecules (δ_d); the energy from dipolar intermolecular force between molecules (δ_p); and the energy from hydrogen bonds between molecules (δ_h), as follows:

Equation I.1. $\delta_d = \frac{\sum F_{di}}{V}$

Equation I.2. $\delta_p = \frac{\sqrt{\sum F_{pi}^2}}{V}$

Equation I.3. $\delta_h = \sqrt{\frac{\sum E_{hi}^2}{V}}$

where F_{di}, F_{pi}, and E_{hi} are the group contributions for different components (dispersion forces, polar interactions, and hydrogen bonding, respectively) of structural groups that are reported in the literature at 25°C [180] and V the molar volume.

The total solubility parameter (δ_t), generally measured in $MPa^{0.5}$, was then determined through the combination of solubility parameters.

Equation I.4. $\delta_{total} = \sqrt{{\delta_d}^2 + {\delta_p}^2 + {\delta_h}^2}$

Details of the calculation of solubility parameters for each polymer and ETR drug are presented in the following tables. To determine the solubility parameters for SLP, which is composed of polyvinyl caprolactam: polyvinyl acetate: polyethylene glycol at a ratio of 57:30:13, the average number of the three monomers was calculated.

Table I.1. Details of the calculation of solubility parameters for ETR.

Compound		ETR		
Structural group	Frequency	F_d $(MJ/m^3)^{0.5}.mol^{-1}$	F_p $(MJ/m^3)^{0.5}.mol^{-1}$	E_h J/mol
CN-	2	860	2200	5000
Phenylene (p)	2	2540	220	0
CH_3-	2	840	0	0
-O-	1	100	400	3000
NH_2-	1	280	0	8400
-NH-	1	160	210	3100
Br-	1	550	0	0
=N-	2	760	200	500
=C<	4	280	0	0
Ring	1	190	0	0
TOTAL		**6560**	**3230**	**20000**
			Solubility parameters δ	-
			δ_d $(MPa^{0.5})$	23.79
			δ_p $(MPa^{0.5})$	11.72
			δ_h $(MPa^{0.5})$	8.52
			δ_t $(MPa^{0.5})$	**27.86**

Table I.2. Details of the calculation of solubility parameters for PEG.

Compound		PEG		
Structural group	Frequency	F_d $(MJ/m^3)^{0.5}.mol^{-1}$	F_p $(MJ/m^3)^{0.5}.mol^{-1}$	E_h J/mol
-O-	1	100	400	3000
$-CH_2$-	2	540	0	0
TOTAL		**640**	**400**	**3000**
			Solubility parameters δ	-
			δ_d $(MPa^{0.5})$	16.41
			δ_p $(MPa^{0.5})$	10.26
			δ_h $(MPa^{0.5})$	8.77
			δ_t $(MPa^{0.5})$	**21.25**

Table I.3. Details of the calculation of solubility parameters for PVP.

Compound		PVP		
Structural group	Frequency	F_d $(MJ/m^3)^{0.5}.mol^{-1}$	F_p $(MJ/m^3)^{0.5}.mol^{-1}$	E_h J/mol
-N<	1	20	800	5000
>C=O	1	290	770	2000
-CH<	1	80	0	0
$-CH_2-$	4	1080	0	0
-CH=	0	0	0	0
$=CH_2$	0	0	0	0
Ring	1	190	0	0
TOTAL		**1660**	**1570**	**7000**
			Solubility parameters δ	**-**
			δ_d $(MPa^{0.5})$	18.67
			δ_p $(MPa^{0.5})$	17.66
			δ_h $(MPa^{0.5})$	8.87
			δ_t $(MPa^{0.5})$	**27.19**

Table I.4. Details of the calculation of solubility parameters for PVPVA.

Compound		PVPVA		
Structural group	Frequency	F_d $(MJ/m^3)^{0.5}.mol^{-1}$	F_p $(MJ/m^3)^{0.5}.mol^{-1}$	E_h J/mol
-N<	1	20	800	5000
>C=O	1	290	770	2000
-CH<	2	160	0	0
$-CH_2-$	5	1350	0	0
-COO-	1	390	490	7000
$-CH_3$	1	420	0	0
Ring	1	190	0	0
TOTAL		**2820**	**2060**	**14000**
			Solubility parameters δ	**-**
			δ_d $(MPa^{0.5})$	18.84
			δ_p $(MPa^{0.5})$	13.76
			δ_h $(MPa^{0.5})$	9.67
			δ_t $(MPa^{0.5})$	**25.26**

Table I.5. Details of the calculation of solubility parameters for SLP.

Compound		SLP (57:30:13 of PVC, PVA, and PEG)		
Structural group	Frequency	F_d	F_p	E_h
N-Vinylcaprolactam		$(MJ/m^3)^{0.5}.mol^{-1}$	$(MJ/m^3)^{0.5}.mol^{-1}$	J/mol
-N<	1	20	800	5000
>C=O	1	290	770	2000
-CH<	1	80	0	0
$-CH_2-$	6	1620	0	0
Ring	1	190	0	0
TOTAL		**2200**	**1570**	**7000**
			Solubility parameters δ	-
			δ_d $(MPa^{0.5})$	16.59
			δ_p $(MPa^{0.5})$	11.84
			δ_h $(MPa^{0.5})$	7.27
			δ_t $(MPa^{0.5})$	**21.64**
Structural group	Frequency	F_d	F_p	E_h
N-vinyl acetate		$(MJ/m^3)^{0.5}.mol^{-1}$	$(MJ/m^3)^{0.5}.mol^{-1}$	J/mol
-COO-	1	390	490	7000
$-CH_3$	1	420	0	0
-CH<	1	80	0	0
$-CH_2-$	1	270	0	0
TOTAL		**1160**	**490**	**7000**
			Solubility parameters δ	-
			δ_d $(MPa^{0.5})$	15.85
			δ_p $(MPa^{0.5})$	6.69
			δ_h $(MPa^{0.5})$	9.78
			δ_t $(MPa^{0.5})$	**19.79**
Structural group	Frequency	F_d	F_p	E_h
Polyethylene glycol		$(MJ/m^3)^{0.5}.mol^{-1}$	$(MJ/m^3)^{0.5}.mol^{-1}$	J/mol
-O-	1	100	400	3000
$-CH_2-$	2	540	0	0
TOTAL		**640**	**400**	**3000**
			Solubility parameters δ	-
			δ_d $(MPa^{0.5})$	16.41
			δ_p $(MPa^{0.5})$	10.26
			δ_h $(MPa^{0.5})$	8.77
			δ_t $(MPa^{0.5})$	**21.25**
Structural group	Frequency	δ_t $(MPa^{0.5})$		
Overall result SLP				
PVC	57	21.64		
PVA	30	19.79		
PEG	13	21.25		
TOTAL		**21.03**		

Table I.6. Details of the calculation of solubility parameters for HPMC.

Compound		HPMC		
Structural group	Frequency	F_d $(MJ/m^3)^{0.5}.mol^{-1}$	F_p $(MJ/m^3)^{0.5}.mol^{-1}$	E_h J/mol
-OH	4	840	2000	80000
-O-	12	1200	4800	36000
-CH<	16	1280	0	0
$-CH_2-$	7	1890	0	0
$-CH_3$	7	2940	0	0
Ring	3	570	0	0
TOTAL		**8720**	**6800**	**116000**
			Solubility parameters δ	**-**
			δ_d $(MPa^{0.5})$	17.77
			δ_p $(MPa^{0.5})$	13.85
			δ_h $(MPa^{0.5})$	15.37
			δ_t $(MPa^{0.5})$	**27.28**

Table I.7. Details of the calculation of solubility parameters for HPMCAS.

Compound		HPMCAS		
Structural group	Frequency	F_d $(MJ/m^3)^{0.5}.mol^{-1}$	F_p $(MJ/m^3)^{0.5}.mol^{-1}$	E_h J/mol
-OH	3	630	1500	60000
-O-	10	1000	4000	30000
-CH<	15	1200	0	0
$-CH_2-$	9	2430	0	0
$-CH_3$	8	3360	0	0
Ring	2	380	0	0
-COOH	1	530	0	0
-COO-	2	780	980	14000
TOTAL		**10310**	**6480**	**104000**
			Solubility parameters δ	**-**
			δ_d $(MPa^{0.5})$	17.55
			δ_p $(MPa^{0.5})$	11.03
			δ_h $(MPa^{0.5})$	13.31
			δ_t $(MPa^{0.5})$	**24.63**

For a system without specific interactions, the χ (Flory-Huggins drug-polymer interaction parameter) may be determined from the solubility parameters of those two components. The interaction parameter characterizes the energy change due to the mixing of one molecule and thus shows the degree of interaction between the molecule and polymer. Thus, it is a parameter dependent on temperature and on the local composition [317]. The relationship between χ and the solubility parameter is given by the following equation [180]:

Equation I.5. $\chi = \frac{V_{site}}{RT}(\delta_{drug} - \delta_{polymer})^2$

where V_{site} is the hypothetical lattice volume, R is the gas constant, T is the absolute temperature, and δ are the solubility parameters of the drug and the polymer, respectively. The molar volume of small molecule drug was chosen as the hypothetical lattice volume, V_{site}, for subsequent calculations [26, 211, 317]. From the equation, it can be concluded that the interaction parameter will approach zero if the solubility parameter of the drug and the polymer are similar. A small value of χ leads to a small magnitude of enthalpy of mixing and a more negative free energy, favoring the mixing [31].

Details of the calculation of χ for each binary composition is portrayed in the following table.

Table I.8. Details of the calculation of Flory-Huggins drug-polymer interaction parameter χ.

Compound	Solubility Parameter δ (acc. to van Krevelen and Hoftyzer)	$\Delta\delta = \delta_{ETR} - \delta_{POL}$	Constants for Equation I.5	Interaction parameter χ
ETR	27.86	-	-	-
PEG	21.25	6.61	V_{site}[a] = 275.7 cm^3 R = 8.31 J·mol^{-1}·K^{-1} T = 298.15 K	4.861
PVP	27.19	0.67		0.049
PVPVA	25.26	2.60		0.752
SLP	21.03	6.82		5.181
HPMC	27.28	0.58		0.037
HPMCAS	24.63	3.22		1.155

δ_{ETR}, solubility parameter of ETR; δ_{POL}, solubility parameter of polymer; $\Delta\delta$, solubility parameter difference between ETR and polymers.

[a]The molar volume of small molecule drug was chosen as the hypothetical lattice volume (V_{site}).

B. High-throughput screening – Physical stability evaluation

Table I.9. Physical stability as evaluated by PLM for 2 months, under exposure to room temperature, desiccator, and 25°C / 60% RH. Crystalline structures were qualitatively evaluated in terms of size and quantity (on a scale from 1 to 5, where 1 is no birefringence and 5 a high number of large crystalline structures). Evaluation of some samples was stopped earlier (before the 2 months of study) due to high crystallization. The plasticizing capacity of the films is also referred (cracks).

System	Desiccator	Room Temperature	Climatic chamber 25°C / 60% RH
ETR Control	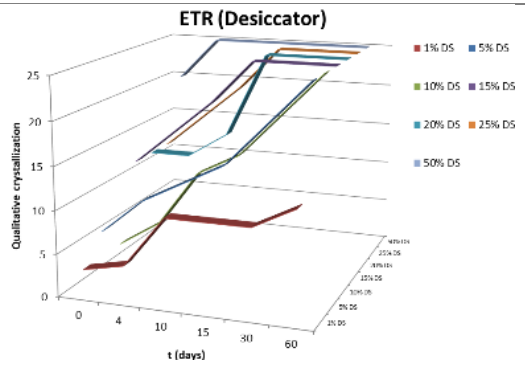	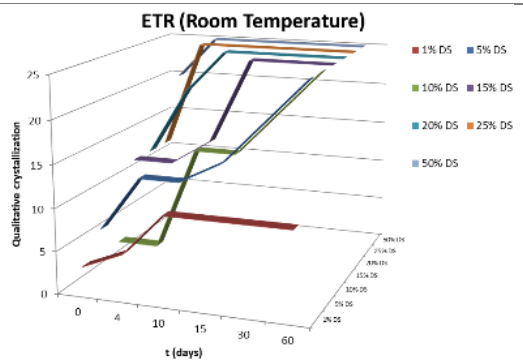	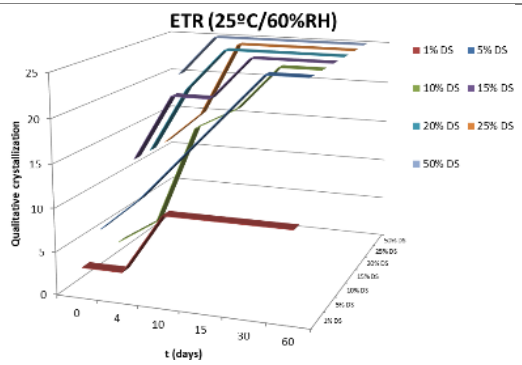

System	Desiccator	Room Temperature	Climatic chamber 25°C / 60% RH
PEG Negative control	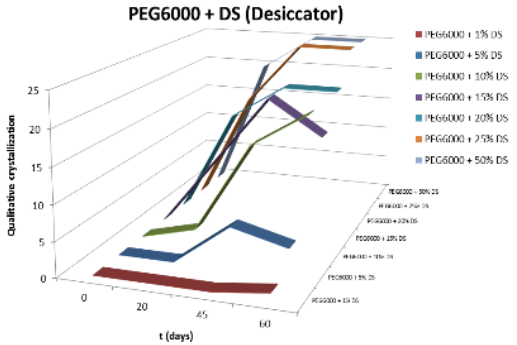	Not performed	Not performed
SLP	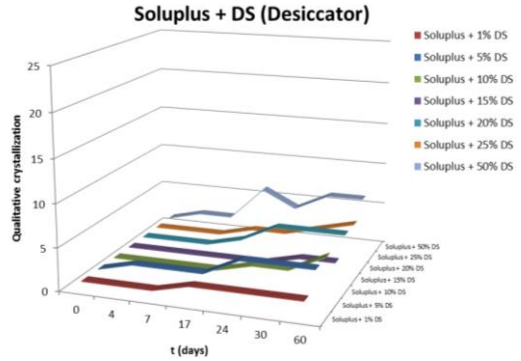	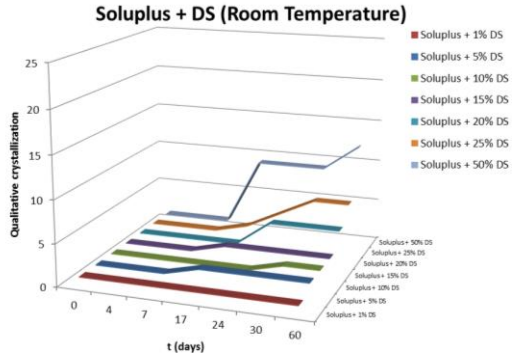	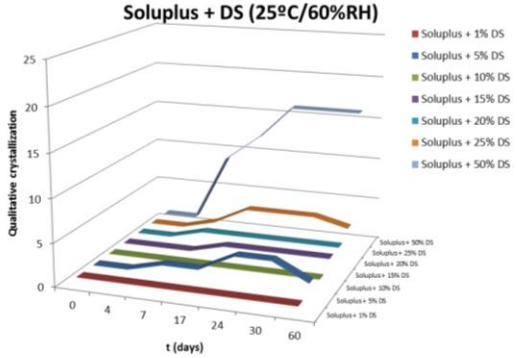

System	Desiccator	Room Temperature	Climatic chamber 25°C / 60% RH
PVPVA [a]	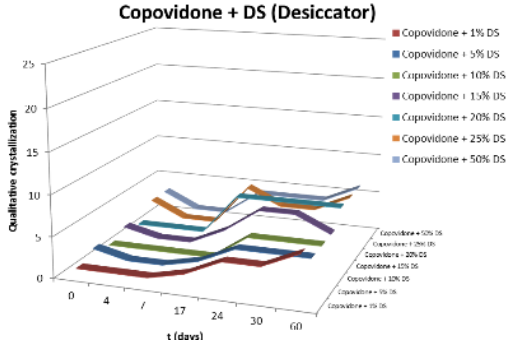	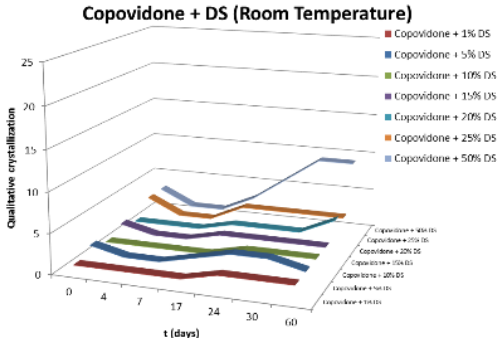	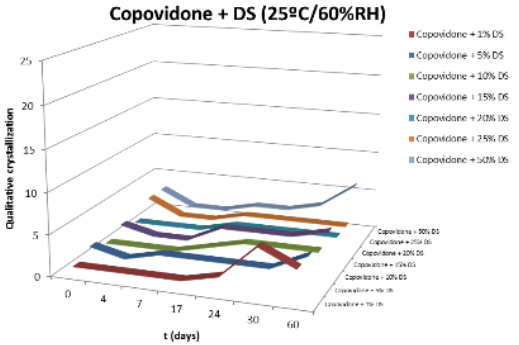
PVP [a]	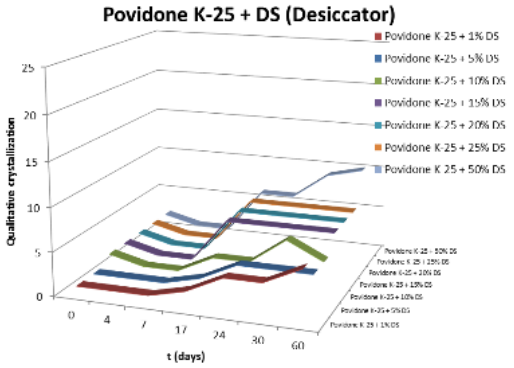	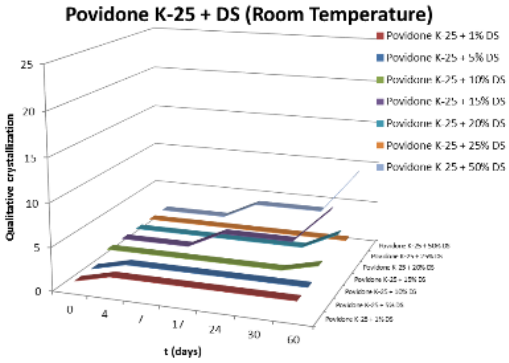	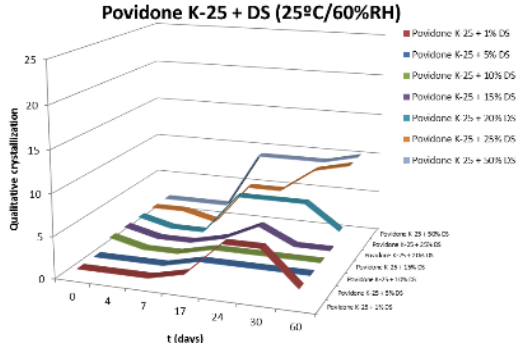

System	Desiccator	Room Temperature	Climatic chamber 25°C / 60% RH
HPMC	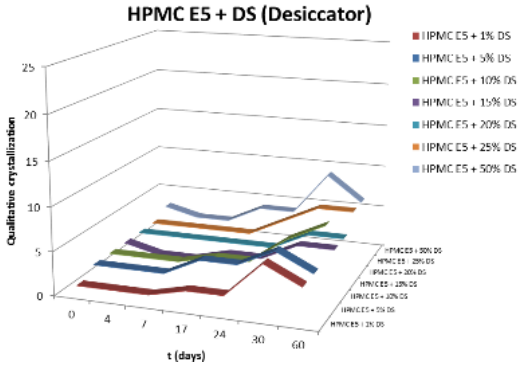	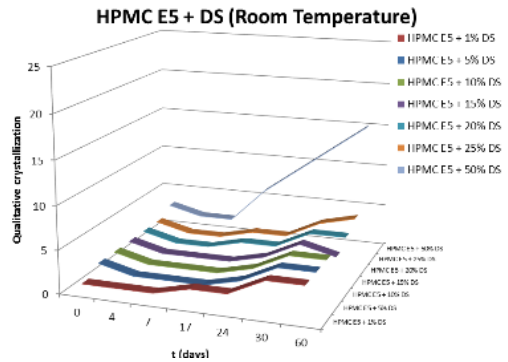	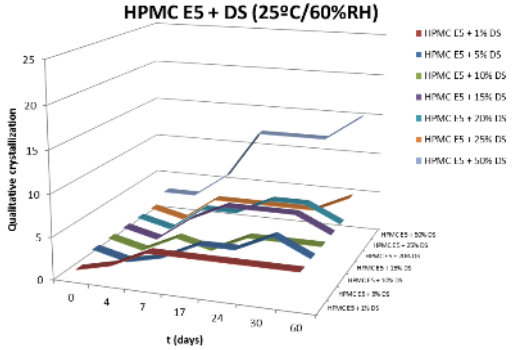
HPMCAS	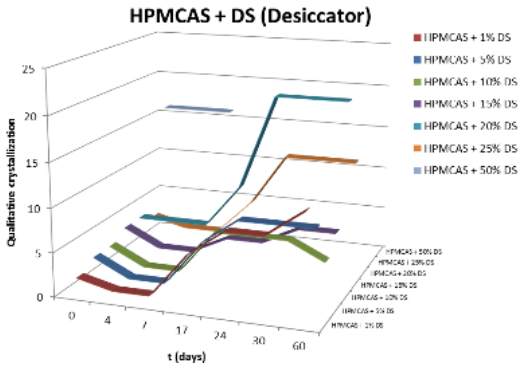	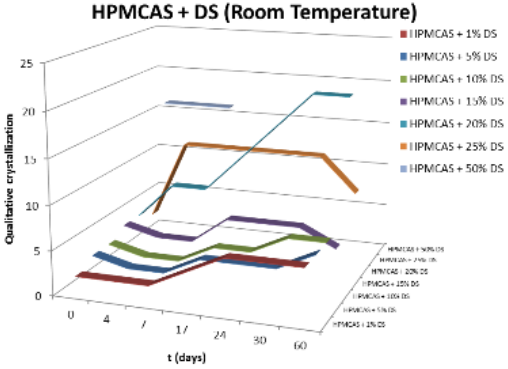	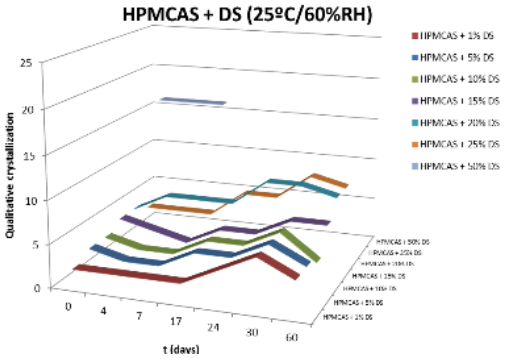

[a] Cracking of these films was noticed when 50% of drug was used, owing to the growth of crystal nuclei.

C. Forced degradation study

A forced degradation study was performed prior to HME tests, to gain insights into the causes of degradation and pathways of ETR drug. To evaluate the effect of dry heat, the powder was exposed to 200°C for 17 hours. For HPLC analysis, a solution of 0.25 mg/mL of ETR was then prepared. The following figures display the reference HPLC chromatogram of thermal degradation under the conditions referred (Figure I.1), and the chromatogram of the standard of impurity 1 injection (Figure I.2). The formation of impurity 1 was identified by comparing the retention time by HPLC with the reference standard, as well as by the analysis of the UV spectrum of the peak (Figure I.3).

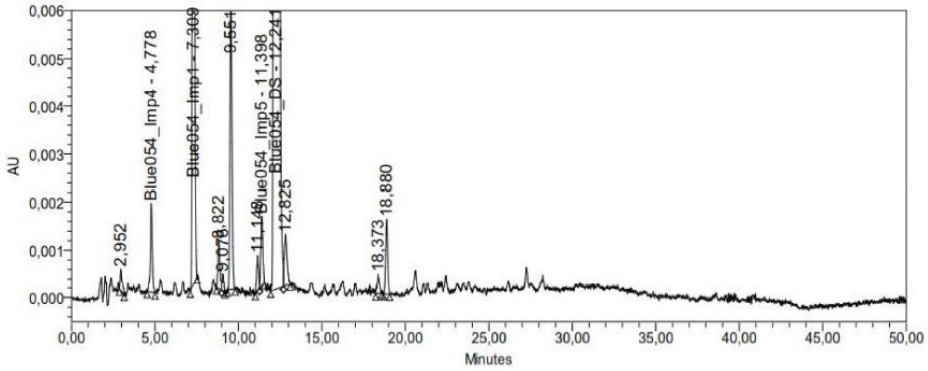

Figure I.1. HPLC chromatogram of etravirine after thermal degradation at 200°C for 17 hours.

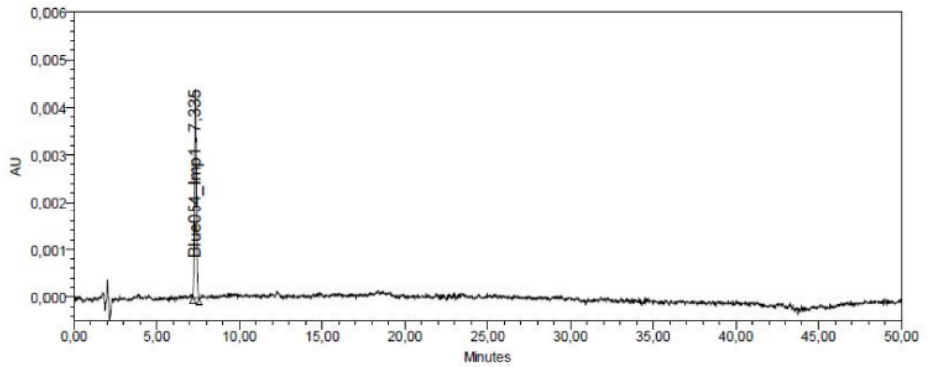

Figure I.2. HPLC chromatogram of the standard of etravirine impurity 1.

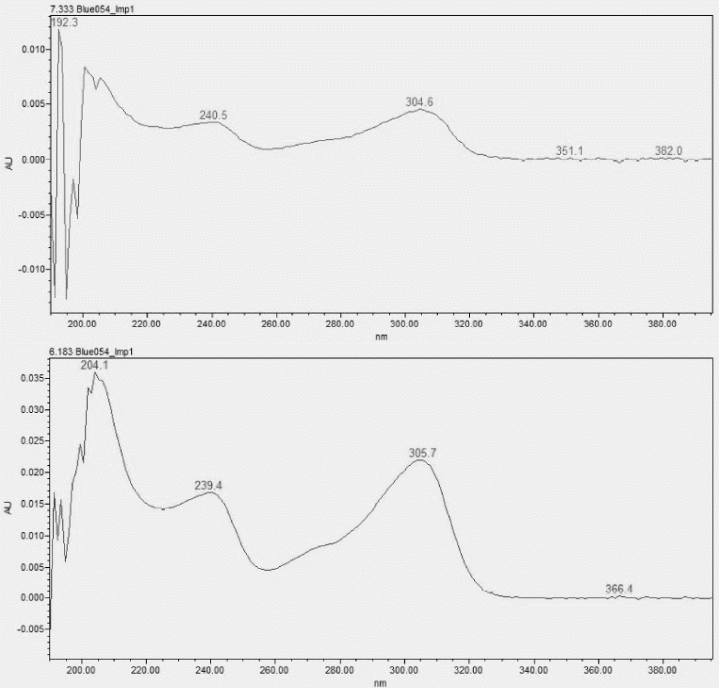

Figure I.3. UV spectra of: up, etravirine impurity 1 standard solution at 0.2%; down, etravirine impurity 1 after forced degradation with dry heat at 200°C for 17h. Peak purity angle is 0.509, and the threshold 0.636. The peak is considered non-impure since peak angle is lower than the threshold, which means that UV spectrum is the same at all point across the peak and no co-elution is observed.

APPENDIX II: IBRUTINIB

A. High-throughput screening – Physical stability evaluation

Additional details on the HTS test are provided below.

Table II.1. General scheme of polymers screening test.

Conc. DS	Test 1	Test 2	Test 3	Test 4	Test 5
	10% DS	20% DS	30% DS	40% DS	50% DS
Polymer	(90% Polymer)	(80% Polymer)	(70% Polymer)	(60% Polymer)	(50% Polymer)
A DS (control)	Sample A1	Sample A2	Sample A3	Sample A4	Sample A5
B PEG6000 (control)	Sample B1	Sample B2	Sample B3	Sample B4	Sample B5
C SLP	Sample C1	Sample C2	Sample C3	Sample C4	Sample C5
D PVPVA	Sample D1	Sample D2	Sample D3	Sample D4	Sample D5
E SLP 65% + HPMCAS 5%	-	-	Sample E3	-	-
F SLP 60% + HPMCAS 10%	-	-	Sample F3	-	-
G SLP 50% + HPMCAS 20%	-	-	Sample G3	-	-
H PVP	Sample H1	Sample H2	Sample H3	Sample H4	Sample H5
I HPMC	Sample I1	Sample I2	Sample I3	Sample I4	Sample I5

The physical evaluation of the binary systems over time by PLM is portrayed below.

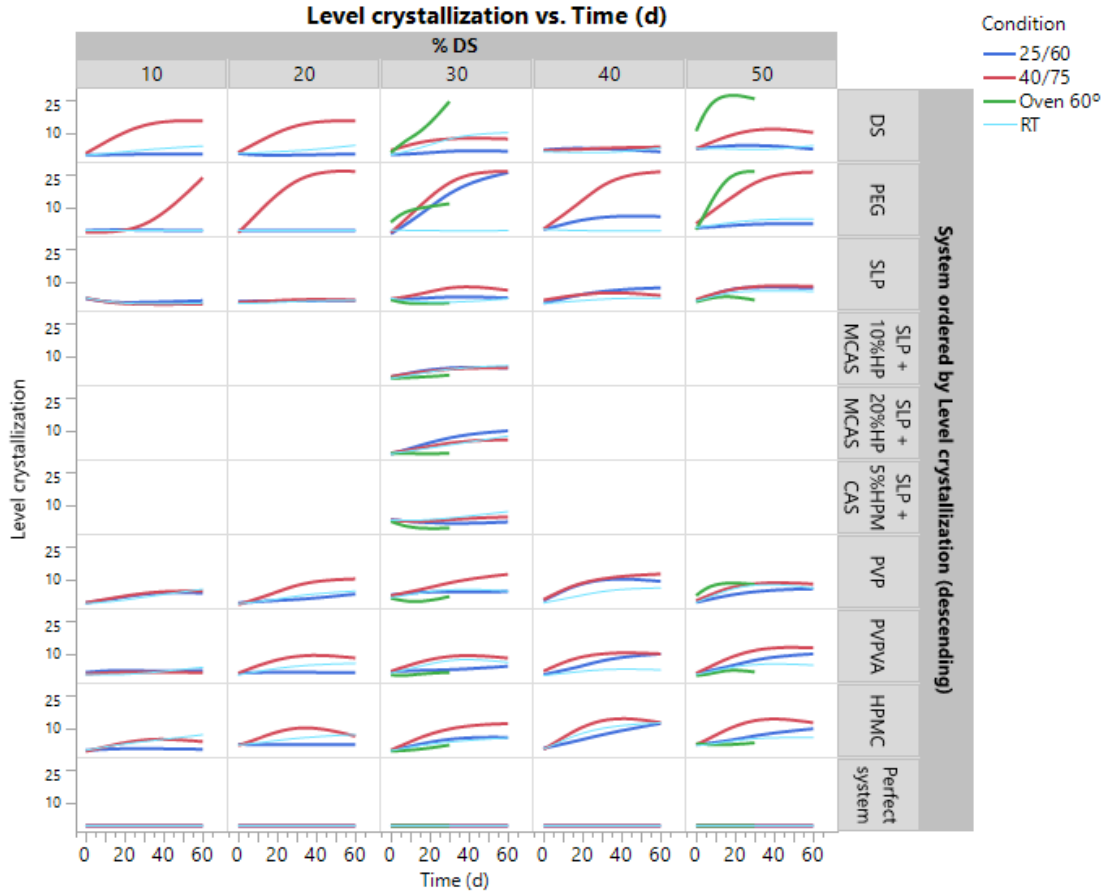

Figure II.1. Physical stability as evaluated by PLM for 2 months, over exposure to 60°C, room temperature, 40°C / 75% RH and 25°C / 60% RH. Crystalline structures were qualitatively evaluated in terms of size and quantity (on a scale from 1 to 5). Evaluation of some samples was stopped earlier (before the 2 months of study) due to high crystallization.

The Raman spectroscopy was used as a validation of PLM observations, to avoid misclassifications. Spectra were classified in crystalline (C), amorphous (A) or partially amorphous (A/C). A typical result from Raman spectroscopy is depicted below, where the amorphous and crystalline IBR spectra are portrayed, as well as a binary system after production and at the end of the stability study. The highlighted areas were used to classify the solid state of IBR in the systems.

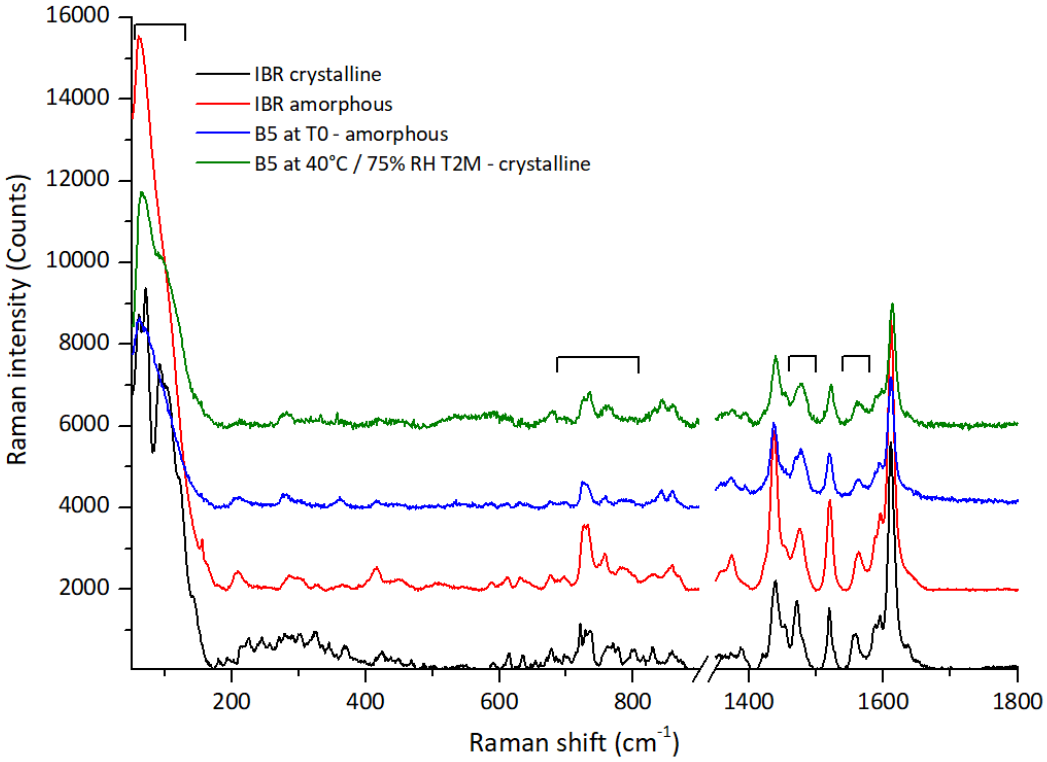

Figure II.2. Example of Raman spectra of amorphous and crystalline form of plain drug, and samples from screening (B5). The spectra were recorded in the 50-1800 cm^{-1} wavenumber range, during 5 to 60 seconds with 5 to 10 accumulations, and excitation at 633 nm. The highlighted areas correspond to changes used to characterize the drug as amorphous or crystalline: the lattice vibration zone (50 - 150 cm^{-1}), the zone between 700 and 800 cm^{-1}, and the shift of 1471 and 1557 cm^{-1} bands to 1476 and to 1564 cm^{-1}.

B. HTS test: PCA analysis per system

To conclude on the effect of individual factors such as temperature, humidity, drug load and time on crystallization, an additional multivariate statistical analysis was performed. Each polymeric composition was assessed through PCA, in order to identify what would be the underlying cause of crystallization and, ultimately, what should we avoid in order to have a stable product. This may be observed by the loading plots depicting the variables (level of crystallization, time, temperature, humidity, and drug load) and the components (1 and 2) (Figure II.3). The closer the value is to 1, the greater the effect of the component on the variable. Depending on the system, three or four principal components were generated with statistical significance ($p < 0.0001$, Bartlett Test), but only two principal components are considered to simplify. They represent and explain the majority of the results variability, around 75% for IBR (control), PEG (control), PVP, PVPVA, HPMC, and SLP systems, and 93% for SLP/HPMCAS systems (Table II.2).

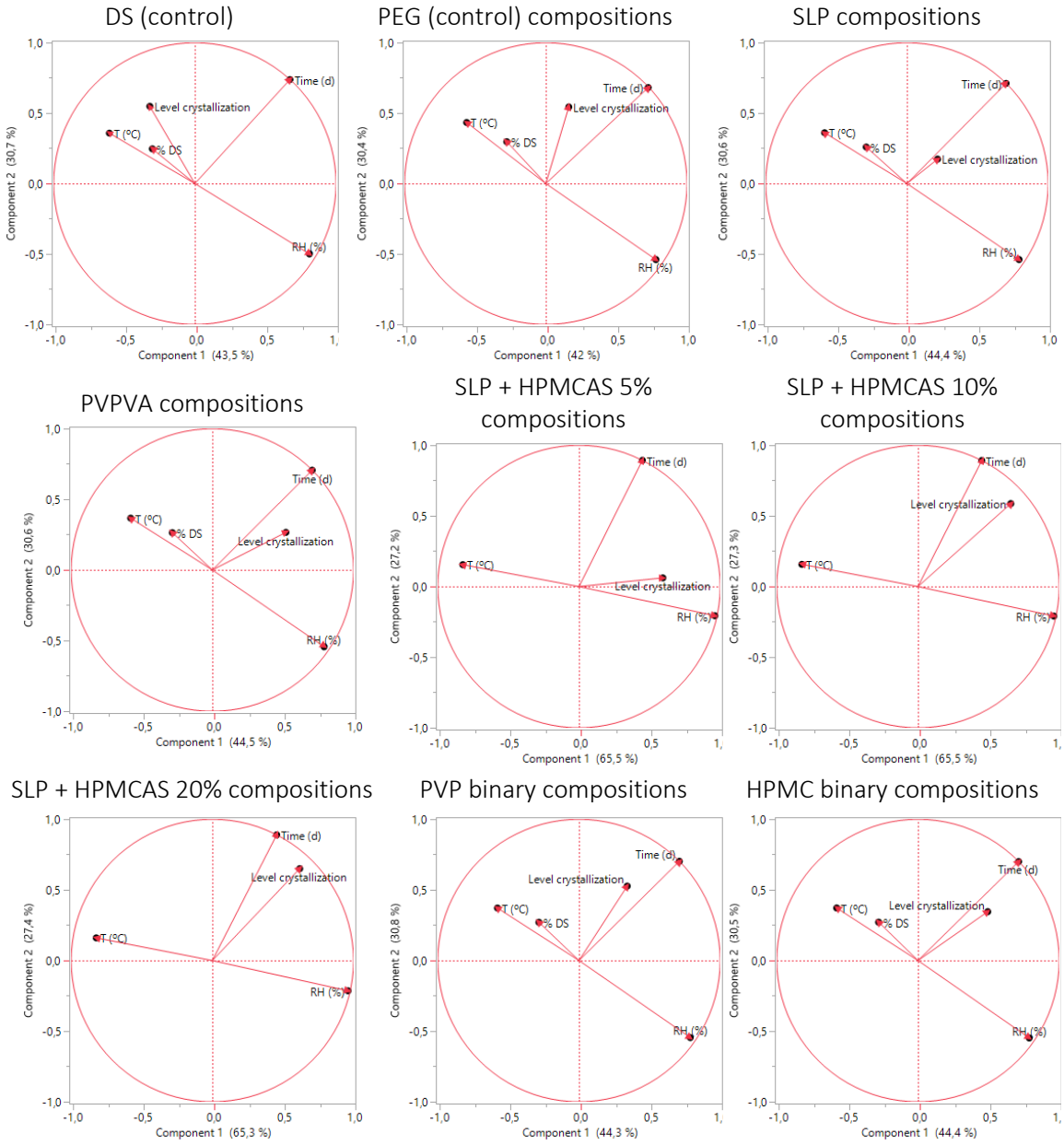

Figure II.3. JMP® 14.0-assisted PCA performed for each system to assess the impact of individual factors as time, temperature, moisture, and drug load in the level of crystallization. Loading plots are depicted, a matrix of two-dimensional representations of factor loadings for the components 1 and 2. The closer the value is to 1, the greater the effect of the component on the variable. Two principal components with statistical significance ($p < 0.0001$, Bartlett Test) are depicted, which explain between approximately 75 and 95% of the results variability.

Table II.2. Eigenvalues table with results of the Bartlett test.

Condition	Component	Eigenvalue	Percent (%)	Cumulative Percent (%)	Prob > ChiSq
DS (control)	1	532.9	43.5	74.2	< 0.0001
	2	376.2	30.7		< 0.0001
PEG (control)	1	531.0	42.0	72.4	< 0.0001
	2	384.3	30.4		< 0.0001
SLP	1	529.7	44.4	75.0	< 0.0001
	2	365.4	30.6		< 0.0001
PVPVA	1	532.1	44.5	75.1	< 0.0001
	2	366.0	30.6		< 0.0001
SLP + HPMCAS 5%	1	880.4	65.5	92.7	< 0.0001
	2	366.6	92.7		< 0.0001
SLP + HPMCAS 10%	1	879.9	65.5	92.8	< 0.0001
	2	365.2	92.6		< 0.0001
SLP + HPMCAS 20%	1	882.5	65.3	92.7	< 0.0001
	2	369.5	27.4		< 0.0001
PVP	1	531.0	44.3	74.8	< 0.0001
	2	368.7	30.8		< 0.0001
HPMC	1	533.2	44.4	74.9	< 0.0001
	2	367.1	30.5		< 0.0001

After comparing the plots obtained for binary/ternary systems to the IBR (drug control), it is seen that it has a different behavior from the other samples, as the position of the vectors is completely different. This is caused by the effect of temperature and/or drug load on the level of crystallization of IBR. From the loading plots, one may conclude that the crystallization of both controls (IBR drug and PEG system) is mainly commanded by humidity and time. For the other binary systems (PVP, HPMC, SLP and PVPVA compositions), the behavior is similar and the main factor leading to crystallization is humidity, followed by time and temperature, to a lesser extent. When the stabilizer is added to SLP, the composition behavior is also changed. Although the effect of drug load has not been studied in these compositions, humidity and temperature seem to be especially important to promote drug crystallization. In summary, there are two very important lessons from this study: humidity is the most important factor that triggers IBR crystallization and, surprisingly, drug load seems not to be relevant for the physical stability of an ASD of IBR.

APPENDIX III: HIGHLY SOLUBLE DRUG

A. Mathematic modeling of dissolution profiles

Several kinetic models were fitted to the dissolution data by JMP® 14.0 from SAS Institute, Inc. Using the non-linear modeling platform, a least-squares loss function to fit the models is run, minimizing the sum of the loss function across the observations. The best model was selected by analyzing the SSE and the RMSE.

The results obtained for the target profile are summarized below. The Weibull function led to the best fitting, with an SSE of 1578.4 and an RMSE of 4.9.

Table III.1. Results of modeling of target dissolution data using the non-linear platform of JMP® 14.0 from SAS Institute, Inc. Eight mathematical models were tested.

Kinetic models	SSE	DFE	MSE	RMSE
Zero-order	16447.88	67	245.49	15.67
First-order	6494.02	67	96.93	9.85
Higuchi	12463.59	68	183.29	13.54
Hixson-Crowell	26785.02	67	399.78	19.99
Korsmeyer-Peppas	10326.38	67	154.13	12.41
Weibull	1578.39	66	23.91	4.89
Hopfenberg	5870.05	68	86.32	9.29
Gompertz	1800.58	57	31.59	5.62

Abbreviations: SSE, sum of squared errors; DFE, degrees of freedom for error; MSE, mean squared error; RMSE, root mean squared error.

The same procedure was applied for the prototype formulation dissolution data, to better understand the mechanistic drug release behavior and determine its kinetics. As described below, the Weibull function led again to the best fitting, with an SSE of 1341.7 and an RMSE of 5.1.

Table III.2. Results of modeling of prototype dissolution data using the non-linear platform of JMP® 14.0 from SAS Institute, Inc. Eight mathematical models were tested.

Kinetic models	SSE	DFE	MSE	RMSE
Zero-order	9797.63	52	188.42	13.73
First-order	2300.33	52	44.24	6.65
Higuchi	4731.78	53	89.28	9.45
Hixson-Crowell	Lack of fit – cannot decrease the objective function (SSE).			
Korsmeyer-Peppas	4368.05	52	84.00	9.17
Weibull	1341.70	51	26.31	5.13
Hopfenberg	1875.72	53	35.39	5.95
Gompertz	23294.00	46	506.39	22.50

Abbreviations: SSE, sum of squared errors; DFE, degrees of freedom for error; MSE, mean squared error; RMSE, root mean squared error.

B. Dataset for the screening of technologies

Table III.3. Formulation tests performed under the scope of the screening of technologies phase.

Co-de	Drug load	Lacto-se	MCC	Eud RL	Eud RS	HP MC	HPMC phase	PV Ac	PVO H	Stearic acid	Pro-cess	Hardness (N)
A	0.08888	0.11022	0.4509	0	0.3	0	no	0	0	0.04	DC	69
B	0.08888	0.11022	0.4509	0.3	0	0	no	0	0	0.04	MUPS	64
C	0.08888	0.3709	0.09022	0.3	0	0.1	in	0	0	0.04	BiTAB	77
D	0.08888	0.3709	0.09022	0	0.3	0.1	out	0	0	0.04	MUPS	62
E	0.08888	0.4509	0.11022	0	0.3	0	no	0	0	0.04	DC	70
F	0.08888	0.09022	0.3709	0.3	0	0.1	out	0	0	0.04	DC	73
G	0.08888	0.3709	0.09022	0	0	0.1	out	0.15	0.15	0.04	MUPS	63
H	0.08888	0.11022	0.4509	0	0	0	no	0.15	0.15	0.04	BiTAB	73
I	0.08888	0.11022	0.4509	0	0	0	no	0.15	0.15	0.04	MUPS	67
J	0.08888	0.4509	0.11022	0	0	0	no	0.15	0.15	0.04	DC	78
K	0.08888	0.09022	0.3709	0	0	0.1	out	0.15	0.15	0.04	DC	73
L	0.08888	0.09022	0.3709	0	0	0.1	in	0.15	0.15	0.04	BiTAB	71
M	0.08888	0.09022	0.3709	0	0	0.1	in	0.15	0.15	0.04	BiTAB	111
N	0.17776	0	0	0	0	0.2	in	0.3	0.3	0.08	BiTAB	75
O	0.17776	0	0	0	0	0.2	in	0.3	0.3	0.08	BiTAB	118
P	0.08888	0.2909	7.022	0	0	0.2	in/out	0.15	0.15	0.04	MUPS	66
Q	0.17776	0.03929	0.16071	0	0	0	no	0.3	0.3	0.08	BiTAB	84
R	0.17776	0.03929	0.16071	0	0	0	no	0.3	0.3	0.08	BiTAB	121
S	0.17776	0.03929	0.16071	0	0	0.2	out	0.3	0.3	0.08	DC	103

Abbreviations: MCC, Microcrystalline cellulose; Eud, Eudragit®; HPMC, hypromellose; PVAc, Polyvinyl Acetate; PVOH, Polyvinyl Alcohol

C. Chromatograms from assay and degradation products UPLC analysis

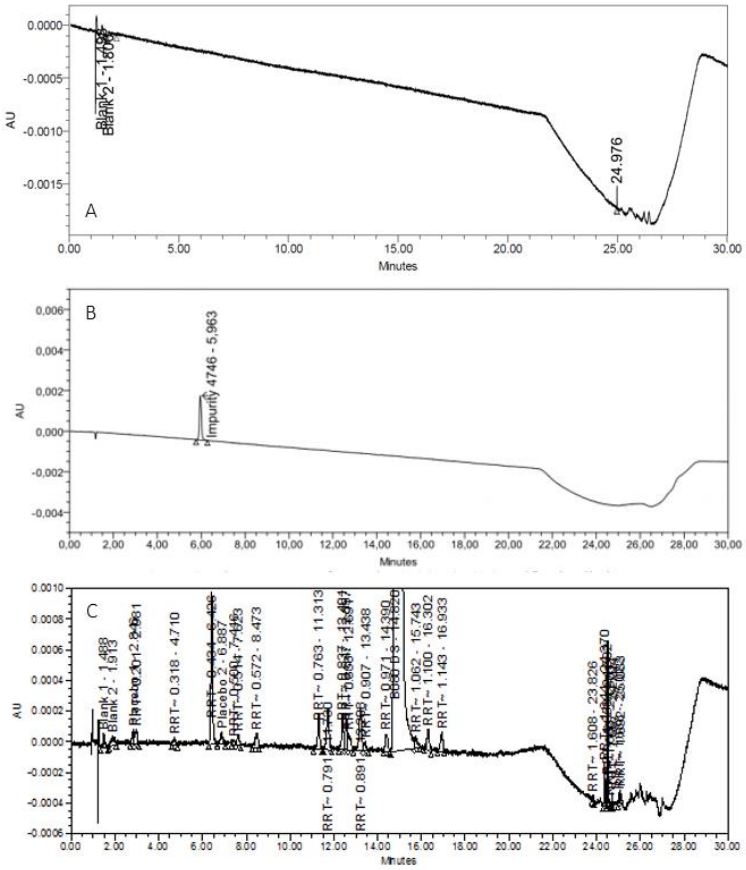

Figure III.1. Chromatograms of UPLC analysis of assay and degradation products of the prototype composition: A, blank; B, known degradation product; C, prototype.

REFERENCES

1. Wilson M, Williams MA, Jones DS, Andrews GP. Hot-melt extrusion technology and pharmaceutical application. Ther Deliv. 2012;3(6):787-97. DOI: 10.4155/tde.12.26

2. Maniruzzaman M, Boateng JS, Snowden MJ, Douroumis D. A review of hot-melt extrusion: process technology to pharmaceutical products. ISRN Pharm. 2012;2012:436763. DOI: 10.5402/2012/436763

3. Malaquias LFB, Sa-Barreto LCL, Freire DO, Silva ICR, Karan K, Durig T, et al. Taste masking and rheology improvement of drug complexed with beta-cyclodextrin and hydroxypropyl-beta-cyclodextrin by hot-melt extrusion. Carbohydr Polym. 2018;185:19-26. DOI: 10.1016/j.carbpol.2018.01.011

4. Tan DCT, Ong JJ, Gokhale R, Heng PWS. Hot melt extrusion of ion-exchange resin for taste masking. Int J Pharm. 2018;547(1-2):385-94. DOI: 10.1016/j.ijpharm.2018.05.068

5. Keating AV, Soto J, Tuleu C, Forbes C, Zhao M, Craig DQM. Solid state characterisation and taste masking efficiency evaluation of polymer based extrudates of isoniazid for paediatric administration. Int J Pharm. 2018;536(2):536-46. DOI: 10.1016/j.ijpharm.2017.07.008

6. McFall H, Sarabu S, Shankar V, Bandari S, Murthy SN, Kolter K, et al. Formulation of aripiprazole-loaded pH-modulated solid dispersions via hot-melt extrusion technology: In vitro and in vivo studies. Int J Pharm. 2019;554:302-11. DOI: 10.1016/j.ijpharm.2018.11.005

7. Vasoya JM, Desai HH, Gumaste SG, Tillotson J, Kelemen D, Dalrymple DM, et al. Development of Solid Dispersion by Hot Melt Extrusion Using Mixtures of Polyoxylglycerides With Polymers as Carriers for Increasing Dissolution Rate of a Poorly Soluble Drug Model. J Pharm Sci. 2019;108(2):888-96. DOI: 10.1016/j.xphs.2018.09.019

8. Zhao Y, Xie X, Zhao Y, Gao Y, Cai C, Zhang Q, et al. Effect of plasticizers on manufacturing ritonavir/copovidone solid dispersions via hot-melt extrusion: Preformulation, physicochemical characterization, and pharmacokinetics in rats. Eur J Pharm Sci. 2019;127:60-70. DOI: 10.1016/j.ejps.2018.10.020

9. Schittny A, Ogawa H, Huwyler J, Puchkov M. A combined mathematical model linking the formation of amorphous solid dispersions with hot-melt-extrusion process parameters. Eur J Pharm Biopharm. 2018;132:127-45. DOI: 10.1016/j.ejpb.2018.09.011

10. Xi L, Song H, Wang Y, Gao H, Fu Q. Lacidipine Amorphous Solid Dispersion Based on Hot Melt Extrusion: Good Miscibility, Enhanced Dissolution, and Favorable Stability. AAPS PharmSciTech. 2018;19(7):3076-84. DOI: 10.1208/s12249-018-1134-9

11. Zhu Y, Shah NH, Malick AW, Infeld MH, McGinity JW. Controlled release of a poorly water-soluble drug from hot-melt extrudates containing acrylic polymers. Drug Dev Ind Pharm. 2006;32(5):569-83. DOI: 10.1080/03639040500528996

12. Vo AQ, Feng X, Morott JT, Pimparade MB, Tiwari RV, Zhang F, et al. A novel floating controlled release drug delivery system prepared by hot-melt extrusion. Eur J Pharm Biopharm. 2016;98:108-21. DOI: 10.1016/j.ejpb.2015.11.015

13. Fukuda M, Peppas NA, McGinity JW. Floating hot-melt extruded tablets for gastroretentive controlled drug release system. J Control Release. 2006;115(2):121-9. DOI: 10.1016/j.jconrel.2006.07.018

14. Sawant KP, Fule R, Maniruzzaman M, Amin PD. Extended release delivery system of metoprolol succinate using hot-melt extrusion: effect of release modifier on methacrylic acid copolymer. Drug Deliv Transl Res. 2018;8(6):1679-93. DOI: 10.1007/s13346-018-0545-1

15. Quintavalle U, Voinovich D, Perissutti B, Serdoz F, Grassi G, Dal Col A, et al. Preparation of sustained release co-extrudates by hot-melt extrusion and mathematical modelling of in vitro/in vivo drug release profiles. Eur J Pharm Sci. 2008;33(3):282-93. DOI: 10.1016/j.ejps.2007.12.008

16. Lu J, Obara S, Liu F, Fu W, Zhang W, Kikuchi S. Melt Extrusion for a High Melting Point Compound with Improved Solubility and Sustained Release. AAPS PharmSciTech. 2018;19(1):358-70. DOI: 10.1208/s12249-017-0846-6

17. Yang R, Wang Y, Zheng X, Meng J, Tang X, Zhang X. Preparation and evaluation of ketoprofen hot-melt extruded enteric and sustained-release tablets. Drug Dev Ind Pharm. 2008;34(1):83-9. DOI: 10.1080/03639040701580572

18. Andrews GP, Jones DS, Diak OA, McCoy CP, Watts AB, McGinity JW. The manufacture and characterisation of hot-melt extruded enteric tablets. Eur J Pharm Biopharm. 2008;69(1):264-73. DOI: 10.1016/j.ejpb.2007.11.001

19. Mehuys E, Remon JP, Vervaet C. Production of enteric capsules by means of hot-melt extrusion. Eur J Pharm Sci. 2005;24(2-3):207-12. DOI: 10.1016/j.ejps.2004.10.011

20. Miller DA, DiNunzio JC, Yang W, McGinity JW, Williams RO, 3rd. Targeted intestinal delivery of supersaturated itraconazole for improved oral absorption. Pharm Res. 2008;25(6):1450-9. DOI: 10.1007/s11095-008-9543-1

21. Bruce LD, Shah NH, Malick AW, Infeld MH, McGinity JW. Properties of hot-melt extruded tablet formulations for the colonic delivery of 5-aminosalicylic acid. Eur J Pharm Biopharm. 2005;59(1):85-97. DOI: 10.1016/j.ejpb.2004.06.007

22. Silva LAD, Almeida SL, Alonso ECP, Rocha PBR, Martins FT, Freitas LAP, et al. Preparation of a solid self-microemulsifying drug delivery system by hot-melt extrusion. Int J Pharm. 2018;541(1-2):1-10. DOI: 10.1016/j.ijpharm.2018.02.020

23. Bhagurkar AM, Repka MA, Murthy SN. A Novel Approach for the Development of a Nanostructured Lipid Carrier Formulation by Hot-Melt Extrusion Technology. J Pharm Sci. 2017;106(4):1085-91. DOI: 10.1016/j.xphs.2016.12.015

24. Patil H, Feng X, Ye X, Majumdar S, Repka MA. Continuous production of fenofibrate solid lipid nanoparticles by hot-melt extrusion technology: a systematic study based on a quality by design approach. AAPS J. 2015;17(1):194-205. DOI: 10.1208/s12248-014-9674-8

25. Verma S, Rudraraju VS. A systematic approach to design and prepare solid dispersions of poorly water-soluble drug. AAPS PharmSciTech. 2014;15(3):641-57. DOI: 10.1208/s12249-014-0093-z

26. Pina MF, Zhao M, Pinto JF, Sousa JJ, Craig DQ. The influence of drug physical state on the dissolution enhancement of solid dispersions prepared via hot-melt extrusion: a case study using olanzapine. J Pharm Sci. 2014;103(4):1214-23. DOI: 10.1002/jps.23894

27. Lakshman JP. Formulation, Bioavailability, and Manufacturing Process Enhancement: Novel Applications of Melt Extrusion in Enabling Product Development. In: Repka MA, Langley N, DiNunzio J, editors. Melt Extrusion: Materials, Technology and Drug Product Design: Springer; 2013.

28. Repka MA, Bandari S, Kallakunta VR, Vo AQ, McFall H, Pimparade MB, et al. Melt extrusion with poorly soluble drugs - An integrated review. Int J Pharm. 2018;535(1-2):68-85. DOI: 10.1016/j.ijpharm.2017.10.056

29. Patil H, Tiwari RV, Repka MA. Hot-Melt Extrusion: from Theory to Application in Pharmaceutical Formulation. AAPS PharmSciTech. 2016;17(1):20-42. DOI: 10.1208/s12249-015-0360-7

30. Tiwari RV, Patil H, Repka MA. Contribution of hot-melt extrusion technology to advance drug delivery in the 21st century. Expert Opin Drug Deliv. 2016;13(3):451-64. DOI: 10.1517/17425247.2016.1126246

31. Lang B, McGinity JW, Williams RO, 3rd. Hot-melt extrusion - basic principles and pharmaceutical applications. Drug Dev Ind Pharm. 2014;40(9):1133-55. DOI: 10.3109/03639045.2013.838577

32. Becker K, Salar-Behzadi S, Zimmer A. Solvent-free melting techniques for the preparation of lipid-based solid oral formulations. Pharm Res. 2015;32(5):1519-45. DOI: 10.1007/s11095-015-1661-y

33. Gao P, Shi Y. Characterization of supersaturatable formulations for improved absorption of poorly soluble drugs. AAPS J. 2012;14(4):703-13. DOI: 10.1208/s12248-012-9389-7

34. Sarode AL, Sandhu H, Shah N, Malick W, Zia H. Hot melt extrusion for amorphous solid dispersions: temperature and moisture activated drug-polymer interactions for enhanced stability. Mol Pharm. 2013;10(10):3665-75. DOI: 10.1021/mp400165b

35. Lakshman JP, Cao Y, Kowalski J, Serajuddin AT. Application of melt extrusion in the development of a physically and chemically stable high-energy amorphous solid dispersion of a poorly water-soluble drug. Mol Pharm. 2008;5(6):994-1002. DOI: 10.1021/mp8001073

36. Lu M, Guo Z, Li Y, Pang H, Lin L, Liu X, et al. Application of hot melt extrusion for poorly water-soluble drugs: limitations, advances and future prospects. Curr Pharm Des. 2014;20(3):369-87. DOI: 10.2174/1381612811319990402

37. Repka MA, Shah S, Lu J, Maddineni S, Morott J, Patwardhan K, et al. Melt extrusion: process to product. Expert Opin Drug Deliv. 2012;9(1):105-25. DOI: 10.1517/17425247.2012.642365

38. Breitenbach J. Melt extrusion: from process to drug delivery technology. Eur J Pharm Biopharm. 2002;54(2):107-17. DOI: 10.1016/s0939-6411(02)00061-9

39. Shah S, Maddineni S, Lu J, Repka MA. Melt extrusion with poorly soluble drugs. Int J Pharm. 2013;453(1):233-52. DOI: 10.1016/j.ijpharm.2012.11.001

40. Stankovic M, Frijlink HW, Hinrichs WL. Polymeric formulations for drug release prepared by hot melt extrusion: application and characterization. Drug Discov Today. 2015;20(7):812-23. DOI: 10.1016/j.drudis.2015.01.012

41. Chaturvedi K, Gajera BY, Xu T, Shah H, Dave RH. Influence of processing methods on physico-mechanical properties of Ibuprofen/HPC-SSL formulation. Pharm Dev Technol. 2018;23(10):1108-16. DOI: 10.1080/10837450.2018.1425430

42. Moradiya HG, Nokhodchi A, Bradley MS, Farnish R, Douroumis D. Increased dissolution rates of carbamazepine - gluconolactone binary blends processed by hot melt extrusion. Pharm Dev Technol. 2016;21(4):445-52. DOI: 10.3109/10837450.2015.1022783

43. Zhang Q, Zhao Y, Zhao Y, Ding Z, Fan Z, Zhang H, et al. Effect of HPMCAS on recrystallization inhibition of nimodipine solid dispersions prepared by hot-melt extrusion and dissolution enhancement of nimodipine tablets. Colloids Surf B Biointerfaces. 2018;172:118-26. DOI: 10.1016/j.colsurfb.2018.08.030

44. Vo AQ, Feng X, Pimparade M, Ye X, Kim DW, Martin ST, et al. Dual-mechanism gastroretentive drug delivery system loaded with an amorphous solid dispersion prepared by hot-melt extrusion. Eur J Pharm Sci. 2017;102:71-84. DOI: 10.1016/j.ejps.2017.02.040

45. Hormann TR, Jager N, Funke A, Murb RK, Khinast JG, Paudel A. Formulation performance and processability window for manufacturing a dual-polymer amorphous solid dispersion via hot-melt extrusion and strand pelletization. Int J Pharm. 2018;553(1-2):408-21. DOI: 10.1016/j.ijpharm.2018.10.035

46. Pimparade MB, Vo A, Maurya AS, Bae J, Morott JT, Feng X, et al. Development and evaluation of an oral fast disintegrating anti-allergic film using hot-melt extrusion technology. Eur J Pharm Biopharm. 2017;119:81-90. DOI: 10.1016/j.ejpb.2017.06.004

47. Speer I, Preis M, Breitkreutz J. Prolonged drug release properties for orodispersible films by combining hot-melt extrusion and solvent casting methods. Eur J Pharm Biopharm. 2018;129:66-73. DOI: 10.1016/j.ejpb.2018.05.023

48. Crowley MM, Zhang F, Koleng JJ, McGinity JW. Stability of polyethylene oxide in matrix tablets prepared by hot-melt extrusion. Biomaterials. 2002;23(21):4241-8. DOI: 10.1016/s0142-9612(02)00187-4

49. Melocchi A, Loreti G, Del Curto MD, Maroni A, Gazzaniga A, Zema L. Evaluation of hot-melt extrusion and injection molding for continuous manufacturing of immediate-release tablets. J Pharm Sci. 2015;104(6):1971-80. DOI: 10.1002/jps.24419

50. Albarahmieh E, Qi S, Craig DQM. Hot melt extruded transdermal films based on amorphous solid dispersions in Eudragit RS PO: The inclusion of hydrophilic additives to develop moisture-activated release systems. Int J Pharm. 2016;514(1):270-81. DOI: 10.1016/j.ijpharm.2016.06.137

51. Nasr M, Karandikar H, Abdel-Aziz RTA, Moftah N, Paradkar A. Novel nicotinamide skin-adhesive hot melt extrudates for treatment of acne. Expert Opin Drug Deliv. 2018;15(12):1165-73. DOI: 10.1080/17425247.2018.1546287

52. Mendonsa NS, Thipsay P, Kim DW, Martin ST, Repka MA. Bioadhesive Drug Delivery System for Enhancing the Permeability of a BCS Class III Drug via Hot-Melt Extrusion Technology. AAPS PharmSciTech. 2017;18(7):2639-47. DOI: 10.1208/s12249-017-0728-y

53. Alhijjaj M, Bouman J, Wellner N, Belton P, Qi S. Creating Drug Solubilization Compartments via Phase Separation in Multicomponent Buccal Patches Prepared by Direct Hot Melt Extrusion-Injection Molding. Mol Pharm. 2015;12(12):4349-62. DOI: 10.1021/acs.molpharmaceut.5b00532

54. Cosse A, Konig C, Lamprecht A, Wagner KG. Hot Melt Extrusion for Sustained Protein Release: Matrix Erosion and In Vitro Release of PLGA-Based Implants. AAPS PharmSciTech. 2017;18(1):15-26. DOI: 10.1208/s12249-016-0548-5

55. Salmoria GV, Sibilia F, Henschel VG, Fare S, Tanzi MC. Structure and properties of polycaprolactone/ibuprofen rods prepared by melt extrusion for implantable drug delivery. Polymer Bulletin. 2017;74(12):4973-87. DOI: 10.1007/s00289-017-1999-x

56. Leelakanok N, Geary SM, Salem AK. Antitumor Efficacy and Toxicity of 5-Fluorouracil-Loaded Poly(Lactide Co-glycolide) Pellets. J Pharm Sci. 2018;107(2):690-7. DOI: 10.1016/j.xphs.2017.10.005

57. Wang A, Liu Y, Liang R, Zhang X, Sun K, Wu Z, et al. Preparation and evaluation of rotigotine-loaded implant for the treatment of Parkinson's disease and its evolution study. Saudi Pharm J. 2016;24(3):363-70. DOI: 10.1016/j.jsps.2016.04.022

58. Martin C. Twin Screw Extruders as Continuous Mixers for Thermal Processing: a Technical and Historical Perspective. AAPS PharmSciTech. 2016;17(1):3-19. DOI: 10.1208/s12249-016-0485-3

59. Bhardwaj V, Kumar MNVR. Drug Delivery Systems to Fight Cancer. In: Siepmann J, Siegel AR, Rathbone JM, editors. Fundamentals and Applications of Controlled Release Drug Delivery. Boston, MA: Springer US; 2012. p. 493-516.

60. Minami J, Numabe A, Andoh N, Kobayashi N, Horinaka S, Ishimitsu T, et al. Comparison of once-daily nifedipine controlled-release with twice-daily nifedipine retard in the treatment of essential hypertension. Br J Clin Pharmacol. 2004;57(5):632-9. DOI: 10.1111/j.1365-2125.2003.02056.x

61. Kesisoglou F, Hermans A, Neu C, Yee KL, Palcza J, Miller J. Development of In Vitro-In Vivo Correlation for Amorphous Solid Dispersion Immediate-Release Suvorexant Tablets and Application to Clinically Relevant Dissolution Specifications and In-Process Controls. J Pharm Sci. 2015;104(9):2913-22. DOI: 10.1002/jps.24362

62. Feng X, Zhang F. Twin-screw extrusion of sustained-release oral dosage forms and medical implants. Drug Deliv Transl Res. 2018;8(6):1694-713. DOI: 10.1007/s13346-017-0461-9

63. Jermain SV, Brough C, Williams RO, 3rd. Amorphous solid dispersions and nanocrystal technologies for poorly water-soluble drug delivery - An update. Int J Pharm. 2018;535(1-2):379-92. DOI: 10.1016/j.ijpharm.2017.10.051

64. EMA, CHMP. Assessment report: Viekirax (ombitasvir / paritaprevir / ritonavir). 2014; Report number EMA/768346/2014.

65. Braeburn Pharmaceuticals, Inc. Full Prescribing Information: PROBUPHINE (buprenorphine) implant for subdermal administration. Revised: 02/2018; Report number 4215185.

66. Population Council, Inc. Full Prescribing Information: ANNOVERA™ (segesterone acetate and ethinyl estradiol vaginal system). Revised: 08/2018; Report number 4305085.

67. Merck Sharp & Dohme, Corp. Full Prescribing Information: BELSOMRA® (suvorexant) tablets, for oral use. Revised: 7/2018; Report number 3610408.

68. Harmon P. A., Variankaval N, inventors; Merck Sharp & Dohme Corp assignee. Solid dosage formulations of an orexin receptor antagonist. US patent US 10098892 B2. 2013.

69. EMA, CHMP. Assessment report: Venclyxto (venetoclax). 2016; Report number EMA/725631/2016.

70. Birtalan E, Hoelig P, Lindley DJ, Sanzgiri YD, Tong P, inventors; AbbVie Deutschland GmbH and Co KG, AbbVie Inc assignee. Melt-extruded solid dispersions containing an apoptosis-inducing agent. US patent US14340435. 2010.

71. EMA, CHMP. Assessment report: Maviret (glecaprevir / pibrentasvir). 2017; Report number EMA/449689/2017.

72. Crowley MM, Zhang F, Repka MA, Thumma S, Upadhye SB, Battu SK, et al. Pharmaceutical applications of hot-melt extrusion: part I. Drug Dev Ind Pharm. 2007;33(9):909-26. DOI: 10.1080/03639040701498759

73. Huang S, O'Donnell KP, Delpon de Vaux SM, O'Brien J, Stutzman J, Williams RO, 3rd. Processing thermally labile drugs by hot-melt extrusion: The lesson with gliclazide. Eur J Pharm Biopharm. 2017;119:56-67. DOI: 10.1016/j.ejpb.2017.05.014

74. Chavan RB, Rathi S, Jyothi V, Shastri NR. Cellulose based polymers in development of amorphous solid dispersions. Asian J Pharm Sci. 2019;14(3):248-64. DOI: 10.1016/j.ajps.2018.09.003

75. Loreti G, Maroni A, Del Curto MD, Melocchi A, Gazzaniga A, Zema L. Evaluation of hot-melt extrusion technique in the preparation of HPC matrices for prolonged release. Eur J Pharm Sci. 2014;52:77-85. DOI: 10.1016/j.ejps.2013.10.014

76. Wilson MR, Jones DS, Andrews GP. The development of sustained release drug delivery platforms using melt-extruded cellulose-based polymer blends. J Pharm Pharmacol. 2017;69(1):32-42. DOI: 10.1111/jphp.12656

77. Yi S, Wang J, Lu Y, Ma R, Gao Q, Liu S, et al. Novel Hot Melt Extruded Matrices of Hydroxypropyl Cellulose and Amorphous Felodipine-Plasticized Hydroxypropyl Methylcellulose as Controlled Release Systems. AAPS PharmSciTech. 2019;20(6):219. DOI: 10.1208/s12249-019-1435-7

78. Dong Z, Choi DS. Hydroxypropyl methylcellulose acetate succinate: potential drug-excipient incompatibility. AAPS PharmSciTech. 2008;9(3):991-7. DOI: 10.1208/s12249-008-9138-5

79. Almutairi M, Almutairy B, Sarabu S, Almotairy A, Ashour E, Bandari S, et al. Processability of AquaSolve LG polymer by hot-melt extrusion: Effects of pressurized CO2 on physicomechanical properties and API stability. J Drug Deliv Sci Technol. 2019;52:165-76. DOI: 10.1016/j.jddst.2019.04.029

80. Xue X, Chen G, Xu X, Wang J, Wang J, Ren L. A Combined Utilization of Plasdone-S630 and HPMCAS-HF in Ziprasidone Hydrochloride Solid Dispersion by Hot-Melt Extrusion to Enhance the Oral Bioavailability and No Food Effect. AAPS PharmSciTech. 2019;20(1):37. DOI: 10.1208/s12249-018-1216-8

81. Wu CY, Lui WB, Peng J. Optimization of Extrusion Variables and Maleic Anhydride Content on Biopolymer Blends Based on Poly(hydroxybutyrate-co-hydroxyvalerate)/Poly(vinyl acetate) with Tapioca Starch. Polymers. 2018;10(8). DOI: 10.3390/polym10080827

82. Fukuda M, Peppas NA, McGinity JW. Properties of sustained release hot-melt extruded tablets containing chitosan and xanthan gum. Int J Pharm. 2006;310(1-2):90-100. DOI: 10.1016/j.ijpharm.2005.11.042

83. Verhoeven E, Vervaet C, Remon JP. Xanthan gum to tailor drug release of sustained-release ethylcellulose mini-matrices prepared via hot-melt extrusion: in vitro and in vivo evaluation. Eur J Pharm Biopharm. 2006;63(3):320-30. DOI: 10.1016/j.ejpb.2005.12.004

84. Bode C, Kranz H, Fivez A, Siepmann F, Siepmann J. Often neglected: PLGA/PLA swelling orchestrates drug release: HME implants. J Control Release. 2019;306:97-107. DOI: 10.1016/j.jconrel.2019.05.039

85. Kamel R, Abbas H. PLGA-based monolithic filaments prepared by hot-melt extrusion: In-vitro comparative study. Ann Pharm Fr. 2018;76(2):97-106. DOI: 10.1016/j.pharma.2017.09.002

86. Heller J, Barr J, Ng S, Shen HR, Gurny R, Schwach-Abdelaoui K, et al. Development of poly(ortho esters) and their application for bovine serum albumin and bupivacaine delivery. J Control Release. 2002;78(1-3):133-41. DOI: 10.1016/s0168-3659(01)00482-5

87. Heller J, Barr J, Ng SY, Shen HR, Schwach-Abdellaoui K, Einmahl S, et al. Poly(ortho esters) - their development and some recent applications. Eur J Pharm Biopharm. 2000;50(1):121-8. DOI: 10.1016/s0939-6411(00)00085-0

88. Verstraete G, Vandenbussche L, Kasmi S, Nuhn L, Brouckaert D, Van Renterghem J, et al. Thermoplastic polyurethane-based intravaginal rings for prophylaxis and treatment of (recurrent) bacterial vaginosis. Int J Pharm. 2017;529(1-2):218-26. DOI: 10.1016/j.ijpharm.2017.06.076

89. Verstraete G, Mertens P, Grymonpre W, Van Bockstal PJ, De Beer T, Boone MN, et al. A comparative study between melt granulation/compression and hot melt extrusion/injection molding for the manufacturing of oral sustained release thermoplastic polyurethane matrices. Int J Pharm. 2016;513(1-2):602-11. DOI: 10.1016/j.ijpharm.2016.09.072

90. Verstraete G, Van Renterghem J, Van Bockstal PJ, Kasmi S, De Geest BG, De Beer T, et al. Hydrophilic thermoplastic polyurethanes for the manufacturing of highly dosed oral sustained release matrices via hot melt extrusion and injection molding. Int J Pharm. 2016;506(1-2):214-21. DOI: 10.1016/j.ijpharm.2016.04.057

91. Li LC, Deng J, Stephens D. Polyanhydride implant for antibiotic delivery - from the bench to the clinic. Adv Drug Deliv Rev. 2002;54(7):963-86. DOI: 10.1016/s0169-409x(02)00053-4

92. Deng JS, Meisters M, Li L, Setesak J, Claycomb L, Tian Y, et al. The development of an injection-molding process for a polyanhydride implant containing gentamicin sulfate. PDA J Pharm Sci Technol. 2002;56(2):65-77.

93. Simoes MF, Pereira A, Cardoso S, Cadonau S, Werner K, Pinto RMA, et al. Five-Stage Approach for a Systematic Screening and Development of Etravirine Amorphous Solid Dispersions by Hot-Melt Extrusion. Mol Pharm. 2020;17(2):554-68. DOI: 10.1021/acs.molpharmaceut.9b00996

94. Evans RC, Bochmann ES, Kyeremateng SO, Gryczke A, Wagner KG. Holistic QbD approach for hot-melt extrusion process design space evaluation: Linking materials science, experimentation and process modeling. Eur J Pharm Biopharm. 2019;141:149-60. DOI: 10.1016/j.ejpb.2019.05.021

95. Ma X, Huang S, Lowinger MB, Liu X, Lu X, Su Y, et al. Influence of mechanical and thermal energy on nifedipine amorphous solid dispersions prepared by hot melt extrusion: Preparation and physical stability. Int J Pharm. 2019;561:324-34. DOI: 10.1016/j.ijpharm.2019.03.014

96. Zi P, Zhang C, Ju C, Su Z, Bao Y, Gao J, et al. Solubility and bioavailability enhancement study of lopinavir solid dispersion matrixed with a polymeric surfactant - Soluplus. Eur J Pharm Sci. 2019;134:233-45. DOI: 10.1016/j.ejps.2019.04.022

97. Ugaonkar SR, Wesenberg A, Wilk J, Seidor S, Mizenina O, Kizima L, et al. A novel intravaginal ring to prevent HIV-1, HSV-2, HPV, and unintended pregnancy. J Control Release. 2015;213:57-68. DOI: 10.1016/j.jconrel.2015.06.018

98. Almeida A, Possemiers S, Boone MN, De Beer T, Quinten T, Van Hoorebeke L, et al. Ethylene vinyl acetate as matrix for oral sustained release dosage forms produced via hot-melt extrusion. Eur J Pharm Biopharm. 2011;77(2):297-305. DOI: 10.1016/j.ejpb.2010.12.004

99. Feng Z, Li M, Wang W. Improvement of dissolution and tabletability of carbamazepine solid dispersions with high drug loading prepared by hot-melt extrusion. Pharmazie. 2019;74(9):523-8. DOI: 10.1691/ph.2019.9008

100. Meng F, Meckel J, Zhang F. Investigation of itraconazole ternary amorphous solid dispersions based on povidone and Carbopol. Eur J Pharm Sci. 2017;106:413-21. DOI: 10.1016/j.ejps.2017.06.019

101. Bhagurkar AM, Darji M, Lakhani P, Thipsay P, Bandari S, Repka MA. Effects of formulation composition on the characteristics of mucoadhesive films prepared by hot-melt extrusion technology. J Pharm Pharmacol. 2019;71(3):293-305. DOI: 10.1111/jphp.13046

102. Palazi E, Karavas E, Barmpalexis P, Kostoglou M, Nanaki S, Christodoulou E, et al. Melt extrusion process for adjusting drug release of poorly water soluble drug felodipine using different polymer matrices. Eur J Pharm Sci. 2018;114:332-45. DOI: 10.1016/j.ejps.2018.01.004

103. Xu X, Siddiqui A, Srinivasan C, Mohammad A, Rahman Z, Korang-Yeboah M, et al. Evaluation of Abuse-Deterrent Characteristics of Tablets Prepared via Hot-Melt Extrusion. AAPS PharmSciTech. 2019;20(6):230. DOI: 10.1208/s12249-019-1448-2

104. Gallet G, Carroccio S, Rizzarelli P, Karlsson S. Thermal degradation of poly(ethylene oxide–propylene oxide–ethylene oxide) triblock copolymer: comparative study by SEC/NMR, SEC/MALDI-TOF-MS and SPME/GC-MS. Polymer. 2002;43(4):1081-94. DOI: 10.1016/s0032-3861(01)00677-2

105. Hughey JR, DiNunzio JC, Bennett RC, Brough C, Miller DA, Ma H, et al. Dissolution enhancement of a drug exhibiting thermal and acidic decomposition characteristics by fusion processing: a comparative study of hot melt extrusion and KinetiSol dispersing. AAPS PharmSciTech. 2010;11(2):760-74. DOI: 10.1208/s12249-010-9431-y

106. Stroyer A, McGinity JW, Leopold CS. Solid state interactions between the proton pump inhibitor omeprazole and various enteric coating polymers. J Pharm Sci. 2006;95(6):1342-53. DOI: 10.1002/jps.20450

107. Watanabe T, Okabayashi M, Kurokawa D, Nishimoto Y, Ozawa T, Kawasaki H, et al. Determination of primary bond scissions by mass spectrometric analysis of ultrasonic degradation products of poly(ethylene oxide-block-propylene oxide) copolymers. J Mass Spectrom. 2010;45(7):799-805. DOI: 10.1002/jms.1771

108. Shojaee S, Cumming I, Kaialy W, Nokhodchi A. The influence of vitamin E succinate on the stability of polyethylene oxide PEO controlled release matrix tablets. Colloids Surf B Biointerfaces. 2013;111:486-92. DOI: 10.1016/j.colsurfb.2013.06.038

109. Carrasco F, Pagès P, Gámez-Pérez J, Santana OO, Maspoch ML. Processing of poly(lactic acid): Characterization of chemical structure, thermal stability and mechanical properties. Polym Degrad Stab. 2010;95(2):116-25. DOI: 10.1016/j.polymdegradstab.2009.11.045

110. Zhang T, Zhou S, Gao X, Yang Z, Sun L, Zhang D. A multi-scale method for modeling degradation of bioresorbable polyesters. Acta Biomater. 2017;50:462-75. DOI: 10.1016/j.actbio.2016.12.046

111. Liu W-C, Halley PJ, Gilbert RG. Mechanism of Degradation of Starch, a Highly Branched Polymer, during Extrusion. Macromolecules. 2010;43(6):2855-64. DOI: 10.1021/ma100067x

112. Hughey JR, Keen JM, Miller DA, Brough C, McGinity JW. Preparation and characterization of fusion processed solid dispersions containing a viscous thermally labile polymeric carrier. Int J Pharm. 2012;438(1-2):11-9. DOI: 10.1016/j.ijpharm.2012.08.032

113. Lu G, Kalyon DM, Yilgör I, Yilgör E. Rheology and extrusion of medical-grade thermoplastic polyurethane. Polym Eng Sci. 2003;43(12):1863-77. DOI: 10.1002/pen.10158

114. Alexy P, Lacík I, Šimková B, Bakoš D, Prónayová Na, Liptaj T, et al. Effect of melt processing on thermo-mechanical degradation of poly(vinyl alcohol)s. Polym Degrad Stab. 2004;85(2):823-30. DOI: 10.1016/j.polymdegradstab.2004.02.011

115. Lin S-Y, Yu H-L, Li M-J. Formation of six-membered cyclic anhydrides by thermally induced intramolecular ester condensation in Eudragit E film. Polymer. 1999;40(12):3589-93. DOI: 10.1016/s0032-3861(98)00488-1

116. Lin S-Y, Yu H-L. Thermal stability of methacrylic acid copolymers of Eudragits L, S, and L30D and the acrylic acid polymer of carbopol. J Polym Sci A Polym Chem. 1999;37(13):2061-7. DOI: 10.1002/(sici)1099-0518(19990701)37:13<2061::aid-pola20>3.0.co;2-y

117. Hancock BC, Shamblin SL, Zografi G. Molecular mobility of amorphous pharmaceutical solids below their glass transition temperatures. Pharm Res. 1995;12(6):799-806. DOI: 10.1023/a:1016292416526

118. Laitinen R, Lobmann K, Strachan CJ, Grohganz H, Rades T. Emerging trends in the stabilization of amorphous drugs. Int J Pharm. 2013;453(1):65-79. DOI: 10.1016/j.ijpharm.2012.04.066

119. Baghel S, Cathcart H, O'Reilly NJ. Polymeric Amorphous Solid Dispersions: A Review of Amorphization, Crystallization, Stabilization, Solid-State Characterization, and Aqueous Solubilization of Biopharmaceutical Classification System Class II Drugs. J Pharm Sci. 2016;105(9):2527-44. DOI: 10.1016/j.xphs.2015.10.008

120. Janssens S, Van den Mooter G. Review: physical chemistry of solid dispersions. J Pharm Pharmacol. 2009;61(12):1571-86. DOI: 10.1211/jpp/61.12.0001

121. Zhu DA, Zografi G, Gao P, Gong Y, Zhang GGZ. Modeling Physical Stability of Amorphous Solids Based on Temperature and Moisture Stresses. J Pharm Sci. 2016;105(9):2932-9. DOI: 10.1016/j.xphs.2016.03.029

122. Bhardwaj SP, Arora KK, Kwong E, Templeton A, Clas SD, Suryanarayanan R. Correlation between molecular mobility and physical stability of amorphous itraconazole. Mol Pharm. 2013;10(2):694-700. DOI: 10.1021/mp300487u

123. Miyanishi H, Nemoto T, Mizuno M, Mimura H, Kitamura S, Iwao Y, et al. Evaluation of crystallization behavior on the surface of nifedipine solid dispersion powder using inverse gas chromatography. Pharm Res. 2013;30(2):502-11. DOI: 10.1007/s11095-012-0896-0

124. Shah N, Sandhu H, Choi DS, Chokshi H, Malick AW. Amorphous Solid Dispersions: Theory and Practice: Springer New York; 2014.

125. Gupta SS, Solanki N, Serajuddin AT. Investigation of Thermal and Viscoelastic Properties of Polymers Relevant to Hot Melt Extrusion, IV: Affinisol HPMC HME Polymers. AAPS PharmSciTech. 2016;17(1):148-57. DOI: 10.1208/s12249-015-0426-6

126. Mao C, Chamarthy SP, Pinal R. Time-dependence of molecular mobility during structural relaxation and its impact on organic amorphous solids: an investigation based on a calorimetric approach. Pharm Res. 2006;23(8):1906-17. DOI: 10.1007/s11095-006-9008-3

127. Surana R, Pyne A, Rani M, Suryanarayanan R. Measurement of enthalpic relaxation by differential scanning calorimetry—effect of experimental conditions. Thermochim Acta. 2005;433(1-2):173-82. DOI: 10.1016/j.tca.2005.02.014

128. Hasegawa S, Ke P, Buckton G. Determination of the structural relaxation at the surface of amorphous solid dispersion using inverse gas chromatography. J Pharm Sci. 2009;98(6):2133-9. DOI: 10.1002/jps.21573

129. Bansal SS, Kaushal AM, Bansal AK. Enthalpy relaxation studies of two structurally related amorphous drugs and their binary dispersions. Drug Dev Ind Pharm. 2010;36(11):1271-80. DOI: 10.3109/03639041003753847

130. Kakumanu VK, Bansal AK. Enthalpy relaxation studies of celecoxib amorphous mixtures. Pharm Res. 2002;19(12):1873-8. DOI: 10.1023/a:1021453810624

131. Mao C, Prasanth Chamarthy S, Byrn SR, Pinal R. A calorimetric method to estimate molecular mobility of amorphous solids at relatively low temperatures. Pharm Res. 2006;23(10):2269-76. DOI: 10.1007/s11095-006-9071-9

132. Karmwar P, Graeser K, Gordon KC, Strachan CJ, Rades T. Investigation of properties and recrystallisation behaviour of amorphous indomethacin samples prepared by different methods. Int J Pharm. 2011;417(1-2):94-100. DOI: 10.1016/j.ijpharm.2010.12.019

133. Mao C, Chamarthy SP, Pinal R. Calorimetric study and modeling of molecular mobility in amorphous organic pharmaceutical compounds using a modified Adam-Gibbs approach. J Phys Chem B. 2007;111(46):13243-52. DOI: 10.1021/jp072577+

134. Aso Y, Yoshioka S, Kojima S. Molecular mobility-based estimation of the crystallization rates of amorphous nifedipine and phenobarbital in poly(vinylpyrrolidone) solid dispersions. J Pharm Sci. 2004;93(2):384-91. DOI: 10.1002/jps.10526

135. Berthier L, Coslovich D. Novel approach to numerical measurements of the configurational entropy in supercooled liquids. Proc Natl Acad Sci U S A. 2014;111(32):11668-72. DOI: 10.1073/pnas.1407934111

136. Qian F, Huang J, Hussain MA. Drug-polymer solubility and miscibility: Stability consideration and practical challenges in amorphous solid dispersion development. J Pharm Sci. 2010;99(7):2941-7. DOI: 10.1002/jps.22074

137. Forster A, Hempenstall J, Tucker, Rades T. The potential of small-scale fusion experiments and the Gordon-Taylor equation to predict the suitability of drug/polymer blends for melt extrusion. Drug Dev Ind Pharm. 2001;27(6):549-60. DOI: 10.1081/ddc-100105180

138. Nair R, Nyamweya N, Gönen S, Martínez-Miranda LJ, Hoag SW. Influence of various drugs on the glass transition temperature of poly(vinylpyrrolidone): a thermodynamic and spectroscopic investigation. Int J Pharm. 2001;225(1-2):83-96. DOI: 10.1016/s0378-5173(01)00767-0

139. Jensen KT, Larsen FH, Lobmann K, Rades T, Grohganz H. Influence of variation in molar ratio on co-amorphous drug-amino acid systems. Eur J Pharm Biopharm. 2016;107:32-9. DOI: 10.1016/j.ejpb.2016.06.020

140. Rask MB, Knopp MM, Olesen NE, Holm R, Rades T. Influence of PVP/VA copolymer composition on drug-polymer solubility. Eur J Pharm Sci. 2016;85:10-7. DOI: 10.1016/j.ejps.2016.01.026

141. O'Donnell KP, Woodward WH. Dielectric spectroscopy for the determination of the glass transition temperature of pharmaceutical solid dispersions. Drug Dev Ind Pharm. 2015;41(6):959-68. DOI: 10.3109/03639045.2014.919314

142. Greenhalgh DJ, Williams AC, Timmins P, York P. Solubility parameters as predictors of miscibility in solid dispersions. J Pharm Sci. 1999;88(11):1182-90. DOI: 10.1021/js9900856

143. Just S, Sievert F, Thommes M, Breitkreutz J. Improved group contribution parameter set for the application of solubility parameters to melt extrusion. Eur J Pharm Biopharm. 2013;85(3 Pt B):1191-9. DOI: 10.1016/j.ejpb.2013.04.006

144. Forster A, Hempenstall J, Tucker I, Rades T. Selection of excipients for melt extrusion with two poorly water-soluble drugs by solubility parameter calculation and thermal analysis. Int J Pharm. 2001;226(1-2):147-61. DOI: 10.1016/s0378-5173(01)00801-8

145. Baghel S, Cathcart H, O'Reilly NJ. Theoretical and experimental investigation of drug-polymer interaction and miscibility and its impact on drug supersaturation in aqueous medium. Eur J Pharm Biopharm. 2016;107:16-31. DOI: 10.1016/j.ejpb.2016.06.024

146. Djuris J, Nikolakakis I, Ibric S, Djuric Z, Kachrimanis K. Preparation of carbamazepine-Soluplus solid dispersions by hot-melt extrusion, and prediction of drug-polymer miscibility by thermodynamic model fitting. Eur J Pharm Biopharm. 2013;84(1):228-37. DOI: 10.1016/j.ejpb.2012.12.018

147. Zhang Y, Luo R, Chen Y, Ke X, Hu D, Han M. Application of carrier and plasticizer to improve the dissolution and bioavailability of poorly water-soluble baicalein by hot melt extrusion. AAPS PharmSciTech. 2014;15(3):560-8. DOI: 10.1208/s12249-013-0071-x

148. Yoo SU, Krill SL, Wang Z, Telang C. Miscibility/stability considerations in binary solid dispersion systems composed of functional excipients towards the design of multi-component amorphous systems. J Pharm Sci. 2009;98(12):4711-23. DOI: 10.1002/jps.21779

149. Yang M, Wang P, Gogos C. Prediction of acetaminophen's solubility in poly(ethylene oxide) at room temperature using the Flory-Huggins theory. Drug Dev Ind Pharm. 2013;39(1):102-8. DOI: 10.3109/03639045.2012.659188

150. Marsac PJ, Shamblin SL, Taylor LS. Theoretical and practical approaches for prediction of drug-polymer miscibility and solubility. Pharm Res. 2006;23(10):2417-26. DOI: 10.1007/s11095-006-9063-9

151. Marsac PJ, Konno H, Taylor LS. A comparison of the physical stability of amorphous felodipine and nifedipine systems. Pharm Res. 2006;23(10):2306-16. DOI: 10.1007/s11095-006-9047-9

152. Tian Y, Booth J, Meehan E, Jones DS, Li S, Andrews GP. Construction of drug-polymer thermodynamic phase diagrams using Flory-Huggins interaction theory: identifying the relevance of temperature and drug weight fraction to phase separation within solid dispersions. Mol Pharm. 2013;10(1):236-48. DOI: 10.1021/mp300386v

153. Shah SM, Jain AS, Kaushik R, Nagarsenker MS, Nerurkar MJ. Preclinical formulations: insight, strategies, and practical considerations. AAPS PharmSciTech. 2014;15(5):1307-23. DOI: 10.1208/s12249-014-0156-1

154. Thakral S, Thakral NK. Prediction of drug-polymer miscibility through the use of solubility parameter based Flory-Huggins interaction parameter and the experimental validation: PEG as model polymer. J Pharm Sci. 2013;102(7):2254-63. DOI: 10.1002/jps.23583

155. Li S, Tian Y, Jones DS, Andrews GP. Optimising Drug Solubilisation in Amorphous Polymer Dispersions: Rational Selection of Hot-melt Extrusion Processing Parameters. AAPS PharmSciTech. 2016;17(1):200-13. DOI: 10.1208/s12249-015-0450-6

156. Hengsawas Surasarang S, Keen JM, Huang S, Zhang F, McGinity JW, Williams RO, 3rd. Hot melt extrusion versus spray drying: hot melt extrusion degrades albendazole. Drug Dev Ind Pharm. 2017;43(5):797-811. DOI: 10.1080/03639045.2016.1220577

157. DiNunzio JC, Martin ZFC, McGinity JW. Melt Extrusion. In: Williams III RO, Watts AB, Miller DA, editors. Formulating Poorly Water Soluble Drugs. New York: Springer; 2012. p. 331-62.

158. Maddineni S, Battu SK, Morott J, Majumdar S, Murthy SN, Repka MA. Influence of process and formulation parameters on dissolution and stability characteristics of Kollidon(R) VA 64 hot-melt extrudates. AAPS PharmSciTech. 2015;16(2):444-54. DOI: 10.1208/s12249-014-0226-4

159. Dinunzio JC, Brough C, Hughey JR, Miller DA, Williams RO, 3rd, McGinity JW. Fusion production of solid dispersions containing a heat-sensitive active ingredient by hot melt extrusion and Kinetisol dispersing. Eur J Pharm Biopharm. 2010;74(2):340-51. DOI: 10.1016/j.ejpb.2009.09.007

160. Thiry J, Krier F, Evrard B. A review of pharmaceutical extrusion: critical process parameters and scaling-up. Int J Pharm. 2015;479(1):227-40. DOI: 10.1016/j.ijpharm.2014.12.036

161. Keen JM, McGinity JW, Williams RO, 3rd. Enhancing bioavailability through thermal processing. Int J Pharm. 2013;450(1-2):185-96. DOI: 10.1016/j.ijpharm.2013.04.042

162. Seibert KD, Collins PC, Fisher E. Milling Operations in the Pharmaceutical Industry. In: Ende DJ, editor. Chemical Engineering in the Pharmaceutical Industry. New Jersey, USA: John Wiley & Sons, Inc.; 2010. p. 365-78.

163. Agrawal A, Dudhedia M, Deng W, Shepard K, Zhong L, Povilaitis E, et al. Development of Tablet Formulation of Amorphous Solid Dispersions Prepared by Hot Melt Extrusion Using Quality by Design Approach. AAPS PharmSciTech. 2016;17(1):214-32. DOI: 10.1208/s12249-015-0472-0

164. Kolter K, Karl M, Gryczke A. Hot-Melt Extrusion with BASF Pharma Polymers: Extrusion Compendium. Germany: BASF SE - Pharma Ingredients and Services; 2012.

165. Iyer R, Hegde S, Zhang YE, Dinunzio J, Singhal D, Malick A, et al. The impact of hot melt extrusion and spray drying on mechanical properties and tableting indices of materials used in pharmaceutical development. J Pharm Sci. 2013;102(10):3604-13. DOI: 10.1002/jps.23661

166. Maniruzzaman M, Nokhodchi A. Continuous manufacturing via hot-melt extrusion and scale up: regulatory matters. Drug Discov Today. 2017;22(2):340-51. DOI: 10.1016/j.drudis.2016.11.007

167. Carley JF, McKelvey JM. Extruder Scale-Up Theory and Experiments. Ind Eng Chem. 1953;45(5):989-92. DOI: 10.1021/ie50521a036

168. Nakatani M. Short communication: Scale-up theory for twin-screw extruder, keeping the resin temperature unchanged. Adv Polym Tech. 1998;17(1):19-22. DOI: 10.1002/(sici)1098-2329(199821)17:1<19::aid-adv2>3.0.co;2-l

169. Chung CI. On the scale-up of plasticating extruder screws. Polym Eng Sci. 1984;24(9):626-32. DOI: 10.1002/pen.760240904

170. Meijer HEH, Elemans PHM. The modeling of continuous mixers. Part I: The corotating twin-screw extruder. Polym Eng Sci. 1988;28(5):275-90. DOI: 10.1002/pen.760280504

171. Agur EE. Extruder scale-up in a corotating twin-screw extrusion compounding process. Adv Polym Tech. 1986;6(2):225-31. DOI: 10.1002/adv.1986.060060208

172. Bigio D, Wang K. Scale-up rules for mixing in a non-intermeshing twin-screw extruder. Polym Eng Sci. 1996;36(23):2832-9. DOI: 10.1002/pen.10684

173. Hughey J. A Practical Guide to Hot-Melt Extrusion Scale-up for Pharmaceutical Applications. Pharm Technol. 2014;Solid Dosage & Excipients:25-9.

174. Agrawal AM, Dudhedia MS, Zimny E. Hot Melt Extrusion: Development of an Amorphous Solid Dispersion for an Insoluble Drug from Mini-scale to Clinical Scale. AAPS PharmSciTech. 2016;17(1):133-47. DOI: 10.1208/s12249-015-0425-7

175. ICH. Q8 (R2) Pharmaceutical Development. August 2009.

176. Censi R, Gigliobianco MR, Casadidio C, Di Martino P. Hot Melt Extrusion: Highlighting Physicochemical Factors to Be Investigated While Designing and Optimizing a Hot Melt Extrusion Process. Pharmaceutics. 2018;10(3). DOI: 10.3390/pharmaceutics10030089

177. Edueng K, Mahlin D, Bergstrom CAS. The Need for Restructuring the Disordered Science of Amorphous Drug Formulations. Pharm Res. 2017;34(9):1754-72. DOI: 10.1007/s11095-017-2174-7

178. Gordon M, Taylor JS. Ideal copolymers and the second-order transitions of synthetic rubbers. i. non-crystalline copolymers. J Appl Chem. 2007;2(9):493-500. DOI: 10.1002/jctb.5010020901

179. Brostow W, Chiu R, Kalogeras IM, Vassilikou-Dova A. Prediction of glass transition temperatures: Binary blends and copolymers. Mater Lett. 2008;62(17-18):3152-5. DOI: 10.1016/j.matlet.2008.02.008

180. Van Krevelen DW, Te Nijenhuis K. Chapter 7 - Cohesive Properties and Solubility. Properties of Polymers (Fourth Edition). Amsterdam: Elsevier; 2009. p. 189-227.

181. DeBoyace K, Wildfong PLD. The Application of Modeling and Prediction to the Formation and Stability of Amorphous Solid Dispersions. J Pharm Sci. 2018;107(1):57-74. DOI: 10.1016/j.xphs.2017.03.029

182. Shmeis RA, Wang Z, Krill SL. A mechanistic investigation of an amorphous pharmaceutical and its solid dispersions, part I: a comparative analysis by thermally stimulated depolarization current and differential scanning calorimetry. Pharm Res. 2004;21(11):2025-30. DOI: 10.1023/b:pham.0000048193.94922.09

183. Khougaz K, Clas SD. Crystallization inhibition in solid dispersions of MK-0591 and poly(vinylpyrrolidone) polymers. J Pharm Sci. 2000;89(10):1325-34. DOI: 10.1002/1520-6017(200010)89:10<1325::aid-jps10>3.0.co;2-5

184. Lehmkemper K, Kyerematen SO, Heinzerling O, Degenhardt M, Sadowski G. Long-Term Physical Stability of PVP- and PVPVA-Amorphous Solid Dispersions. Mol Pharm. 2017;14(1):157-71. DOI: 10.1021/acs.molpharmaceut.6b00763

185. Liu C, Xu CQ, Yu J, Pui Y, Chen H, Wang S, et al. Impact of a Single Hydrogen Substitution by Fluorine on the Molecular Interaction and Miscibility between Sorafenib and Polymers. Mol Pharm. 2019;16(1):318-26. DOI: 10.1021/acs.molpharmaceut.8b00970

186. Knopp MM, Olesen NE, Holm P, Lobmann K, Holm R, Langguth P, et al. Evaluation of drug-polymer solubility curves through formal statistical analysis: comparison of preparation techniques. J Pharm Sci. 2015;104(1):44-51. DOI: 10.1002/jps.24207

187. Breitkreutz J. Prediction of intestinal drug absorption properties by three-dimensional solubility parameters. Pharm Res. 1998;15(9):1370-5. DOI: 10.1023/a:1011941319327

188. Hoy K. New values of the solubility parameters from vapor pressure data. J Paint Tech. 1970;1970:76–118.

189. Turpin ER, Taresco V, Al-Hachami WA, Booth J, Treacher K, Tomasi S, et al. In Silico Screening for Solid Dispersions: The Trouble with Solubility Parameters and chiFH. Mol Pharm. 2018;15(10):4654-67. DOI: 10.1021/acs.molpharmaceut.8b00637

190. Wlodarski K, Zhang F, Liu T, Sawicki W, Kipping T. Synergistic Effect of Polyvinyl Alcohol and Copovidone in Itraconazole Amorphous Solid Dispersions. Pharm Res. 2018;35(1):16. DOI: 10.1007/s11095-017-2313-1

191. Vay K, Scheler S, Friess W. Application of Hansen solubility parameters for understanding and prediction of drug distribution in microspheres. Int J Pharm. 2011;416(1):202-9. DOI: 10.1016/j.ijpharm.2011.06.047

192. Pawar J, Suryawanshi D, Moravkar K, Aware R, Shetty V, Maniruzzaman M, et al. Study the influence of formulation process parameters on solubility and dissolution enhancement of efavirenz solid solutions prepared by hot-melt extrusion: a QbD methodology. Drug Deliv Transl Res. 2018;8(6):1644-57. DOI: 10.1007/s13346-018-0481-0

193. Penumetcha SS, Gutta LN, Dhanala H, Yamili S, Challa S, Rudraraju S, et al. Hot melt extruded Aprepitant-Soluplus solid dispersion: preformulation considerations, stability and in vitro study. Drug Dev Ind Pharm. 2016;42(10):1609-20. DOI: 10.3109/03639045.2016.1160105

194. Sarode AL, Sandhu H, Shah N, Malick W, Zia H. Hot melt extrusion (HME) for amorphous solid dispersions: predictive tools for processing and impact of drug-polymer interactions on supersaturation. Eur J Pharm Sci. 2013;48(3):371-84. DOI: 10.1016/j.ejps.2012.12.012

195. Wlodarski K, Sawicki W, Haber K, Knapik J, Wojnarowska Z, Paluch M, et al. Physicochemical properties of tadalafil solid dispersions - Impact of polymer on the apparent solubility and dissolution rate of tadalafil. Eur J Pharm Biopharm. 2015;94:106-15. DOI: 10.1016/j.ejpb.2015.04.031

196. Chew NY, Shekunov BY, Tong HH, Chow AH, Savage C, Wu J, et al. Effect of amino acids on the dispersion of disodium cromoglycate powders. J Pharm Sci. 2005;94(10):2289-300. DOI: 10.1002/jps.20426

197. Davidson IG, Langner EJ, Plowman SV, Blair JA. Release mechanism of insulin encapsulated in trehalose ester derivative microparticles delivered via inhalation. Int J Pharm. 2003;254(2):211-22. DOI: 10.1016/s0378-5173(03)00035-8

198. Desai D, Sandhu H, Shah N, Malick W, Zia H, Phuapradit W, et al. Selection of Solid-State Plasticizers as Processing Aids for Hot-Melt Extrusion. J Pharm Sci. 2018;107(1):372-9. DOI: 10.1016/j.xphs.2017.09.004

199. Rask MB, Knopp MM, Olesen NE, Holm R, Rades T. Comparison of two DSC-based methods to predict drug-polymer solubility. Int J Pharm. 2018;540(1-2):98-105. DOI: 10.1016/j.ijpharm.2018.02.002

200. Hu XY, Lou H, Hageman MJ. Preparation of lapatinib ditosylate solid dispersions using solvent rotary evaporation and hot melt extrusion for solubility and dissolution enhancement. Int J Pharm. 2018;552(1-2):154-63. DOI: 10.1016/j.ijpharm.2018.09.062

201. Chen Y, Pui Y, Chen H, Wang S, Serno P, Tonnis W, et al. Polymer-Mediated Drug Supersaturation Controlled by Drug-Polymer Interactions Persisting in an Aqueous Environment. Mol Pharm. 2019;16(1):205-13. DOI: 10.1021/acs.molpharmaceut.8b00947

202. Chakravarty P, Lubach JW, Hau J, Nagapudi K. A rational approach towards development of amorphous solid dispersions: Experimental and computational techniques. Int J Pharm. 2017;519(1-2):44-57. DOI: 10.1016/j.ijpharm.2017.01.003

203. Jog R, Gokhale R, Burgess DJ. Solid state drug-polymer miscibility studies using the model drug ABT-102. Int J Pharm. 2016;509(1-2):285-95. DOI: 10.1016/j.ijpharm.2016.05.068

204. Chen Y, Wang S, Wang S, Liu C, Su C, Hageman M, et al. Initial Drug Dissolution from Amorphous Solid Dispersions Controlled by Polymer Dissolution and Drug-Polymer Interaction. Pharm Res. 2016;33(10):2445-58. DOI: 10.1007/s11095-016-1969-2

205. Qian F, Wang J, Hartley R, Tao J, Haddadin R, Mathias N, et al. Solution behavior of PVP-VA and HPMC-AS-based amorphous solid dispersions and their bioavailability implications. Pharm Res. 2012;29(10):2765-76. DOI: 10.1007/s11095-012-0695-7

206. Knopp MM, Tajber L, Tian Y, Olesen NE, Jones DS, Kozyra A, et al. Comparative Study of Different Methods for the Prediction of Drug-Polymer Solubility. Mol Pharm. 2015;12(9):3408-19. DOI: 10.1021/acs.molpharmaceut.5b00423

207. Dukeck R, Sieger P, Karmwar P. Investigation and correlation of physical stability, dissolution behaviour and interaction parameter of amorphous solid dispersions of telmisartan: a drug development perspective. Eur J Pharm Sci. 2013;49(4):723-31. DOI: 10.1016/j.ejps.2013.05.003

208. Huang S, O'Donnell KP, Keen JM, Rickard MA, McGinity JW, Williams RO, 3rd. A New Extrudable Form of Hypromellose: AFFINISOL HPMC HME. AAPS PharmSciTech. 2016;17(1):106-19. DOI: 10.1208/s12249-015-0395-9

209. Keen JM, Martin C, Machado A, Sandhu H, McGinity JW, DiNunzio JC. Investigation of process temperature and screw speed on properties of a pharmaceutical solid dispersion using corotating and counter-rotating twin-screw extruders. J Pharm Pharmacol. 2014;66(2):204-17. DOI: 10.1111/jphp.12106

210. Huang J, Li Y, Wigent RJ, Malick WA, Sandhu HK, Singhal D, et al. Interplay of formulation and process methodology on the extent of nifedipine molecular dispersion in polymers. Int J Pharm. 2011;420(1):59-67. DOI: 10.1016/j.ijpharm.2011.08.021

211. Zhao Y, Inbar P, Chokshi HP, Malick AW, Choi DS. Prediction of the thermal phase diagram of amorphous solid dispersions by Flory-Huggins theory. J Pharm Sci. 2011;100(8):3196-207. DOI: 10.1002/jps.22541

212. Sun Y, Tao J, Zhang GG, Yu L. Solubilities of crystalline drugs in polymers: an improved analytical method and comparison of solubilities of indomethacin and nifedipine in PVP, PVP/VA, and PVAc. J Pharm Sci. 2010;99(9):4023-31. DOI: 10.1002/jps.22251

213. Marsac PJ, Li T, Taylor LS. Estimation of drug-polymer miscibility and solubility in amorphous solid dispersions using experimentally determined interaction parameters. Pharm Res. 2009;26(1):139-51. DOI: 10.1007/s11095-008-9721-1

214. Piccinni P, Tian Y, McNaughton A, Fraser J, Brown S, Jones DS, et al. Solubility parameter-based screening methods for early-stage formulation development of itraconazole amorphous solid dispersions. J Pharm Pharmacol. 2016;68(5):705-20. DOI: 10.1111/jphp.12491

215. Matsunami Y, Ichikawa K. Characterization of the structures of poly(urea-urethane) microcapsules. Int J Pharm. 2002;242(1-2):147-53. DOI: 10.1016/s0378-5173(02)00138-2

216. Anderson BD. Predicting Solubility/Miscibility in Amorphous Dispersions: It Is Time to Move Beyond Regular Solution Theories. J Pharm Sci. 2018;107(1):24-33. DOI: 10.1016/j.xphs.2017.09.030

217. Lehmkemper K, Kyeremateng SO, Heinzerling O, Degenhardt M, Sadowski G. Impact of Polymer Type and Relative Humidity on the Long-Term Physical Stability of Amorphous Solid Dispersions. Mol Pharm. 2017;14(12):4374-86. DOI: 10.1021/acs.molpharmaceut.7b00492

218. Gumaste SG, Gupta SS, Serajuddin ATM. Investigation of Polymer-Surfactant and Polymer-Drug-Surfactant Miscibility for Solid Dispersion. AAPS J. 2016;18(5):1131-43. DOI: 10.1208/s12248-016-9939-5

219. Unga J, Tajarobi F, Norder O, Frenning G, Larsson A. Relating solubility data of parabens in liquid PEG 400 to the behaviour of PEG 4000-parabens solid dispersions. Eur J Pharm Biopharm. 2009;73(2):260-8. DOI: 10.1016/j.ejpb.2009.06.003

220. Weuts I, Kempen D, Decorte A, Verreck G, Peeters J, Brewster M, et al. Phase behaviour analysis of solid dispersions of loperamide and two structurally related compounds with the polymers PVP-K30 and PVP-VA64. Eur J Pharm Sci. 2004;22(5):375-85. DOI: 10.1016/j.ejps.2004.04.002

221. Arnum PV. Exploring excipient functionality. Pharm Technol. 2011;35:6-11.

222. Adam G, Gibbs JH. On the Temperature Dependence of Cooperative Relaxation Properties in Glass-Forming Liquids. J Chem Phys. 1965;43(1):139-46. DOI: 10.1063/1.1696442

223. Graeser KA, Patterson JE, Zeitler JA, Rades T. The Role of Configurational Entropy in Amorphous Systems. Pharmaceutics. 2010;2(2):224-44. DOI: 10.3390/pharmaceutics2020224

224. Graeser KA, Patterson JE, Zeitler JA, Gordon KC, Rades T. Correlating thermodynamic and kinetic parameters with amorphous stability. Eur J Pharm Sci. 2009;37(3-4):492-8. DOI: 10.1016/j.ejps.2009.04.005

225. Wyttenbach N, Janas C, Siam M, Lauer ME, Jacob L, Scheubel E, et al. Miniaturized screening of polymers for amorphous drug stabilization (SPADS): rapid assessment of solid dispersion systems. Eur J Pharm Biopharm. 2013;84(3):583-98. DOI: 10.1016/j.ejpb.2013.01.009

226. Parikh T, Gupta SS, Meena AK, Vitez I, Mahajan N, Serajuddin AT. Application of film-casting technique to investigate drug-polymer miscibility in solid dispersion and hot-melt extrudate. J Pharm Sci. 2015;104(7):2142-52. DOI: 10.1002/jps.24446

227. Sotthivirat S, McKelvey C, Moser J, Rege B, Xu W, Zhang D. Development of amorphous solid dispersion formulations of a poorly water-soluble drug, MK-0364. Int J Pharm. 2013;452(1-2):73-81. DOI: 10.1016/j.ijpharm.2013.04.037

228. Shanbhag A, Rabel S, Nauka E, Casadevall G, Shivanand P, Eichenbaum G, et al. Method for screening of solid dispersion formulations of low-solubility compounds - miniaturization and automation of solvent casting and dissolution testing. Int J Pharm. 2008;351(1-2):209-18. DOI: 10.1016/j.ijpharm.2007.09.042

229. Kyeremateng SO, Pudlas M, Woehrle GH. A fast and reliable empirical approach for estimating solubility of crystalline drugs in polymers for hot melt extrusion formulations. J Pharm Sci. 2014;103(9):2847-58. DOI: 10.1002/jps.23941

230. Auch C, Harms M, Mader K. Melt-based screening method with improved predictability regarding polymer selection for amorphous solid dispersions. Eur J Pharm Sci. 2018;124:339-48. DOI: 10.1016/j.ejps.2018.08.035

231. Enose AA, Dasan PK, Sivaramakrishnan H, Shah SM. Formulation and Characterization of Solid Dispersion Prepared by Hot Melt Mixing: A Fast Screening Approach for Polymer Selection. J Pharm (Cairo). 2014;2014:105382. DOI: 10.1155/2014/105382

232. Lauer ME, Maurer R, Paepe AT, Stillhart C, Jacob L, James R, et al. A Miniaturized Extruder to Prototype Amorphous Solid Dispersions: Selection of Plasticizers for Hot Melt Extrusion. Pharmaceutics. 2018;10(2). DOI: 10.3390/pharmaceutics10020058

233. Zecevic DE, Wagner KG. Rational development of solid dispersions via hot-melt extrusion using screening, material characterization, and numeric simulation tools. J Pharm Sci. 2013;102(7):2297-310. DOI: 10.1002/jps.23592

234. Shah N, Sandhu H, Choi DS, Kalb O, Page S, Wyttenbach N. Structured Development Approach for Amorphous Systems. In: Williams Iii RO, Watts AB, Miller DA, editors. Formulating Poorly Water Soluble Drugs. New York, NY: Springer New York; 2012. p. 267-310.

235. Alhijjaj M, Belton P, Fabian L, Wellner N, Reading M, Qi S. Novel Thermal Imaging Method for Rapid Screening of Drug-Polymer Miscibility for Solid Dispersion Based Formulation Development. Mol Pharm. 2018;15(12):5625-36. DOI: 10.1021/acs.molpharmaceut.8b00798

236. Maclean J, Medina C, Daurio D, Alvarez-Nunez F, Jona J, Munson E, et al. Manufacture and performance evaluation of a stable amorphous complex of an acidic drug molecule and Neusilin. J Pharm Sci. 2011;100(8):3332-44. DOI: 10.1002/jps.22583

237. Gajera BY, Shah DA, Dave RH. Investigating a Novel Hot Melt Extrusion-Based Drying Technique to Solidify an Amorphous Nanosuspension Using Design of Experiment Methodology. AAPS PharmSciTech. 2018;19(8):3778-90. DOI: 10.1208/s12249-018-1189-7

238. Zhang D, Lee YC, Shabani Z, Frankenfeld Lamm C, Zhu W, Li Y, et al. Processing Impact on Performance of Solid Dispersions. Pharmaceutics. 2018;10(3):142. DOI: 10.3390/pharmaceutics10030142

239. Ma D, Djemai A, Gendron CM, Xi H, Smith M, Kogan J, et al. Development of a HPMC-based controlled release formulation with hot melt extrusion (HME). Drug Dev Ind Pharm. 2013;39(7):1070-83. DOI: 10.3109/03639045.2012.702350

240. Evans RC, Kyerematen SO, Asmus L, Degenhardt M, Rosenberg J, Wagner KG. Development and Performance of a Highly Sensitive Model Formulation Based on Torasemide to Enhance Hot-Melt Extrusion Process Understanding and Process Development. AAPS PharmSciTech. 2018;19(4):1592-605. DOI: 10.1208/s12249-018-0970-y

241. Pudlas M, Kyerematen SO, Williams LAM, Kimber JA, van Lishaut H, Kazarian SG, et al. Analyzing the impact of different excipients on drug release behavior in hot-melt extrusion formulations using FTIR spectroscopic imaging. Eur J Pharm Sci. 2015;67:21-31. DOI: 10.1016/j.ejps.2014.10.012

242. Desai PM, Hogan RC, Brancazio D, Puri V, Jensen KD, Chun JH, et al. Integrated hot-melt extrusion - injection molding continuous tablet manufacturing platform: Effects of critical process parameters and formulation attributes on product robustness and dimensional stability. Int J Pharm. 2017;531(1):332-42. DOI: 10.1016/j.ijpharm.2017.08.097

243. Alshetaili AS, Almutairy BK, Alshahrani SM, Ashour EA, Tiwari RV, Alshehri SM, et al. Optimization of hot melt extrusion parameters for sphericity and hardness of polymeric face-cut pellets. Drug Dev Ind Pharm. 2016;42(11):1833-41. DOI: 10.1080/03639045.2016.1178769

244. Patwardhan K, Asgarzadeh F, Dassinger T, Albers J, Repka MA. A quality by design approach to understand formulation and process variability in pharmaceutical melt extrusion processes. J Pharm Pharmacol. 2015;67(5):673-84. DOI: 10.1111/jphp.12370

245. Islam MT, Maniruzzaman M, Halsey SA, Chowdhry BZ, Douroumis D. Development of sustained-release formulations processed by hot-melt extrusion by using a quality-by-design approach. Drug Deliv Transl Res. 2014;4(4):377-87. DOI: 10.1007/s13346-014-0197-8

246. Ghosh I, Vippagunta R, Li S, Vippagunta S. Key considerations for optimization of formulation and melt-extrusion process parameters for developing thermosensitive compound. Pharm Dev Technol. 2012;17(4):502-10. DOI: 10.3109/10837450.2010.550624

247. Ghosh I, Snyder J, Vippagunta R, Alvine M, Vakil R, Tong WQ, et al. Comparison of HPMC based polymers performance as carriers for manufacture of solid dispersions using the melt extruder. Int J Pharm. 2011;419(1-2):12-9. DOI: 10.1016/j.ijpharm.2011.05.073

248. LaFountaine JS, McGinity JW, Williams RO, 3rd. Challenges and Strategies in Thermal Processing of Amorphous Solid Dispersions: A Review. AAPS PharmSciTech. 2016;17(1):43-55. DOI: 10.1208/s12249-015-0393-y

249. Yu LX. Pharmaceutical quality by design: product and process development, understanding, and control. Pharm Res. 2008;25(4):781-91. DOI: 10.1007/s11095-007-9511-1

250. Sangshetti JN, Deshpande M, Zaheer Z, Shinde DB, Arote R. Quality by design approach: Regulatory need. Arab J Chem. 2017;10:S3412-S25. DOI: https://doi.org/10.1016/j.arabjc.2014.01.025

251. Mishra V, Thakur S, Patil A, Shukla A. Quality by design (QbD) approaches in current pharmaceutical set-up. Expert Opin Drug Deliv. 2018;15(8):737-58. DOI: 10.1080/17425247.2018.1504768

252. Zhang L, Mao S. Application of quality by design in the current drug development. Asian J Pharm Sci. 2017;12(1):1-8. DOI: 10.1016/j.ajps.2016.07.006

253. Yu LX, Amidon G, Khan MA, Hoag SW, Polli J, Raju GK, et al. Understanding pharmaceutical quality by design. AAPS J. 2014;16(4):771-83. DOI: 10.1208/s12248-014-9598-3

254. Markarian J. Defining Design Space in Hot-Melt Extrusion. Pharmaceutical Technology; 2012 [cited 2019 2 Ago]; Available from: http://www.pharmtech.com/defining-design-space-hot-melt-extrusion.

255. Gupta A, Khan M. Hot-Melt Extrusion: An FDA Perspective on Product and Process Understanding. In: Douroumis D, editor. Hot-Melt Extrusion: Pharmaceutical Applications: John Wiley & Sons, Ltd; 2012. p. 323-31.

256. Lionberger RA, Lee SL, Lee L, Raw A, Yu LX. Quality by design: concepts for ANDAs. AAPS J. 2008;10(2):268-76. DOI: 10.1208/s12248-008-9026-7

257. Chaves LL, Vieira AC, Reis S, Sarmento B, Ferreira DC. Quality by design: discussing and assessing the solid dispersions risk. Curr Drug Deliv. 2014;11(2):253-69. DOI: 10.2174/15672018116661402111110943

258. Aho J, Edinger M, Botker J, Baldursdottir S, Rantanen J. Oscillatory Shear Rheology in Examining the Drug-Polymer Interactions Relevant in Hot Melt Extrusion. J Pharm Sci. 2016;105(1):160-7. DOI: 10.1016/j.xphs.2015.11.029

259. Chan SY, Qi S, Craig DQ. An investigation into the influence of drug-polymer interactions on the miscibility, processability and structure of polyvinylpyrrolidone-based hot melt extrusion formulations. Int J Pharm. 2015;496(1):95-106. DOI: 10.1016/j.ijpharm.2015.09.063

260. FDA. Quality by Design for ANDAs: An Example for Immediate-Release Dosage Forms. April 2012.

261. FDA. Quality by Design for ANDAs: An Example for Modified Release Dosage Forms. December 2011.

262. Rantanen J, Khinast J. The Future of Pharmaceutical Manufacturing Sciences. J Pharm Sci. 2015;104(11):3612-38. DOI: 10.1002/jps.24594

263. Pramod K, Tahir MA, Charoo NA, Ansari SH, Ali J. Pharmaceutical product development: A quality by design approach. Int J Pharm Investig. 2016;6(3):129-38. DOI: 10.4103/2230-973X.187350

264. Wu JX, van den Berg F, Sogaard SV, Rantanen J. Fast-track to a solid dispersion formulation using multi-way analysis of complex interactions. J Pharm Sci. 2013;102(3):904-14. DOI: 10.1002/jps.23409

265. Pawar J, Tayade A, Gangurde A, Moravkar K, Amin P. Solubility and dissolution enhancement of efavirenz hot melt extruded amorphous solid dispersions using combination of polymeric blends: A QbD approach. Eur J Pharm Sci. 2016;88:37-49. DOI: 10.1016/j.ejps.2016.04.001

266. Lang B, McGinity JW, Williams RO, 3rd. Dissolution enhancement of itraconazole by hot-melt extrusion alone and the combination of hot-melt extrusion and rapid freezing - effect of formulation and processing variables. Mol Pharm. 2014;11(1):186-96. DOI: 10.1021/mp4003706

267. Saerens L, Ghanam D, Raemdonck C, Francois K, Manz J, Kruger R, et al. In-line solid state prediction during pharmaceutical hot-melt extrusion in a 12 mm twin screw extruder using Raman spectroscopy. Eur J Pharm Biopharm. 2014;87(3):606-15. DOI: 10.1016/j.ejpb.2014.03.002

268. Reitz E, Vervaet C, Neubert RH, Thommes M. Solid crystal suspensions containing griseofulvin - preparation and bioavailability testing. Eur J Pharm Biopharm. 2013;83(2):193-202. DOI: 10.1016/j.ejpb.2012.09.012

269. Baronsky-Probst J, Moltgen CV, Kessler W, Kessler RW. Process design and control of a twin screw hot melt extrusion for continuous pharmaceutical tamper-resistant tablet production. Eur J Pharm Sci. 2016;87:14-21. DOI: 10.1016/j.ejps.2015.09.010

270. Chen M, Lu J, Deng W, Singh A, Mohammed NN, Repka MA, et al. Influence of processing parameters and formulation factors on the bioadhesive, temperature stability and drug release properties of hot-melt extruded films containing miconazole. AAPS PharmSciTech. 2014;15(3):522-9. DOI: 10.1208/s12249-013-0029-z

271. Debevec V, Srcic S, Horvat M. Scientific, statistical, practical, and regulatory considerations in design space development. Drug Dev Ind Pharm. 2018;44(3):349-64. DOI: 10.1080/03639045.2017.1409755

272. ICH. Q9 Quality Risk Management. November 2005.

273. ICH. Q10 Pharmaceutical Quality System. June 2008.

274. ICH. Q11 Development and Manufacture of Drug Substances (Chemical Entities and Biotechnological/Biological Entities). May 2012.

275. FDA. Guidance for industry PAT - A framework for innovative pharmaceutical manufacturing and quality assurance. September 2004.

276. Wesholowski J, Prill S, Berghaus A, Thommes M. Inline UV/Vis spectroscopy as PAT tool for hot-melt extrusion. Drug Deliv Transl Res. 2018;8(6):1595-603. DOI: 10.1007/s13346-017-0465-5

277. Kelly AL, Gough T, Isreb M, Dhumal R, Jones JW, Nicholson S, et al. In-process rheometry as a PAT tool for hot melt extrusion. Drug Dev Ind Pharm. 2018;44(4):670-6. DOI: 10.1080/03639045.2017.1408641

278. Islam MT, Scoutaris N, Maniruzzaman M, Moradiya HG, Halsey SA, Bradley MS, et al. Implementation of transmission NIR as a PAT tool for monitoring drug transformation during HME processing. Eur J Pharm Biopharm. 2015;96:106-16. DOI: 10.1016/j.ejpb.2015.06.021

279. Moradiya HG, Islam MT, Scoutaris N, Halsey SA, Chowdhry BZ, Douroumis D. Continuous Manufacturing of High Quality Pharmaceutical Cocrystals Integrated with Process Analytical Tools for In-Line Process Control. Cryst Growth Des. 2016;16(6):3425-34. DOI: 10.1021/acs.cgd.6b00402

280. Gryczke A. Hot-Melt Extrusion Process Design Using Process Analytical Technology. In: Repka AM, Langley N, DiNunzio J, editors. Melt Extrusion: Materials, Technology and Drug Product Design. New York, NY: Springer New York; 2013. p. 397-431.

281. Hitzer P, Bauerle T, Drieschner T, Ostertag E, Paulsen K, van Lishaut H, et al. Process analytical techniques for hot-melt extrusion and their application to amorphous solid dispersions. Anal Bioanal Chem. 2017;409(18):4321-33. DOI: 10.1007/s00216-017-0292-z

282. Schlindwein W, Bezerra M, Almeida J, Berghaus A, Owen M, Muirhead G. In-Line UV-Vis Spectroscopy as a Fast-Working Process Analytical Technology (PAT) during Early Phase Product Development Using Hot Melt Extrusion (HME). Pharmaceutics. 2018;10(4). DOI: 10.3390/pharmaceutics10040166

283. Vo AQ, He H, Zhang J, Martin S, Chen R, Repka MA. Application of FT-NIR Analysis for In-line and Real-Time Monitoring of Pharmaceutical Hot Melt Extrusion: a Technical Note. AAPS PharmSciTech. 2018;19(8):3425-9. DOI: 10.1208/s12249-018-1091-3

284. Malaquias LFB, Schulte HL, Chaker JA, Karan K, Durig T, Marreto RN, et al. Hot Melt Extrudates Formulated Using Design Space: One Simple Process for Both Palatability and Dissolution Rate Improvement. J Pharm Sci. 2018;107(1):286-96. DOI: 10.1016/j.xphs.2017.08.014

285. Haser A, Huang S, Listro T, White D, Zhang F. An approach for chemical stability during melt extrusion of a drug substance with a high melting point. Int J Pharm. 2017;524(1-2):55-64. DOI: 10.1016/j.ijpharm.2017.03.070

286. Banerjee S, Shankar KR, Prasad YR. Formulation development and systematic optimization of stabilized ziprasidone hydrochloride capsules devoid of any food effect. Pharm Dev Technol. 2016;21(7):775-86. DOI: 10.3109/10837450.2015.1055764

287. Maddineni S, Battu SK, Morott J, Soumyajit M, Repka MA. Formulation optimization of hot-melt extruded abuse deterrent pellet dosage form utilizing design of experiments. J Pharm Pharmacol. 2014;66(2):309-22. DOI: 10.1111/jphp.12129

288. Marsac PJ, Rumondor AC, Nivens DE, Kestur US, Stanciu L, Taylor LS. Effect of temperature and moisture on the miscibility of amorphous dispersions of felodipine and poly(vinyl pyrrolidone). J Pharm Sci. 2010;99(1):169-85. DOI: 10.1002/jps.21809

289. Thiry J, Lebrun P, Vinassa C, Adam M, Netchacovitch L, Ziemons E, et al. Continuous production of itraconazole-based solid dispersions by hot melt extrusion: Preformulation, optimization and design space determination. Int J Pharm. 2016;515(1-2):114-24. DOI: 10.1016/j.ijpharm.2016.10.003

290. Rege B. Amorphous Solid Dispersions: Scientific and Regulatory Considerations. Baltimore, USA: AAPS Arden Conference; 2016.

291. FDA. Guidance for Industry: Size, Shape and Other Physical Attributes of Generic Tablets and Capsules. June 2015.

292. Drake AC, Lee Y, Burgess EM, Karlsson JOM, Eroglu A, Higgins AZ. Effect of water content on the glass transition temperature of mixtures of sugars, polymers, and penetrating cryoprotectants in physiological buffer. PLoS One. 2018;13(1):e0190713. DOI: 10.1371/journal.pone.0190713

293. Sanghvi T, Katstra J, Quinn BP, Thomas H, P H. Scientific and Regulatory Considerations in Product Development. In: Gad S, editor. Pharmaceutical Sciences Encyclopedia: John Wiley & Sons, Inc; 2015.

294. Gupta A, Khan MA. Consistency of Pharmaceutical Products: An FDA Perspective on Hot-Melt Extrusion Process. In: Repka MA, Langley N, DiNunzio J, editors. Melt Extrusion: Materials, Technology and Drug Product Design. New York, NY: Springer New York; 2013. p. 435-45.

295. Yang LP. Suvorexant: first global approval. Drugs. 2014;74(15):1817-22. DOI: 10.1007/s40265-014-0294-5

296. FDA. CDER. Chemistry Review(s). Application number: 204569Orig1s000 (Belsomra®), NDA 204569. 2014; Report number 3601330.

297. FDA. CDER. Clinical Pharmacology and Biopharmaceutics Review(s). Application number: 204569Orig1s000 (Belsomra®), NDA 204569. 2013; Report number 3532089.

298. FDA. CDER. Clinical Pharmacology and Biopharmaceutics Review(s). Application number: 206619Orig1s000 (Viekira Pak®), NDA 206619. 2014; Report number 3631325.

299. FDA. CDER. Clinical Pharmacology and Biopharmaceutics Review(s). Application number: 207931Orig1s000 (Technivie®), NDA 207931. 2015; Report number 3785394.

300. FDA. CDER. Clinical Pharmacology and Biopharmaceutics Review(s). Application number: 208573Orig1s000 (Venclexta®), NDA 208573. 2016; Report number 3901940.

301. FDA. CDER. Chemical Review(s). Application number: 208573Orig1s000 (Venclexta®), NDA 208573. 2015; Report number OPQ-XOPQ-TEM-0001 v02.

302. Emami Riedmaier A, Lindley DJ, Hall JA, Castleberry S, Slade RT, Stuart P, et al. Mechanistic Physiologically Based Pharmacokinetic Modeling of the Dissolution and Food Effect of a Biopharmaceutics Classification System IV Compound-The Venetoclax Story. J Pharm Sci. 2018;107(1):495-502. DOI: 10.1016/j.xphs.2017.09.027

303. FDA. CDER. Product Quality Review(s). Application number: 209394Orig1s000 (Mavyret®), NDA 209394. 2017; Report number 4136686.

304. FDA. CDER. Clinical Pharmacology and Biopharmaceutics Review(s). Application number: 209394Orig1s000 (Mavyret®), NDA 209394. 2017; Report number 4104227.

305. Oberoi RK, Zhao W, Sidhu DS, Viani RM, Trinh R, Liu W. A Phase 1 Study to Evaluate the Effect of Crushing, Cutting Into Half, or Grinding of Glecaprevir/Pibrentasvir Tablets on Exposures in Healthy Subjects. J Pharm Sci. 2018;107(6):1724-30. DOI: 10.1016/j.xphs.2018.02.015

306. Huang S, Williams RO, 3rd. Effects of the Preparation Process on the Properties of Amorphous Solid Dispersions. AAPS PharmSciTech. 2018;19(5):1971-84. DOI: 10.1208/s12249-017-0861-7

307. Trivino A, Gumireddy A, Meng F, Prasad D, Chauhan H. Drug-polymer miscibility, interactions, and precipitation inhibition studies for the development of amorphous solid dispersions for the poorly soluble anticancer drug flutamide. Drug Dev Ind Pharm. 2019;45(8):1277-91. DOI: 10.1080/03639045.2019.1606822

308. Andries K, Azijn H, Thielemans T, Ludovici D, Kukla M, Heeres J, et al. TMC125, a novel next-generation nonnucleoside reverse transcriptase inhibitor active against nonnucleoside reverse transcriptase inhibitor-resistant human immunodeficiency virus type 1. Antimicrob Agents Chemother. 2004;48(12):4680-6. DOI: 10.1128/AAC.48.12.4680-4686.2004

309. Weuts I, Van Dycke F, Voorspoels J, De Cort S, Stokbroekx S, Leemans R, et al. Physicochemical properties of the amorphous drug, cast films, and spray dried powders to predict formulation probability of success for solid dispersions: etravirine. J Pharm Sci. 2011;100(1):260-74. DOI: 10.1002/jps.22242

310. Janssen Pharmaceuticals I. Full Prescribing Information: INTELENCE (etravirine) tablets for oral use. Revised: August 2014; Report number 3106676.

311. Scholler-Gyure M, Kakuda TN, Raoof A, De Smedt G, Hoetelmans RM. Clinical pharmacokinetics and pharmacodynamics of etravirine. Clin Pharmacokinet. 2009;48(9):561-74. DOI: 10.2165/10895940-000000000-00000

312. Ramesh K, Chandra Shekar BC, Khadgapathi P, Bhikshapathi DVRN. A Comparative Study of Etravirine Solid Dispersions Using Hot Melt Extrusion and Spray Drying Technique. Am J PharmTech Res. 2014;4(6):595-617.

313. Ramesh K, Shekar BC, Khadgapathi P, Bhikshapathi DVRN, Gourav N. Enhancement of Solubility and Bioavailability of Etravirine Solid Dispersions by Solvent Evaporation Technique with Novel Carriers. IOSR-JPBS. 2015;10(4):30-41.

314. Kommavarapu P, Maruthapillai A, Palanisamy K, Koya RT. Physical characterization and dissolution performance assessment of Etravirine solid dispersions prepared by spray drying process. Pak J Pharm Sci. 2016;29(6):2023-31.

315. Bochmann ES, Neumann D, Gryczke A, Wagner KG. Micro-scale solubility assessments and prediction models for active pharmaceutical ingredients in polymeric matrices. Eur J Pharm Biopharm. 2019;141:111-20. DOI: 10.1016/j.ejpb.2019.05.012

316. Simoes MF, Pinto RMA, Simoes S. Hot-melt extrusion in the pharmaceutical industry: toward filing a new drug application. Drug Discov Today. 2019;24(9):1749-68. DOI: 10.1016/j.drudis.2019.05.013

317. Zhu J, Lu X, Balieu R, Kringos N. Modelling and numerical simulation of phase separation in polymer modified bitumen by phase-field method. Mater Des. 2016;107:322-32. DOI: 10.1016/j.matdes.2016.06.041

318. Wang J-s, Porter RS. On the viscosity-temperature behavior of polymer melts. Rheol Acta. 1995;34(5):496-503. DOI: 10.1007/bf00396562

319. Hansen CM. Chapter 1: Solubility Parameters - an introduction. In: Hansen CM, editor. Hansen Solubility Parameters: a User's Handbook. 2nd ed. Florida, USA: CRC Press, Taylor & Francis Group; 2007. p. 1-26.

320. Liu J, Cao F, Zhang C, Ping Q. Use of polymer combinations in the preparation of solid dispersions of a thermally unstable drug by hot-melt extrusion. Acta Pharm Sin B. 2013;3(4):263-72. DOI: 10.1016/j.apsb.2013.06.007

321. Meng F, Dave V, Chauhan H. Qualitative and quantitative methods to determine miscibility in amorphous drug-polymer systems. Eur J Pharm Sci. 2015;77:106-11. DOI: 10.1016/j.ejps.2015.05.018

322. Kini A, Patel SB. Phase behavior, intermolecular interaction, and solid state characterization of amorphous solid dispersion of Febuxostat. Pharm Dev Technol. 2017;22(1):45-57. DOI: 10.3109/10837450.2016.1138130

323. Qi S, Weuts I, De Cort S, Stokbroekx S, Leemans R, Reading M, et al. An investigation into the crystallisation behaviour of an amorphous cryomilled pharmaceutical material above and below the glass transition temperature. J Pharm Sci. 2010;99(1):196-208. DOI: 10.1002/jps.21811

324. Saboo S, Mugheirbi NA, Zemlyanov DY, Kestur US, Taylor LS. Congruent release of drug and polymer: A "sweet spot" in the dissolution of amorphous solid dispersions. J Control Release. 2019;298:68-82. DOI: 10.1016/j.jconrel.2019.01.039

325. Craig DQ. The mechanisms of drug release from solid dispersions in water-soluble polymers. Int J Pharm. 2002;231(2):131-44. DOI: 10.1016/s0378-5173(01)00891-2

326. Chen Y, Liu C, Chen Z, Su C, Hageman M, Hussain M, et al. Drug-polymer-water interaction and its implication for the dissolution performance of amorphous solid dispersions. Mol Pharm. 2015;12(2):576-89. DOI: 10.1021/mp500660m

327. Lu Y, Tang N, Lian R, Qi J, Wu W. Understanding the relationship between wettability and dissolution of solid dispersion. Int J Pharm. 2014;465(1-2):25-31. DOI: 10.1016/j.ijpharm.2014.02.004

328. Ghadi R, Dand N. BCS class IV drugs: Highly notorious candidates for formulation development. J Control Release. 2017;248:71-95. DOI: 10.1016/j.jconrel.2017.01.014

329. Gupta S, Kesarla R, Omri A. Formulation strategies to improve the bioavailability of poorly absorbed drugs with special emphasis on self-emulsifying systems. ISRN Pharm. 2013;2013:848043. DOI: 10.1155/2013/848043

330. Tran P, Pyo YC, Kim DH, Lee SE, Kim JK, Park JS. Overview of the Manufacturing Methods of Solid Dispersion Technology for Improving the Solubility of Poorly Water-Soluble Drugs and Application to Anticancer Drugs. Pharmaceutics. 2019;11(3):132. DOI: 10.3390/pharmaceutics11030132

331. Skrdla PJ, Floyd PD, Dell'Orco PC. Predicting the solubility enhancement of amorphous drugs and related phenomena using basic thermodynamic principles and semi-empirical kinetic models. Int J Pharm. 2019;567:118465. DOI: 10.1016/j.ijpharm.2019.118465

332. Novakovic D, Isomaki A, Pleunis B, Fraser-Miller SJ, Peltonen L, Laaksonen T, et al. Understanding Dissolution and Crystallization with Imaging: A Surface Point of View. Mol Pharm. 2018;15(11):5361-73. DOI: 10.1021/acs.molpharmaceut.8b00840

333. Karagianni A, Kachrimanis K, Nikolakakis I. Co-Amorphous Solid Dispersions for Solubility and Absorption Improvement of Drugs: Composition, Preparation, Characterization and Formulations for Oral Delivery. Pharmaceutics. 2018;10(3). DOI: 10.3390/pharmaceutics10030098

334. Lin X, Hu Y, Liu L, Su L, Li N, Yu J, et al. Physical Stability of Amorphous Solid Dispersions: a Physicochemical Perspective with Thermodynamic, Kinetic and Environmental Aspects. Pharm Res. 2018;35(6):125. DOI: 10.1007/s11095-018-2408-3

335. Miller DA, McConville JT, Yang W, Williams RO, 3rd, McGinity JW. Hot-melt extrusion for enhanced delivery of drug particles. J Pharm Sci. 2007;96(2):361-76. DOI: 10.1002/jps.20806

336. Shi X, Song S, Ding Z, Fan B, Huang W, Xu T. Improving the Solubility, Dissolution, and Bioavailability of Ibrutinib by Preparing It in a Coamorphous State With Saccharin. J Pharm Sci. 2019;108(9):3020-8. DOI: 10.1016/j.xphs.2019.04.031

337. Sathisaran I, Dalvi SV. Engineering Cocrystals of PoorlyWater-Soluble Drugs to Enhance Dissolution in Aqueous Medium. Pharmaceutics. 2018;10(3):108. DOI: 10.3390/pharmaceutics10030108

338. Pharmacyclics, LLC. Full Prescribing Information: IMBRUVICA®. Revised: 08/2018; Report number 3694103.

339. PubChem: Compound Summary for CID 24821094 (Ibrutinib) [database on the Internet]. [cited 8 Jan 2019]. Available from: https://pubchem.ncbi.nlm.nih.gov/compound/24821094.

340. EMA, CHMP. Assessment report: Imbruvica. 2014; Report number EMEA/H/C/003791/0000.

341. Heinz A, Strachan CJ, Gordon KC, Rades T. Analysis of solid-state transformations of pharmaceutical compounds using vibrational spectroscopy. J Pharm Pharmacol. 2009;61(8):971-88. DOI: 10.1211/jpp/61.08.0001

342. Zvoníček V, Skořepová E, Dušek M, Babor M, Žvátora P, Šoóš M. First Crystal Structures of Pharmaceutical Ibrutinib: Systematic Solvate Screening and Characterization. Cryst Growth Des. 2017;17(6):3116-27. DOI: 10.1021/acs.cgd.7b00047

343. Yoshioka M, Hancock BC, Zografi G. Inhibition of indomethacin crystallization in poly(vinylpyrrolidone) coprecipitates. J Pharm Sci. 1995;84(8):983-6. DOI: 10.1002/jps.2600840814

344. Kianfar F, Ayensu I, Boateng JS. Development and physico-mechanical characterization of carrageenan and poloxamer-based lyophilized matrix as a potential buccal drug delivery system. Drug Dev Ind Pharm. 2014;40(3):361-9. DOI: 10.3109/03639045.2012.762655

345. Fulop I, Gyeresi A, Kiss L, Deli MA, Croitoru MD, Szabo-Revesz P, et al. Preparation and investigation of mefenamic acid - polyethylene glycol - sucrose ester solid dispersions. Acta Pharm. 2015;65(4):453-62. DOI: 10.1515/acph-2015-0035

346. Baird JA, Van Eerdenbrugh B, Taylor LS. A classification system to assess the crystallization tendency of organic molecules from undercooled melts. J Pharm Sci. 2010;99(9):3787-806. DOI: 10.1002/jps.22197

347. Meng F, Gala U, Chauhan H. Classification of solid dispersions: correlation to (i) stability and solubility (ii) preparation and characterization techniques. Drug Dev Ind Pharm. 2015;41(9):1401-15. DOI: 10.3109/03639045.2015.1018274

348. Zvoníček V, Skořepová E, Dušek M, Žvátora P, Šoóš M. Ibrutinib Polymorphs: Crystallographic Study. Cryst Growth Des. 2018;18(3):1315-26. DOI: 10.1021/acs.cgd.7b00923

349. Wheless JW, Phelps SJ. A Clinician's Guide to Oral Extended-Release Drug Delivery Systems in Epilepsy. J Pediatr Pharmacol Ther. 2018;23(4):277-92. DOI: 10.5863/1551-6776-23.4.277

350. Derosa G, D'Angelo A, Romano D, Maffioli P. Effects of metformin extended release compared to immediate release formula on glycemic control and glycemic variability in patients with type 2 diabetes. Drug Des Devel Ther. 2017;11:1481-8. DOI: 10.2147/DDDT.S131670

351. Childress AC, Komolova M, Sallee FR. An update on the pharmacokinetic considerations in the treatment of ADHD with long-acting methylphenidate and amphetamine formulations. Expert Opinion on Drug Metabolism & Toxicology. 2019;15(11):937-74. DOI: 10.1080/17425255.2019.1675636

352. Siddique S, Khanam J, Bigoniya P. Development of sustained release capsules containing "coated matrix granules of metoprolol tartrate". AAPS PharmSciTech. 2010;11(3):1306-14. DOI: 10.1208/s12249-010-9501-1

353. Abdelbary A, El-Gazayerly ON, El-Gendy NA, Ali AA. Floating tablet of trimetazidine dihydrochloride: an approach for extended release with zero-order kinetics. AAPS PharmSciTech. 2010;11(3):1058-67. DOI: 10.1208/s12249-010-9468-y

354. 5 - Mathematical models of drug release. In: Bruschi ML, editor. Strategies to Modify the Drug Release from Pharmaceutical Systems: Woodhead Publishing; 2015. p. 63-86.

355. Liu L, Khang G, Rhee JM, Lee HB. Monolithic osmotic tablet system for nifedipine delivery. J Control Release. 2000;67(2-3):309-22. DOI: 10.1016/s0168-3659(00)00222-4

356. Liu L, Ku J, Khang G, Lee B, Rhee JM, Lee HB. Nifedipine controlled delivery by sandwiched osmotic tablet system. J Control Release. 2000;68(2):145-56. DOI: 10.1016/s0168-3659(00)00243-1

357. Waterman KC, MacDonald BC, Roy MC. Extrudable core system: development of a single-layer osmotic controlled-release tablet. J Control Release. 2009;134(3):201-6. DOI: 10.1016/j.jconrel.2008.11.017

358. Thombre AG, Appel LE, Chidlaw MB, Daugherity PD, Dumont F, Evans LA, et al. Osmotic drug delivery using swellable-core technology. J Control Release. 2004;94(1):75-89. DOI: 10.1016/j.jconrel.2003.09.009

359. Hu M, Zhu Z, Wu Y, Meng Q, Luo J, Wang H. Exploring the Potential of Hydrophilic Matrix Combined with Insoluble Film Coating: Preparation and Evaluation of Ambroxol Hydrochloride Extended Release Tablets. AAPS PharmSciTech. 2020;21(3):93. DOI: 10.1208/s12249-020-1628-0

360. Qazi F, Shoaib MH, Yousuf RI, Nasiri MI, Ahmed K, Ahmad M. Lipids bearing extruded-spheronized pellets for extended release of poorly soluble antiemetic agent-Meclizine HCl. Lipids Health Dis. 2017;16(1):75. DOI: 10.1186/s12944-017-0466-x

361. Danckwerts MP, van der Watt JG, Moodley I. Zero-order release of theophylline from a core-in-cup tablet in sequenced simulated gastric and intestinal fluid. Drug Dev Ind Pharm. 1998;24(2):163-7. DOI: 10.3109/03639049809085601

362. Sundy E, Danckwerts MP. A novel compression-coated doughnut-shaped tablet design for zero-order sustained release. Eur J Pharm Sci. 2004;22(5):477-85. DOI: 10.1016/j.ejps.2004.05.004

363. Ijaz H, Qureshi J, Danish Z, Zaman M, Abdel-Daim M, Hanif M, et al. Formulation and in-vitro evaluation of floating bilayer tablet of lisinopril maleate and metoprolol tartrate. Pak J Pharm Sci. 2015;28(6):2019-25.

364. Abouelatta SM, Aboelwafa AA, Khalil RM, ElGazayerly ON. Floating lipid beads for the improvement of bioavailability of poorly soluble basic drugs: in-vitro optimization and in-vivo performance in humans. Eur J Pharm Biopharm. 2015;89:82-92. DOI: 10.1016/j.ejpb.2014.11.011

365. Tomuta I, Leucuta SE. The influence of formulation factors on the kinetic release of metoprolol tartrate from prolong release coated minitablets. Drug Dev Ind Pharm. 2007;33(10):1070-7. DOI: 10.1080/03639040601180002

366. Huang KK, Wang DP, Meng CL. Development of extended release dosage forms using non-uniform drug distribution techniques. Drug Dev Ind Pharm. 2002;28(5):593-9. DOI: 10.1081/ddc-120003455

367. Fina F, Goyanes A, Rowland M, Gaisford S, A WB. 3D Printing of Tunable Zero-Order Release Printlets. Polymers. 2020;12(8). DOI: 10.3390/polym12081769

368. Vo AQ, Zhang J, Nyavanandi D, Bandari S, Repka MA. Hot melt extrusion paired fused deposition modeling 3D printing to develop hydroxypropyl cellulose based floating tablets of cinnarizine. Carbohydr Polym. 2020;246:116519. DOI: 10.1016/j.carbpol.2020.116519

369. Giri BR, Song ES, Kwon J, Lee JH, Park JB, Kim DW. Fabrication of Intragastric Floating, Controlled Release 3D Printed Theophylline Tablets Using Hot-Melt Extrusion and Fused Deposition Modeling. Pharmaceutics. 2020;12(1). DOI: 10.3390/pharmaceutics12010077

370. Zhang J, Yang W, Vo AQ, Feng X, Ye X, Kim DW, et al. Hydroxypropyl methylcellulose-based controlled release dosage by melt extrusion and 3D printing: Structure and drug release correlation. Carbohydr Polym. 2017;177:49-57. DOI: 10.1016/j.carbpol.2017.08.058

371. Bisharat L, Alkhatib HS, Abdelhafez A, Barqawi A, Aljaberi A, Qi S, et al. Hot melt extruded zein for controlled delivery of diclofenac sodium: Effect of drug loading and medium composition. Int J Pharm. 2020;585:119503. DOI: 10.1016/j.ijpharm.2020.119503

372. Alqahtani F, Belton P, Ward A, Asare-Addo K, Qi S. An investigation into the use of low quantities of functional additives to control drug release from hot melt extruded solid dispersions for poorly soluble drug delivery. Int J Pharm. 2020;579:119172. DOI: 10.1016/j.ijpharm.2020.119172

373. Cheng L, Li T, Dong L, Wang X, Huo Q, Wang H, et al. Design and Evaluation of Bilayer Pump Tablet of Flurbiprofen Solid Dispersion for Zero-Order Controlled Delivery. J Pharm Sci. 2018;107(5):1434-42. DOI: 10.1016/j.xphs.2017.12.026

374. Zhang X, Wang M, Li P, Wang A, Liang R, Gai Y, et al. Application of hot-melt extrusion technology for designing an elementary osmotic pump system combined with solid dispersion for a novel poorly water-soluble antidepressant. Pharm Dev Technol. 2016;21(8):1006-14. DOI: 10.3109/10837450.2015.1089896

375. Thommes M, Baert L, Rosier J. 800 mg Darunavir tablets prepared by hot melt extrusion. Pharm Dev Technol. 2011;16(6):645-50. DOI: 10.3109/10837450.2010.508077

376. Verhoeven E, De Beer TR, Van den Mooter G, Remon JP, Vervaet C. Influence of formulation and process parameters on the release characteristics of ethylcellulose sustained-release mini-matrices produced by hot-melt extrusion. Eur J Pharm Biopharm. 2008;69(1):312-9. DOI: 10.1016/j.ejpb.2007.10.007

377. Lu T, Ten Hagen TLM. A novel kinetic model to describe the ultra-fast triggered release of thermosensitive liposomal drug delivery systems. J Control Release. 2020;324:669-78. DOI: 10.1016/j.jconrel.2020.05.047

378. Dash S, Murthy PN, Nath L, Chowdhury P. Kinetic modeling on drug release from controlled drug delivery systems. Acta Pol Pharm. 2010;67(3):217-23.

379. Papadopoulou V, Kosmidis K, Vlachou M, Macheras P. On the use of the Weibull function for the discernment of drug release mechanisms. Int J Pharm. 2006;309(1-2):44-50. DOI: 10.1016/j.ijpharm.2005.10.044

380. Heinze G, Wallisch C, Dunkler D. Variable selection - A review and recommendations for the practicing statistician. Biom J. 2018;60(3):431-49. DOI: 10.1002/bimj.201700067

381. Sainani KL. Explanatory Versus Predictive Modeling. PM&R. 2014;6(9):841-4. DOI: https://doi.org/10.1016/j.pmrj.2014.08.941

382. Hameed HA, Khan S, Shahid M, Ullah R, Bari A, Ali SS, et al. Engineering of Naproxen Loaded Polymer Hybrid Enteric Microspheres for Modified Release Tablets: Development, Characterization, in silico Modelling and in vivo Evaluation. Drug Des Devel Ther. 2020;14:27-41. DOI: 10.2147/DDDT.S232111

383. Shi X, Fan N, Zhang G, Sun J, He Z, Li J. Quercetin amorphous solid dispersions prepared by hot melt extrusion with enhanced solubility and intestinal absorption. Pharm Dev Technol. 2020;25(4):472-81. DOI: 10.1080/10837450.2019.1709502

384. Delaney SP, Nethercott MJ, Mays CJ, Winquist NT, Arthur D, Calahan JL, et al. Characterization of Synthesized and Commercial Forms of Magnesium Stearate Using Differential Scanning Calorimetry, Thermogravimetric Analysis, Powder X-Ray Diffraction, and Solid-State NMR Spectroscopy. J Pharm Sci. 2017;106(1):338-47. DOI: 10.1016/j.xphs.2016.10.004

385. Raijada D, Mullertz A, Cornett C, Munk T, Sonnergaard J, Rantanen J. Miniaturized approach for excipient selection during the development of oral solid dosage form. J Pharm Sci. 2014;103(3):900-8. DOI: 10.1002/jps.23840

386. Haque MK, Roos YH. Crystallization and X-ray diffraction of spray-dried and freeze-dried amorphous lactose. Carbohydr Res. 2005;340(2):293-301. DOI: 10.1016/j.carres.2004.11.026

387. Wu L, Miao X, Shan Z, Huang Y, Li L, Pan X, et al. Studies on the spray dried lactose as carrier for dry powder inhalation. Asian J Pharm Sci. 2014;9(6):336-41. DOI: 10.1016/j.ajps.2014.07.006

388. Mudie DM, Amidon GL, Amidon GE. Physiological parameters for oral delivery and in vitro testing. Mol Pharm. 2010;7(5):1388-405. DOI: 10.1021/mp100149j

389. Bermejo M, Hens B, Dickens J, Mudie D, Paixao P, Tsume Y, et al. A Mechanistic Physiologically-Based Biopharmaceutics Modeling (PBBM) Approach to Assess the In Vivo Performance of an Orally Administered Drug Product: From IVIVC to IVIVP. Pharmaceutics. 2020;12(1). DOI: 10.3390/pharmaceutics12010074

390. Silva TND, Reynaud F, Picciani PHS, de Holanda ESKG, Barradas TN. Chitosan-based films containing nanoemulsions of methyl salicylate: Formulation development, physical-chemical and in vitro drug release characterization. Int J Biol Macromol. 2020;164:2558-68. DOI: 10.1016/j.ijbiomac.2020.08.117

391. Kosmidis K, Argyrakis P, Macheras P. A reappraisal of drug release laws using Monte Carlo simulations: the prevalence of the Weibull function. Pharm Res. 2003;20(7):988-95. DOI: 10.1023/a:1024497920145